

THE FORMATION AND PROPERTIES OF COHERENT FLOCS  
IN FIBRE SUSPENSIONS

by

ROBERT MARIAN SOSZYŃSKI

B.D. Tech. School Energ., Warsaw, 1966  
Mgr. Inż., Warsaw Polytechnic, 1973

A THESIS SUBMITTED IN PARTIAL FULFILLMENT OF  
THE REQUIREMENTS FOR THE DEGREE OF  
DOCTOR OF PHILOSOPHY

in

THE FACULTY OF GRADUATE STUDIES  
Department of Chemical Engineering

We accept this thesis as conforming  
to the required standard

UNIVERSITY OF BRITISH COLUMBIA

June 1987

© Robert Marian Soszyński, 1987

In presenting this thesis in partial fulfillment of the requirements for an advanced degree at the University of British Columbia, I agree that the Library shall make it freely available for reference and study. I further agree that permission for extensive copying of this thesis for scholarly purposes may be granted by the Head of my Department or by his or her representatives. It is understood that copying or publication of the thesis for financial gain shall not be allowed without my written permission.

Department of Chemical Engineering

University of British Columbia  
2075 Wesbrook Place  
Vancouver, Canada  
V6T 1W5

Date: June, 1987

**ABSTRACT**

Fibres in concentrated suspensions are in continuous contact with other fibres and may interlock through elastic bending to form coherent networks. Such interlocking is termed Type-C cohesion. The process by which Type-C cohesion forms among fibres and the resulting structure and tensile strength of individual flocs of fibres have been examined in experimental study in which relatively straight, smooth nylon (6-6) fibres of aspect ratios from 65 to 189 were suspended in aqueous-sugar solutions. The fibres were in most cases neutrally buoyant. The suspensions were caused to flow in a partially filled, inclined-to-the-horizontal or horizontally-oriented cylinder rotated about its principal axis to produce a recirculating and moderately unsteady flow. At a well-defined and reproducible "threshold concentration" Type-C coherent flocs formed. The flocs were verified to be of Type-C by heat treatment. The heat treatment caused stress relaxation in elastically bent fibres resulting in reduced floc strength. Visual observations of floc formation and velocity measurements with Laser Doppler Anemometer indicated that the flocs originated in the zone in which flow decelerated. In this zone flocs formed by compaction of crowded fibres. The threshold concentration depended on fibre geometry and viscosity of the suspending liquid. Below an aspect ratio of approximately 50 and above a suspending liquid viscosity of approximately 0.013 Pa·s, Type-C coherent flocs did not form at any concentration of fibres. Under the test conditions of this work, the threshold concentration was unaffected by the cylinder

rotational speed, cylinder diameter, and angle of incline to the horizontal, provided that sufficient shear was induced in the cylinder to create recirculating flow. The structure and strength of Type-C coherent flocs were examined. The number of contact points per fibre was less than values estimated from theoretical, statistical models in the literature. The tensile strength of individual Type-C flocs measured in a tester with a unique comb support showed values larger than strengths reported in the literature for either man-made or wood-pulp fibre networks. A mathematical model developed to describe tensile strength based on frictional fibre-to-fibre interaction accounted for only a part of the total floc strength.

**Table of Contents**

1	INTRODUCTION .....	1
2	LITERATURE REVIEW .....	7
2.1	Flocculation in Dilute Fibre Suspensions .....	7
2.2	Flocculation in Semiconcentrated Fibre Suspensions .....	11
2.2.1	Fibre interactions and collisions .....	11
2.2.2	Fibre cohesion .....	18
2.3	Flocculation in Concentrated Fibre Suspensions .....	22
2.3.1	Process of network formation .....	23
2.3.2	Structure of coherent networks .....	33
2.3.3	Network strength .....	38
2.3.4	Cohesion forces .....	54
2.4	Classification of Findings from the Literature Review ...	59
2.5	Summary of Literature Review .....	63
2.6	Thesis Objectives .....	68
3	EXPERIMENTAL PROGRAM .....	70
3.1	Preparation of fibres .....	70
3.1.1	Choice of fibrous material .....	70
3.1.2	Determination of fibre geometry .....	72
3.1.3	Moisture absorption by nylon fibres .....	73
3.1.4	Determination of fibre elastic properties .....	74
3.1.5	Determination of wet-friction coefficient .....	75
3.2	Creation of Coherent Flocs .....	75
3.2.1	Observation of the phenomenon of flocculation .....	78
3.2.2	Sediment concentration .....	78
3.3	Experimental Variables .....	79
3.3.1	Fibre concentration .....	80

3.3.2	Density of the suspending liquid .....	81
3.3.3	Cylinder diameter, angle of incline, and rotational speed .....	81
3.3.4	Fibre dimensions - length and diameter .....	82
3.3.5	Viscosity of the suspending liquid .....	82
3.4	Flow Patterns in Horizontal Rotating Cylinder .....	83
3.5	Studies of Floc Structure .....	85
3.6	Floc Strength Measurement .....	86
4	RESULTS AND DISCUSSION .....	88
4.1	Effect of Fibre Concentration on Floc Formation .....	88
4.2	Observations of Origin and Growth of Type-C Flocs .....	94
4.3	Effect of Key Variables on Threshold Concentration .....	98
4.3.1	Cylinder (flow) variables .....	100
4.3.2	Suspending liquid viscosity .....	104
4.3.3	Fibre geometry .....	109
4.4	Evaluation of Criteria for Threshold Concentration .....	113
4.5	Flow Conditions under which Coherent Flocs Form .....	124
4.5.1	Dissimilarities between flows in horizontal cylinder .....	126
4.5.2	Other types of flow .....	135
4.6	Observations of Floc Structure .....	136
4.7	Tensile Strength of Type-C Flocs .....	139
4.5	Mathematical Model of Tensile Strength of Type-C Flocs	150
5	SUMMARY .....	156
6	RECOMMENDATIONS FOR FURTHER WORK .....	159
	NOMENCLATURE .....	160
	LIST OF REFERENCES .....	163
	GLOSSARY .....	173

APPENDIX I. Water Retention Ratio of Wood Pulp Fibres .....	176
APPENDIX II. Apparent Density of Wood Pulp Fibres in Aqueous Suspensions .....	179
APPENDIX III. Estimates of Magnitudes of Various Cohesion Forces .....	185
APPENDIX IV. Filament Cutting Procedure .....	187
APPENDIX V. Measurement of Fibre Length and Curvature .....	189
APPENDIX VI. Water Absorption by Nylon Fibres .....	197
APPENDIX VII. Relationships Between Mass and Volume Concentration of Hydrophilic Particles Suspended in Aqueous-Solute Solutions .....	201
APPENDIX VIII. Measurement of the Elastic Moduli of Fibres ..	205
APPENDIX IX. Friction Between Wet Fibre Surfaces .....	215
APPENDIX X. Rotating Cylinder Apparatus .....	219
APPENDIX XI. Suspension Preparation and Type-C Floc Formation .....	221
APPENDIX XII. Sediment Concentration Measurements .....	223
APPENDIX XIII. Flow Velocity Measurement in Fibre Suspensions in Horizontal Rotating Cylinder .....	224
APPENDIX XIV. Floc Preparation and Contact Counting Procedures .....	236
APPENDIX XV. Tensile Strength of Wet Nylon Floccs .....	239
APPENDIX XVI. Computer Model of Fibre Deposition into 3-D networks .....	245
APPENDIX XVII. Mathematical Analysis of the Tensile Strength of Type-C Floccs .....	248
APPENDIX XVIII. Conductivity and pH Measurements .....	254

APPENDIX XIX. Data Collection Program For Fibre Length and Fibre Curvature Measurements .....	258
APPENDIX XX. Data Collection Program for Water Absorption by Nylon Fibres .....	261
APPENDIX XXI. Fibre Bending. Data Processing Program, Raw Data File, Averages and Standard Deviations of Fibre Deflections, Bulk Reynolds Numbers. Eye-Piece-Micrometer and GILMONT Flowmeter Calibration Data .....	263
APPENDIX XXII. Data Acquisition Program for Flow Velocity Measurements .....	270
APPENDIX XXIII. Data Acquisition Program for Tensile Tests of Wet, Type-C Nylon Floccs .....	276
APPENDIX XXIV. Data Collection Program for Determination of Break Area .....	280
APPENDIX XXV. FORTRAN Program Processing Conductivity Data. Data Listing .....	283
APPENDIX XXVI. Data from Threshold Concentration Measurements .....	286
APPENDIX XXVII. Data from Velocity Measurements in Horizontal Rotating Cylinder .....	295
APPENDIX XXVIII. Data from Tensile Strength Measurements ....	303
APPENDIX XXIX. Data from Sedimentation Experiments .....	307
APPENDIX XXX. Data from Coefficient of Friction Measurements .....	315
APPENDIX XXXI. Average Velocities and Root-Mean-Squares of Velocity Fluctuation .....	317

## List of Tables

Table	Page
I. Factors Affecting Flocculation of Wood-Pulp Fibres .....	5
II. Number of Fibre Contacts per Fibre in Compacted Mats [E4] and Calculated from Equation (2) and (3) .....	39
III. Yield Stress of Nylon Fibre Slurries .....	42
IV. Shear Strength of Fibre Suspensions. Direct Methods. Quasi-Static Tests .....	46
V. Shear Strength of Fibre Suspensions. Indirect Methods. Quasi-Static Tests .....	47
VI. Tensile Strength of Fibre Networks. Quasi-Static Tests ..	49
VII. Tensile Strength of Dry Wood-Pulp Flocs .....	53
VIII. Threshold Concentration for 15 Denier Nylon Fibres in Water and in Aqueous-Sugar Solution .....	99
IX. System Characteristics for Suspensions of Nylon Fibres (L=4.97 mm, d=0.0442 mm) in the Suspending Media of Various Viscosities .....	106
X. Nylon Fibre Dimensions in Wet State .....	110
XI. Threshold Concentrations and Sediment Concentrations ....	114
XII. Crowding Factors Calculated from Equation (6) and (7) at the Onset of Type-C Floc Formation .....	121
XIII. Limits of Equations (14) to (17) .....	123
XIV. Fit Coefficients and Limits for Number of Fibres in a Cubical Volume .....	124
XV. Power Fit Parameters of Tensile Strength Data .....	148
XVI. Evaluation of the Mathematical Model of Tensile Strength .....	153

I-XVII.	Average Dimensions of Wood Fibres and Pulp Fibres ...	178
II-XVIII.	WRR at the "Knee" for Various Never-dried Pulps ...	181
II-XIX.	Apparent Density of Wood Pulp Fibres at Selected WRRk Values .....	183
III-XX.	Forces Deflecting Simply Supported Fibres .....	186
V-XXI.	Nylon Fibres in Wet State. Fibre Length Statistics ..	194
V-XXII.	Nylon Fibres in Wet State. Curvature Statistics ....	195
VI-XXIII.	Water Absorption by Nylon Fibres in 98% Relative Humidity Environment .....	200
VII-XXIV.	Relationships Between Mass and Volume Concentration of Hydrophilic Particles in Suspensions .....	204
VIII-XXV.	Elastic Moduli of 3 and 6 Denier Nylon Filaments ..	209
VIII-XXVI.	Elastic Moduli and Stiffness of Wet Nylon Fibres .	213
IX-XXVII.	Static and Dynamic Coefficient of Friction for Wet Nylon Fibres .....	218
XIV-XXVIII.	Contact Points in Type-C Floccs .....	238
XVIII-XXIX.	Fit Parameters for Two Straight Lines Shown in Figure XVIII-65 .....	256

## List of Figures

Figure	Page
1. The Principle of Type-C (a) and Type-B (b) Cohesion .....	3
2. Shear Modulus versus Suspending Liquid Viscosity .....	25
3. Concepts of Fibre Crowding in Suspensions and Experimental Investigations with Man-made Fibres .....	60
4. Concepts of Fibre Crowding in Suspensions and Experimental Investigations with Wood-pulp Fibres .....	62
5. Surface Texture and Shape of Nylon (dark) and Wood-pulp Fibres. Magnification 120x .....	71
6. Rotating Cylinder Apparatus .....	77
7. Experimental Setup for Velocity Measurements in a Horizontal Rotating Cylinder .....	84
8. Schematic of Initial Comb Positioning in Tensile Tests ....	86
9. Increasing Cloudiness with an Increase in Fibre Concentration .....	89
10. a. Cloudiness; b. Granularity; c. Granules in rediluted Suspension .....	91
11. Floc Concentration versus Suspension Concentration .....	96
12. Floc Weighing 0.12 g Suspended in the Air by Few Fibres ..	97
13. Effect of Cylinder Diameter on Threshold Concentration ..	101
14. Effect of Cylinder Incline on Threshold Concentration ...	102
15. Effect of Angular Speed on Threshold Concentration .....	103
16. Threshold Concentration versus Viscosity of the Suspending Liquid .....	105
17. Effect of Fibre Length and Diameter on Threshold Concentration .....	111

18. Threshold Concentration versus $d^4$ .....	112
19. Threshold Concentrations and Sediment Concentrations versus Fibre Aspect Ratio .....	115
20. Sediment Concentrations and Mathematical Models. ....	116
21. Mathematical Models and Concentrations of Fibres in Suspensions at the Onset of Type-C Floc Formation .....	118
22. Flow Pattern in a Horizontal Rotating Cylinder .....	125
23. Velocity Vectors for the Case 1 Flow .....	127
24. Velocity Vectors for the Case 2 Flow .....	128
25. Velocity Vectors for the Case 3 Flow .....	130
26. Flow Velocities at $r/R=0.85$ and $\beta$ from 0 to 100 degrees. Cylinder peripheral velocity is 0.295 m/s .....	131
27. Flow Velocities at $r/R=0.96$ and $\beta$ from 0 to 100 degrees. Cylinder peripheral velocity is 0.295 m/s .....	132
28. Number of Contacts per Fibre versus Fibre Concentration in Flocs ( $L=6.26$ mm, $d=44.2$ $\mu\text{m}$ ) .....	137
29. Number of Contacts per Fibre versus Fibre Concentration in Flocs ( $L=45.9$ mm, $d=559$ $\mu\text{m}$ ) .....	138
30. Typical Shape of Load-separation Curve .....	140
31. Tensile Stress versus Floc Apparent Volume Concentration ( $L=6.2$ mm, $d=44.2$ $\mu\text{m}$ ) .....	141
32. Tensile Stress versus Floc Apparent Volume Concentration ( $L=4.9$ mm, $d=44.2$ $\mu\text{m}$ ) .....	142
33. Tensile Stress versus Floc Apparent Volume Concentration ( $L=2.9$ mm, $d=44.2$ $\mu\text{m}$ ) .....	142
34. Tensile Stress versus Floc Apparent Volume Concentration ( $L=4.6$ mm, $d=27.9$ $\mu\text{m}$ ) .....	144

35. Tensile Stress versus Floc Apparent Volume Concentration (L=3.7 mm, d=27.9 $\mu\text{m}$ ) .....	145
36. Tensile Stress versus Floc Apparent Volume Concentration (L=2.7 mm, d=27.9 $\mu\text{m}$ ) .....	146
37. Tensile Stress versus Floc Apparent Volume Concentration (L=3.7 mm, d=19.7 $\mu\text{m}$ ) .....	146
38. Breaking Stress versus Suspension Apparent Volume Concentration .....	149
39. Concepts of Fibre Crowding in Suspensions and Fitted Lines to the Threshold Concentration Data .....	156
I-40. Apparent Volume Concentration versus Mass Concentration for Wood-pulp Fibres .....	176
IV-41. Multifilament Preparation for Cutting .....	187
V-42. Sample of Fibres deposited on the Slide Mount and Closed in It .....	189
V-43. Principle of Fibre Length and Radius of Curvature Measurements .....	190
V-44. Data Acquisition System for Fibre Length and Fibre Curvature Measurements .....	192
VI-45. Experimental Setup for Water Absorption by Nylon Fibres .....	197
VI-46. Water Absorption by Nylon Fibres in 98% RH Environment .....	198
VIII-47. Typical Load-elongation Curves for 3 Denier Nylon Filaments in Wet and Dry State .....	207
VIII-48. Simply supported Fibre deflects in a Cross-flow ....	210
VIII-49. Fibre Deflection versus Bulk Reynolds Number .....	212

IX-50. Method of Friction Measurement .....	215
IX-51. Wet-friction Coefficients versus Sled Loading for 3 Denier Nylon Filaments .....	216
IX-52. Wet-friction Coefficient Versus Sled Loading for 6 Denier Nylon Filaments .....	217
X-53. Rotating Cylinder Apparatus .....	219
XIII-54. Experimental Setup for Velocity Measurements in a Horizontal Rotating Cylinder .....	224
XIII-55. Beam Crossing Geometry at an Instant in Time .....	226
XIII-56. Locations of Measuring Points within the Central Plane of the Cylinder .....	228
XIII-57. Change in Focal Length caused by Various Indices of Refraction .....	230
XIV-58. Progressive Dismemberment of Type-C Floc .....	237
XV-59. Coherent Floc removed from the Suspension by the Fork .....	239
XV-60. Tensile Test Equipment .....	240
XV-61. Device for Tensile Testing of Nylon Flocs .....	241
XV-62. Plane View of the Break Zone .....	243
XVI-63. Parallelepiped in which Fibre deposition was Modeled .....	246
XVII-64. Bending Forces acting on Fibre .....	251
XVIII-65. Standard and Seibold Conductivities versus KCl Concentration in Solutions .....	255

## ACKNOWLEDGEMENTS

This dissertation is, apart from explicit reference, the original work of the author.

However, I am deeply indebted to my supervisor, Dr. Richard J. Kerekes, Honorary Professor of Chemical Engineering, and to my colleague Dr. Peter A. Tam Doo for many hours of valuable discussion.

I thank the People of Canada who contributed to the existence and operation of the University of British Columbia, the Pulp and Paper Research Institute of Canada, the Natural Sciences and Engineering Research Council of Canada, and MacMillan Bloedel Limited. By doing this, they provided me with a place of study and financial assistance.

## DEDICATION

I dedicate this work to my wife, Irena, and my son, Antoine.

## 1 INTRODUCTION

Flocculation of wood-pulp fibres in suspension is an important factor in pulp rheology, cleaning, screening, washing, beating, and mixing as well as in relation to the design of the wet end of paper machines. In consequence, flocculation affects the properties of the end product-paper. The competitive environment demands improved paper quality and production efficiency. The improvement of both cannot happen without understanding the factors affecting them. This is the rationale for doing research in the area of flocculation of wood-pulp fibres.

From past work, fibre flocculation has emerged as a complex phenomenon that has to date defied precise definition. Nevertheless, three general aspects of fibre flocculation have become distinguishable: state, process and nature. The state of flocculation relates to the degree of suspension nonuniformity at a given instant of time. Hence, the state of flocculation can be observed in decaying turbulence, fully-developed flow, or in an immobile suspension. The process of flocculation relates to the dynamics of the suspension between two flocculation states separated by an interval of time. It deals with relative fibre motion and interaction between suspending medium and fibres. The nature of flocculation is uniquely related to forces of interaction at fibre contact points in a given state of flocculation.

Broadly speaking, the flocculation of fibres in suspension consists of relative fibre motion, fibre collisions, and cohesion. The forces of cohesion can be of a colloidal or mechanical nature. Colloidal forces are the result of molecular and surface charge interactions whereas mechanical forces the result of physical entanglement/interlocking of fibres. In a wood-pulp fibre suspension of papermaking consistency, the forces of mechanical cohesion dwarf the effects of colloidal attraction. Historically, an electro-chemical cohesion was recognized first [B5,B6,B12,E6,R9,W8]; then mechanical cohesion was shown to be more significant [A5,A8,J3,J4,J5,J6,M1,P3,S12]. While mechanical cohesion is now accepted as being dominant, its precise nature is not known.

A recent review of current knowledge of fibre flocculation [K7] pointed out that two distinctly different forms of mechanical cohesion may exist - fibre linking and fibre interlocking. For sake of convenience these have been called Type-B and Type-C cohesion: Type-B cohesion occurs as a result of linking or hooking between fibres; Type-C cohesion is the result of constraint imposed on elastically bent fibres in a fibre network. Figure 1 shows the principles of these two cohesions. In Type-C cohesion, the normal forces at fibre contact points develop along with the network and give rise to the surface friction forces which prevent relative fibre movement. In Type-B cohesion, the normal forces at contact points are unnecessary for the network to exist but they would develop along with the frictional forces if the network was strained. The subject of

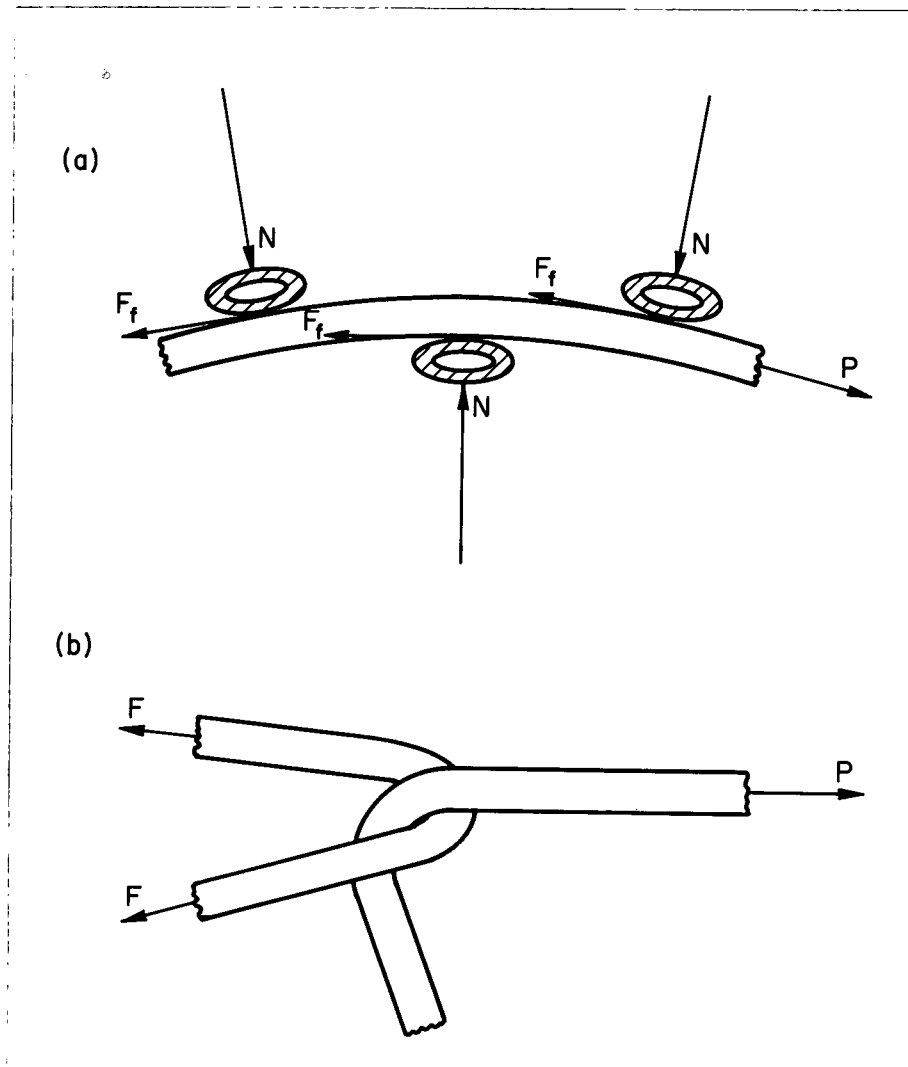


Figure 1. Principle of Type-C (a) and Type-B (b) Cohesion. In (a), normal forces are represented by letter N and frictional forces by F. Figure taken from [K7]

this dissertation is Type-C cohesion, its nature and formation.

The two particular approaches to studies of fibre flocculation are statistical and phenomenological. The statistical approach inquires exclusively about variations in the mass distribution of fibres and/or variations in the number of flocs [A3,A4,A6,A8,A10,E7,H5,H8,I2,J1,J2,L1,M17,N3,N4,R4,R5,T3,W2]. The phenomenological approach, on the other hand, which sees flocculation as a process having various fibre-to-fibre or

fibre-to-liquid interactions [A5,H8,J3,J4,J5,J6,S12] is much more demanding than the statistical approach because it requires understanding and control of a greater number of factors. Table I lists the majority of known factors that affect flocculation. The phenomenological approach was chosen for this study because improved understanding of the process and the nature of flocculation could result. Numerous factors were eliminated or controlled through use of a model fibre system - nylon fibres suspended in an aqueous-sugar solution. Type-C cohesion was isolated experimentally to determine the conditions under which it occurs. The Type-C coherent flocs were dismantled to explore their structure and were strained to measure their strength.

This dissertation begins with a systematic review of the literature (Section 2) on the flocculation of wood-pulp fibres<sup>1</sup> and man-made fibres in suspension. The process and the nature of flocculation for man-made fibres and wood-pulp fibres are discussed separately in three sub-chapters corresponding to the three sub-ranges of concentration: dilute, semiconcentrated and concentrated. The boundaries of these sub-ranges which depend on fibre aspect ratio and fibre concentration are well defined only for the fibres of uniform length and diameter. This review shows that, despite considerable research, mechanical cohesion has not been investigated and remains unexplored. The literature is replete with suppositions and guesses on fibre

---

<sup>1</sup> This term refers exclusively to pulps obtained through the pulping processes which produce undamaged, elongated particles from wood fibres or tracheids.

Table I. Factors Affecting Flocculation of Wood-pulp Fibres.

SUSPENSION CONCENTRATION	PHYSICAL AND CHEMICAL FACTORS		HYDRODYNAMIC FACTORS
	FIBRE CHARACTERISTICS	WATER CHARACTERISTICS	
<p>CONCENTRATION [C1, F1, G5, H8, W8]</p> <p>CRITICAL CONCENTRATION [B11, M5, M6]</p> <p>SEDIMENT CONCENTRATION [A5, T8, T9]</p> <p>LIMITING CONCENTRATION [M10, T9]</p>	<p>FIBRE LENGTH [F1, H8, M6, T8]</p> <p>FIBRE DIAMETER [T8]</p> <p>WALL THICKNESS, SWELLING [J3, J4]</p> <p>FIBRE SHAPE (HOOKS, KINKS, BENDS) [M5]</p> <p>FIBRILLATION, SURFACE ROUGHNESS [E6, F1, M5, J5, J6, T8, W8]</p> <p>FIBRE FLEXIBILITY [E6, F1, M6, J3, J4, T8]</p> <p>SURFACE CHEMISTRY [C1, J1, J2, J5, J6, M6]</p>	<p>pH OF WATER [A5, C1]</p> <p>ION TYPES AND CONCENTRATION [C1, R2]</p> <p>ADDITIVES [B6, C1, E6, H8, R2, W8]</p> <p>PRESENCE OF AIR [B6, G4, H9, K2, M4, T12]</p> <p>TEMPERATURE [E6, J1, W8]</p>	<p>CHANNEL GEOMETRY [A9, K5, K6, K7]</p> <p>FLOW VELOCITY [F1, H8, R5]</p> <p>TURBULENCE (SCALE, INTENSITY) [A9, G5, K7, R5]</p> <p>SHEAR RATE SHEAR DURATION [H8, K1, K7, M4, W8]</p> <p>WATER VISCOSITY [J1]</p> <p>FIBRE-WATER RELATIVE VELOCITY</p>

cohesion in general and Type-C cohesion in particular. The Summary of the Literature Review (Section 2.5) discusses experimental findings and focusses on the subject of the dissertation. The Literature Review concludes with the statement of objectives for this research work.

Section 3 presents an experimental program for study of a fibre system whose main characteristics are:

1. The nylon fibres suspended in an aqueous-sugar solution are neutrally buoyant.
2. The viscosity of the suspending medium is 3.7 times that of water.
3. The fibre length distributions are narrow. The range of lengths was selected to correspond to the naturally occurring lengths of wood-pulp fibres.
4. The fibre diameters were selected to match the flexibility of wood-pulp fibres.

The experimental program is divided into three topics: Type-C floc formation, floc structure, and floc strength. Section 4 reports and discusses the experimental results; Section 5 summarizes the new findings; Section 6 recommends further work.

The numerous appendices which are referred to throughout the text were introduced to record information which would obscure the clarity of the main text. This information is, nevertheless, of primary importance, and the subjects discussed in them are interrelated.

## **2 LITERATURE REVIEW**

Many concepts concerning fibre flocculation were published in the 1950's and 1960's. Some of these studies have been referred to extensively in the literature in the years since, but misinterpretations which subsequently have been repeated have often resulted. In some cases, concepts originating from one work have been extrapolated beyond their applicability so that an erroneous picture of flocculation emerged. In other cases, concepts not clearly stated at first were clarified later or not clarified at all. Frequently, reported observations have been wrongly interpreted or have remained unexplained. The absence of a global view on the process and nature of fibre flocculation in part accounts for this. For minimal misinterpretation, of the kind that has occurred, the literature review that follows directly quotes original publications and provides a unified picture of fibre behaviour in suspension.

### **2.1 Flocculation in Dilute Fibre Suspensions**

A suspension is defined here as dilute when fibres are free to move without interaction with other fibres. This does not mean that interaction cannot happen. It means only that the distances between fibres are several times larger than the fibre length and, if the interaction occurs, it is a chance interaction. This regime of fibre concentration is reviewed to illustrate the complexity of fibre motion under the simplest flow conditions, i.e., sedimentation or simple shear. The studies of suspensions of fibres which are of well-defined regular shape

(man-made fibres) are addressed separately from the studies of suspensions of wood-pulp fibres which are of irregular shape.

#### Man-made fibres.

Mason and his colleagues studied motion of individual cylindrical particles in the corn syrup subjected to uniform shear [M5,M7,T11]. Observations were made in a Couette system consisting of two concentric glass cylinders rotated in the opposite directions by the independent mechanical drives having continuously variable speeds. The particles were made of glass filament  $9.5 \mu\text{m}$  in diameter and were cut to lengths which gave a range of fibre aspect ratios,  $L/d$ 's, from 17.8 to 132 [T11]. The applied rates of shear were less than  $2 \text{ s}^{-1}$ . The periodic rocking motion of individual particles was observed. The particles rotated irregularly around the axis perpendicular to the plane of shear with the periods of rotation varying inversely with the rate of shear. The ends of a single particle described trajectories the projections of which on the plane of shear were ellipses. At the same time, the particle was spinning about its principal axis.

In another study [N2], the motion of longer particles was observed. Rayon fibres of  $9.5 \mu\text{m}$  diameter and aspect ratios of 43.2, 113, 173, 240 and 356 were suspended in castor oil of  $2.5 \text{ Pa}\cdot\text{s}$  viscosity. Uniform,  $10 \text{ s}^{-1}$  rate of shear was applied to the dispersion medium. Short particles ( $L/d=43.2$  & 113) rotated in spherical elliptical orbits described in the preceding paragraph. Longer fibres were seen to undergo increasing amounts

of bending during rotations. Fibres of  $L/d=176$  showed slight springiness; fibres of  $L/d=240$  showed increased springiness; fibres of  $L/d=356$  showed springiness and flexibility during rotations. Thus, fibre length adds new features to the already complex motion of short and stiff fibres.

The interaction between cylindrical particles was observed in another similar study [M8]. Dacron Polyester cylinders were suspended in a corn syrup (viscosity about  $5 \text{ Pa}\cdot\text{s}$  and density about  $1300 \text{ kg/m}^3$ ) which was uniformly sheared with rates lower than  $2.5 \text{ s}^{-1}$ . The Dacron cylinders had  $12.4 \mu\text{m}$  mean diameter. Very dilute suspensions were prepared having volume concentrations,  $C_v$ 's, of 0.0000026, 0.0000062, 0.0000031 for fibre aspect ratio of 20, 68 and 115 respectively.<sup>1</sup> *As a result of the velocity gradient in the liquid, two rotating cylinders can be carried by translation into proximity and thus interact. On approaching one another, the two participating cylinders become associated for a time, separate and rotate in orbits which differ from those which prevailed before interaction. Such sudden changes in orbits were always associated with the close approach of another particle. The interaction did not involve apparent collision of the two particles but merely a close approach and possibly an interpenetration of their orbits.* [M8]

Andersson [A2] studied interactions of pairs of sedimenting cylindrical particles. He observed in a travelling microscope the pairs of glass fibres of equal diameter but of different

---

<sup>1</sup> In this dissertation all concentrations are reported as fractions. Nomenclature gives definitions of symbols.

length sedimenting in a pure glycerol ( $\rho=1260 \text{ kg/m}^3$ ,  $\mu=1.76 \text{ Pa}\cdot\text{s}$ ). The motion of glass fibres during interaction was complicated. No collision between interacting particles was ever observed although efforts to attain a physical contact were made. Andersson tried to simulate collisions in other sedimentation systems. *Such model systems were nylon fibres suspended in organic liquids swelling nylon, rayon fibres suspended in CMC solution or viscose solution, but in no case was any flocculating tendency observed.* [A8]

### Wood-pulp fibres.

Motion of wood-pulp fibres in a uniform shear flow was also studied [A11,F1,F2,M7]. In [A11] the suspending medium was a corn syrup of  $5 \text{ Pa}\cdot\text{s}$  viscosity. Douglas fir pulps of various yields were fractionated (20/28-mesh fraction). Fifty fibres of a mean length close to  $2 \text{ mm}$  were selected from each yield fraction. The fibres were visually observed during rotations induced by  $3.5 \text{ s}^{-1}$  rate of shear. *Visual observations showed that in each pulp there existed a spectrum of flexibility of individual fibres; it was therefore not surprising that in any sample a multitude of rotation patterns was observed* [A11]. A simple classification of fibre orbits was made [A11]:

1. Rigid Fibres. Rigid fibres executed the same type of rotations as rigid cylinders.
2. Flexible Fibres.
  - a. Group 1. The fibre undergoes axial spin in the course of which it periodically straightens and bends into an arc.

- b. Group 2. The flexible spin described is superimposed on a spherical elliptical orbit.
- c. Group 3. This group is preferred by flexible fibres. The modes of rotation in this group may be further subdivided in order of increasing flexibility: Springy Rotation, Snake Turn and S-Turn.

It is noteworthy that, because the corn syrup used was about 5000 times more viscous than water is, the motions of fibres observed by Mason et al. [A11,F1,F2,M7] in the corn syrup may not be encountered in water. From the nature of these rotations, it is apparent that the volume swept out by one rotating fibre is considerably greater than fibre's actual volume. When two swept volumes intercept, fibre collision can occur.

## **2.2 Flocculation in Semiconcentrated Fibre Suspensions**

A suspension is defined here as semiconcentrated when the distances between fibre centres are smaller than the average fibre length. In such suspensions, the fibres move relative to one another with interactions and/or collisions. The review of the literature pertinent to this concentration regime will be made to illustrate how experimental findings from this regime influenced understanding of fibre flocculation in general.

### **2.2.1 Fibre interactions and collisions**

#### **Man-made fibres.**

Blakeney [B11] studied the effect of fibre concentration on the interaction of straight, rigid fibres. He used nylon fibres

16.9 and 43.1  $\mu\text{m}$  in diameter with aspect ratios of 19.2 and 20.3 respectively. Measurements were conducted in a concentric cylinder viscometer at shear rates between 0.1 and 0.5  $\text{s}^{-1}$ . The fibres were suspended in tetrachloroethane-paraffin oil solution adjusted to the density of fibres. Analysis of the *orientation factor*<sup>1</sup> revealed that it remained constant up to the concentration  $C_v=0.0042$ . Above this concentration, the formation of groups of two or three fibres increased rapidly. Between concentrations of  $C_v=0.0042$  and 0.0050, the interacting fibres changed their orbits to more horizontal, i.e., closer to the plane of shear. It was concluded that below  $C_v=0.0042$  the interaction between fibres was negligible. This concentration agreed closely with Mason's estimate of the *critical concentration* which was defined as:

*The concentration above which unrestrained motion of all the fibres is no longer possible is defined as the critical concentration [M6].*

Mason later estimated the critical concentration quantitatively as:

*An estimate of the order of magnitude of critical concentration can be made by assuming that the statistically averaged shape of the space enclosed by a rotating fibre is a sphere whose diameter equals the particle length. [M7]*

This definition leads to an expression for the critical volumetric concentration of cylindrical particles  $C_{v,cr}$ :

$$C_{v,cr} = \frac{3}{2} \cdot \left(\frac{d}{L}\right)^2 \quad (1)$$

---

<sup>1</sup> See Glossary.

Attanasio et al. [A18] studied viscosity of suspensions of rayon fibres in the capillary (3 and 120  $\text{s}^{-1}$  rate of shear) and Couette (100 to 500  $\text{s}^{-1}$  rate of shear) viscometers. The aqueous-sucrose solution with 67% sucrose content by weight was used as the suspending medium ( $\rho=1300 \text{ kg/m}^3$ ,  $\mu=0.18 \text{ Pa}\cdot\text{s}$ ). The volumetric concentration of fibres ranged from  $C_v=0.0015$  to 0.01. The fibre aspect ratios were 11.3, 16.2, 17.7, 18.2 and 69.5. The analysis of experimental results revealed an almost linear relationship between the *limiting viscosity number*<sup>1</sup> and the aspect ratio for all aspect ratios but for 69.5. This irregularity indicates the presence of intense fibre interaction between the longest fibres for which the critical concentration  $C_{v,cr}=0.0003$  is well below the range of experimental concentrations. Since the critical concentration for the second longest fibres is  $C_{v,cr}=0.0045$  and is only slightly less than the upper limit of experimental concentrations, the linear relationship between the *limiting viscosity number* and the aspect ratio appears to occur below the critical concentration defined by equation (1).

Numerous publications relate to the rheology of fibre suspensions to which Attanasio et al. [A18] work belongs. The latest review of the literature in this area was published by Ganani and Powell [G1]. Most rheological works, however, say nothing about the process and the nature of fibre interactions.

---

<sup>1</sup> See Glossary.

## Wood-pulp fibres.

In a shear flow and at very low concentrations, wood-pulp fibres can rotate independently of one another and can undergo *chance collisions*, i.e., collisions of low frequency [M6]. As the concentration is increased, the frequency of two-body encounters increases as the fibre orbits become more and more crowded until a point is reached at which a rotating fibre is under more or less continuous interaction of *forced collisions*. These were described in [M7]:

*At very low concentrations of wood-pulp fibres, e.g., less than 0.0005 by weight, which is the upper limit of concentration at which single fibres can be followed in the microscope field, the encounters are very frequent and cause the particles to move in erratic orbits.*

For example, an average fibre length for never-dried softwoods is 3.37 mm and an average width is 30.3  $\mu\text{m}$  giving  $L_w/w=111$ .<sup>1</sup> The collection of such fibres would have the critical volumetric concentration of  $C_{v,cr}=0.000154$ . This would correspond to the consistency of  $C_{m,cr}=0.000054$  if the water retained by fibres was 2 g per 1 g of dry fibre mass [E5]. An average, never-dried, hardwood fibre is 1.23 mm long and 17.6  $\mu\text{m}$  wide giving  $L_w/d=70$ . The suspension of such fibres would have  $C_{v,cr}=0.000391$ . This would correspond to the consistency of  $C_{m,cr}=0.000136$  if the water retained by fibres was 1.7 g per 1 g of dry fibre mass [E5]. These simple calculations reveal how small the critical concentrations for wood-pulp fibres are. Thus, in any suspension of practical consistency, the

---

<sup>1</sup> See Table I-XVII in Appendix I.

interactions and/or collisions between fibres are forced.

Arlov et al. [A11] measured the steady-state distribution of orbits in a suspension of 28/48-mesh fraction ( $L=1.6$  mm [T7]) of an unbeaten, unbleached softwood sulphite pulp at consistency less than  $C_m=0.0005$  after shearing for 15 hours at  $2 \text{ s}^{-1}$  rate of shear. The orbits of wood-pulp fibres, as those of smooth rigid cylinders [M8], had preferred instantaneous orientations in the plane of shear under forced fibre interactions. The orbits changed frequently as a result of "collisions."<sup>1</sup> The distribution of orbits was said to have reached a *dynamic equilibrium*.

Andersson [A8] conducted sedimentation experiments of wood-pulp fibres in aqueous-glycerol mixtures having viscosities from 0.02 to 0.2 Pa·s (region of "creeping motion"). Initial fibre consistencies ranged from  $C_m=0.0001$  to 0.0006. Fibre approaches within particle pairs occurred due to differential speed of sedimentation. Hydrodynamic repulsion counteracted such approaches; however, due to the fibres' irregular shape, they approached each other close enough to establish physical contact. *In an experiment where the approaching fibre was shaped as a bow, concave downwards, the hydrodynamic forces acted in vain, and the approaching fibre landed right on the other fibre, which was slightly curved in the opposite direction* [A2]. In dilute fibre suspensions, the man-made fibres which were rigid and straight did not collide. On the other hand, wood-pulp fibres, which were neither stiff nor straight, were found to collide.

---

<sup>1</sup> Quotations marks around the word collisions were used in [A11] without explanation.

In 1938, Wollwage, in a thesis titled "The Flocculation of Papermaking Fibres" [W7] described experiments [W7,W8] with wood-pulp fibre suspensions having consistencies,  $C_m$ , from 0.00005 to 0.0002, and flowing with bulk speeds from 0.005 to 0.0274 mm/s (Re from 3.8 to 20.8)<sup>1</sup> in a vertical glass pipe. Estimated shear rates based on the maximum speeds were from 0.26 to 1.4 s<sup>-1</sup>. The pipe was 8-foot long and 3-inch in diameter. A controlled *laminar flow of a well-dispersed suspension, free from eddy currents*, was visually observed and photographed. The distance from the top of the pipe to the point at which flocculation occurred was a dependent variable.

*Evaluations of the flocculation end-points were made where definite fibre bunches could be seen, as well as small portions of the dispersing medium which are devoid of fibres. Above this point there existed a relatively complete degree of dispersion of the fibres, but below it, the condition was one of definite flocculation. [W8]*

This equipment and technique permitted a dynamic study of the flocculation of wood-pulp fibres. Erspamer [E6] and Beasley [B6] used the same experimental setup though Beasley ran it under slightly different conditions. Beasley's experimental conditions were:  $C_m$  from 0.00002 to 0.0005, 0.0168 m/s bulk speed (Re=12.8) and 0.88 s<sup>-1</sup> estimated shear rate. A summary of common, non-contradictory results from these three investigations shows:

1. Factors Enhancing Flocculation: Alum flock (in small amount), hydrophilic bentonite clay, starch, air, increasing consistency, beating action and increasing fibre length.
2. Factors Suppressing Flocculation: Alum flock (in large

---

<sup>1</sup> Reynolds numbers are based on the bulk speed, pipe inner diameter and viscosity of water at 25°C.

amount), deacetylated Karaya gum, Locust bean gum, methylcellulose, mannogalactan, decreasing consistency, low water temperature.

3. Factors Having No Effect: calcium carbonate, surface-active agents (surface tension), sodium hexametaphosphate, water pH.

Wollwage concluded that *non-mechanical factors play important roles in the phenomenon of fibre flocculation.* Wollwage's and Erspamer's publications (1939,1940) [W8,E6] popularized the subject of colloidal cohesion. In 1953, Beasely received the Shibley Award from TAPPI for his paper. This event indicates the popularity of colloidal cohesion among papermakers in the 1940's and 1950's. Though cohesion between fibres was considered to be dominantly colloidal in nature, it was recognized that *the mechanism by which the flocculating fibres are brought together differs fundamentally from that of colloid sol in that an entirely different type of particle motion is involved.* [M4]

Wollwage was fully aware of this fact in 1939.

*As the dispersion moves down the column, fibres are acted upon by viscous forces due to relative motions in the fluid, individual fibres being rotated, moved about, and brought into contact, and groups of two or more fibres which may be adhering together tending to be sheared apart. At some point down the flow tube, the number of fibres colliding with each other and tending to adhere will exceed the number being sheared apart and separated by the fluid motion and, at this point, fibre bunching or flocculation should be observed. Since the shearing forces will vary with changes in fluid velocity in the tube, the flocculation point will depend on the flow rate.* [W8]

Wood-pulp fibres which have dimensions between  $10^{-5}$  to  $10^{-3}$  m are thus outside the actual colloidal region of particle sizes which range from  $10^{-9}$  to  $10^{-6}$  m [N1]. They, contrary to colloid particles, cannot be brought into contact by Brownian motion because, in the case of suspension of large particles such as cellulose fibres, this motion is non-detectable and therefore insignificant. The distances between fibres are also large, about one fibre length,  $10^{-3}$  m, while the interaction range of electro-chemical forces is about  $10^{-8}$  m. The importance of fibre motion in suspension as an element of flocculation was recognized by Mason in 1948 [M4]. Under Mason's leadership, a series of rigorous studies of fibre motion was initiated. Some of those studies have already been reviewed in this chapter.

### 2.2.2 Fibre cohesion

When collision has taken place, fibres may cohere to form flocs which may subsequently disperse in a shear flow [K1,W8]. Mason et al. [M4] described this process:

*Shear motion provides a mechanism whereby fibres can be brought into contact and, if an attractive force exists, can adhere to form the nucleus of a floc which can grow by further collisions. The floc itself will also tend to rotate and in the process will be subjected to shear and tensile stresses which tend to stretch it and disrupt it, the disruptive stresses increasing with increased rate of shear. Thus the motion which allows flocs to form will also tend to destroy them.*

If sufficient time is allowed, a *dynamic equilibrium* is established between floc formation and floc destruction.

*At low concentrations where individual flocs could be observed they were continuously formed and broken up and ... the size of the flocs at equilibrium appeared to increase with decreasing shear rates. [M4] The*

*equilibrium moreover could be reproduced repeatedly by restoring a given rate of shear even though the equilibrium was disturbed in the interval. [H8]*

The existence of dynamic equilibrium was shown experimentally [H8] when pulp suspension (100/200-mesh, bleached sulphite,  $L=0.45$  mm [T7]) was subjected to varying rates of shear, from 19 to  $70 \text{ s}^{-1}$  in a Couette type apparatus. Fibre mass concentration was  $C_m=0.0004$ . During dynamic equilibrium two counteracting elements clearly are in balance: the rate of floc dispersion and the rate of floc formation. The cohesion forces developed at fibre contact points found at the floc peripheries equal the dispersion forces resulting from the drag imposed on fibres.

Andersson [A5] observed that, under differential sedimentation conditions, the fibres have frequently remained in contact after collision. He speculated on the possible nature of cohesion:

*This suggests the existence of adhesion between fibre surfaces. Such adhesion may be due to protruding fibre elements being like barbs, or it may also be due to adhesive forces of an electrical or chemical nature. [A5]*

Mason [M6] envisaged fibre cohesion:

*When the fibres come into contact with one another there are two possible ways by which they can stick together. Perhaps the most obvious is by inter-particle attraction in the same way, for example, as the particles of coagulated sol are held together. For convenience we shall call this chemical flocculation. The other is by intermeshing or mechanical entanglement, and to distinguish it from the first, will be called mechanical flocculation. From the nature of the processes involved one would anticipate chemical flocculation to be determined in part by the surface condition and mechanical flocculation by the geometric shape of fibre.*

Here, Mason should have used the word "cohesion" instead of "flocculation" since he had already distinguished "collision" from "cohesion" as two steps of wood-pulp fibre flocculation [M4]. This distinction could have eliminated much of the ambiguity from his discussions of flocculation.

If fibres have strong electrostatic surface charge, there is normally a repulsion force between the fibres. However, if they are forcibly brought into intimate contact, e.g., through collision in the shear flow, the repulsion barrier can be overcome and a force of attraction is generated between them. The fibres are held together by van der Waals forces. Erspamer's and Wollwage's [E6,W8] experiments left no doubt that electro-chemical cohesion occurred when fibres had been brought into contact by hydrodynamic forces and varied, within limits, with addition of certain materials. Their experiments, however, were conducted at shear rates not larger than  $1.4 \text{ s}^{-1}$ . Hubley et al. [H8] studied the effects of the addition of varying amounts of thorium chloride, aluminum sulphate, deacetylated Karaya gum and methyl cellulose to the suspensions of pulp-fines ( $L < 0.2 \text{ mm}$ ) of consistency  $C_m = 0.0007$ . The applied rate of shear was  $16 \text{ s}^{-1}$ . The observed changes in the *flocculation index*<sup>1</sup> were small, from 0.55 to 0.76. An exception was the excessive addition of deacetylated Karaya gum. The flocculation index in this case changed from 0.411 to 2.06.

The effect of shear rate on the flocculation of 100/200-mesh ( $L = 0.45 \text{ mm}$  [T7]) bleached sulphite pulp at  $C_m = 0.0004$  was also

---

<sup>1</sup> See Glossary.

studied [H8]. The change of shear rate from 70 to  $19 \text{ s}^{-1}$  increased the flocculation index from 0.470 to 2.66. The increase in the flocculation index was also produced by the increased presence of longer fibres in the suspension. Suspension concentration was maintained constant, at  $C_m=0.0008$ , but the proportion of 48/100-mesh fibres ( $L=0.7 \text{ mm}$ ) and pass-200-mesh fines ( $L<0.2 \text{ mm}$ ) was varied. At 100% fines, the flocculation index was 0.540 and, at 20% fines, it rose to 2.54. The effects of shear rate and fibre length may be regarded as purely mechanical in nature [M4]. Hence, the effects of electro-chemical interaction between fibres of finer pulp fraction were, in most cases, small compared with the variations resulting from varied shear and fibre length [H8].

The whole-pulp fibres were observed to form large stable flocs, presumably because of increased mechanical cohesion [H8]. Shear rates greater than  $50 \text{ s}^{-1}$  were necessary to break up these flocs appreciably. This strong cohesion rendered the whole-pulp fibres unsuitable for studying the electro-chemical effects. How this strong cohesion developed was not described. The picture presented by Mason [M5,M6] is in part speculative.

*In pulp suspensions we deal with particles which possess a measure of flexibility, and are bent and twisted. Fibrillation provides surfaces with innumerable hooks which can join fibres together. All of these factors will tend to favor interlocking of the particles. The tendency to clot mechanically will increase markedly as the aspect ratio is increased. It will be aided further by fibrillation, which will facilitate interlocking, and by increasing flexibility, which will allow the fibres to bend and interweave. [M5]*

No direct investigation has ever been conducted to evaluate the importance of fibre fibrillation, flexibility or aspect ratio on flocculation.

### 2.3 Flocculation in Concentrated Fibre Suspensions

In semiconcentrated suspension as the concentration is increased, the fibres form larger flocs and the space occupied by the relatively free fibres diminishes. At some point, large flocs merge to form a *continuous network* [M5] or *connected structure* [H8]. A suspension is defined here as concentrated when all fibres are in continuous contact with other fibres and form one network between confining boundaries. This network is sometimes called a "plug." The lowest concentrations at which plug flows of wood-pulp fibres occur are slightly below sediment concentrations [A9]. The connected networks of measurable strength were produced at concentrations as low as  $C_m=0.002$  [G5,V1].

Andersson [A5] measured consistencies of sedimented fibre mats formed from  $C_m=0.0005$  consistency suspensions of rewetted and defibrated Swedish softwood pulp laps. The reported sediment consistencies were:

	$C_m$
1. Spruce, unbleached sulphite.....	0.0032
2. Spruce, bleached sulphite.....	0.0030
3. Pine, unbleached kraft.....	0.0032
4. Pine, bleached kraft.....	0.0028

Thalen and Wahren [T8] reported sediment consistencies for much wider spectrum of pulp fibres. They used the same initial consistency as in [A5]. The sediment consistencies for hardwood fibres are only cited here to demonstrate that shorter fibres sediment into denser mats.

$$C_m$$

1. Birch, NSSC, 80% yield.....0.0046
2. Aspen, sulphite, beaten.....0.0058
3. Birch, bleached kraft, beaten.....0.0033

### 2.3.1 Process of network formation

#### Man-made fibres.

Meyer and Wahren [M10] noted that elongated particles such as glass, Teflon and Perlon fibres may form a unique type of mechanically entangled, 3-dimensional (3-D), coherent network. The coherence of such a network was not ascribed to chemical bonding but was primarily due to normal forces associated with the bending stresses in fibres and to frictional forces produced by these normal forces acting at contact points between fibres [S12]. Meyer and Wahren [M10] carefully worded the concept of such network formation and cohesion:

*When a fibre suspension is agitated, the fibres are exposed to viscous and dynamic forces, which bend and twist fibres. When agitation ceases, the fibres tend to regain their original unstrained shape. However, if there are many fibres per unit volume, the fibres cannot straighten out freely but will come to rest in contact with other fibres. A fraction of the fibres will come in contact with so many other fibres that they will come to rest in strained positions, and forces will be transmitted from fibre to fibre. These fibres become interlocked by normal and frictional forces and*

*constitute a fibre network, where forces can be transmitted through the fibres and from fibre to fibre.*

This concept remained unaltered in later publications by Wahren et al. [S12,W1,W3,W4] and has been assumed to apply to wood-pulp fibres [C1,E2,P3,W1,W3,W4,W10]. The existence of such a network has not been verified experimentally. Steenberg et al. [S12] have presented some evidence of it by describing the circumstances of suspension preparation:

*If bundles of straight Perlon fibres or any other man-made fibres of a suitable length-to-radius ratio are put into water, they settle to the bottom of the container and do not form a network, even after gentle stirring with a spoon. If, however, the suspension is vigorously agitated - for instance, with a propeller - the fibres are dispersed randomly and form a network that fills the whole available volume and possesses elastic properties. [S12]*

Steenberg et al. [S12] witnessed the change in suspension appearance and described conditions under which this change occurred, but they never directly verified the process of network formation.

Steenberg et al. [S12] showed that, using different viscosities of the suspending medium, networks varying in rigidity were formed. Equal amounts of fibres (Perlon) were dispersed in aqueous-sugar solutions of different viscosities and the shear modulus was measured. The volumetric concentration of fibres was  $C_v=0.015$ . It was observed that the shear modulus decreased as the viscosity of the suspending medium increased. This is illustrated in Figure 2. The authors concluded that no fibre networks formed at very high viscosities of the suspending medium. They satisfied themselves with the following

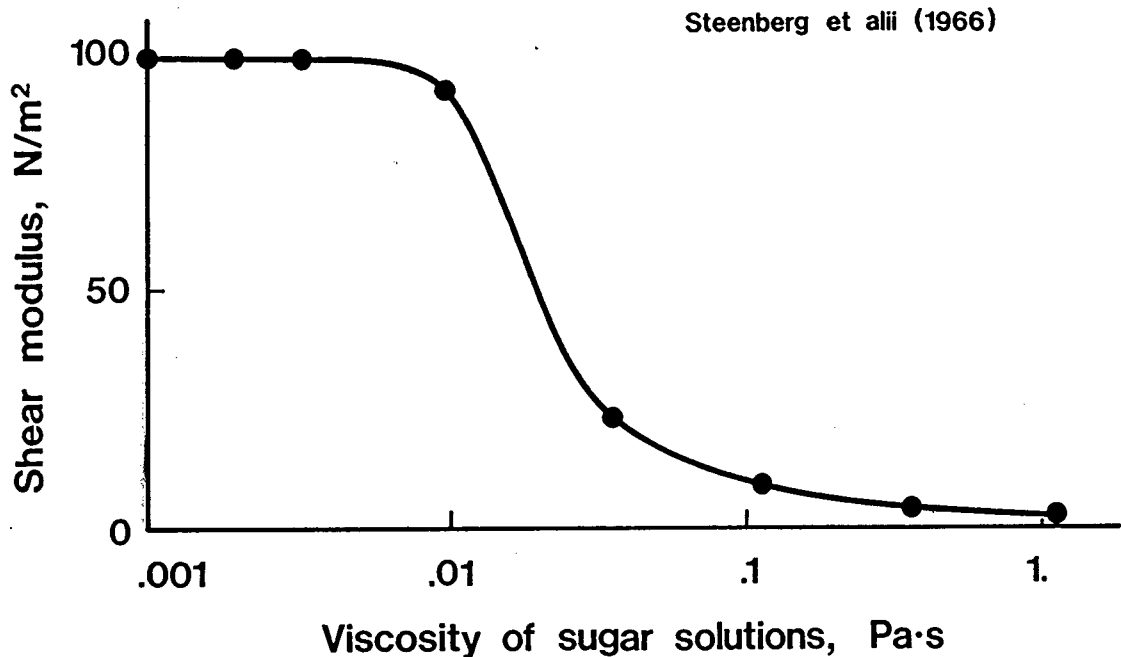


Figure 2. Shear Modulus versus Suspending Liquid Viscosity. Figure redrawn from [S12].

explanation:

*It takes longer for fibres to come to rest after agitation in a more viscous medium; hence, the elastic energy of many of them may be dissipated and unstrained configurations will result. Once the fibres have lost their elastic energy, they cannot become actively engaged in the network however much time elapses. [S12]*

This explanation is incomplete because fibre-to-fibre interactions were not mentioned. At the concentration used,  $C_v=0.015$ , there is ubiquitous contact between fibres during and after agitation. Logically, less time should be required for fibres and the entire suspension to come to rest after agitation in a more viscous medium since the only dissipating forces are the viscous forces. Further comments on this work cannot be made because no information on fibre geometry was given. Attanasio

et al. [A17] provided alternate explanation to the effect of viscosity on network rigidity:

*This effect, observed with suspensions of Perlon fibres in glucose solutions (the drop is found at  $\mu$  values between 0.01 and 0.05 Pa·s) shows that the medium has a lubricating effect on the contact points. [A17]*

Thalen and Wahren [T9] presented some testimony to the ever-present nonuniformity of fibre networks and to the frictional character of fibre-to-fibre contact:

*Considerable difficulties were encountered when trying to get uniform networks of the Perlon and glass fibres, especially at high concentrations and with long (6 mm) fibres. The networks formed at high concentrations were uneven also after intense stirring. Although the Teflon fibres were of the order of 6 mm long, they were much easier to disperse and the network that formed had an even appearance. The networks of fibres having low coefficient of friction (Teflon) are easier to disperse evenly, thus giving higher values for the shear modulus. [T9]*

Not only does fibre material affect the fibre-to-fibre interactions but also the type of suspending liquid. Elias [E4] has found that compression behaviour of the glass fibre mats was significantly affected by the immersion liquid. It is possible that the immersion liquids could alter fibre surface properties and thereby affect the frictional interaction at fibre contact points.

#### **Wood-pulp fibres.**

As the concentration is increased well above the critical concentration, the *interweaving* of fibres becomes more pronounced and, eventually, more or less *continuous network* of *entangled* fibres will be formed, possessing a structural rigidity [M5].

Forgacs, Robertson and Mason [F1] were first to demonstrate that fibres in pulp suspensions form *coherent fibre networks* which exhibit tensile strength at concentrations as low as  $C_m=0.003$ . They coined the term "coherent fibre networks" and suggested that networks are held together by *inter-fibre friction*. A term "interlocked networks" was introduced by Chang & Robertson [C1] in their studies of tensile strength of pendent plugs. The network preparation was done by fast recirculation of pulp suspension around a closed flow loop and sudden stoppage of flow. The formation of plugs was promoted by increased fibre length, fibre flexibility, number of hooks and bends, fibrillation, surface roughness and concentration of fibres [F1].

When concentrated suspension is pumped through the tubes or pipes, it exhibits three flow regimes: *plug*, *mixed*, and *distributed* [R4] or *turbulent* [C4,F1]. There are two transition velocities between these regions. Robertson et al. [R4] described the regimes as follows:

*Below the first transition velocity, the stock could be observed to flow as a solid plug with the entire velocity gradient concentrated in a narrow boundary at the wall. The plug may be regarded as a continuous network of interlocked fibres whose independent movement (rotational or translational) is inhibited by the close packing; this network is rigid in the sense that it resists disruption by the shear stress at the wall. Above the second transition velocity, the network was disrupted into a series of fibres and fibre flocs with velocity gradients extending across the tube. [R4]*

In studies in which plugs were formed for tensile strength tests [A9,C1,F1,G5,R2], the objective was to disperse fibres as uniformly as possible in the turbulent type of flow and freeze this uniform dispersion by suddenly stopping the flow.

*In the case of abruptly stopping the circulation process, the turbulent state of flow becomes, to a certain extent, "frozen" into the just formed network of the plug but only when the transition from turbulent flow to the state of rest or, at least, to laminar flow takes place suddenly. [G5]*

Giese and Giese [G5] experimented with two pumps of different dispersing potentials and showed that the degree of homogenization is critical to the plug tensile strength. The peristaltic pump, working on the displacement principle, had no mixing and no deflocculating effects. The agitation of the suspension in the recirculating tube was gentle because of low flow rates. The centrifugal pump gave good mixing and faster flow which produced more agitation in the recirculating tube. The plugs produced with the centrifugal pump exhibited much higher tensile strength than those produced with the peristaltic pump. Thus, the appearance and strength of plugs depends on the conditions of plug formation, more uniform plug giving higher strength [G5] or exhibiting better elastic properties [T8].

It was not clear how cohesion occurred but there was unanimous consensus that fibre-to-fibre cohesion is predominantly of a mechanical nature [C1,F1,G5,R2]. Two important properties of a coherent plug were identified: fibre-to-fibre cohesion and the plug structure which includes plug nonuniformity.

A series of experiments of great importance in the study of wood-pulp fibre flocculation was carried out by Jacquelin [J3,J4,J5,J6]. He exposed pulp suspensions to unique flow conditions in partly filled, rotating cylindrical vessels. The vessels were rotated about their longitudinal axis while

remaining horizontal or inclined at 45 degree to the horizontal. Jacquelin agitated about 4 liters of suspension in a 20 cm diameter cylinder at the cylinder linear speed of about 40 m/min (about 42 rad/s) for a few hours and obtained very dense, almost spherical flocs which he named "coherent flocs" [J3]. He used the ratio between the weight of dry fibres constituting the flocs and the total weight of dry fibres from a given batch as a dependent variable. He called this ratio "taux des flocs cohérent"<sup>1</sup> and denoted it for convenience as T.F.C. The maximum reported T.F.C. was 94%.

Observing the evolution of the number of coherent flocs Jacquelin saw the number stabilized more quickly than T.F.C., in one case less than 5 hours instead of more than 15 hours for T.F.C. This, he concluded, shows that, after an initial period of aggregation of coherent flocs, the growth of flocs happens mainly by capture of the suspended fibres having physical characteristics suitable to enter into these flocs. The remaining fibres in the suspension were progressively reduced in number and the process of capture slowed [J3].

Within the consistency range from  $C_m=0.0075$  to 0.049, Jacquelin found the concentration sub-ranges related to fibre nature and conditions of agitation which favoured the formation of coherent flocs. The maxima in T.F.C. were attained at consistencies about three times larger than the sediment consistencies [J3].<sup>2</sup> They were:

---

<sup>1</sup> Mass content of coherent flocs.

<sup>2</sup> Sediment consistencies were cited at the beginning of Section 2.3.

from 0.01 to 0.012 for unbleached softwood monosulphite, from 0.013 to 0.015 for unbleached softwood kraft, from 0.015 to 0.017 for unbleached softwood bisulphite, and from 0.026 to 0.028 for bleached birch kraft.

The observed difference between maxima for softwoods and hardwood can be attributed to the difference in fibre lengths. This important point has not been explored by Jacquelin. His empirical investigations inclined toward studying fibre flexibility as a variable. He was influenced by the contemporary concept of fibre network formation which was postulated in 1964 by Meyer and Wahren [M10] and described earlier in this section as one in which fibre elasticity played a key role in the formation process as well as in the mode of cohesion.

Jacquelin found predominant quantities of thick-wall fibres in coherent flocs and the thin-wall fibres in the suspension. Similarly, high-yield softwood fibres were more apt to form coherent flocs than did low yield fibres. He concluded that the flexible fibres are unable to accumulate enough energy in their elastic deformation and do not aggregate. He also noted that very stiff fibres, like certain fibres of semichemical pulps or mechanical pulps, are unable to form coherent networks. He concluded that these fibres are unable to deform sufficiently under existing conditions of agitation so that the optimum fibre flexibility should exist at a given condition of agitation and that outside this optimum the cohesion of networks cannot arise from the elastic deformation of fibres [J3,J4].

Modification of fibre flexibility through refining brought unexpected results. It was observed that slight refining greatly reduced the ability of fibres to form coherent flocs. Determination of the *flexibility index* by Mason's method [R7] revealed that, in the case of kraft pulp, the changes in fibre flexibility were small between 13° and 18°SR [J6]. In addition, it seemed that the surfaces of fibres which were drastically modified showed fibrils and microfibrils. These gently refined fibres formed relatively weak aggregates and their existence impaired the development of coherent flocs. Jacquelin realized that the nature of cohesion had changed and classified flocs into two groups: (1) the *fragile* flocs which impart to the suspension a cloudy appearance; (2) the *coherent* flocs which form slowly under rather peculiar conditions and have a somewhat button-like appearance. He described them [J5]:

*Whereas the first and more common type of floc forms rapidly and has neither a defined structure nor cohesion, the second, of slow and progressive formation has good structure and cohesion.*

*The important point is that all factors liable to favor the formation of the first type of flock impair the development of the second type, and vice versa. Particularly in the field which is of special interest here the "cloudy" non-cohesive flocculation, will interfere with the formation of cohesive flocs and consequently reduce the T.F.C. In fact, when the attraction between fibres is very strong, a rapid formation of structureless units will ensue to the detriment of the slow bonding of cohesive networks. These latter require a certain liberty of individual fibre movement.*

Lee [L2] produced flocs using Jacquelin's technique for his studies of individual floc dispersion. He described the mechanism of floc formation by the rolling method as a two-step

process: network truncation into flocs and floc compaction [L2]:

*The secondary flow caused by the rolling motion separates the mat of fibres into large patches or lumps on the order of several centimeters. As time progresses, further fragmentation and flocculation take place. The patches larger than the final equilibrium size will undergo further breaking or shedding, while the ones smaller than the equilibrium size will undergo flocculation. At this stage, the aggregates are not highly entangled and the boundaries of the aggregates are not sharply defined. The shape of the aggregates is also irregular. These loose aggregates at their equilibrium size then undergo compaction as a result of their interactions. The compaction is a process in which the aggregates grind against one another. The surface fibres bend and adhere to the surface or detach from the aggregate. Thus the surface of the aggregate is smoothed and loose surface fibres are removed. At the same time, the grinding action compresses the aggregate causing rearrangement of the internal fibres and a spheroidal floc with a very strong network takes form. By increasing the rolling time, flocs of more uniform shape and higher compaction can be obtained. Surface smoothness also increases as time progresses.*

Lee did not notice any fundamental difference in the form of cohesion or the structure of flocs he studied.

The author of this dissertation attempted to observe the formation of wood-pulp fibre networks in decaying turbulence at sediment concentration. Turbulence was created in a suspension by a grid being moved through 13 mm deep plexiglas channel [K7]. The grid speed of 0.28 m/s produced a jet speed of 1.3 m/s from the grid openings. With high-speed cinematography, the motion of dyed fibres in decaying turbulent shear was recorded. An area of 15 mm by 10 mm was filmed to observe individual fibre motion. Suspensions of bleached softwood kraft fibres having a consistency of  $C_m=0.003$  and containing about 10% of dyed fibres were used. Individual fibres experienced substantial bending which stopped in 0.13 s after passage of the grid. If fibres

interlocked by regaining their unbent configurations, the process of network formation must have been fast. Complete cessation of motion in the suspension occurred after 0.84 s. Interactions between colored and non-colored fibres could not be observed because of large amount of light scatter through the suspension.

### 2.3.2 Structure of coherent networks

In 1962, Corte and Kallmes [C5] reported on a theoretical analysis of random 3-D structures of fibres. They cited a private communication with R.E. Miles on his Ph.D. thesis in which he showed that the volumetric concentration is related to the number of contacts per fibre, fibre length and fibre diameter:

$$C_v = \frac{n_c \cdot d}{4 \cdot L} \quad (2)$$

This model was developed for fibres having uniform lengths and diameters.

The second published analysis of 3-D fibre networks was that of Meyer and Wahren [M10]. They refined the statistical model of Onogi and Sasaguri [O2] to account for fibre length. Their model assumed that the fibre length and the fibre radius have variable distributions expected to cover the *normally occurring radius and fibre length distributions* [M10]. The concepts of the number fibre fraction at a given length with a given number of contact points and the partial segment length were applied. The segment is a part of an active fibre between two consecutive contact points. The segment length is the distance along the fibre

centerline between the segment ends. The partial segment length distribution (or contact point distribution) was assumed to be a Poisson distribution starting at  $n_c=3$  and normalized from  $n_c=3$  to infinity. The partial segment length distribution has been chosen to fit the assumption that every unit length of fibre has the same probability of receiving a contact point. With the final assumption that every fibre in the population has the identical length and diameter and is in contact with at least  $n_c$  other fibres, the expression for the volumetric concentration reaches a minimum. From their mathematical approach the relationship has emerged between the fibre volume concentration, the number of contact points per fibre, and fibre length-to-diameter ratio. This relationship is:

$$C_{v,\min} = \frac{16 \cdot \pi \cdot L/d}{\left(\frac{2 \cdot L}{n_c \cdot d} + \frac{n_c}{n_c - 1}\right)^3 \cdot (n_c - 1)} \quad (3)$$

Equation (3) indicates the existence of a *limiting concentration* [M10] for fibres of uniform length and diameter all actively engaged in the network. The fibre length-to-diameter ratio exerts a strong influence on the limiting concentration.

The models of Miles and Meyer & Wahren are suitable for experimental evaluation of uniformly long and thick fibres. One difficulty, however, remains. An implicit assumption was made in the development of these models that the network is isotropic and unbound. In reality, large networks are always nonuniform [T9]. It is possible that this factor inhibited direct experimental

verification of equations (2) and (3).

Thalen and Wahren [T9] detected the lowest concentrations at which a shear modulus of suspensions could be measured. These minimum concentrations were only slightly higher than the corresponding sediment concentrations. The postulation that coherent networks are not formed at concentrations lower than the sediment concentrations seemed, therefore, natural.

Elias [E4] elaborated on the number of contact points between fibres in the sedimented networks:.

*During the formation of a sediment, as fibre is deposited upon a partly formed bed it will be supported at two points, as it would be a rare coincidence for three or more of points of suspension to occur in the same straight line. As each point of support on the bottom of a fibre is paired with one on the top of another fibre, each fibre will also, as a rule, contact two fibres along its top surface. Each fibre will then touch an average of four other fibres in a sediment.*

Since all fibres in sedimented networks have four contact points, the sediment concentration should exceed  $C_{v,\min}$  at  $n_c=3$ . This is, in fact, what Thalen and Wahren observed by comparing sediment concentrations with the limiting concentration calculated at  $n_c=3$  [T9].

In a more recent publication, Wahren [W4] stated that attempts at an experimental verification of the formula for the limiting concentration have indicated that  $n_c=4$  is closer to reality. Indeed, better agreement is observed between the sediment concentrations and the limiting concentrations calculated at  $n_c=4$  [T9]. This agreement is surprising because the sedimented network is not an isotropic, 3-D network [E4].

Whether suspended fibres form a coherent network or are in some other state (sediment), the number of fibres in the suspension is finite. If all fibres are uniformly distributed, the number of fibres in any volume smaller than the total suspension volume is constant so that the number of fibres  $N_f$  in the volume  $V$  can be related to the volumetric concentration  $C_v$  when the average fibre length  $L$  and diameter  $d$  are known:

$$C_v = \frac{N_f \cdot \pi \cdot d^2 \cdot L}{4 \cdot V} \quad (4)$$

or

$$N_f = \frac{4 \cdot C_v \cdot V}{\pi \cdot d^2 \cdot L} \quad (5)$$

The number of fibres,  $N_f$ , was used as an indicator of *fibre crowding* [K7] in one instance and as a *number density* [B9] in another. Kerekes et al. [K7] chose a sphere having diameter  $L$  for volume  $V$ :

$$N_{fS} = \frac{2}{3} \cdot C_v \cdot \left(\frac{L}{d}\right)^2 \quad (6)$$

Bibbo et al. [B9], on the other hand, selected a cube with side  $L$  for  $V$ :

$$N_{fC} = \frac{4}{\pi} \cdot C_v \cdot \left(\frac{L}{d}\right)^2 \quad (7)$$

In both cases  $N_f$  was a useful parameter in the description of the state of fibre crowding. For fibres of identical proportions, for example, the softwood fibres from Section 2.2 at  $C_v=0.01$  and  $L_w/w=111$ , the number of fibres in the sphere is

$N_{fs} \approx 82$ , and in the cube  $N_{fc} \approx 157$ . The potential for interaction between fibres in such suspension is great. Numbers of fibre contacts per fibre calculated from equation (2) and (3) are  $n_c \approx 4.4$  and  $n_c \approx 4$  respectively.

Bibbo et al. [B9], studying the shear properties of semiconcentrated suspensions, defined this regime using  $N_{fc}$  as a parameter. For semiconcentrated suspensions,  $1/\pi < N_{fc} < L/(\pi \cdot d)$  was suggested; for dilute suspension,  $N_{fc} < 1/\pi$ . Doi and Kuzuu [D3] stated that a fibre suspension behaves as a viscoelastic liquid if  $N_{fc} \lesssim L/(\pi \cdot d)$ , and as an elastic material if  $N_{fc} \gtrsim L/(\pi \cdot d)$ . These concepts, though unrefined, are worthy of mention since they constitute the beginning of the systematic classification of fibre suspensions with respect to fibre behaviour.

#### **Man-made fibres.**

No experimental work has been published on the structure of truly random, three-dimensional (3-D) fibre networks. Elias [E4] investigated the behaviour of individual glass fibres during the mechanical compression of thick, filtration-formed mats. Though the mats were undeniably 3-D, the arrangement of fibres in them was not random. More than 90% of fibres were inclined to the horizontal at angles of less than 10 degrees whereas in an isotropic network an average angle between fibres and horizontal is 32.7 degree [W3].

From photographs showing the shapes of the fibres in the loaded beds, Elias [E4] determined the *minimum* number of fibres touched by a given silvered fibre. The term "minimum" was used

because one fibre could touch another without producing a detectable bending of either fibre. The experimental data are given in the first three columns of Table II. Volume concentrations shown in second column were calculated from Elias's *solids fraction* assuming a glass density of  $2600 \text{ kg/m}^3$ . The number of fibre contacts per fibre,  $n_c$ , was calculated from equations (2) and (3) using Elias's data; the results are given in columns 4 and 5 of Table II. Clearly, the calculated numbers of contacts are greater than observed.

Wahren considered [W3] the deflections of fibres in the coherent network from their original nearly straight shape as small. Elias's observations of fibre deflections in the compressed mats of glass fibres support Wahren's opinion. In mats, the deflections were about one fibre diameter [E4].

### 2.3.3 Network strength

Devising methods of efficient floc dispersion requires a knowledge of network strength. For a uniform suspension, flocs must be dispersed into individual fibres, i.e., a suspension must be homogenized. Homogenized suspension is required for fibres to be evenly accessible to chemicals or to produce a uniform sheet of paper.

#### Man-made fibres.

In 1958, Forgacs et al. [F1] reported that, at  $C_m=0.008$  concentration, the chopped rayon fibres ( $d=10 \mu\text{m}$ ,  $L=1.5 \text{ mm}$ ) had no tensile strength. The limiting concentration calculated at

Table II. Number of Fibre Contacts per Fibre in Compacted Mats [E4] and Calculated from Equation (2) and (3).

ASPECT RATIO L/d	VOLUME CONCENTRATION OF FIBRES $c_v$	OBSERVED NUMBER OF CONTACTS [E4]	CALCULATED NUMBER OF CONTACTS eq. (2)	CALCULATED NUMBER OF CONTACTS eq. (3)
313	0.0119	7.3	14.9	13.6
313	0.0187	11.4	23.5	17.3
313	0.0209	12.6	26.2	18.4
151	0.0231	6.5	13.9	9.1
151	0.0284	6.5	17.2	10.2
630	0.0221	21.6	55.7	38.6
179	0.0254	7.2	18.2	11.5

$n_c=3$  for these rayon fibres is  $C_{v,min}=0.003$ . Forgacs et al. were unsuccessful in forming a coherent network at a concentration of almost three times the limiting concentration in a device which produced enough agitation to entangle wood-pulp fibres of similar dimensions and flexibility.

Horie and Pinder [H6,H7], experimenting with *artificial slurries* of regularly sized nylon fibres in aqueous solutions of polyethylene glycol, sodium chloride, and dextrose, employed a coaxial cylinder viscometer with a gap of 10.9 mm. The surfaces of both the cup and the bob with grooves in the axial direction prevented slip of fibres at the walls. The effects of fibre aspect ratio, fibre and salt concentration on the yield stress, the equilibrium stress and variation of thickness of flowing layer with time were examined. The fibres of uniform diameter of 43.1  $\mu\text{m}$  and various lengths (0.987, 1.62, 3.01, 5.03 and 6.72 mm), gave a range of aspect ratios from 22.9 to 156. The volumetric fibre concentrations in slurries ranged from  $C_v=0.04$  to 0.17.

Three of Horie and Pinder's [H7] numerous observations are of interest to this study:

1. The higher the fibre concentration, the higher the yield stress.
2. The higher the aspect ratio, the higher the yield stress at any concentration. It would appear, however, that there is a limiting value of maximum yield stress independent of fibre length since the points for  $L/d$  ratios greater than the 37.4

lie on a single curve, i.e., the points for  $L/d=68.8$ , 116, and 156.

3. At a fixed fibre concentration, the yield stress decreased with increasing dispersing medium viscosity which varied from 0.00745 to 0.22 Pa·s.

These observations applied to the equilibrium stress as well. The second observation indicates that slurries made of long fibres behave alike within a range of  $C_v$  from 0.04 to 0.11. The third observation is in agreement with Steenberg et al. [S12]. Relationships between the yield stress and the volumetric concentration were analyzed by the original data being fitted to a power relationship of the form:

$$\tau_y = a \cdot C_v^b \quad (8)$$

Since such relationships have been widely used in the comparison of shear strengths of wood-pulp fibre suspensions, this relationship is used here for the same reason. Values for  $a$  and  $b$  along with the original data for  $L/d=69.8$ , 116, and 156 are shown in Table III. These values are used later in this dissertation in the analysis and discussion of experimental results.

#### Wood-pulp fibres.

Numerous researchers used two main approaches in studying network strength: shear strength and tensile strength measurements. These studies can be classified as direct and indirect. The direct methods comprise experimental techniques in

Table III. Yield Stress of Nylon Fibre Slurries. Data taken from [H6].

$$\tau_y (N/m^2) = a C_v (\%)^b$$

ASPECT RATIO	VOLUME CONC.	DEXTROSE + 1 MOLE NaCl in 10% PEG - H <sub>2</sub> O $\mu=0.0074Pa.s$		DEXTROSE + 1 MOLE NaCl in 30% PEG - H <sub>2</sub> O $\mu=0.0553Pa.s$		DEXTROSE + 1 MOLE NaCl in 40% PEG - H <sub>2</sub> O $\mu=0.103Pa.s$		DEXTROSE + 1 MOLE NaCl in 50% PEG - H <sub>2</sub> O $\mu=0.220Pa.s$	
		YIELD STRESS N/m <sup>2</sup>	a N/m <sup>2</sup>	b	YIELD STRESS N/m <sup>2</sup>	a N/m <sup>2</sup>	b	YIELD STRESS N/m <sup>2</sup>	a N/m <sup>2</sup>
69.8	0.05		0.001	7.42					
	0.06								
	0.07								
	0.08								
	0.09								
	0.10								
116.	0.05	593	3.11	3.72	355	2.06	3.65	0.070	4.82
	0.06	1060			603				
	0.07	2610			1700				
	0.08	4500			2450				
	0.09								
156.	0.04	394	0.717	4.43	338	4.87	3.04	2.65	3.13
	0.05	642			646				
	0.06	2180			1090				
	0.07	4220			1890				
	0.08								
	0.09								

which the force is applied to the body of the network so that the break area is restricted; the force and the area are directly measured. The indirect method has, in all cases, some uncertainty arising from the estimates of either the breaking force or the load-bearing area or both.

Studies of shear and tensile strength of fibre networks by the direct methods are:

1. Shear strength studies of suspended fibre networks in shear testers under quasi-static test conditions (low shear rates) in which only network-network interface transmits the load. The applied torque is measured directly and the break area is predetermined [D4,D5,K10,T12].
2. Tensile strength of dry wood-pulp fibres. The load and break area of the network is directly measured so that the breaking stress is easily calculated [G2].

Strength studies by the indirect methods are:

1. Tensile strength of fibre plugs. The plugs which are formed in tubes have a predefined cross-sectional area. However, because the load is not applied at a well-defined cross-section, the plug breaks always in the weakest spot, i.e., at the floc boundaries at which the network discontinuity may exist. The length of the pendent plug after rupture, is used in the calculation of the breaking stress [C1,E3,F1,G5,V1].
2. Shear strength studies of fibre suspensions in the shear testers under dynamic flow conditions (large rates of shear)

and/or where the network-solid boundary interface transmits the load under either quasi-static or dynamic conditions. Under dynamic flow conditions when pulp suspension moves relative to the smooth walls in a shear tester, fibres migrating away from the walls form a clear water annulus between the walls and the pulp network surface [M16]. Similarly, when the pulp suspension flows in a pipe, fibres migrate away from the pipe wall [C4].

- a. The shear stress is evaluated at the inner cylinder surface and at a given cylinder speed [B8,M13,R1,T8].
  - b. The shear stress is evaluated at the network (plug) dispersive surface at a given cylinder speed [G6,H3].
  - c. The shear stress is evaluated at the outer cylinder surface at the onset of turbulent agitation of the entire suspension [G8].
3. Shear strength studies of flowing fibre networks in pipes, i.e., plug surface disruption in pipe flow.
- a. The shear strength was calculated at the pipe radius which was evaluated from the estimate of the water annulus thickness at the onset of turbulence in it [D1,D2,G7,K4,M14,M15,R5,S9].
  - b. The shear strength was calculated at the visually assessed radius of the plug disruption surface [D4,D5].
  - c. The shear strength was calculated at the radius taken from the velocity profile studies [D4,D5,M12].
  - d. The shear strength was assumed to be the same as the wall shear stress at the onset of drug reduction in pipe flow [B1,P2].

Publications include enough data for valid comparison of quasi-static test methods. The comparison can be made employing the mathematical relationship most commonly cited in the literature.

$$\tau = a' \cdot C_m^{b'} \quad (9)$$

Since this relationship has not been derived from basic principles it does not have theoretical justification for its coefficients. The fit coefficients  $a'$  and  $b'$  for the direct shear measurement studies (Table IV) are consistently greater than those for the indirect shear measurement studies (Table V). This implies that the ultimate shear strength of networks was probably measured by the application of the direct methods. This finding should guide those who undertake any experimental investigations of network strength.

The power coefficients obtained from the fits of

$$\sigma = a'' \cdot C_m^{b''} \quad (10)$$

to the data of tensile strength studies, shown in Table VI, are generally lower than those from the indirect methods of shear measurement shown in Table V. The reason could lie in the different ranges of consistencies in which the experiments were performed. Since the fit coefficients do not have clear physical meaning, this observation cannot be interpreted.

The tensile strength studies produced more experimental evidence on the complexity of fibre-to-fibre interaction than did

Table IV. Shear Strength of Fibre Suspensions. Direct Methods. Quasi-Static Tests.

$$\tau(N/m^2) = a' C_m(\%)^{b'}$$

FIBRE TYPE	AUTHORS	PULP TYPE	CONSISTENCY RANGE %	a' N/m <sup>2</sup>	b' --	- a' N/m <sup>2</sup>	- b' --
Long Fibre Chemical Pulps (Softwoods)	DUFFY [D5]	Unbleached kraft from pine Bleached kraft from pine Pine kraft	0.9-3.1 0.95-4.6 1.5-4.1	24.6 16.3 6.62	2.21 2.12 2.73	13.1	2.46
	DUFFY, TITCHENER [D4]	Unbleached, unrefined kraft from Pinus Radiata Bleached kraft from Pinus Radiata	2.4-3.9 2.6-5.0	22.4 6.64	2.27 2.73		
	TURNER et al. [T12]	Unbleached kraft from pine Bleached kraft from pine	1.0-5.0 1.0-5.0	9.80 7.87	2.83 2.69		
	KRYSKI [K10]	Softwood kraft	0.94-12.3	10.8	2.14		
Short Fibre Chemical Pulps (Hardwoods)	DUFFY [D5]	Hardwood sulphite Birch kraft	1.7-5.7 1.6-4.0	3.37 2.51	3.03 3.21	3.90	2.96
	DUFFY, TITCHENER [D4]	Semi-bleached aspen sulphite	2.2-3.5	3.50	3.01		
	TURNER [T12]	Bleached kraft from birch Semi-bleached aspen sulphite	1.0-5.0 1.0-5.0	5.42 4.72	2.60 2.85		
Groundwoods	DUFFY [D5]	Refiner groundwood Stone groundwood	1.6-5.3 1.8-5.3	2.57 2.15	2.95 3.11	2.36	3.03

Table V. Shear Strength of Fibre Suspensions. Indirect Methods. Quasi-Static Tests.

$$r(N/m) = a' C (\%)^{b'}$$

FIBRE TYPE	AUTHORS	PULP TYPE	CONSISTENCY RANGE %	a' N/m <sup>2</sup>	b'	a' N/m <sup>2</sup>	b'
Long Fibre Chemical Pulps (Softwoods)	RAIJ, WAHREN [R1]	High yield spruce sulphite	2.1-3.2	0.21	4.16	2.87	2.24
		Unbleached sulphite from spruce	1.3-1.9	2.51	2.42		
		Bleached sulphite from spruce	0.72-1.7	1.91	1.77		
		Unbleached kraft from spruce	0.6-1.9	2.98	2.63		
	THALEN, WAHREN [T8]	Spruce sulphite 15.9° SR	0.55-4.5	1.84	1.62		
		68.0° SR	0.64-5.6	2.95	1.81		
		Bleached sulphite from spruce 18° SR	0.41-5.5	2.18	1.58		
		46° SR	0.40-4.8	2.77	1.38		
	BERGMAN TAKAMURA [B8]	Spruce sulphite, 60.5% yield 47.4% yield	0.81-2.21	5.56	2.99		
			0.63-1.78	4.50	2.64		
Short Fibre Chemical Pulps (Hardwoods)	THALEN, WAHREN [T8]	Aspen sulphite, 27.5° SR	0.82-3.9	2.13	1.68	1.96	1.69
		Bleached sulphite from birch, 17.0° SR	0.78-4.0	1.80	1.70		
Groundwoods	RAIJ & WAHREN [R1]	Spruce groundwood 102mL CSF	0.98-5.3	1.01	3.10	1.78	2.25
			1.10-7.2	1.62	2.03		
	THALEN, WAHREN [T8]	Spruce groundwood 191mL CSF Spruce groundwood 91mL CSF	1.10-5.0	1.62	1.99		
			0.68-5.1	2.88	1.88		

the shear strength studies. For this reason, the tensile strength studies are discussed here in more detail. Each tensile test consisted of two steps: the first step was plug preparation; the second step was plug extrusion. Section 2.3.1 describes the preparation of plugs.

The majority of investigators allowed the downward extruded plug to break under its own buoyed weight. Andersson [A9], on the other hand, pushed the plug upward to a predetermined length and disrupted it in an annular flow of water whose flow-rate increased linearly with time. Only a few investigators used neutrally buoyant rings [C1,R2] to lower the friction between the plug column and the sides of the glass tube.

In general, a fibre plug is pushed downward to protrude from the glass tube into another tube of larger diameter and concentrically arranged. Until the plug breaks, it emerges from the tube into water flowing at the same velocity. Experiments show that the plug-breaking length, is independent of the tube diameter when other variables are kept constant provided that the diameter is large enough to permit uniform fibre dispersion [F1]. However, the plug-breaking length is dependent on the speed of extrusion, water temperature, and presence of air [G5,R3]. All air bubbles must be evacuated. Speed of extrusion and water temperature should be kept constant. The extrusion speeds are listed in Table VI.

If any changes in plug dimensions due to elongation of the network are neglected, the stress at the break is readily shown

Table VI. Tensile Strength of Fibre Networks. Quasi-Static Tests.

$$\sigma(\text{N/m}^2) = a'' c_m(\%)^{b''}$$

AUTHORS	EXTRUSION SPEED mm/s	PULP TYPE	CONSISTENCY RANGE %	a'' N/m <sup>2</sup>	b'' --	a'' N/m <sup>2</sup>	b'' --
FORGACS, ROBERTSON,, MASON [F1]	1.13	68% yield spruce sulphite, 740mL CSF 662mL CSF 539mL CSF 440mL CSF 318mL CSF	0.30-0.96	1.19	1.25	1.86	1.59
			0.68-1.22	1.84	1.25		
			0.68-1.08	1.87	1.55		
			0.64-1.00	2.38	1.47		
			0.56-1.03	3.01	1.74		
CHANG, ROBERTSON [C1]	1.0	Standard kraft pulp, 400mL CSF	0.30-1.30	2.49	1.85		
GIESE, GIESE [G5]	0.8	F1-S1-Cellulose, 47' SR F1-S1-Cellulose, 42' SR Mechanical pulp, 52' SR Mechanical pulp, 52' SR	0.40-1.60	1.86	1.48		
			0.18-0.99	1.36	1.37		
			0.56-1.33	1.75	2.02		
			0.32-1.06	1.20	1.74		
VEINOV et al. [V1]	1.1	Unknown pulp, 19' SR Unknown pulp, 42' SR	0.20-1.06	1.31	1.36		
			0.38-1.32	2.08	2.05		

to be:

$$\sigma = g \cdot C_m \cdot PL \cdot \left(1 - \frac{\rho_w}{\rho_{fm}}\right) \quad (11)$$

A linear relationship was found between the measured plug length, PL, and the mass concentration of fibres  $C_m$  within a range of  $C_m$  from 0.004 to 0.01 [C1]. At higher concentrations, reliable values of PL were difficult to obtain because increasingly poor fibre dispersion created weak spots in the plug structure [F1]. Furthermore, the faulty spots existed at plug edges so that premature breaks resulted. Giese and Giese [G5] experimented with two pumps of different dispersing potentials and demonstrated that the degree of homogenization was critical to PL. The same pulp dispersed by centrifugal and peristaltic pumps exhibited different strength relationships with consistency. PL did not increase monotonously with increased consistency of the long fibre pulps which were prepared with the peristaltic pump; rather, it levelled off and started to drop beyond 0.006 consistency [G5].

Contrary to Forgacs et al. [F1], Giese and Giese [G5] demonstrated that groundwood pulps develop networks whose strength can be measured. However, chemical pulps formed stronger plugs than groundwood pulps at the same consistency. A similar trend emanates from shear strength experiments. Softwood pulps (long fibres) formed stronger networks at the same consistency than hardwood pulps (short fibres) which, in turn, formed stronger networks than groundwood pulps (Table IV and V).

In the pendant plug tests, differentiation was made as far as the character of a break zone was concerned between smooth and fibrous breaks. A pulp with short and rigid fibres, such as mechanical pulp, gave smooth break surfaces. On the other hand, pulps having long and flexible fibres which gave brushy break surfaces indicated that long fibres were pulled from the plug over distances comparable to the fibre length.

Andersson [A9] studied the disruptive velocities of 20 mm long plugs of different mass concentration, from  $C_m=0.0046$  to 0.015. The median velocity of water was plotted versus plug concentration and nearly linear relationship between the breaking velocity of the liquid and the plug concentration was observed. At this plug length, the second order term of velocity dominated the stress equation, and Andersson concluded that this result agrees well with the observation that the network strength varies closely with the second power of concentration as indicated by Chang and Robertson [C1], Table VI.

The dependence of tensile strength on various parameters considered in pendant plug tests is summarized below:

1. The tensile strength increased as the beating level increased for black-spruce sulphite [F1].
2. Increase in strength was observed as yield of Douglas-fir and black spruce sulphites decreased until an apparent maximum was reached below 60% yield [F1].
3. Increase in strength was observed with the increased degree of beating applied to Fi-Si-cellulose until a maximum at 45°SR was reached [G5].

4. Moderate addition of electrolytes or polymers produced sizable changes in the tensile strength [C1,R2].
5. Mixtures of softwood chemical and mechanical pulps produced stronger networks as the content of chemical fibres increased [G5].
6. Strength of the plugs increased with the increased degree of plug homogenization [G5].

Some questions remain unanswered, e.g., 1, what are the mechanical cohesion forces that prevent or hamper the relative displacement of individual fibres, and 2, were plugs of *coherent* or *fragile* nature in Jacquelin's sense [J5,J6].

Recently, a unique study of the tensile strength of dry wood-pulp flocs has been published by Garner [G2]. This study is unique for two reasons: it is the only study done on dry flocs and one of only two devoted to the strength of single flocs [G2,L2]. For all pulps investigated, the floc strength exhibited a power-law relationship with the bulk density. The fits were made to the digitized data from Figure 3 of [G2]. The exponents ranged from 2.29 to 3.60 as shown in Table VII. The exponents for two Refiner Mechanical Pulps were greater than for bleached hardwood and softwood krafts. These results, similar to those found from the shear strength studies of pulp suspensions (Table IV, Direct Methods), suggest that similar mechanisms of fibre interaction during network disruption may be operating in "wet" and "dry" fibre networks. The most probable fibre-to-fibre interaction is of a frictional nature.

Table VII. Tensile Strength of Dry Wood-pulp Flocs.

$$\sigma(\text{N/m}^2) = a'''' \cdot C_b(\text{kg/m}^3)^{b''''}$$

TYPE OF WOOD-PULP	BULK DENSITY RANGE	a''''	b''''
	kg/m <sup>3</sup>	N/m <sup>2</sup>	--
Bleached softwood kraft	6.2-29.7	2.94x10 <sup>-1</sup>	2.29
Bleached hardwood kraft	14.4-39.1	2.14x10 <sup>-2</sup>	2.57
Refiner mechanical pulp 1	23.4-67.1	1.30x10 <sup>-4</sup>	3.60
Refiner mechanical pulp 2	25.9-72.9	1.85x10 <sup>-3</sup>	3.17

The effect of rate of straining on the tensile strength was undetected because the measurements were within the scatter of data. This wide scatter of data was attributed to the experimental difficulties, nonuniformity within flocs, and errors of measurement in the floc dimensions [G2]. On the other hand, the effect of straining would be small if the fibre-to-fibre interaction was predominantly of a frictional nature because the dynamic coefficient of friction is constant. Thus, the supposition of frictional interactions between fibres during floc straining is supported.

#### 2.3.4 Cohesion forces

The elastic interlocking of whole fibres is expected to occur in concentrated suspensions.

##### Man-made fibres.

In 1964, Meyer and Wahren [M10] indicated that *a fibre network is a system of fibres in contact where every fibre is locked in position in the network by contact with at least three other fibres in the network and in such a way as to be able to transmit forces*. It was unclear how one fibre can be locked in position and have at least three contacts with other fibres. In 1972, Parker [P3] understood this as interlocking by three alternate contact points and illustrated it using fingers for fibres (Figure 1.18 in [P3]). In 1979, Wahren [W3] agreed. The principle of this interlocking is shown in Figure 1a.

Thalen and Wahren [T9] wrote: *the results of the experiments indicate that specific attraction forces between fibres are not needed for the formation of coherent networks, but that the coherence of networks is due to physical bonding by entanglement of the fibres*. It is not clear on which experimental evidence this statement was built since the magnitudes of the specific attraction forces are not reported.

##### Wood-pulp fibres.

Wollwage [W7] attempted to measure fibre-to-fibre cohesion forces with a torsion balance. He used unbleached spruce sulphite fibres. The results were *not entirely satisfactory*,

*principally because of lack of sensitivity. The exploratory experiments made to date indicated that fiber-to-fiber adhesion forces do exist and are of the order of  $10^{-4}$  dynes ( $10^{-9}$  N).* This was a direct approach in the determination of a force normal to the plane of contact between the two fibres. This method focussed solely on the attractive electro-chemical interaction between two crossed fibres.

Without doubt the cohesion forces between wood-pulp fibres result from electro-chemical and/or mechanical interactions. The question of their relative importance was raised by Chang & Robertson [C1] and Reeves & Gerischer [R2]. Chang and Robertson published results of the dependence of the pendent plug strength and zeta potential of kraft-pulp fibres on the concentration of additives: electrolytes KCl, CaCl<sub>2</sub>, FeCl<sub>3</sub>, and ThCl<sub>4</sub> and poly-(1,2 dimethyl-5-vinyl-piridinium methyl sulphate) or shortly poly-(DMVPMS). Changes in plug breaking length, PL, of the kraft pulp beaten to 400 mL CSF [C9,T5] and at  $C_m=0.007$  were: about 2.5 cm due to charge neutralization, about 1.5 cm due to ThCl<sub>4</sub>, and about 3 cm due to poly-(DMVPMS). Change in PL due to change in suspension concentration from  $C_m=0.003$  to 0.011 was about 6 cm. Clearly, electro-chemical interactions affected strength half as much as the change in suspension concentration. Reeves and Gerischer [R2], who used Alum (Al<sub>2</sub>(SO<sub>4</sub>)<sub>3</sub>·18H<sub>2</sub>O) and modified polyethyleneimine (PEI) as additives to the bleached, long fibre, kraft pulp of  $C_m=0.006$ , noticed similar effects. Addition of Alum produced about 1 cm change in PL, and addition of PEI only 0.3 cm. These changes constituted less than 30% of the initial

breaking length of plugs.

Moderate additions of electrolytes and polymers producing noticeable changes in the strengths showed that the surface charge which is so significant in the stability of colloid systems also has a measurable effect on fibre-to-fibre interactions in fibre plugs. However, it can also be concluded from these experiments that the chemical bonding between fibres is not the primary cause of coherence in fibre plugs but that they are coherent mainly through entanglement of fibres.

It is noteworthy that the strength of pendent plugs was the lowest ever recorded for fibre networks. Hence, the electro-chemical effects were noticeable only in the weakest of produced networks. Studies of electro-chemical effects on shear strength of fibre networks have never been reported, the possible reason being that these effects were unnoticeable.

Jacquelin [J5,J6] observed the formation of two types of flocs in wood-pulp fibre suspensions: *fragile* and *coherent*. Gentle mechanical treatment applied to fibres which normally formed hard (*coherent*) flocs changed them into fibres having a soft (*fragile*), floc-forming tendency. Experiments with chemical additives shed more light on this transformation and the importance of fibre surface interactions, e.g., addition of polyethyleneimine (PEI) in the presence of Alum to the gently-refined pulp produced large changes in T.F.C.<sup>1</sup> whereas the same addition did not do so for unrefined pulp. This indicates

---

<sup>1</sup> Mass content of coherent flocs.

that the extent of the electro-chemical effects can be altered by mechanical modification of fibre surfaces [J5], i.e., it increases with the creation of fibrils and microfibrils. Jacquelin also experimented with Alum in combination with sodium hydroxide sizing of unrefined and gently refined pulps with and without PEI, galactomannan, starch and diastase (cellulose enzyme). These experiments confirmed the importance of the interfacial physico-chemical actions on the behaviour of fibre in suspension. It appears that when wood-pulp fibres have developed surface features, the size of which falls into the colloid region, e.g., fibrils, the interaction of these added up to a significant electro-chemical force between fibres.

Surface tension forces deserve mention because numerous publications refer to small air bubbles as a cause of fibre flocculation [F3,G4,H9,K2]. The commonly accepted description of the phenomenon is given in [G4]:

*Water repellent parts of fibres are easily contacted by gas bubbles and a bubble contacting two or several fibres at the same time will hold them together with a force that is actually the surface tension of water. In dilute fibre suspension it is sometimes possible to see fibre flocs built up around gas bubbles which seem to act as a kind of cement.*

Turner, Titchener and Duffy [T12] measured *disruptive shear stress* quasi-statically in the Fisher & Porter Tester to evaluate the contribution of air bubbles to the network strength. They used the technique described by Duffy and Titchener [D4] to test original and deaerated pulps. The disruptive shear of the deaerated pulps did not appear to differ within experimental error from that for the original pulp at the same consistency.

Undeniably, surface tension forces must be present since the bubbles attached to fibre surfaces exist. However, how they could contribute to the network strength is unknown.

#### General classification of cohesion forces.

The mechanical strength of fibre networks results from cohesion forces developed at the fibre-to-fibre contacts. In a recent literature review, Kerekes et al. [K7] classified these forces into four types and for convenience labelled them Type-A, B, C and D:

##### *Type-A Colloidal:*

*These are the well-known electrostatic and electrokinetic forces which exist between small particles. Their strength depends on intimacy of contact, which is difficult to achieve between the rough surfaces of fibres, and on chemical additives that modify the negative charge found on fibre surfaces.*

##### *Type-B Mechanical Surface Linkage:*

*This is a hooking force caused by mechanical entanglement of fibres having kinked or curled configurations, or fibrillated surfaces. When a force is applied to separate fibres, the reaction force caused by hooking at contact points opposes relative movement between them. This type of cohesion depends on surface fibrillation, the degree to which fibres are contorted, and fibre stiffness.*

##### *Type-C Elastic Fibre Bending:*

*Here the cohesive force between fibres is caused by frictional resistance induced by normal forces at fibre contact points. The normal forces arise when elastically bent fibres are restrained from straightening as a result of contact with other fibres. The ultimate source of this cohesive force is therefore an internal stress within individual fibres rather than an externally imposed stress on the network.*

##### *Type-D Surface Tension:*

*Bubbles of undissolved gas (usually air) at fibre interstices produce cohesive forces as a result of surface tension.*

This classification combined the experimental evidence and the postulates on cohesion of man-made and wood-pulp fibres. Type-C cohesion was singled out from other mechanical cohesion because Kerekes et al. [K7] anticipated the experimental findings of this research. No direct study of Type-B cohesion has been published. The classification could be expanded by the inclusion of another type of mechanical cohesion: fibre stringing [S5,V2,W9] which is distinct from either Type-B or Type-C. For the remainder of this dissertation the term "Type-C cohesion" instead of somewhat lengthy wording "interlocking by the elastic fibre bending" is used.

#### 2.4 Classification of Findings from the Literature Review

Fibre geometry and suspension concentration have the most profound effect on the process of flocculation. These two factors are used to classify fibre suspensions in terms of fibre behaviour into: dilute, semiconcentrated and concentrated. Other parameters such as the physico-chemical properties of fibres or suspending medium are also important, but their significance is predetermined primarily by the suspension concentration and fibre geometry. Thus, fibre geometry and concentration are the most suitable in the construction of a space for graphic representation of the regimes of fibre flocculation. This is shown in Figure 3 in which the aspect ratio ( $L/d$ ) is plotted on the vertical axis and the volumetric concentration of fibres on the horizontal axis. Both axes are logarithmic. The graph contains five lines which represent the geometric concepts on fibre crowding. From left to right they are:

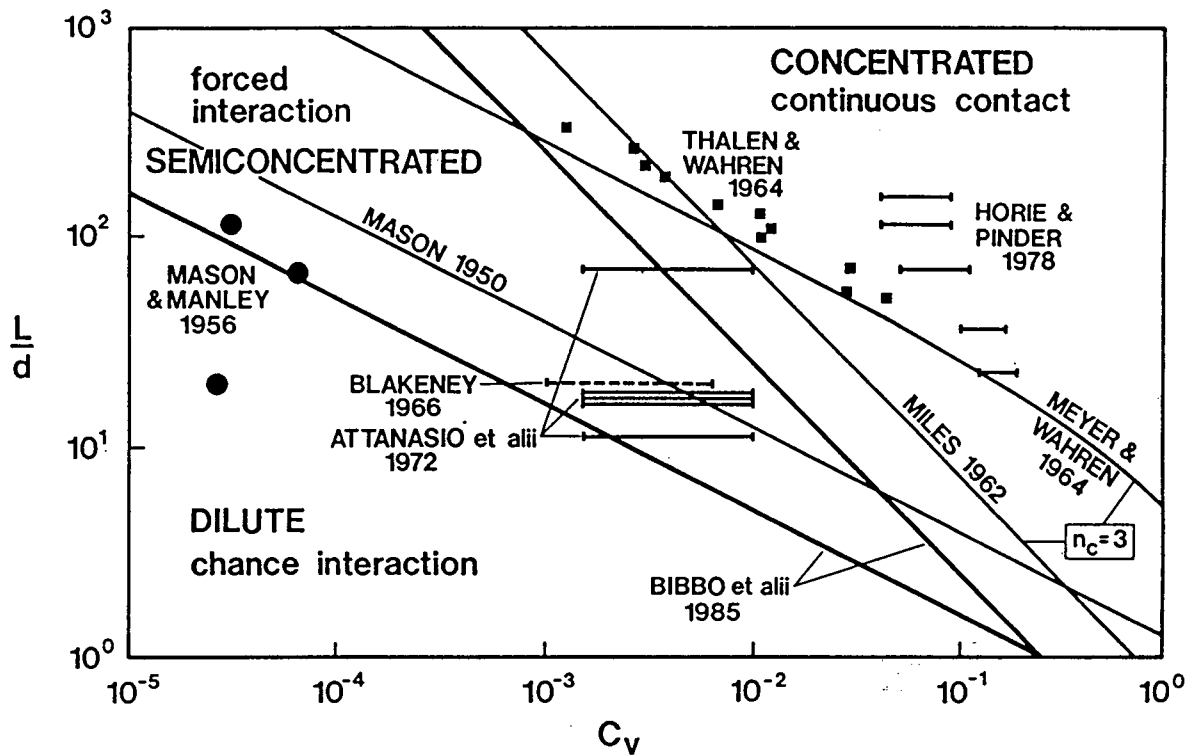


Figure 3. Concepts of Fibre Crowding in Suspensions and Experimental Investigations with Man-made Fibres.

1. The concentration below which suspensions are dilute as defined by Bibbo et al. [B9],
2. The concentration at which only one fibre is in a spherical volume having a diameter equal to the fibre length, as defined by Mason [M7] (equation (1)).
3. The concentration which constitutes the upper boundary of semiconcentrated suspensions, as defined by Bibbo et al. [B9]. Below this concentration, the suspension behaved as viscoelastic liquid but, above it, as an elastic material, according to Doi and Kuzuu [D3].
4. The concentration below which continuous networks having three contact points per fibre should not exist, as defined

by Meyer and Wahren [M10] (equation (3) at  $n_c=3$ ).

5. The concentration defined by equation (2) [C5] and calculated for  $n_c=3$  since  $n_c=3$  was suggested by others [M10].

Only analysis of experimental observations can show which one of these concepts is valid. The experimental investigations with man-made fibres are shown in Figure 3 to identify the regimes of flocculation to which they belong. The experimental evidence, though scarce, is sufficient to support some cautious conclusions. It could be suggested that the boundary between dilute and semiconcentrated suspensions be delineated by Mason's critical concentration on the basis of Blakeney's [B11] and Attanasio et al. [A18] results, and the boundary between semiconcentrated and concentrated suspensions be delineated by Meyer-Wahren's limiting concentration at  $n_c=3$  [M10]. In this case, the boundaries proposed by Bibbo et al. [B9] seem to be out of place. Verification of these conditions requires further research.

Classification of fibre suspensions into three types, dilute, semiconcentrated, and concentrated, provides systematic organization of the scattered experimental data reported in the literature so that a useful basis for the understanding of fibre interactions in suspensions is provided.

The experimental studies with wood-pulp fibre suspensions are presented in Figure 4 to identify the regimes of flocculation to which they belong. Calculation of volume concentration from the mass concentration was made under

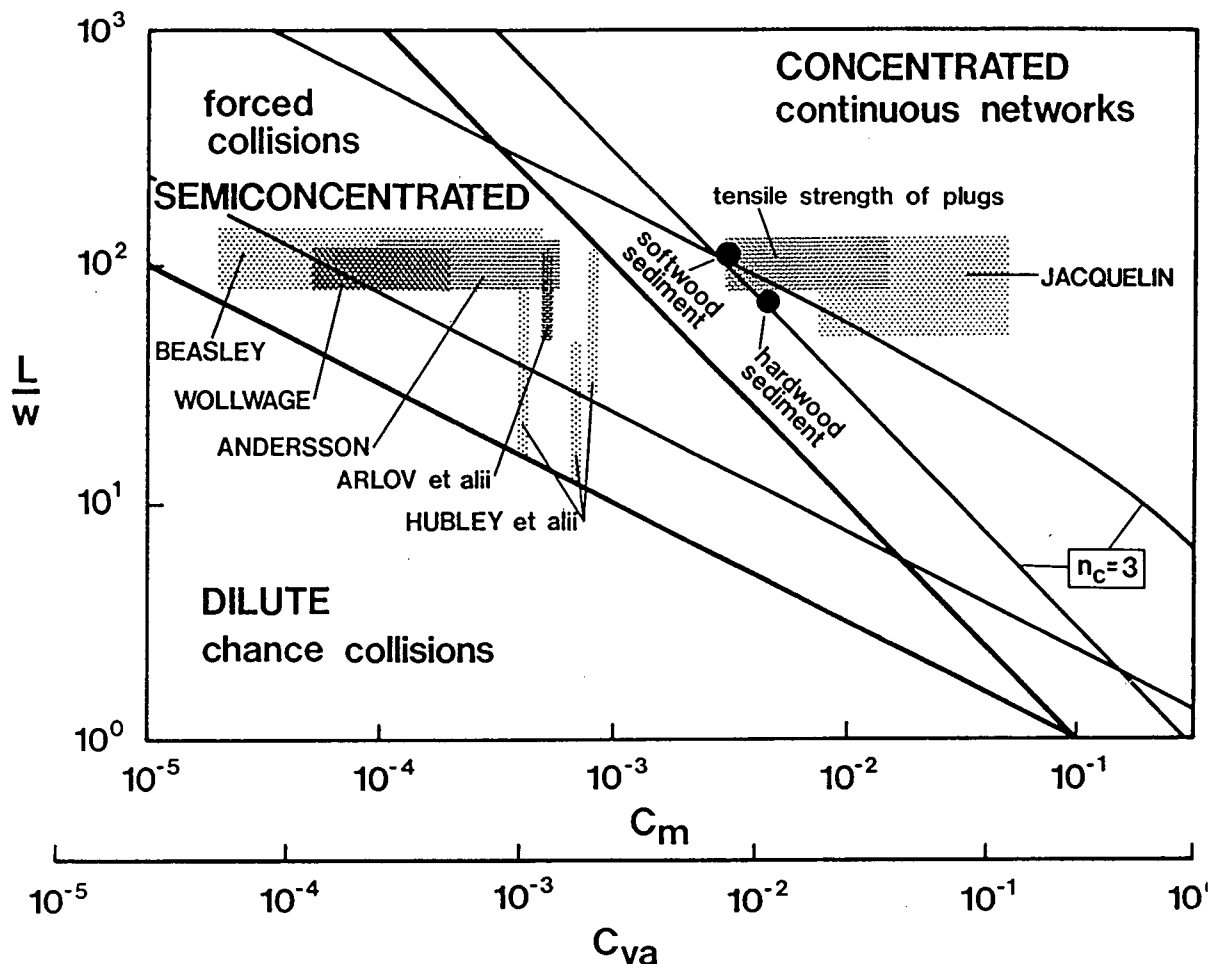


Figure 4. Concepts of Fibre Crowding in Suspensions and Experimental Investigations with Wood-pulp Fibres.

assumption that: the water retained by fibres is 2 g/g [E5]; the water density is 998 kg/m<sup>3</sup> [C10]; and the density of dry fibre matter is 1500 kg/m<sup>3</sup> [S4]. The ranges of fibre aspect ratio were not reported in the literature but are presented in Figure 4 with some degree of approximation. The data are insufficient to draw any general conclusions regarding the location of the boundaries separating the three regions of fibre behaviour. Location of sediment data indicates that Meyer-Wahren limiting concentration may be accepted as a boundary between

semiconcentrated and concentrated suspensions.

## 2.5 Summary of Literature Review

### Dilute suspensions.

Short, rigid, cylindrical particles spin, rotate and oscillate in a simple shear flow. However, long, cylindrical particles spin, rotate, oscillate and flex in a simple shear flow. The motion of both types of particles is complex. In any case, the space swept by the single particle is much larger than the space defined by the particle volume.

Wood-pulp fibres exhibit more complex motion in a simple shear than man-made fibres because of their irregular shape and higher flexibility. Wood-pulp fibres deform in various ways. Their modes of deformation depend on the degree of fibre flexibility. In simple shear flow, deformation of a flexible fibre is superimposed on the basic rotational and translational motion of a rigid fibre. The volume swept by the flexible fibre may be smaller than the volume swept by the rigid fibre of identical dimensions.

Rigid, cylindrical particles do not collide in simple shear flow or under differential sedimentation conditions; they only interact on approach. These are chance interactions which manifest themselves by a drastic change in particle orbits. Wood-pulp fibres, on the other hand, collide in a simple shear and under differential sedimentation conditions. These are chance collisions which occur below the critical concentration.

### Semiconcentrated suspensions.

The interaction of straight, rigid fibres increases with concentration in shear flows. It was found that the critical concentration delineates the regime of chance interactions and forced interactions. For the straight nylon fibres of  $L/d \approx 20$  this concentration was  $C_v = 0.0042$  (Blakeney, 1966). Slightly above critical concentration, the formation of groups of two and three fibres increased rapidly. The interaction of straight, rigid fibres increases with increase in fibre length as well.

Forced collisions between wood-pulp fibres occur at and above the critical concentration. When collision occurs in a Couette type apparatus, the fibres may cohere and form a floc. Cohesion may be of a colloidal or mechanical nature. For the short fibre fraction of softwood-pulp, the forces of colloidal nature are, in most cases, small in comparison with mechanical effects, i.e., fibre length variation and shear rate changes.

A dynamic equilibrium in the flocculation process was observed in a Couette-type apparatus with fine-fraction of fibres. The existing flocs shed peripheral fibres and acquired new fibres at the same rate. The cohesion forces developed at the contact points found at floc peripheries equalled the dispersion forces which resulted from the viscous drag imposed on fibres.

In the semiconcentrated suspensions, only flocculation of wood-pulp fibres was documented. The flocculation mechanism consisted of two steps; first, forced collision, and second,

cohesion. Collisions occurred as the result of orbit overlap in the shear arising from suspension circulation. Cohesion resulted from chemical or mechanical interactions. The cohesion developed between the whole-pulp fibres was much stronger than the cohesion between the fine-fraction of fibres. This increase in strength was attributed to the mechanical entanglement. Whether the colloidal or mechanical cohesion is predominant depends not only on fibre geometry or suspension concentration but also on fibre surface properties (fibrils) and flow conditions. The colloidal cohesion is predominant only in the dilute suspensions and under low rates of shear.

Mason termed mechanical cohesion of wood-pulp fibres in many ways - clotting, hooking, intermeshing, interlocking, interweaving and entanglement - and used this terminology liberally to distinguish wood-pulp fibre flocculation from colloidal aggregation [M4,M5,M6,M7]. None of these terms was precisely defined or documented in any investigation.

#### **Concentrated suspensions.**

It has been observed that coherent networks form when man-made fibres of suitable length settle and are subsequently vigorously agitated. Such networks are always nonuniform. Better uniformity is achieved if the viscosity of the suspending liquid is increased. However, at very high viscosities, the network may not form at all. How these networks formed has never been documented. Inference not experiment indicated that fibres interlocked elastically.

It has been demonstrated that wood-pulp fibres form form continuous networks, e.g., a sediment mat or a plug in plug flow. The term "continuous" implies that the network entirely fills the volume of a container or a conduit. It has been also demonstrated that coherent networks form under favorable flow conditions, i.e., through a specific process of plug formation. The structure of continuous coherent network depended on flow conditions, i.e., well dispersed (homogenized) or poorly dispersed (floccy) networks were formed. Neither the process nor the structure of those networks has been studied.

Jacquelin produced individual, well-defined networks which he classified as "coherent flocs." These flocs possessing organized structure and sizable strength, he distinguished from "fragile" flocs with no visible structure or significant strength. The coherent flocs could only be formed from the long fibre chemical-pulps never exposed to even gentle mechanical treatment (beating). Neither strength nor the structure of those flocs was investigated by Jacquelin.

Two models of 3-D, isotropic fibre networks pertain to fibres of uniform length and diameter. The Meyer-Wahren model developed for networks having three and more contact points per fibre has never been verified empirically. It has only been conjectured from the sediment and shear modulus experimental data. Neither Miles's model nor Meyer-Wahren model has been verified to apply to 3-D, isotropic fibre networks. Thus far, the estimated numbers of contact points per fibre calculated from both models do not agree with those counted in the compressed

fibre mats. It was also postulated that the man-made fibres interlock by the three alternate contact point arrangement. This detail of the form of interlocking has never been checked experimentally.

The strength of fibre networks varies widely over several orders of magnitude. The lowest strength was recorded for wood-pulp fibre networks under tension. The highest strength was obtained from shearing the nylon fibre slurries. The tensile stress ranged from 0.2 to 4 N/m<sup>2</sup> whereas the shear yield stress ranged from 400 to 4500 N/m<sup>2</sup> in suspending liquids of comparable viscosity. The exponents from all power fits ranged from 1.59 to 4.43.

A trend was observed for the exponents from the direct test methods in the case of wood-pulp fibres (Table IV and VII). The exponents were the largest for mechanical pulps (3.03 & 3.6) followed by those for hardwood-pulps (2.96 & 2.57) and those for softwood-pulps (2.46 & 2.29). This trend indicates that the mechanism of fibre separation in tension and in shear may be similar.

Nylon fibres did not form coherent networks in a flow loop under conditions that produced coherent networks from wood-pulp fibres [F1] although the volumetric concentration was almost three times larger than  $C_{v,min}$ . This behaviour seems contrary to the observations made in another case [M10] in which the continuous coherent networks were produced by vigorous stirring of fibres with an impeller and sudden decay of agitation at

concentrations corresponding to  $C_{v,min}$ .

The only estimate of the order of magnitude of cohesion force due to colloidal attraction between two crossed wood-pulp fibres is that of Wollwage,  $10^{-9}$  N. The electro-chemical forces, though smaller than mechanical entanglement forces, are nevertheless significant in the cohesion of flocs or continuous networks when myriads of fibrils interact.

The presence of small air bubbles enhances flocculation but shows no effect on the disruptive shear stress.

## 2.6 Thesis Objectives

The principal goal of this thesis, that of answering major questions concerning the existence and properties of Type-C cohesion, is pursued by meeting the following objectives:

1. To verify the existence of Type-C cohesion experimentally by isolating it from other types of cohesion.
2. To identify the process of Type-C network formation by exploring the conditions under which Type-C networks exist and by paying particular attention to the limiting concentration below which such networks do not form as postulated by Wahren *et alii*.
  - a. To investigate fibre properties and flow conditions under which Type-C cohesion can or cannot exist.
  - b. To explain the effect of suspending liquid viscosity on the formation process of Type-C cohesion.
  - c. To verify the mechanism of elastic fibre interlocking proposed by Wahren *et alii*.

- d. To verify whether the sediment concentration approximates the limiting concentration.
3. To identify the structure of 3-D, Type-C coherent networks.
    - a. To verify experimentally the predictive power of two existing theories relating  $C_v$  to  $L/d$  and  $n_c$ .
    - b. To gather direct evidence of alternate contact point interlocking.
  4. To measure strength of Type-C networks.
    - a. To reveal whether the relationship between stress and concentration yields the same exponent as indicated by the shear and/or tensile strength studies.
    - b. To verify whether friction forces developed at contact points are the source of network strength.

### 3 EXPERIMENTAL PROGRAM

#### 3.1 Preparation of Fibres

A study of flocculation of wood-pulp fibres is hampered by numerous independent variables created by tremendous heterogeneity of any collection of natural fibres. These variables cannot be controlled, but can be eliminated by using substitute fibres such as man-made fibres.

##### 3.1.1 Choice of fibrous material

Wood tracheids and fibres which are elongated tubular objects tapered at both ends have irregular geometry and surface features due partly to morphology and partly to the pulping process by which they were separated from wood. Morphological characteristics of deciduous tree fibres or coniferous tree tracheids vary between species as well as within one species. In addition, each tree has fibres or tracheids of various lengths, cross-sections and wall thicknesses [I3,P1,R10,S18]. Some pulping processes can change a straight tubular shape into a kinked, contorted and collapsed shape. Other processes may roughen the tube wall or even tear the tube apart, in both cases exposing the fibrillated wall structure [C2].

This broad nonuniformity of shape and surface roughness creates various mechanical entanglements [M5] and enhances electro-chemical interaction [C1,J5]. Accordingly, no exclusive type of cohesion can be produced while wood-pulp fibres are used. For Type-C cohesion to be isolated, the features that produce other types of cohesion had to be eliminated. For this reason

the experimental work of this thesis used model fibres which had smooth surfaces and straight configuration.

Apart from the need to produce exclusively Type-C cohesion, it was important that the model fibres required similar flexibility and density as those of wood-pulp fibres. Nylon 6-6 was selected because it has an apparent density of  $1130 \text{ kg/m}^3$  in water which is close to that of wood pulp fibres.<sup>1</sup> Nylon fibres and wood-pulp fibres are compared in Figure 5.

Since fibre stiffness was shown to be crucial to Type-C cohesion [J3,T9], nylon 6-6 filaments were obtained in various

---

<sup>1</sup> See Appendix II for further details.

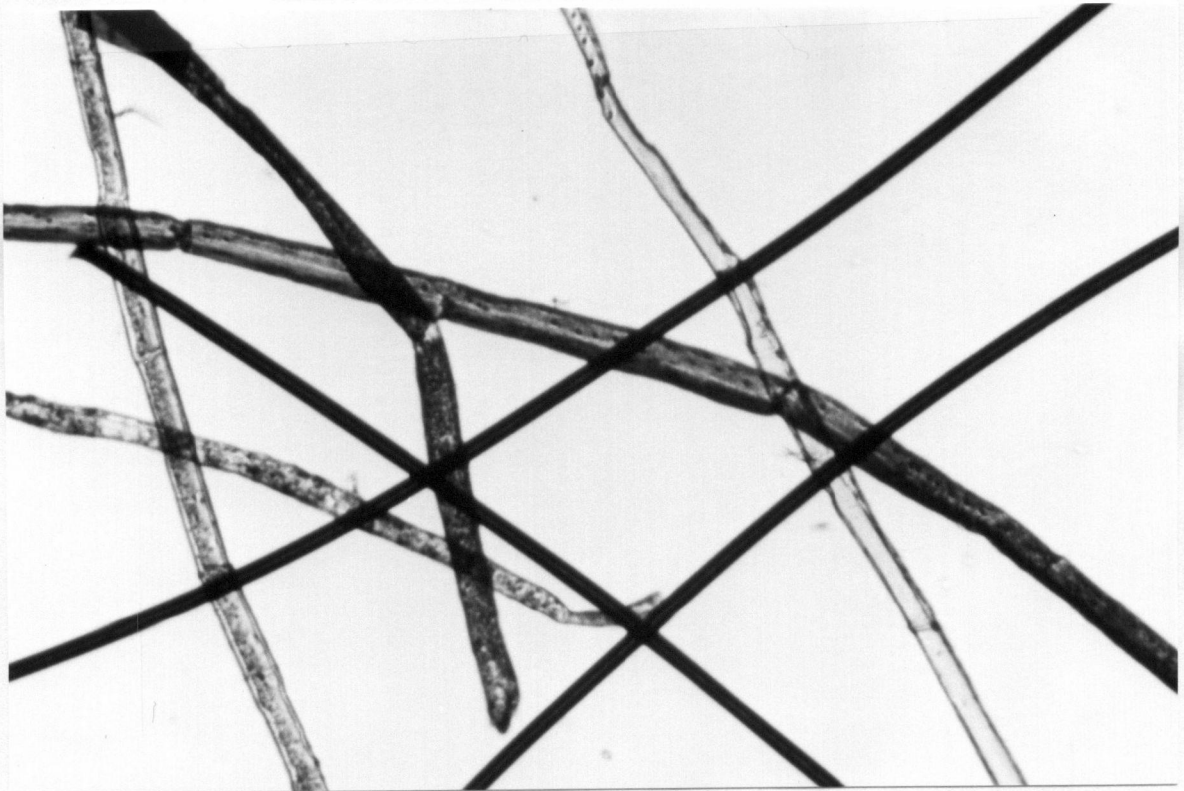


Figure 5. Surface Texture and Shape of Nylon (dark) and Wood-pulp Fibres. Magnification 120x.

diameters to cover the range of wood-pulp fibre stiffness. The stiffness range for the wet nylon filaments was expected to be from  $8 \cdot 10^{-12}$  to  $200 \cdot 10^{-12}$  N·m<sup>2</sup>, based on elastic modulus  $E = 1.17 \cdot 10^9$  N/m<sup>2</sup> [M9], whereas wood pulp fibre stiffness was reported to range from  $0.21 \cdot 10^{-12}$  to  $157 \cdot 10^{-12}$  N·m<sup>2</sup> [S1,S6,S11,T1,T2]. The nylon filaments were cut to the desired lengths with a technique that produced a narrow length distribution, a crucial requirement to meet to test equations (2) and (3). After nylon 6-6 filaments were cut, the fibre lengths spanned the full spectrum of naturally-occurring lengths of softwood and hardwood fibres [I3,P1,R10,W6].

The choice of nylon 6-6 material made electro-chemical attractive forces between fibres in aqueous-sugar solution insignificant compared to mechanical bending forces which are postulated to be the source of Type-C cohesion. The magnitude of the electro-chemical attraction between two fibres was estimated to be 1000 times smaller than the interaction due to elastic fibre bending.<sup>1</sup>

### 3.1.2 Determination of fibre geometry

Thalen and Wahren [T9], and Jacquelin [J3,J4] have observed that fibre geometry has strong influence on formation and properties of coherent networks. It was anticipated that fibre length and diameter would be primary independent variables.

Fibres were cut from multifilaments with a technique described in Appendix IV. After being cut, the fibres were

---

<sup>1</sup> Appendix III contains details of this estimate.

washed with mild detergent in hot water for removal of impurities acquired during manufacturing process. Subsequently, they were thoroughly rinsed in deionized water, dewatered in Buchner funnel, and dried at 105°C for four hours. This time was sufficient for stable dry weight to be ascertained. At this point, oven-dry samples were weighed for floc formation tests. Much smaller samples were taken for length and curvature measurements. Length and curvature measurements followed drying because the latter shortens fibres permanently by about 7 to 8% [D7,K9]. It is understood that relaxation of latent stresses incurred during manufacture of filaments causes this shortening by rearrangement of molecules.

Fibre samples were rewetted for 48 hours in preparation for length and curvature measurements. The measurement method relied on projecting a magnified fibre image on a digitizer and processing the digital information on the computer. The details of this method are given in Appendix V.

### 3.1.3 Moisture absorption by nylon fibres

The theoretical models of three-dimensional (3-D) fibre networks governed by equations (2) and (3) [C5,M10] can be verified only when accurate and precise data on their parameters are available. Two parameters, fibre length and diameter, have already been discussed. The third geometrical parameter, the apparent volumetric concentration, is difficult to measure directly; it can however, be calculated from the mass concentration. Because this calculation requires knowledge of

the amount of water retained by saturated nylon 6-6, the water retention of nylon 6-6 was investigated by exposing nylon to a 98% relative humidity (RH) environment. Moisture uptake was continuously monitored with a computer-balance system until it levelled off.<sup>1</sup> The apparent volumetric concentration was determined from equations derived in Appendix VII by the substitution of the levelled off moisture uptake for WRRk.<sup>2</sup>

#### 3.1.4 Determination of fibre elastic properties

Jacquelin [J3] found optimum fibre flexibility at a given intensity of agitation above and below which coherent flocs formed with more difficulty. Since fibre flexibility was shown to determine the network elastic properties [M10], a close estimate of the flexibility of nylon fibres was necessary.

Fibre flexibility is defined as a reciprocal of fibre stiffness in bending,  $S$ , which is the product of elastic modulus,  $E$ , and the moment of inertia,  $I$  ( $S = E \cdot I$ ). The moment of inertia for a circular cross-section is defined as  $I = \pi d^2 / 64$ , in which  $d$  denotes fibre diameter. Fibre diameters were calculated from the weight per standard length and the density data provided by DuPont Canada [D7]. The diameters were corrected for water swelling. The moment of inertia could then be calculated. However, since no reliable data on the elastic modulus of water saturated nylon 6-6 were available, the modulus of elasticity was determined empirically. Two methods were used: a tensile method [A12,A14] and a bending method [T1,T2]. Both tests are described

---

<sup>1</sup> Details of this experimental approach are in Appendix VI.

<sup>2</sup> Discussion of WRRk is in Appendix I and II.

in Appendix VIII.

### 3.1.5 Determination of wet-friction coefficient

As described earlier, Meyer and Wahren [M10] postulated that fibres interlock through elastic bending and frictional forces so that wet-friction coefficient should be important to Type-C cohesion. Static and dynamic coefficients of friction were measured employing an inclined plane method [A15,T4]. The experimental setup and procedures for this test are described in Appendix IX.

### 3.2 Creation of Coherent Floccs

Experimental verification of the relationships (2) and (3) requires construction of large, uniform fibre networks of a given fibre concentration. In practice, such networks cannot be formed because fibres in suspension tend to flocculate into mass concentrations (flocs) [T9,G5]. The experimental effort, for this reason, was directed toward production of relatively uniform flocs. The method of producing such flocs from wood-pulp fibres was described by Jacquelin [J3,J4,J7]. He applied continuous, moderate agitation to the concentrated suspensions and produced unique, mechanically entangled, aggregates. They were formed in a partially filled, rotating cylinder either horizontally oriented or inclined at 45 degrees to the horizontal. Jacquelin called them "coherent flocs."

Preliminary experiments of this study showed that the agitation of a suspension of nylon fibres under the conditions

specified by Jacquelin produced regularly-shaped flocs suitable for studies of network properties. The flocculation phenomenon observed by Jacquelin seemed to be preserved despite the radical change in the type of fibres used, i.e., nylon fibres in place of wood-pulp fibres. The nature of cohesion, though expected to be Type-C, was enigmatic. Qualitative experiments determined whether the nylon flocs derive their strength from the energy stored in the elastically bent fibres.

A few flocs were heated in water at a slow rate to 90°C temperature at which they remained for 5 minutes. The nylon temperature, raised above its glass transition point (65°C [H4]), permitted the bending stresses to relax. After subsequent cooling, the heat-treated flocs were placed in a large volume of water with never-heated flocs and their relative strength was evaluated by slow increase of the intensity of suspension agitation. The heat-treated flocs dispersed easily under gentle agitation whereas the never-heated flocs required intense agitation to be dispersed. The outcome of this experiment justified further systematic study. The nature of cohesion was of Type-C.

The design of a versatile rotating cylinder apparatus was based on Jacquelin's device. In this apparatus, shown in Figure 6, various cylinder diameters could be accommodated by the relocation of one roller (A). All cylinders were 164 mm long. The frame (B) that houses rollers (A,C) can be inclined to the horizontal at 15 degree increments from 0 to 60 degrees. The cylinder (D) which rests on rollers (A,C) and is prevented from

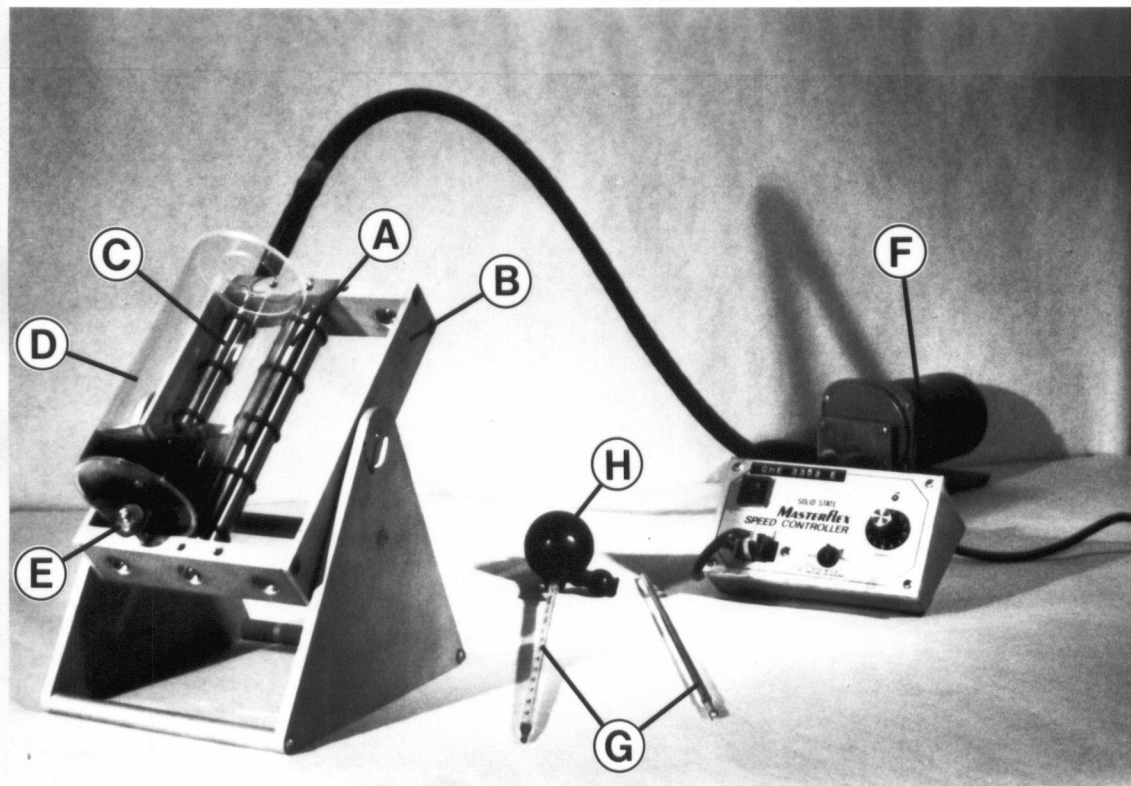


Figure 6. Rotating Cylinder Apparatus.

sliding off the frame by the third roller (E). Rotation of the cylinder (D) is induced by the roller (C) which is driven by the speed-controlled, electric motor (F).

The suspension in the cylinder is concentrated by gradual removal of the suspending liquid with the pipet (G) and the pipet filler (H). This feature was especially useful in the experimental evaluation of the limiting concentration, i.e., the concentration below which coherent networks cannot exist. The suspension volume was chosen so that the flat base was always covered with the suspension. This was necessary to assure only one type of recirculating flow. Details of the apparatus are given in Appendix X.

### 3.2.1 Observation of the phenomenon of flocculation

The first steps in the exploration of the unknown process of floc formation were visual observations. The appearance of the suspension was assessed and photographed. The dynamic behaviour of flocs was observed and in some cases videotaped. Changes in the suspension appearance with the increase in concentration were studied. These observations were facilitated by the use of multicolored fibres. Most tests were carried out in an 82 mm internal diameter (ID), plexiglas cylinder inclined at 45-degrees to the horizontal and rotated at the constant speed of 8.9 rad/s. The cylinder length was 164 mm. Details of fibre suspension preparation, test conditions, and experimental procedure are in Appendix XI.

In addition to the production of flocs in recirculating flow in a rotating cylinder, the formation of Type-C flocs in other flows was attempted. The other flows occurred: in the zone between rotating concentric cylinders under laminar and turbulent conditions; in a tank with the suspension agitated by a stirrer; in a stationary channel through which a grid was passed cyclically.

### 3.2.2 Sediment concentration

Thalen and Wahren [T9] observed that the lowest concentrations of Perlon fibres in suspension at which a shear modulus could be measured were only slightly higher than the corresponding sediment concentrations. It seemed natural for them to postulate that coherent networks are not formed at

concentrations lower than the sediment concentration. For this study to test this postulate, the sediment concentration for each type of fibre was determined and compared with the concentration at which nylon flocs formed. The sediment pads were formed by the usual method of fibres being allowed to settle gently from a dilute suspension. The sedimentation took place in a one-liter graduated glass cylinder. The detailed procedure is described in Appendix XII.

### 3.3 Experimental Variables

Since little was known about the process of Type-C floc formation, each independent variable was investigated. The examined variables and their ranges are:

Fibre volume concentration (.0001-0.1)

Cylinder rotational speed (1.5-22 rad/s)

Cylinder incline (0,15,30,45,60,90 deg.)

Cylinder internal diameter (32-146 mm)

Fibre length (0.91-6.26 mm)

Fibre diameter (19.8, 27.9, 44.2  $\mu\text{m}$ )

Viscosity of the suspending liquid (0.001-0.14 Pa·s)

density (998-1315  $\text{kg/m}^3$ )

The effect of these variables on the appearance and behaviour of the suspension, specifically the formation of coherent flocs, was determined by visual observation and photographic techniques to be described later.

### 3.3.1 Fibre concentration

As described in Section 2.4, fibre concentration is a variable of the utmost importance in flocculation. The effect of this variable was studied by a dilute suspension being placed in the rotating cylinder and the suspension being thickened.

In the thickening procedure, a sample of rewetted fibres was first placed in a one-liter graduated cylinder fully filled with the suspending liquid. The concentration was low, about one tenth of the sediment concentration. At this concentration any fibre aggregates were easily dispersed with several strokes of a plunger having at one end a perforated rubber disk which fitted loosely inside the graduated cylinder. Next, the suspension was thickened by slow removal of liquid by suction into a 100 mL pipet. The pipet's tip covered with a 200-mesh screen prevented fibre removal. When the suspension volume in the graduated cylinder reached 500 mL, the suspension was transferred to the plexiglas cylinder.

The plexiglas cylinder was mounted on the rolling mechanism and rotated at constant speed. Further liquid removal was achieved by suction into a pipet which was inserted through the open top-end of the cylinder. The suspending liquid was removed in 5 mL increments until first occurrence of Type-C flocs, then the suspension volume was measured. The precision of volume measurement in a 500 mL graduated cylinder was  $\pm 5$  mL. For recognition of Type-C flocs from other flocs to be enhanced, the removal of the liquid was done in steps, i.e., each time 25 mL

was removed, 20 mL was reintroduced.

### 3.3.2 Density of the suspending liquid

The density difference between water and nylon which produced fibre sedimentation created visible fibre concentration near the bottom of the inclined cylinder so that the average suspension concentration did not represent the concentration at every zone in the suspension. This effect was eliminated by an aqueous-sugar solution that matched the apparent density of nylon fibres being used as the suspending liquid. Hence, most of the experimental work used the neutrally buoyant fibres in the aqueous-sugar solution. One exception was the experiment involving varying viscosities of the suspending liquid described in Section 3.3.5.

### 3.3.3 Cylinder diameter, angle of incline, and rotational speed.

The effects of physical dimensions of the rotating cylinder, cylinder angle of incline, and rotational speed on floc formation were examined.

Flocculation behaviour was observed in eight cylinders of internal diameters (ID): 32, 45, 56, 70, 82, 96, 121, and 146 mm. The 82 mm ID cylinder was rotated under various angles of incline to the horizontal: 0, 15, 30, 45, and 60 degrees. At a 45 degree incline, the 82 mm ID cylinder was rotated at various speeds. The rotational speed, controlled by a variable speed-drive, was changed from 5.2 to 78 rad/s on the driving roller. This range

of rotational speeds created velocities ranging from 0.061 to 0.90 m/s at the inner cylinder surface.

#### **3.3.4 Fibre dimensions - length and diameter**

Thalen and Wahren [T9] found that the fibre aspect ratio profoundly affected the sediment concentration which, in turn, corresponded to the concentration at which the shear modulus became a measurable quantity. Anticipating a major effect of fibre geometry on the limiting concentration below which Type-C flocs do not form [J3,J4,M10,S12,T9], thirteen fibre samples of various lengths and diameters were prepared. In this study, the aspect ratios for the thirteen fibre samples ranged from 32.7 to 189.1. Detailed information on fibre geometry is in Appendix V.

#### **3.3.5 Viscosity of the suspending liquid**

Steenberg et al. [S12] observed that the viscosity of the suspending liquid greatly influenced the elastic properties of the Perlon fibre networks in suspension. When Perlon suspensions having 0.015 volume concentration were tested in a double cylinder viscometer, the fibre network suspended in a viscous liquid showed much smaller shear modulus than the network suspended in a low viscosity liquid. Gradual change in the viscosity of the suspending liquid produced a step change in the shear modulus. This interesting behaviour required further investigation, specifically, verification of Type-C floc existence in high viscosity suspending media. This investigation varied the viscosity of the suspending liquid from 0.001 Pa·s to 0.14 Pa·s, covering the range in which a sudden drop in shear

modulus was reported by Steenberg et al. [S12]. Addition of sugar to water changes the viscosity and density of the suspending liquid, e.g., aqueous-sugar solution containing 64% sugar by weight has a density of  $1310 \text{ kg/m}^3$  and viscosity  $0.12 \text{ Pa}\cdot\text{s}$  [C10]. It should be noted that Perlon [T9] and nylon 6-6 have the same density.

### 3.4 Flow Patterns in Horizontal Rotating Cylinder

The flow field in a partly filled, inclined, rotating cylinder is unique and difficult to be characterized and measured. No description of it even for a single phase could be found in the fluid mechanics literature. A simpler flow which also produced coherent flocs of wood-pulp fibres occurs in a partially filled, horizontally oriented, long rotating cylinder [J3]. A description of flow of liquids (not suspensions) in such a cylinder has been given by Haji-Sheiks et al. [H1]. The flow field in a horizontal cylinder was more easily characterized but not measured. The length of the cylinder (172 mm) was too large to be penetrated by two beams of the Laser Doppler Anemometer. A shorter cylinder of length 36 mm was therefore used. Experiments showed that the flow in this short cylinder produced Type-C nylon flocs at the conditions found in the longer inclined cylinders.

The velocity profiles in the central plane of the 36 mm deep, 94 mm ID cylinder were determined with the TSI Laser Doppler Anemometer (LDA). Figure 7 shows the experimental setup. Details are given in Appendix XIII. Three flow cases were studied: one produced by a high viscosity suspending liquid

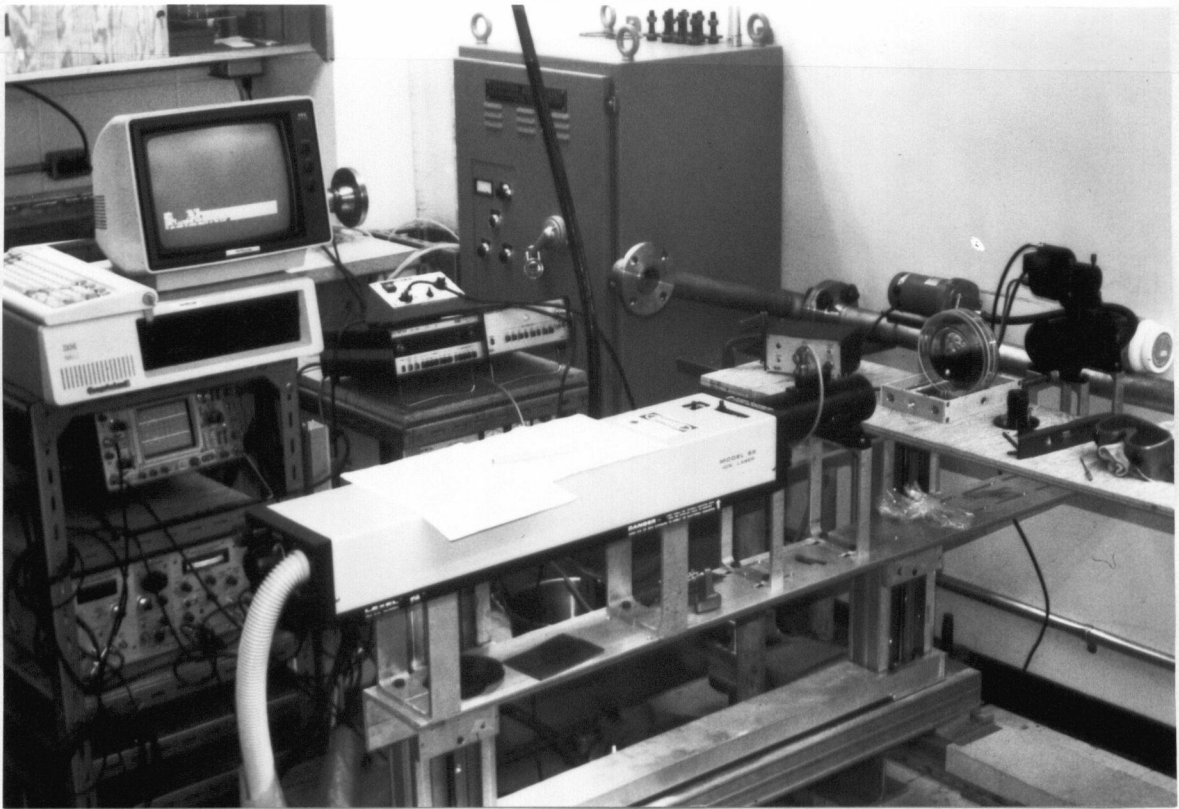


Figure 7. Experimental Setup for Velocity Measurements in a Horizontal Rotating Cylinder.

(0.14 Pa·s) where flocs did not form, and two others involving low viscosity suspending liquid (0.00375 Pa·s) before and after the Type-C flocs formed. These three flow cases were expected to reveal the mechanism by which the Type-C coherent flocs form. The experimental approach included an analysis of suspension flow patterns recorded by video-taping and cine-filming and was complemented by the measurements of the velocity profiles with the LDA. In all cases the cylinder was half-full of a suspension of 4.97 mm long, 44.2  $\mu\text{m}$  diameter nylon fibres. The cylinder was rotated at the constant angular speed of  $2\pi$  rad/s. The low and high viscosity suspending liquids had densities 1130 and 1315  $\text{kg/m}^3$  respectively.

### 3.5 Studies of Floc Structure

The physical properties of any 3-D fibre network are determined by the properties of individual fibres and their arrangement in space. While fibre properties are relatively easily measured, the spatial arrangement of fibres in the network is not. This explains why the theoretical models of fibre network proposed more than twenty years ago [M10,C5] have not been verified experimentally (equations (2) and (3)).

This study examined relationship between fibre concentration and the number of contact points per fibre in Type-C nylon flocs which were formed in the rotating cylinder at increasing levels of fibre concentration. The selected flocs removed from suspension were dried. During drying, sugar from the suspending liquid deposited on fibre surfaces and at fibre-to-fibre contact points. This deposition led to bonding between fibres. Those visible bonds which were close to the floc extremity were broken first. This freed some fibres which were subsequently removed from the floc. The newly exposed bonds were ruptured and next fibres were removed. The sequence of bond breaking and fibre removal continued until the floc was dismembered. The broken bonds and the removed fibres were counted. This tedious, time-consuming procedure was carried out on several flocs as described in Appendix XIV.

### 3.6 Floc Strength Measurement

The strength of individual flocs was measured. While flocs can be ruptured in certain flows, e.g., in a shear flow [L2] or in an extensional flow [K1], the disruptive force and the break zone are never certain. On the other hand, applying rupture force directly by physically restraining the floc with the load-sensing elements [G2] results in easy control of the mode of failure (shear, tensile or compression), the break zone, and the rate of floc deformation. This approach was used here. The tensile mode was selected because it seemed suitable for the verification of the concept of frictional fibre interlocking due to elastic bending.

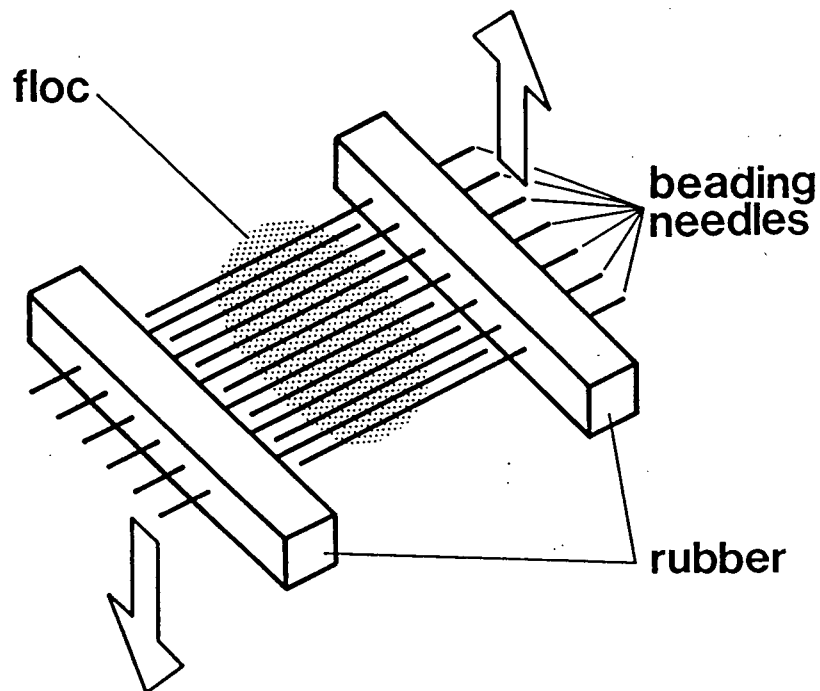


Figure 8. Schematic of Initial Comb Positioning in Tensile Tests.

The tensile strength of flocs formed at various concentrations in the rotating cylinder was measured. The flocs, removed from the suspension and placed in a tensile tester, were pierced by two intermeshing combs of beading needles<sup>1</sup> as shown in Figure 8. The needles secured to two rubber supports formed a retractable comb-like structure. The needles of one comb evenly interspaced those of the other comb. The floc was pulled apart as the combs separated in the direction indicated by the arrows. Details of this test method are in Appendix XV.

---

<sup>1</sup> Needles of small diameter used to string small pieces of glass, wood, stone etc. for ornamentation.

## 4 RESULTS AND DISCUSSION

The experimental investigation accentuates three aspects of Type-C cohesion: formation, structure, and strength of Type-C flocs.

### 4.1 Effect of Fibre Concentration on Floc Formation

Preliminary experiments had shown that flocs of nylon fibres, similar to wood-pulp fibre "coherent flocs" formed by Jacquelin [J3,J4], could be produced in an inclined rotating cylinder. Fibre concentration was increased by removal of the suspending liquid with a pipet while the suspension was in motion. The suspension was observed visually for formation of coherent flocs. Although, visual observations are subjective and therefore biased, in this case the observations were made simple through the careful selection of the experimental system as described in Section 3.1.1. The subjective evaluation was limited to simple a "yes" or "no" decision. A strong spotlight illuminating the entire suspension enabled assessment of the suspension state at any depth. Cyclic, unsteady flow produced good mixing which forced fibres and flocs to the surface or to approach transparent cylinder walls so that the detection of Type-C flocs was facilitated. The inclined cylinder arrangement made the suspension handling and the removal of the suspending liquid easy.

With increasing concentration, the suspension appearance changed from uniformly dispersed, (Figure 9a) to cloudy (Figure 9b). The cloudiness intensified with increasing

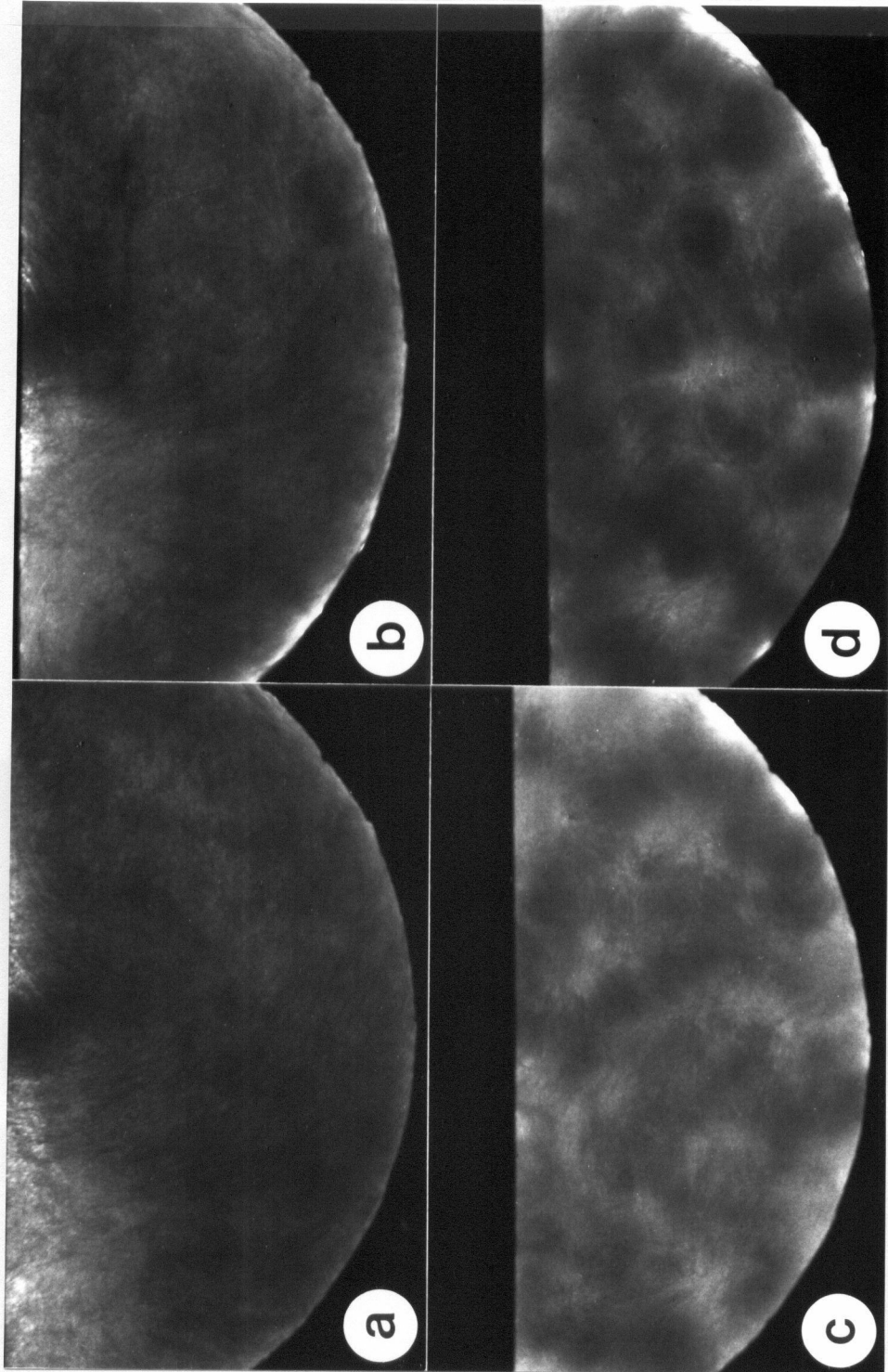


Figure 9. Increasing Cloudiness with Increase in Fibre Concentration.

concentration, (Figure 9b,c,d), but the individual clouds (flocs) formed and then disappeared. While flocs were always present in the flow, they did not remain for long in the flow as entities. Rather, flocs appeared to be in a state of continual dispersion and formation. This process was similar to the "dynamic equilibrium" described by Mason [M4], and experimentally demonstrated by Hubley [H8]. It should be noted that the dynamic state observed in this study occurred at concentrations of one order of magnitude greater than those of Hubley et al. [H8], i.e.,  $C_{va}=0.02$  versus  $C_{va}=0.001$  for fibres of similar aspect ratio.<sup>1</sup>

The cloudy nature of the suspension could be diminished at any time by reintroduction of the suspending liquid into the suspension. The cloudy appearance could be eliminated altogether if the suspension was rediluted to the initial concentration. This indicates a reversible process of floc (cloud) formation.

Further increases of suspension concentration by removal of liquid resulted in a condition in which the suspension appearance changed from cloudy to grainy, as shown in Figure 10a,b. This change in appearance was accompanied by the formation of nylon flocs that persisted through the recirculating flow as identifiable entities, i.e., coherent flocs. Moreover, these flocs did not disperse even when the suspension was rediluted, as shown in Figure 10c, provided the rotational speed was not increased. In Figure 10c, the average fibre concentration, is

---

<sup>1</sup> Assuming  $WRRk=2$  g/g for wood-pulp fibres which had  $L=0.45$  mm,  $d=30$   $\mu$ m giving an average  $L/d=52.5$ .  $WRRk$  is discussed in Appendix I and II.

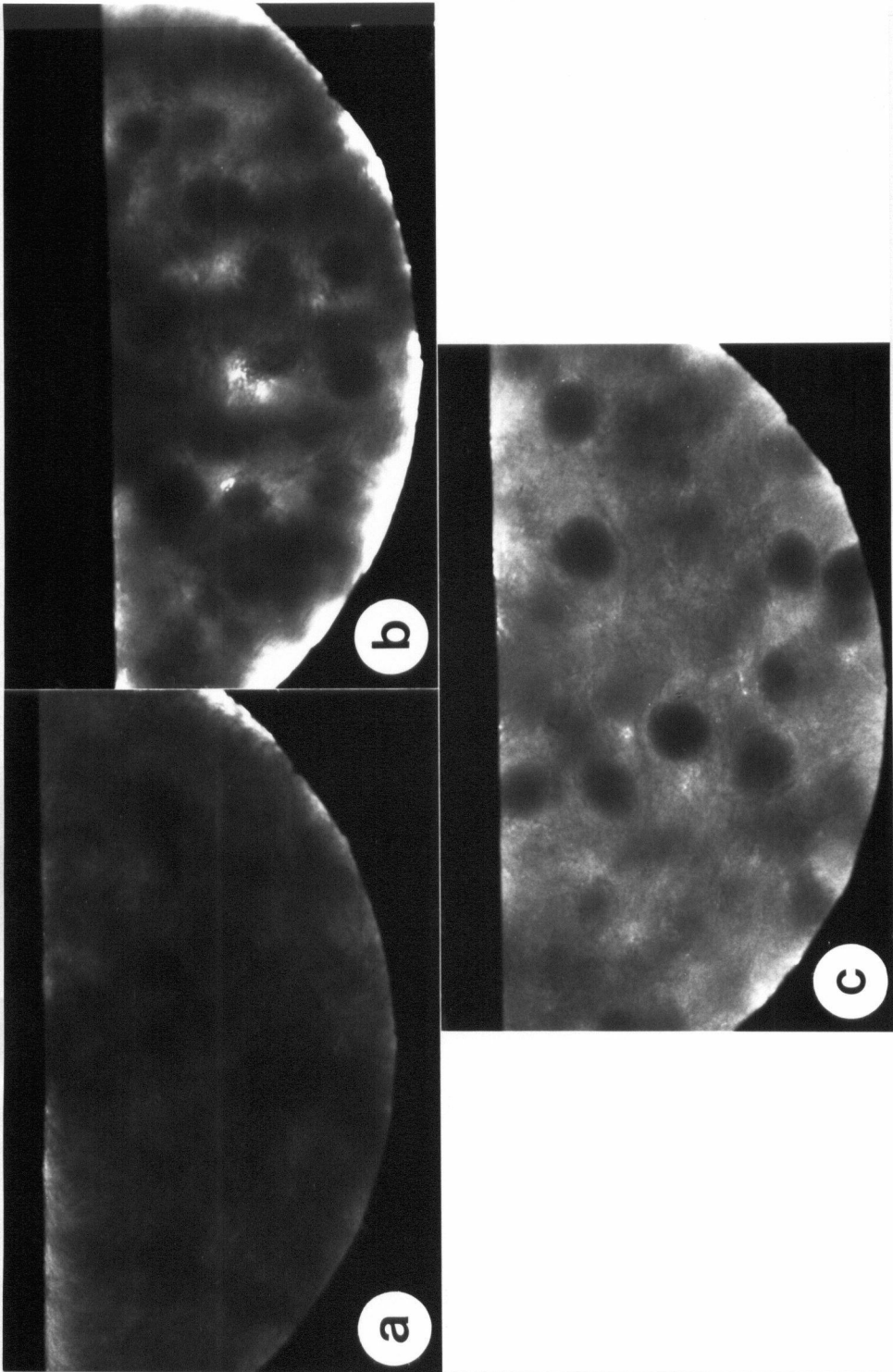


Figure 10. a. Cloudiness; b. Granularity; c. Granules in rediluted Suspension.

the same as the initial fibre concentration in Figure 9a. This illustrates the permanent change in suspension appearance. Suspension redilution helped visual identification of flocs and demonstrated the irreversible process of floc formation.

It had been shown earlier by selection of fibres and the experimental conditions that only Type-C cohesion existed in the suspension of fibres. Thus, these flocs may be labelled Type-C coherent flocs. For convenience, they will be called Type-C flocs through the remainder of this study.

Experiments with dyed fibres confirmed the existence of the irreversible process of floc formation. First, two separate batches of fibres were prepared. One batch contained translucent fibres and the other red-dyed fibres. Second, red Type-C flocs were formed and individually transferred to the batch of translucent fibres. The suspension rotation started and its concentration was gradually increased to produce translucent Type-C flocs. After five minutes, rotation was halted and all flocs were examined by dissection. Not one translucent fibre was found inside the red floc centres. This shows that the initially formed flocs always remained coherent. In another experiment, red fibres were added to the suspension of translucent fibres at the cloudy state of suspension appearance, i.e., at fibre concentration below the threshold concentration. Subsequently, concentration was increased to form Type-C flocs. Examined flocs were found to be a mixture of colored fibres.

These observations indicate that flocs of significant strength can form and resist rupture by the hydrodynamic forces exerted upon them in their cyclic flow within the cylinder. As stated earlier, the floc strength must have come from elastic bending because the possibility of other forms of cohesion had been eliminated. With the procedure described in Section 3.2, the existence of elastic interlocking was verified by comparison of the relative strength of heat-treated (above the glass transition temperature) flocs and never-heated flocs. Gentle stirring easily dispersed the former flocs but the latter flocs did not disperse at all. In fact, vigorous agitation was required to disperse the never-heated flocs. It therefore appears that the source of floc strength is truly one from fibre interlocking by elastic bending.

The tests involving increasing suspension concentration in the rotating cylinder also showed that, for a given fibre type and at given flow conditions, there exists a reproducible concentration at which Type-C flocs form and do not disperse on continuous passage through the flow. This leads to the conclusion that Type-C flocs have acquired sufficient strength to withstand hydrodynamic forces acting upon them at a reproducible level of fibre crowding. The concentration at which Type-C flocs form is termed the threshold concentration, and marked  $C_{va}^*$ .<sup>1</sup> When this concentration had been exceeded, the Type-C flocs formed instantaneously, i.e., within a period of time which was

---

<sup>1</sup> Threshold concentration is expressed as an apparent volumetric concentration throughout this dissertation. Its numerical values are reported as fractions.

necessary to concentrate suspension, between 10 to 20 seconds. The process of Type-C floc formation was fast, unlike that described by Jacquelin [J3] for coherent flocs of wood-pulp fibres. His coherent flocs formed over hours of stirring.

It must be emphasized that the threshold concentration is not an absolute concentration at which Type-C cohesion initiates, but it is an experimental condition required for Type-C flocs formation in a unique type of flow. Subsequent sections show that the threshold concentration is independent of some experimental variables and strongly dependent on others.

#### 4.2 Observations of Origin and Growth of Type-C Flocs

Experiments were carried out to determine the mechanism by which Type-C flocs formed. The dyed fibres helped visual observations. At low concentrations below the threshold concentration, it was observed that, during circulation, the suspension truncated into groups of fibres, (earlier termed "clouds"). As the concentration was increased, some of these clouds become denser and transformed into Type-C flocs. These flocs acted as nuclei; they grew by acquisition of new fibres and became denser with increased suspension concentration. Thus, the forming process of Type-C flocs appears to consist of two stages - nucleus formation and fibre accumulation. A similar mechanism of coherent floc formation was described by Jacquelin [J3] and Lee [L2] for wood-pulp fibres. However, they formed coherent flocs starting with "concentrated" suspensions, whereas in this study the initial suspensions were "semiconcentrated" as defined

in the Literature Review and illustrated in Figure 4. The shape of Type-C flocs appeared to be spheroidal.

At a given concentration, after Type-C flocs formed and after prolonged rolling over many minutes, all flocs adopted a smoother "surface" and became more spherical. The number of flocs became fixed. That an increase in the floc density was not detectable suggests that the prolonged rolling produced only changes in the floc's appearance. In comparison, Jacquelin found that, for wood-pulp fibres, stabilization in floc number occurred after about five hours and that the maximum in T.F.C. was reached after about 12 hours of rolling. These seemingly diverse observations are the result of different experimental approaches. In this study, suspension concentration was gradually increased from semiconcentrated to a level above the threshold concentration. In Jacquelin's experiments, the initial suspension concentration was already well above the threshold concentration. In this study, the development of Type-C flocs was paralleled by the dilution of the remaining suspension so that the formation of additional Type-C flocs was hindered. These events occurred within the short time required (about one-half minute) for the suspension to be concentrated. In Jacquelin's experiments, on the other hand, the formation and densification of coherent flocs occurred simultaneously. As the suspension truncated into coherent flocs which were gradually compacted and reshaped, the concentration of the suspension external to these flocs remained high so that new flocs formed, changed shape and became denser. This sequence of events may

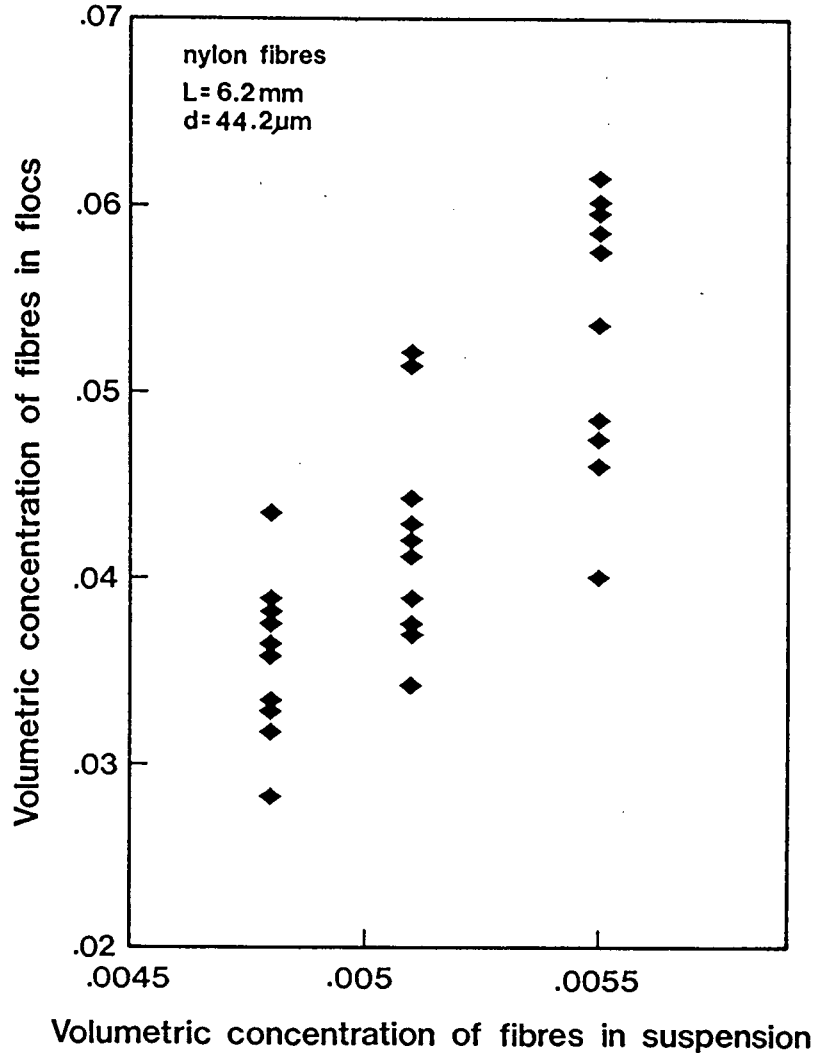


Figure 11. Floc Concentration versus Suspension Concentration.

explain the long times (hours) needed for a stable number of coherent flocs of wood-pulp fibres to be reached. The maximum in T.F.C. was reached even later, probably due to the processes associated with the growth and compaction of flocs that seem to be slower in the case of wood-pulp fibres.

The increase in suspension concentration when Type-C flocs had formed led to the densification of all Type-C flocs. Some flocs appearing more dense than the others indicated that floc

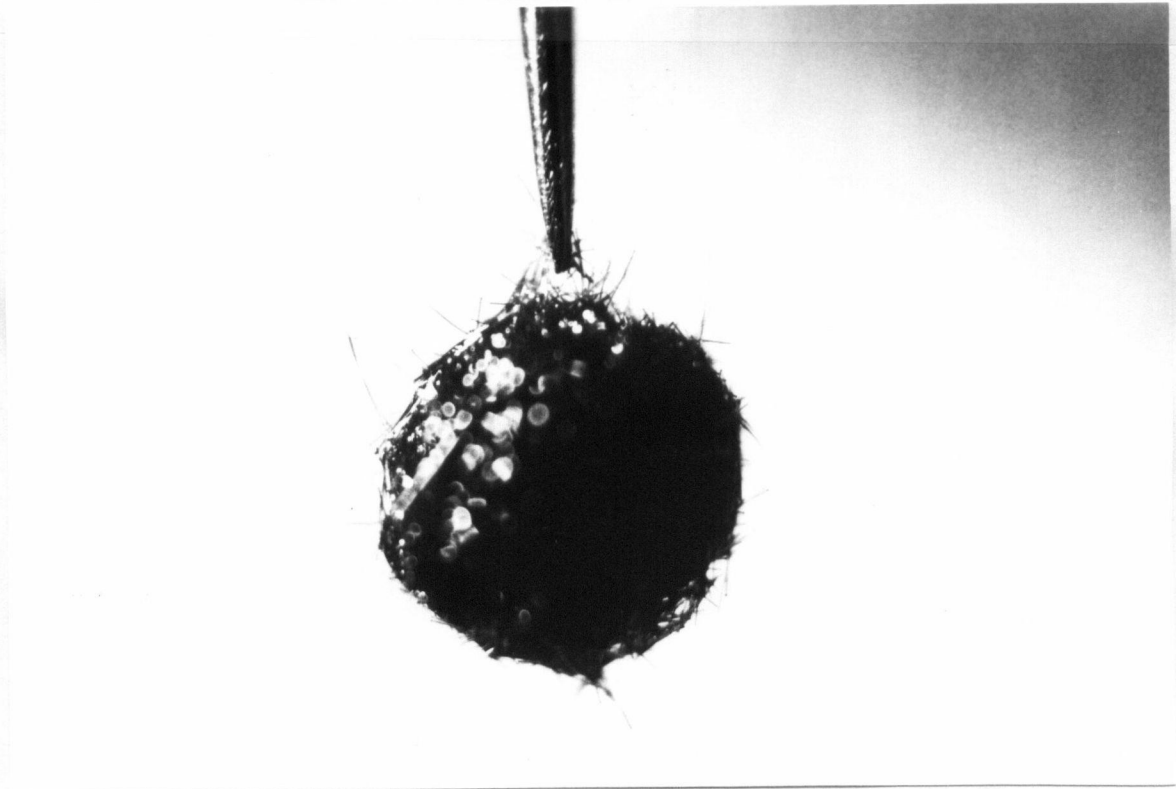


Figure 12 Floc Weighing 0.12 g Suspended in the Air by Few Fibres.

formation was not uniform. The densification process occurred instantaneously with the 10 to 30 second removal of the suspending liquid. The densification seems to result from gradual reduction of the space within which a certain number of flocs exists. Since the suspension volume is reduced, the flocs grind against surrounding fibres and against cylinder walls, or protrude through the free surface. Which of these actions or which combination of them contribute most to floc densification is not known. It is known that floc density increases with increased suspension concentration, as shown in Figure 11. Three samples of ten flocs each were drawn from the same suspension but at different concentrations. Although variations

in floc density are large within each sample, the increase in floc concentration with an increase in suspension concentration is clearly visible. When the prolonged rolling was combined with the gradual increase in suspension concentration, very strong cohesion developed, e.g., by pulling of a few fibres protruding from the surface, Type-C floc could be lifted from the suspension, as shown in Figure 12.

#### 4.3 Effect of Key Variables on Threshold Concentration

The next step in this experimental program was to establish the dependence of the threshold concentration on fibre and flow properties.

As stated in Section 3.3.2, the density difference between nylon fibres and water caused fibre sedimentation which created a zone of high fibre concentration at the lowest part of the cylinder. Accordingly, aqueous-sugar solutions of the same density as that of nylon fibres were used as the suspending medium. The effect of the density difference on the threshold concentration was examined with all other variables constant. Table VIII shows the difference between the threshold concentrations for the nylon fibres in pure water and in aqueous-sugar solutions.<sup>1</sup> Null hypotheses for the averages were tested using Student-t distribution. Calculated 't' values exceeded the tabulated values [B7] even at the 0.001 level of significance (see Table VIII). The null hypotheses were rejected, i.e., the effect of the suspending liquid density on

---

<sup>1</sup> Tables of experimental data are in Appendix XXVI.

Table VIII. Threshold Concentrations for 15 Denier Nylon Fibres in Water and in Aqueous-sugar Solution.

FIBRE LENGTH mm	THRESHOLD CONCENTRATION STATISTICS						t-TEST OF NULL HYPOTHESIS (MEAN1-MEAN2)	
	FIBRES IN WATER			FIBRES IN AQUEOUS-SUGAR SOLUTION			CALCULATED t	DEGREES OF FREEDOM
	No. OF TESTS	MEAN1	STANDARD DEVIATION	No. OF TESTS	MEAN2	STANDARD DEVIATION		
2.947	6	.01892	.0005224	8	.02221	.0006022	-10.68	12
4.973	8	.007004	.0001925	9	.007915	.0002300	- 8.780	15
6.261	8	.003620	.0001577	7	.004469	.0002267	- 8.518	13

the threshold concentration was significant in all cases. In fact, fibre sedimentation resulted in localized crowding of fibres in the lowest part of the cylinder. The average suspension concentration in such a case was lower than that recorded in a neutrally buoyant fibre suspension. The sedimentation effect was eliminated when the nylon fibres were suspended in the aqueous-sugar solutions to render them neutrally buoyant in all experiments but one - that determining the effect of suspending liquid viscosity on the threshold concentration.

#### 4.3.1 Cylinder (flow) variables

The effect of flow variables on the threshold concentration was first examined with various cylinder diameters, angles of incline and rotational speeds. Every possible variable was investigated since Type-C nylon flocs have been formed for the first time in the partially filled rotating cylinder. Fibres 4.97 mm long and 44.2  $\mu\text{m}$  diameter were used in these investigations.

In cylinders having internal diameters from 56 to 146 mm Type-C flocs formed and the cylinder diameter had no effect on threshold concentration. This is illustrated in Figure 13 where 95% confidence limits are also shown.<sup>1</sup> In these cylinders partly filled with suspensions, a complex recirculating flow formed. In cylinders of internal diameter 32 mm and 45 mm, such flow did not exist. Rather, fibres aggregated into large bodies which rolled

---

<sup>1</sup> Threshold concentration is expressed as an apparent volumetric concentration throughout this dissertation. Its numerical values are reported as fractions.

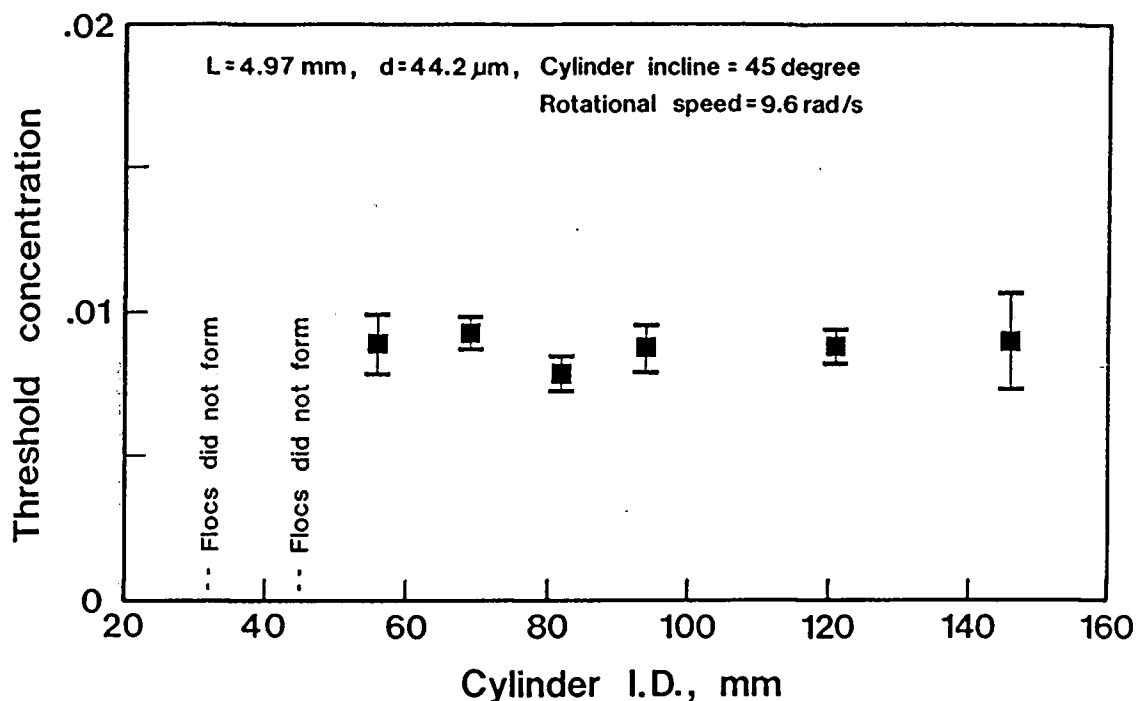


Figure 13. Effect of Cylinder Diameter on Threshold Concentration.

erratically within cylinders and Type-C flocs did not form. It can be postulated that an internal diameter of a cylinder should be more than  $(2 \cdot R/L \approx 9)$ , i.e., nine times larger than fibre length for a proper recirculating flow for Type-C floc formation to be produced.

Angles of incline from 0 to 45 degree had no effect on the threshold concentration, as shown in Figure 14. However, no flocs formed at angles of 60 and 90 degrees at which the suspension was observed to adopt solid body rotation, whereas at lower angles it had a complex recirculating flow pattern. Thus, the supposition based on the results of this and the previous experiment can be made that a recirculating flow is needed to produce Type-C nylon flocs. This flow is analyzed in further

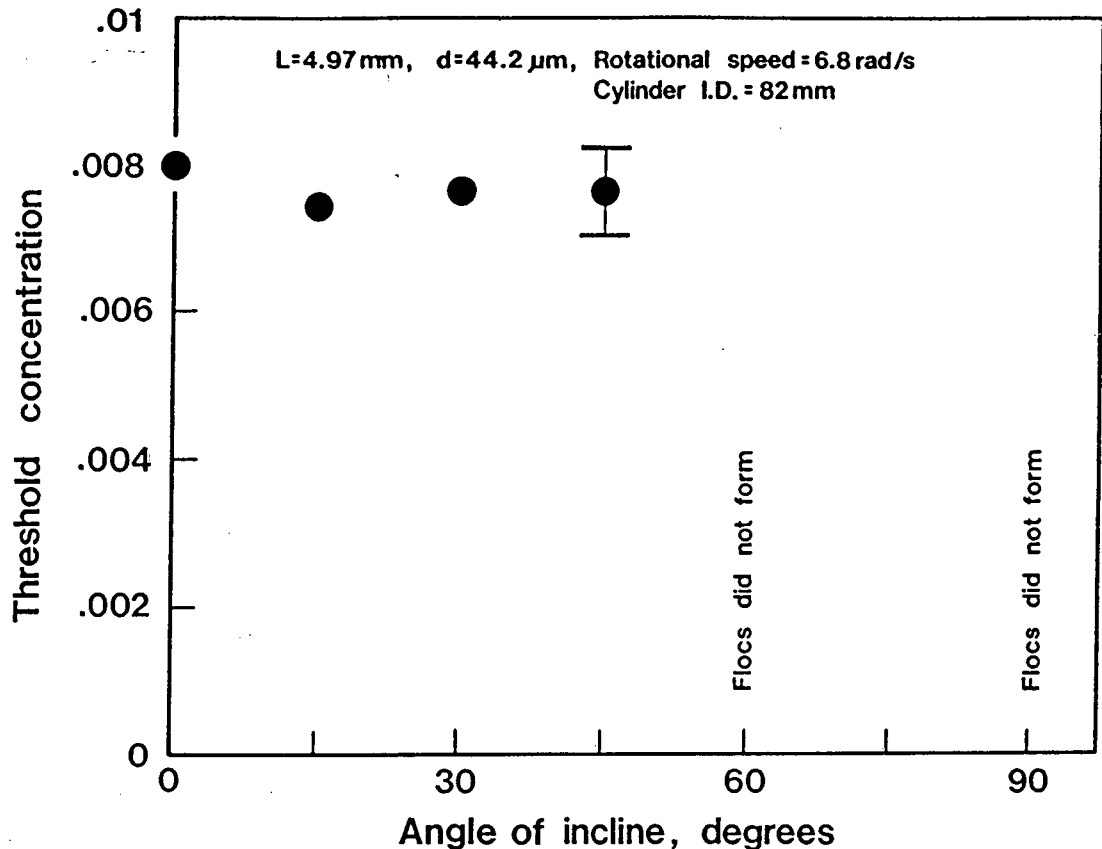


Figure 14. Effect of Cylinder Incline on Threshold Concentration.

detail in Section 4.5.

It was found that a minimum angular speed was necessary for relative motion in the suspension to be created. Below this minimum the suspension was relatively stationary as the cylinder rotated. The velocity gradient was confined to a thin annulus between the cylinder wall and the fibre suspension; there was no relative motion within the suspension. This flow condition is similar to the "plug flow" regime of pulp suspensions in pipes [C4,R6] but with one difference that the wall is moving and the suspension is stationary. At higher angular speeds above 4

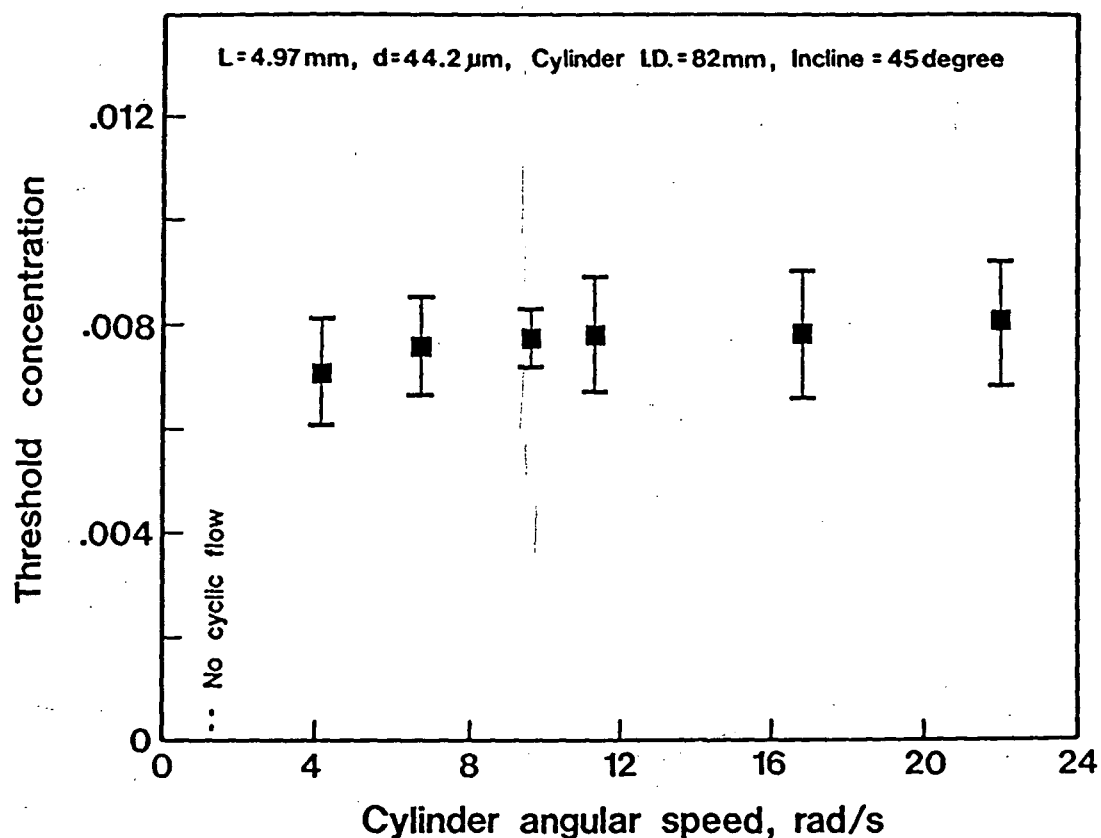


Figure 15. Effect of Angular Speed on Threshold Concentration.

rad/s, the recirculating motion was produced within the fibre suspension in the 82 mm ID cylinder. Under such a condition, Type-C flocs formed as soon as the threshold concentration was reached. When the angular speed had exceeded 4 rad/s, the threshold concentration was unaffected by it. This is illustrated in Figure 15 where 95% confidence limits are also shown.

As the rolling speed increased, the total number of Type-C flocs visibly decreased, but the threshold concentration was unaffected. The shear layer at the cylinder walls at which

fibres were well dispersed grew in thickness with increasing rotational speed. It seems that the floc-forming phenomenon was countered by the dispersive action of this shear layer. Jacquelin [J3] also noted the reduction in the mass content of coherent flocs (T.F.C.) as the rolling speed increased. The absence of coherent networks in Forgacs et al. [F1] apparatus could have been caused by high shear rates present there.

The data and statistics for experiments described in this chapter are in Appendix XXVI.

#### 4.3.2 Suspending liquid viscosity

The effect of suspending liquid viscosity on the threshold concentration was examined with aqueous-sugar solutions of varying sugar content and one type of fibres (length=4.97 mm and diameter=44.2  $\mu\text{m}$ ). The results are shown in Figure 16. The data and statistics are in Appendix XXVI. Initially, the threshold concentration increased with viscosity. In conjunction with this, smaller numbers of weaker flocs formed. However, above 0.013 Pa·s, Type-C flocs did not form at all. At viscosity 0.033 Pa·s, the suspension adopted a cloudy appearance, but at 0.14 Pa·s the suspension appeared uniform. At viscosities higher than 0.013 Pa·s, no Type-C flocs formed. Indeed, the concentration was increased to the point at which all fibres formed a "solid," i.e., there was insufficient suspending liquid to have a suspension.

The magnitude of viscous interaction between fluid and fibres can be illustrated by the calculation of the terminal

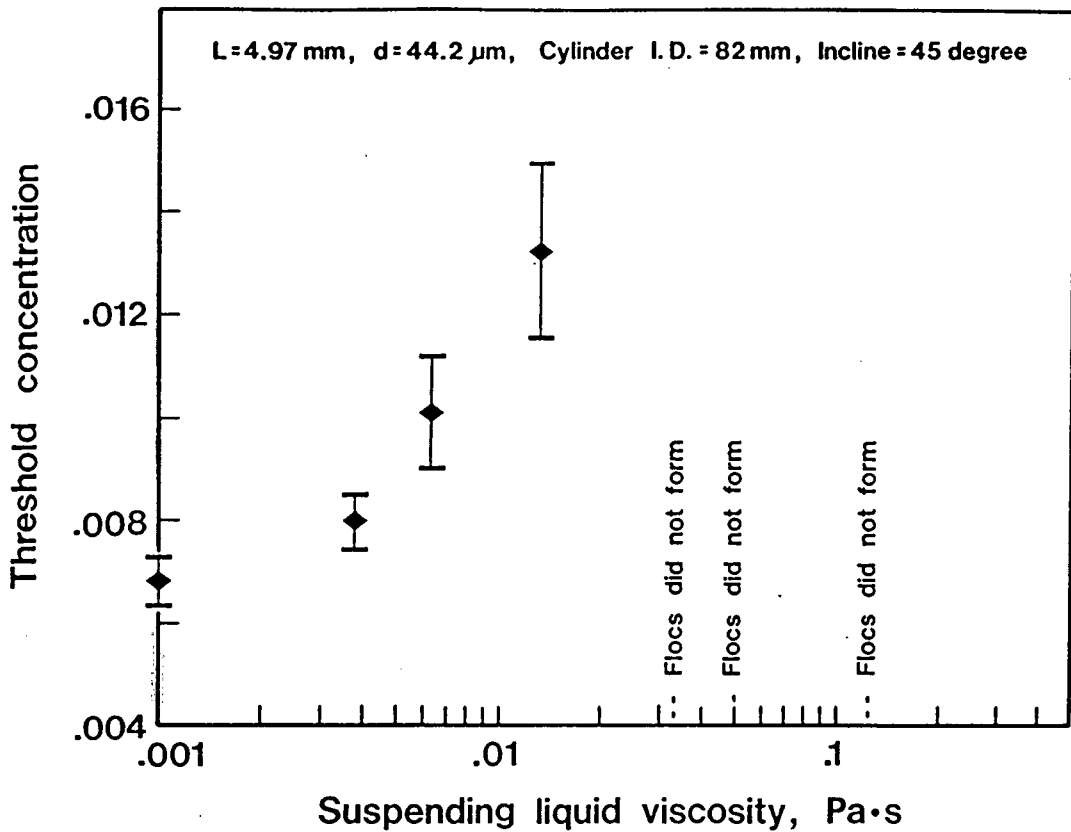


Figure 16. Threshold Concentration versus Viscosity of the Suspending Liquid.

velocity and the terminal Reynolds number for a single fibre [C6,C7] in the examined suspending liquids. The results of such calculations, shown in Table IX, indicate that a single particle or a collection of particles in a dilute, stationary suspension would undergo creeping rise or sedimentation. Thus, the motion of fibres under net buoyancy forces is very slow. It is a reasonable conclusion that fibres follow the steady flow very closely, i.e., the relative velocity between individual fibres and fluid is very small.

Table IX. System Characteristics for Suspensions of Nylon Fibres (L=4.97 mm, d=0.0442 mm) in the Suspending Media of Various Viscosities.

SUSPENDING MEDIUM		DENSITY RATIO $\rho_p/\rho$	TERMINAL VELOCITY		TERMINAL REYNOLDS NUMBERS *	
DENSITY $\rho$ kg/m <sup>3</sup>	VISCOSITY $\mu$ Pa.s		AXIAL MOTION $U_{T1}$ mm/s	CROSS-AXIAL MOTION $U_{T2}$ mm/s	AXIAL MOTION $Re_{T1}$ --	CROSS-AXIAL MOTION $Re_{T2}$ --
998	0.00100	1.13	1.4565	0.8862	$6.42 \times 10^{-2}$	$3.91 \times 10^{-2}$
1130	0.00336	1.00	0.0	0.0	0.0	0.0
1175	0.00602	0.96	0.0825	0.0502	$7.11 \times 10^{-4}$	$4.33 \times 10^{-4}$
1220	0.0129	0.926	0.0770	0.0468	$3.22 \times 10^{-4}$	$1.96 \times 10^{-4}$
1265	0.0327	0.893	0.0455	0.0277	$7.79 \times 10^{-5}$	$4.74 \times 10^{-5}$
1280	0.0498	0.882	0.0332	0.0202	$3.77 \times 10^{-5}$	$2.30 \times 10^{-5}$
1315	0.144	0.859	0.0142	0.0086	$5.72 \times 10^{-6}$	$3.48 \times 10^{-6}$

\* Based on the terminal velocity, fibre diameter, and kinematic viscosity of suspending liquid.

The flow in a partly filled, inclined, rotating cylinder is unsteady; it decelerates and accelerates while changing directions. The fibres do not tend to follow such a flow closely, they crowd where the flow decelerates and accelerates. The degree of crowding depends on the viscosity of the suspending liquid and the concentration of fibres, both counteracting each other. As the viscosity increased and the crowding tendency of fibres decreased, this had to be compensated for by increased fibre concentration for Type-C coherence to be produced, as is clearly visible in Figure 16. There existed, however, a viscosity above which the crowding did not result in Type-C floc formation. This viscosity must be slightly higher than 0.013 Pa·s under these experimental conditions.

Comparison of these findings with those reported by Steenberg et al. [S12] is interesting. They examined the effect of suspending liquid viscosity on the shear modulus of suspensions of Perlon fibres at the volumetric concentration of 0.015 and reported that the shear modulus decreased as the viscosity of the suspending medium increased. Their data show a dramatic drop in the shear modulus from  $100 \text{ N/m}^2$  in water (0.001 Pa·s), to less than  $3 \text{ N/m}^2$  in a very viscous medium (1.0 Pa·s).<sup>1</sup> The steep drop occurred within a viscosity change from 0.01 to 0.05 Pa·s. Steenberg et al. attributed the drop to *the change in the relationship between viscous forces from the suspending liquid and the elastic forces of fibres*. Referring to intense agitation as the process of coherent network formation,

---

<sup>1</sup> These data have been reproduced in Figure 3 of this dissertation.

they reasoned that *it takes longer for the fibres to come to rest after agitation in more viscous medium; hence, the elastic energy of many of them may be dissipated and unstrained configurations will result. Once fibres lost their elastic energy, they cannot become actively engaged in the network however much time elapses.*

Because this explanation does not consider the restraining action of surrounding fibres at the concentration in question, their explanation is incomplete. It is not clear how the fluid viscosity can play the predominant role in dissipating the elastic energy of fibres when the latter are in a continuous, multiple contact with one another.

In summary, the gradual increase in the suspending liquid viscosity produced flow conditions that progressively eliminated the fibre interlocking into flocs. Clearly the viscosity plays a strong role in Type-C floc formation in the recirculating flow which is unsteady (this study) as well as in the highly agitated flow which decayed (other studies). In the recirculating flow, the fibres may align themselves to avoid formation of the isotropic 3-D networks or can follow the flow so closely that the fibre crowding is nonexistent. It is also conceivable that both effects occur at the same time. In the highly agitated suspension the picture of fibre motion is more complex, but it may include these effects.

Although the density of the suspending liquid changed with viscosity, it only changed by the factor of 1.32 whereas the viscosity changed more than one hundred times.

### 4.3.3 Fibre geometry

The threshold concentration was found to be profoundly affected by the dimensions of fibres. The dimensions of wet fibres used in these experiments are shown in Table X. As fibre length,  $L$ , increased, the threshold concentration decreased (Figure 17). Experimental data concerning the effect of fibre geometry on the threshold concentration are in Appendix XXVI. Moreover, for a given diameter,  $d$ , there appears to be a lower limit of fibre length,  $L$ , below which no Type-C flocs form in the circulating suspension regardless of how high fibre concentration is. This suggests a lower limit of fibre length or possibly lower limit of fibre aspect ratio at which Type-C flocs cannot form. This subject is expanded in Section 4.4.

Another rarely discussed variable related to the three alternate contact interlocking is fibre deflection. Intuition suggests that fibres deflect more as they are brought more closely together in the Type-C network. Similarly, short fibres must bend more to interlock since the distances between their centers are smaller as indicated by the increased fibre concentration in Figure 17, i.e., cohesion cannot develop if the fibre-bending forces (compaction forces) are too low. This seems to be the case for floc formation in rotating cylinders because Type-C flocs can be formed from the shortest fibres of this study by fibres being compacted between fingers. Thus, it may be concluded that the limiting condition for floc formation in rotating cylinders was not fibre length, but the intensity of fibre crowding. Nevertheless, it is reasonable to expect that

Table X. Nylon Fibre Dimensions in Wet State.

TYPE OF FIBRE	DIAMETER $d$	SAMPLE SIZE	FIBRE LENGTH		ASPECT RATIO $L/d$	CURVATURE	
			AVERAGE LENGTH $L$	STANDARD DEVIATION		AVERAGE $1/R$ **	STANDARD DEVIATION
denier*	$\mu\text{m}$		mm	mm		$\text{mm}^{-1}$	$\text{mm}^{-1}$
3	19.76	1062	0.9158	0.08484	46.35	0.3094	0.2132
		1054	1.875	0.09244	94.88	0.2553	0.1719
		1231	2.815	0.1019	142.5	0.2811	0.1933
		1117	3.737	0.1122	189.1	0.2855	0.1881
6	27.95	1237	0.9139	0.08322	32.70	0.1696	0.1453
		1138	1.832	0.09898	65.55	0.1522	0.1113
		1042	2.757	0.1267	98.65	0.1618	0.1195
		1049	3.718	0.1576	133.0	0.1297	0.1003
		1024	4.666	0.1338	166.9	0.1370	0.1034
15	44.19	1038	1.560	0.1009	35.30	0.08366	0.08033
		1162	2.947	0.1081	66.69	0.07240	0.06239
		1001	4.973	0.1762	112.5	0.07107	0.05731
		1006	6.261	0.1769	141.7	0.06060	0.05105

\* Denier is a weight in grams of 9000 meters long monofilament.

\*\* R denotes a radius of curvature.

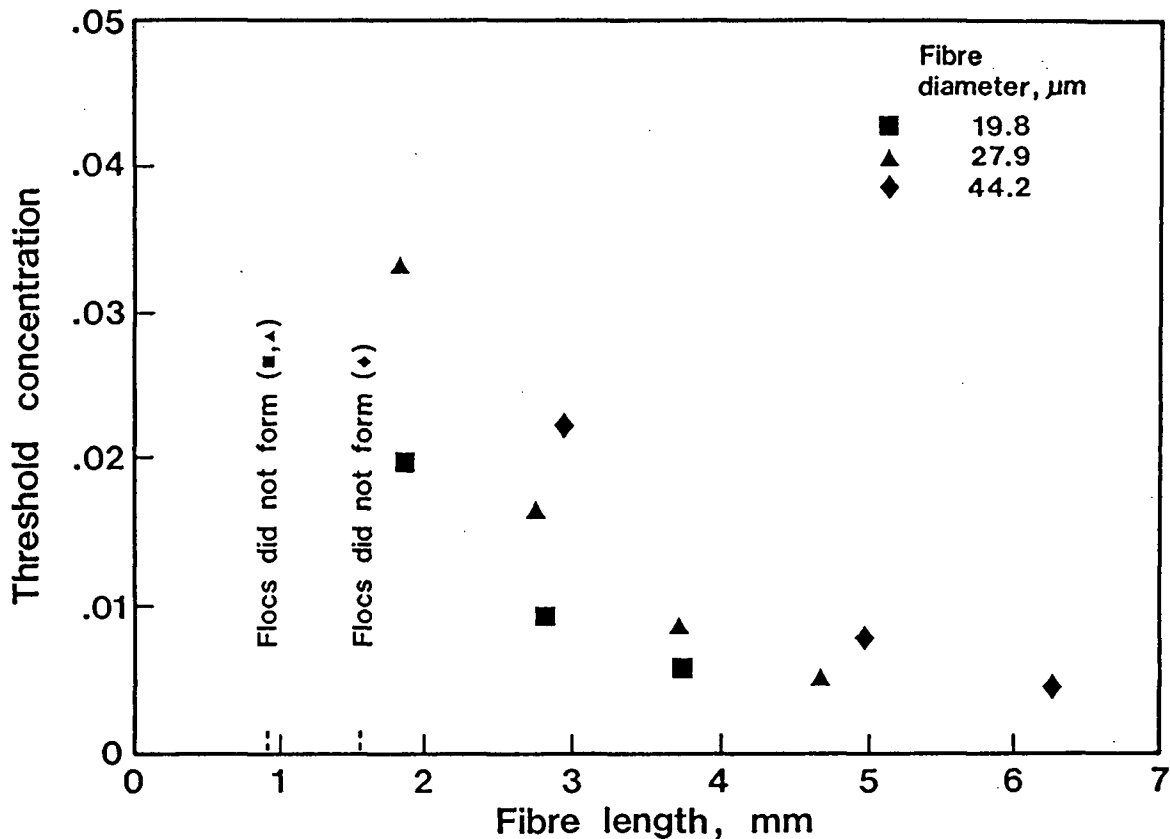


Figure 17. Effect of Fibre Length and Diameter on Threshold Concentration.

the lower limit of fibre length or fibre aspect ratio should exist below which fibres cannot interlock elastically in a 3-D network. This interlocking cannot develop regardless of the magnitude of the fibre bending forces.

A strong effect of fibre diameter,  $d$ , on the threshold concentration is also visible. As fibre diameter increases for a given fibre length, the threshold concentration increases. It should be noted, however, that doubling of fibre diameter in a random 3-D network should increase the volumetric concentration about three times. The estimated increase, based on Figure 17,

is slightly less than three when the fibre diameter more than doubles: 19.8 to 44.2  $\mu\text{m}$ . It must also be noted that the total number of fibres in a unit volume should double if the diameter is halved. Values close to that have been observed, and are discussed in the next section. Thus, the effect of fibre diameter on threshold concentration is accounted for in large part on the basis of network geometry.

Fibre diameter is a key factor affecting fibre stiffness,  $S$ , where  $S = \pi \cdot E \cdot d^4 / 64$ . Figure 18 shows the threshold concentration plotted versus  $d^4$  for a constant fibre length,  $L$ , as well as for

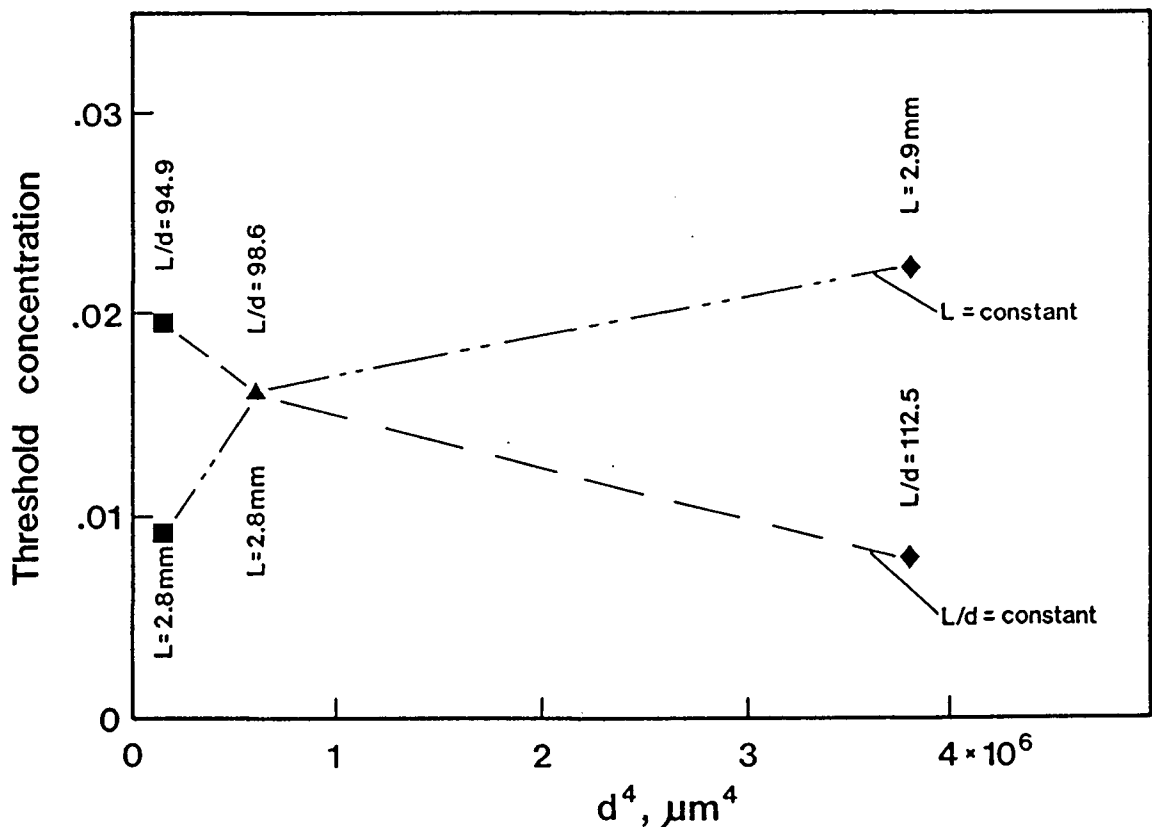


Figure 18. Threshold Concentration versus  $d^4$ .

a constant fibre aspect ratio,  $L/d$ . Such a plot is justified because the differences between the elastic moduli of the wet nylon fibres are small. The elastic moduli were determined experimentally and are reported in Appendix VIII. At a constant  $L$ , the increasingly stiffer fibres produce cohesion at higher concentrations whereas at a constant  $L/d$ , the trend is reversed. The fibre length and diameter clearly affect the threshold concentration in a complex way.

#### 4.4 Evaluation of Criteria for Threshold Concentration

The criteria for threshold concentration are evaluated with the experimental observations of this investigation.

##### Threshold and Sediment Concentrations.

It was proposed [T9] that the sediment concentration is an estimate of the lowest concentration at which coherent network strength may be detected. This postulate can be tested by the sediment concentrations being compared to the threshold concentrations measured in this study. For fibres having diameters 19.8 and 27.9  $\mu\text{m}$ , the sediment concentrations are systematically lower than the threshold concentrations, as shown in Figure 19 and in Table XI.<sup>1</sup> On the other hand, for the 44.2  $\mu\text{m}$  diameter fibres, the situation is reversed. There is no systematic agreement between the sediment and the threshold concentrations, though both have similar trends with respect to  $L/d$ . This finding indicates that the sedimented fibres form

---

<sup>1</sup> The data and statistics from sedimentation experiments are in Appendix XXIX.

Table XI. Threshold Concentrations and Sediment Concentrations.

FIBRE DIAMETER (WET) d $\mu\text{m}$	AVERAGE FIBRE LENGTH (WET) L mm	FIBRE ASPECT RATIO L/d	THRESHOLD CONCENTRATION		SEDIMENT CONCENTRATION	
			APPARENT VOLUMETRIC $C_{va}^*$	STANDARD DEVIATION $\sigma$	APPARENT VOLUMETRIC $C_{va}^s$	STANDARD DEVIATION $\sigma$
19.76	0.9158	46.35	NO FLOCS	-	.03517	.0005677
	1.875	94.88	.01972	.0005615	.01154	.001637
	2.815	142.5	.009334	.0002908	.005373	.0006473
	3.737	189.1	.005791	.0004115	.003132	.0003314
27.95	0.9139	32.70	NO FLOCS	-	.04786	.003088
	1.832	65.55	.03314	.001350	.02182	.001091
	2.757	98.65	.01641	.001124	.008173	.001220
	3.718	133.0	.008549	.0007753	.006043	.0008337
	4.666	166.9	.005099	.0001874	.003812	.0003147
44.19	1.560	35.30	NO FLOCS	-	.05572	.004084
	2.947	66.69	.02221	.0006021	.02427	.001249
	4.973	112.5	.007915	.0002300	.00976	.0007970
	6.261	141.7	.004469	.0002266	.005416	.0005382

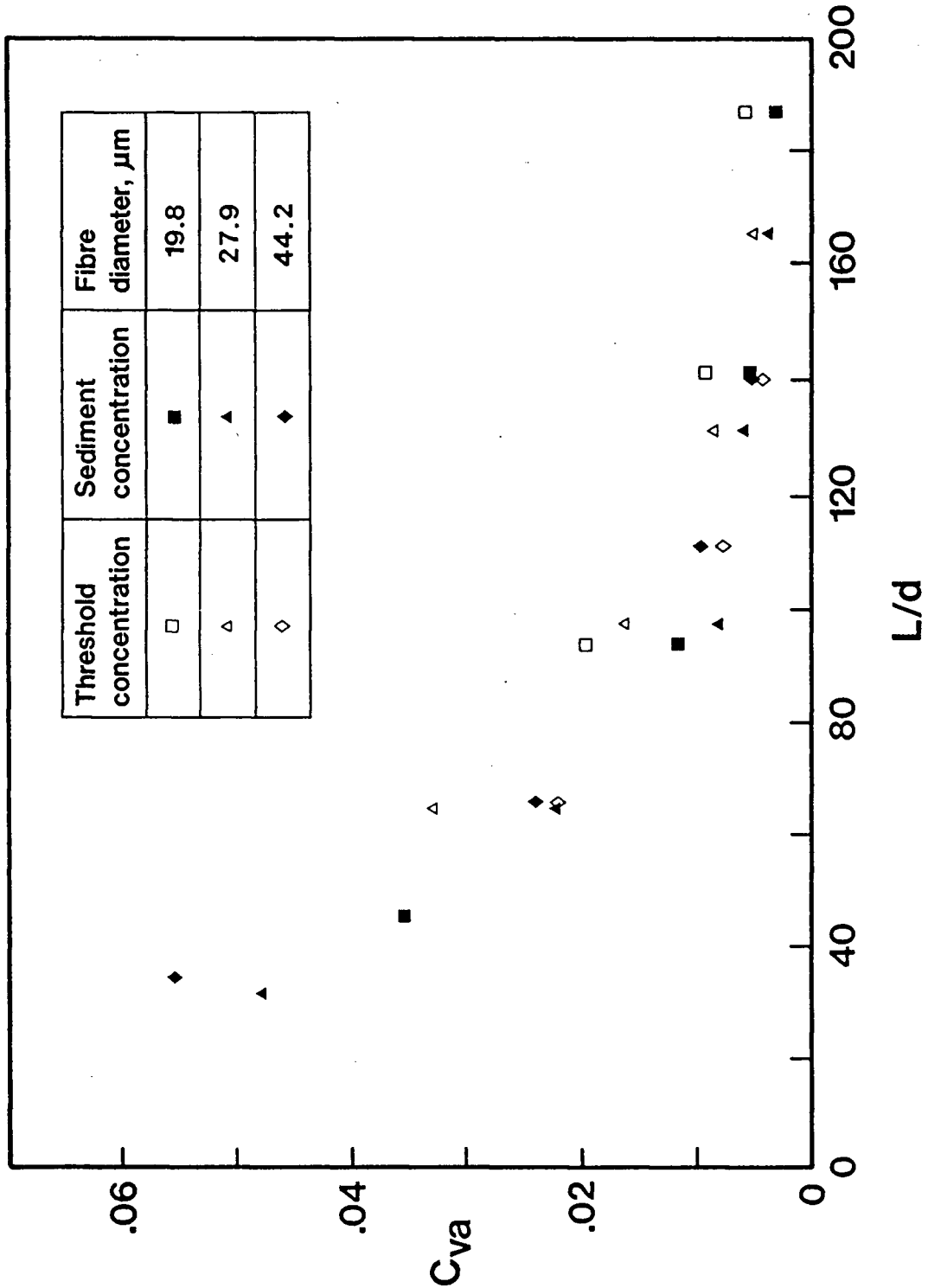


Figure 19. Threshold and Sediment Concentrations versus Fibre Aspect Ratio.

distinctly different networks from the networks circulating in an inclined rotating cylinder.

### Sediment Concentration and Mathematical Models.

In the literature [T9], the limiting concentrations calculated from equation (3) were compared with the sediment concentrations of various man-made fibres. The agreement of the sediment data with the equation (3) at  $n_c$  from 3 to 5 gave reason to advance the postulate that, above the limiting concentration, the fibres interlock by three alternate contact points [P3,W3].

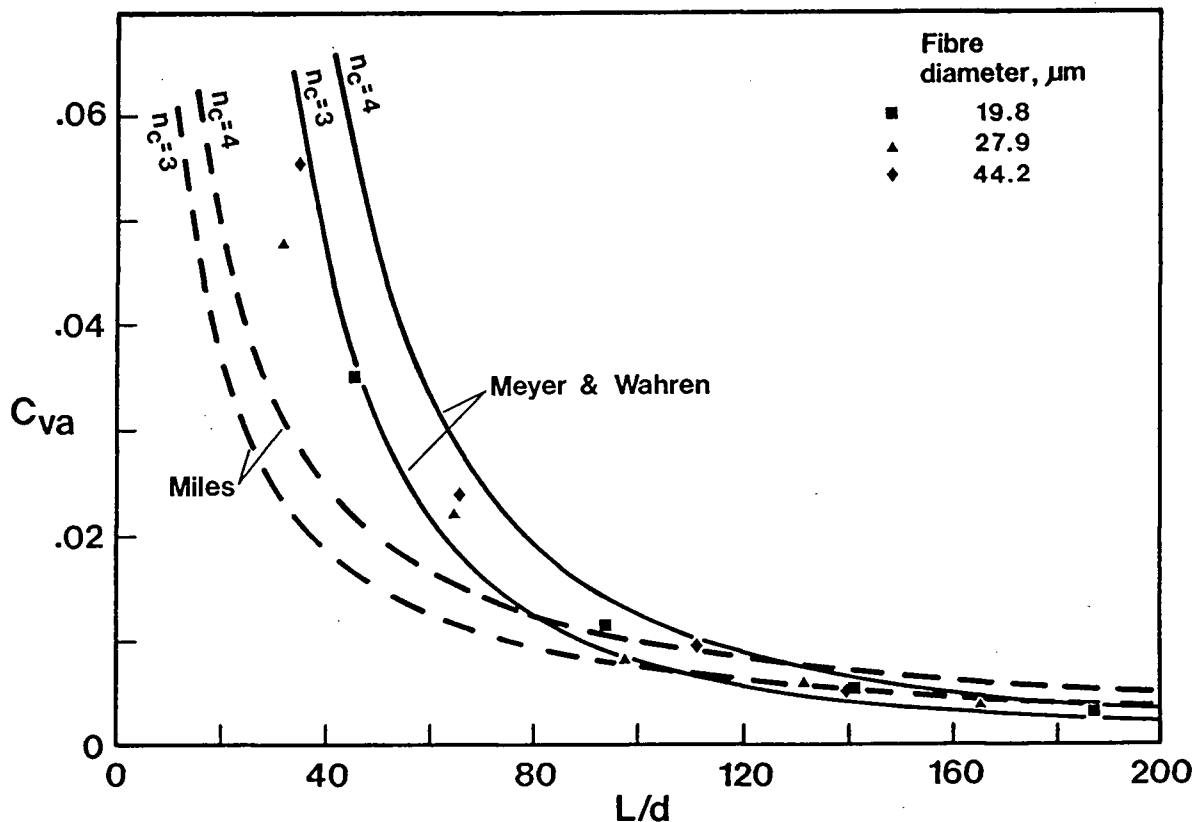


Figure 20. Sediment Concentrations and Mathematical Models.

The experimental data for sediment concentrations from this investigation (Appendix XXIX) indicate that, for large fibre aspect ratios ( $L/d > 100$ ), all sediment concentrations fall between the theoretical lines calculated from equation (3), with  $n_c = 3$  and  $n_c = 4$ , as shown in Figure 20. Below the aspect ratio of 100, the theoretical lines start to overestimate the sediment concentrations. Similar results were obtained by Thalen and Wahren [T9], with the one difference that most of their sediment concentrations were located between  $n_c = 4$  and  $n_c = 5$  lines. Miles's model, represented by dashed lines (Figure 20), agrees with the experimental data to a lesser extent than does the Meyer-Wahren model, especially at fibre aspect ratios lower than 100.

The sediment concentrations and the predictions from statistical models appear to agree for the aspect ratios larger than 100. Below the aspect ratio of 100, only the Meyer-Wahren model at  $n_c = 3$  agrees with the sediment data. This result is surprising because the sedimented network is not an isotropic 3-D network; the fibres are preferentially oriented at low angles to the horizontal in sedimented networks, especially long fibres ( $L/d > 100$ ). In addition, in all sedimented networks, each fibre should have four ordinary contact points with other fibres [E4]. Thus, a sedimented network has a larger number of contact points per fibre than an isotropic, 3-D network at the same concentration. This explains why both concentrations coincide. In general, the comparison of sedimented fibre networks with the isotropic, 3-D networks should not be made because they differ significantly in spatial fibre orientation.

### Threshold Concentration and Mathematical Models.

The threshold concentrations of this study were compared to the limiting concentrations calculated from equation (2) and (3) at  $n_c=4$  since it was said to be *closer to reality* [W4]. The comparison is shown in Figure 21. The solid line is a plot of Meyer-Wahren theoretical relationship for a continuous, isotropic, 3-D network of uniformly long and thick fibres.

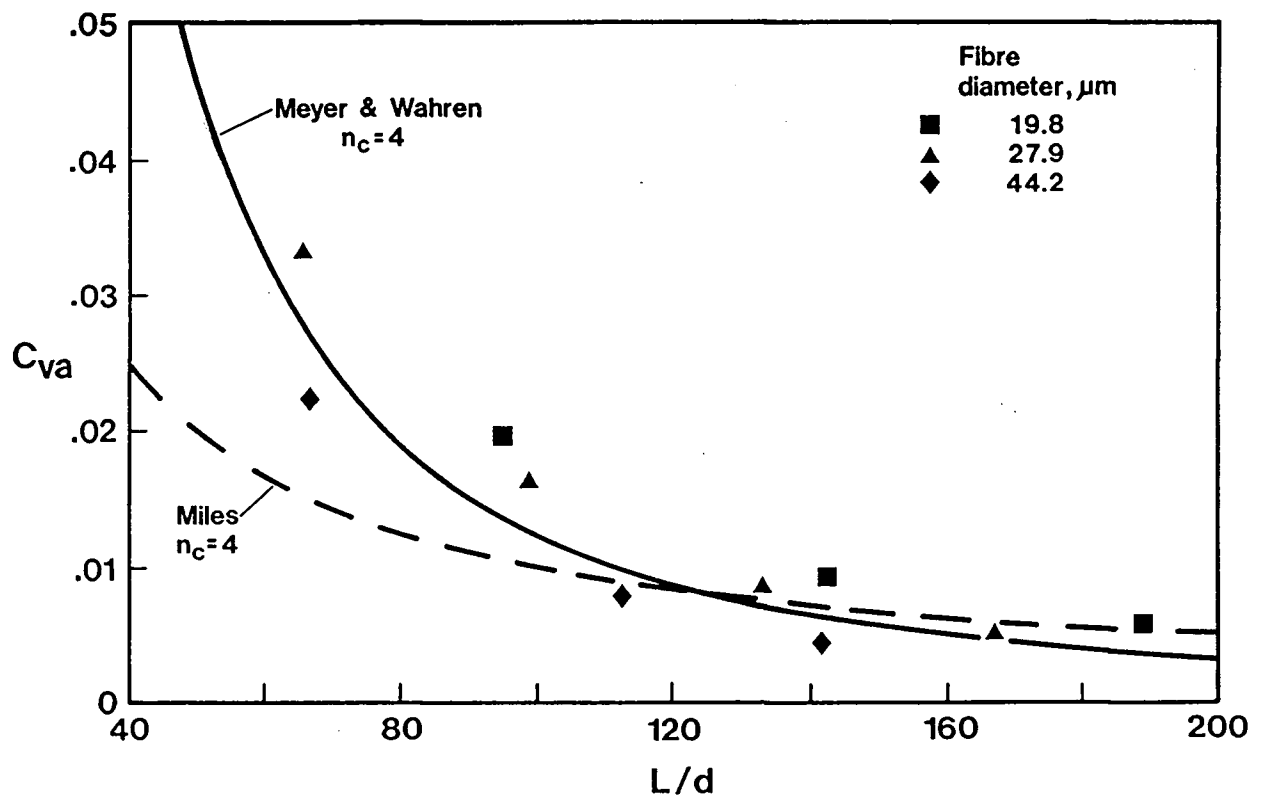


Figure 21. Mathematical Models and Concentrations of Fibres in Suspensions at the Onset of Type-C Floc Formation.

$$C_{va} = \frac{16 \cdot \pi \cdot L}{\left(\frac{L}{2 \cdot d} + \frac{4}{3}\right)^3 \cdot 3 \cdot d} \quad (12)$$

The dotted line is a plot of Miles's model at  $n_c=4$ .

$$C_{va} = \frac{d}{L} \quad (13)$$

At high  $L/d$ , both lines follow the trend of the experimental data points, but not completely. Overall, the Meyer-Wahren model fits the experimental data well. Miles's model agrees poorly with the data at  $L/d$ 's less than 120 at which the most significant changes in threshold concentration take place. It is noteworthy that neither of these models accounts for the effect of fibre diameter evident from the experimental observations shown in Figure 21. This raises doubt about the applicability of both statistical models.

#### Crowding Factor and Number Density.

"Crowding factor" and "number density" are the alternate criteria for the characterization of the threshold concentration. Kerekes et al. [K7] proposed the "crowding factor" extrapolating from Mason's concept of "critical concentration" [M5,M6,M7]. The "crowding factor,"  $N_{fs}$ , represents the number of fibres in a spherical volume having diameter equal to one fibre length as expressed by equation (6). Bibbo et al. [B9] used a cube of side  $L$  instead and coined the term "number density,"  $N_{fc}$  as

expressed by equation (7). Both concepts carry an assumption that the fibre length is finite, i.e., it is not zero or infinity. At the threshold concentration,  $C_{va}^*$ , these terms are denoted  $N_{fs}^*$  and  $N_{fc}^*$  and are large as shown in Table XII. This unequivocally points to the presence of strong fibre interaction. Examination of Table XII reveals that for a given diameter,  $N_{fs}^*$  and  $N_{fc}^*$  are relatively constant over a range of fibre lengths. This suggests that, for a given diameter, the threshold concentration occurs at a constant number of fibres in a given volume. Moreover, the number of fibres diminishes with increases fibre diameter. This result warrants further consideration of the character of the relationship between  $N_f^*$ 's and fibre diameter. For brevity, further discussion is limited to  $N_{fc}^*$  as defined:

$$C_{va}^* = \frac{\pi}{4} \cdot N_{fc}^* \cdot \left(\frac{d}{L}\right)^2 \quad (14)$$

With  $N_{fc}^*$  assumed to depend solely on fibre diameter, the following hyperbolic, logarithmic and exponential relationships were selected to relate these two variables:

$$N_{fc}^* = \frac{K_1}{d+K_2} \quad (15)$$

$$N_{fc}^* = K_3 - \ln(1+d \cdot K_4) \quad (16)$$

Table XII. Crowding Factors Calculated from Equations (6) and (7) at the Onset of Type-C Floc Formation.

FIBRE DIAMETER (WET) d $\mu\text{m}$	AVERAGE FIBRE LENGTH (WET) L mm	FIBRE ASPECT RATIO L/d	THRESHOLD CONCENTRATION $C_{va}^*$	AVERAGE NUMBER OF FIBRES IN A SPHERE WHICH DIAMETER IS EQUAL TO THE AVERAGE FIBRE LENGTH $N_{fs}^*$	AVERAGE NUMBER OF FIBRES IN A CUBE WHICH SIDE IS EQUAL TO THE AVERAGE FIBRE LENGTH $N_{fc}^*$
19.76	0.9158 1.875 2.815 3.737	46.35 94.88 142.5 189.1	NO FLOCS .01972 .009334 .005791	-- 118.4 126.3 141.0	-- 226.1 241.2 269.3
27.95	0.9139 1.832 2.757 3.718 4.666	32.70 65.55 98.65 133.0 166.9	NO FLOCS .03314 .01641 .008549 .005099	-- 94.92 106.4 100.8 94.74	-- 181.3 203.3 192.6 180.9
44.19	1.560 2.947 4.973 6.261	35.30 66.69 112.5 141.7	NO FLOCS .02221 .007915 .004469	-- 65.85 66.83 62.79	-- 125.8 127.6 119.9

$$N_{fc}^* = K_5^{(1-d \cdot K_6)} \quad (17)$$

Selection of these simple relationships respected geometrical limits shown in Table XIII because the domain of fibre diameter in these relationships is  $(0, L]$  at any finite  $L$ .

#### Limit (1).

As  $d$  approaches zero,  $N_{fc}^*$  approaches  $CONSTANT_1$ .  $CONSTANT_1$  represents a number of straight line segments of length  $L$  in a cube of side  $L$ .  $C_{va}^*$  then, of course, approaches zero.

#### Limit (2).

As  $d$  approaches  $L$ ,  $N_{fc}^*$  approaches  $CONSTANT_2$  making  $C_{va}^*$  approach  $(\pi/4) \cdot CONSTANT_2$ .

The geometric interpretation of the second limit is difficult. The limit dependence on fibre length is cumbersome. Certainly the relationships (14) to (17) do not apply at small aspect ratios, i.e., where Type-C networks do not form. In this case the upper limit of fibre diameter must be  $d=d_{limit}$ . Regardless of whether  $(d/L)_{limit}$  or  $L_{limit}$  exist,  $N_{fc,limit}^*$  represents the minimum number of fibres required to form Type-C floc for given  $L$  and  $d$ . These experiments indicate that the limiting  $L/d$  is large, about 50, and in practice  $d$  never equals  $L$ , contrary to what mathematical limit (2) stipulates.

Table XIII. Limits of Equations (14) to (17).

	LIMIT (1)	LIMIT (2)
	$d \rightarrow 0$	$d \rightarrow L$
$C_{va}^*$	$\rightarrow 0$	$\rightarrow \frac{\pi}{4} \cdot \text{CONSTANT}_2$
$N_{fc}^*$	$\rightarrow \text{CONSTANT}_1$	$\rightarrow \text{CONSTANT}_2$

Nonlinear fits made to all data from Table XII determine K-coefficients with the NL2SOL Fortran subprogram available from the UBC Computing Centre. The calculated parameters are shown in Table XIV. The second column containing the sum of least squares indicates the goodness of fit. The fit coefficients and limits are shown in the next two columns.

To supplement these observations, the computer program described in Appendix XVI was written to model fibre sedimentation. In this program, a depositing fibre contacts the topmost fibre of previously deposited mat lying on its path of descent, then rotates and/or slides to rest on the top of the mat or penetrates the mat. The program was run with fibre diameter set to zero after an initial sedimentation with fibres of finite diameter. The number of sedimented line segments of  $L=140$  "distance units" in a cube of side  $L$  was 253. This number of line segments is comparable to the LIMIT (1) obtained from three fits, cf. Table XIV. This is only an illustration of

Table XIV. Fit Coefficients and Limits for Number of Fibres in a Cubical Volume.

$N_{fc}^*$	$\Sigma$ squares	COEFFICIENTS	LIMIT (1)
$\frac{K_1}{d+K_2}$	$4.32 \cdot 10^{-6}$	$K_1=6.8221\text{mm}$ $K_2=0.00933\text{mm}$	731
$K_3 - \ln(1+d \cdot K_4)$	$1.17 \cdot 10^{-4}$	$K_3=170.71$ $K_4=5000.1\text{mm}^{-1}$	171
$K_5(1-d \cdot K_6)$	$4.02 \cdot 10^{-6}$	$K_5=370.06$ $K_6=4.1519\text{mm}^{-1}$	370

finiteness of CONSTANT<sub>1</sub>.

#### 4.5 Flow Conditions under which Coherent Flocs Form

Observations and measurements of the flows were made to identify the hydrodynamic conditions that lead to formation of Type-C flocs. The differences between flows that caused and did not cause Type-C floc formation were sought. Visual observations and LDA velocity measurements were made under selected conditions in the 36 mm deep, 94 mm ID rolling cylinder described in Section 3.4. One type of nylon fibres was used: 44.2  $\mu\text{m}$  in diameter and 4.97 mm long, ( $L/d=112.5$ ). The ratio of cylinder depth to fibre length was 7.2.

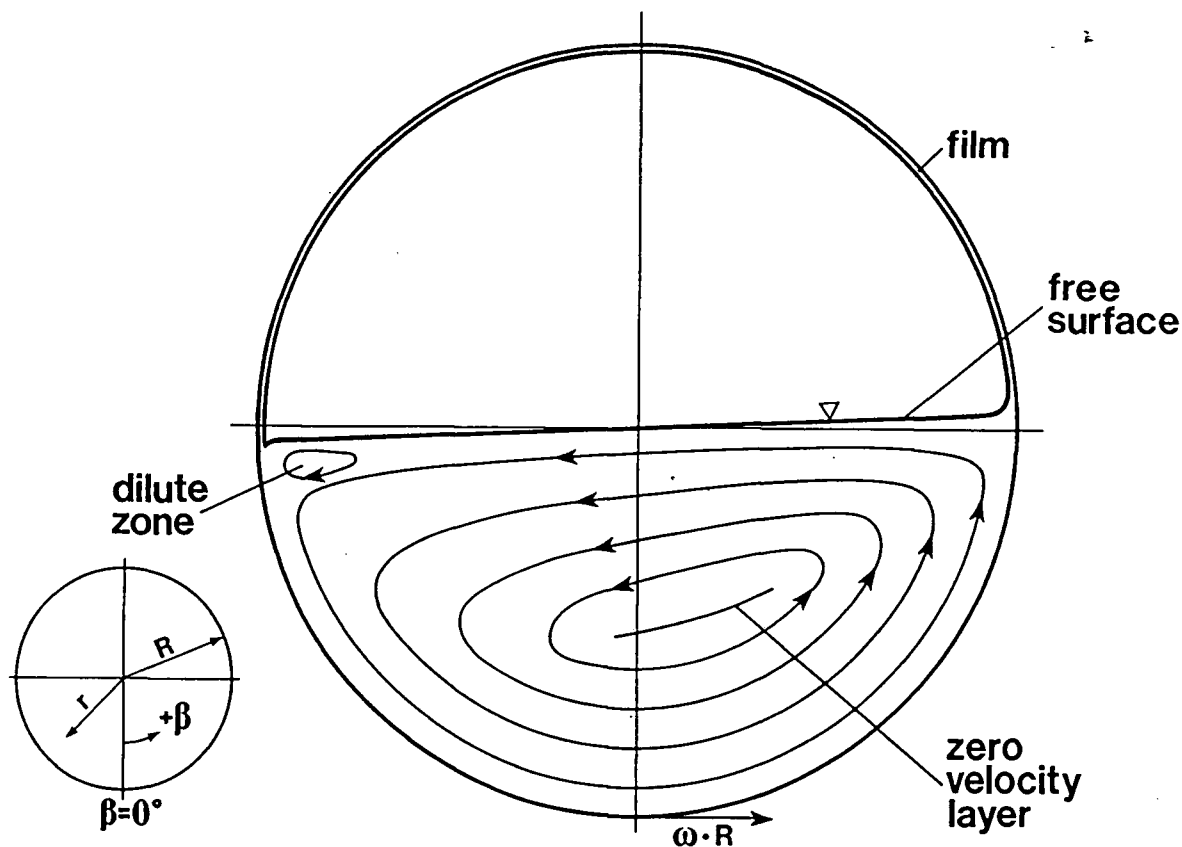


Figure 22. Flow Pattern in a Horizontal Rotating Cylinder.

A typical flow pattern observed visually with the cylinder half full and rotating at a constant angular speed of  $2\pi$  rad/s is shown in Figure 22. The cylinder rotation is counter-clockwise, as marked by the velocity vector at the lowest point of the cylinder. The cylinder walls imparting motion to the suspension exploit the adhesive and viscous forces. The viscous forces combine with the gravitational forces to accelerate suspension in the lower-left quadrant ( $-\pi/2 < \beta < 0$ ) of the cylinder cross-section. In the lower-right quadrant ( $0 < \beta < \pi/2$ ), the inertia and gravitational forces oppose the viscous forces. In the zone near the free surface and close to the cylindrical wall ( $\pi/4 < \beta < \pi/2$  and

$0.65R < r < R$ ), the suspension decelerates in the tangential direction, turns sharply towards the cylinder axis, and accelerates in the radial direction across the cylinder. On reaching the opposite cylindrical wall, the suspension turns again to follow the downward direction of this wall movement. A small portion of the upwardly flowing suspension adheres to the cylinder walls and moves as a film. This film carries some fibres and produces a dilution zone at  $\beta \approx -\pi/2$ . In the lower half of the cylinder ( $-\pi/2 < \beta < \pi/2$ ), a layer of zero velocity (evaluated with respect to a stationary observer outside the cylinder) exists as if a midfeather were placed there. Other features of this general flow pattern are discussed in the following section.

#### 4.5.1 Dissimilarities between flows in horizontal cylinder

In a suspending liquid of low viscosity, Type-C flocs formed when the threshold concentration was exceeded. In the suspending liquid of high viscosity, flocs never formed. It was expected that studying the dissimilarities between these flows could lead to understanding of the mechanism of coherent floc formation. Three flow cases were compared:

Case 1. Low viscosity suspending liquid ( $\mu = 0.00375 \text{ Pa}\cdot\text{s}$ ) with fibre concentration ( $C_{va} = 0.0076$ ) slightly below the threshold concentration. Type-C flocs did not form.

Case 2. Low viscosity suspending liquid, as in Case 1, with fibre concentration ( $C_{va} = 0.0114$ ) above the threshold concentration. Type-C flocs formed.

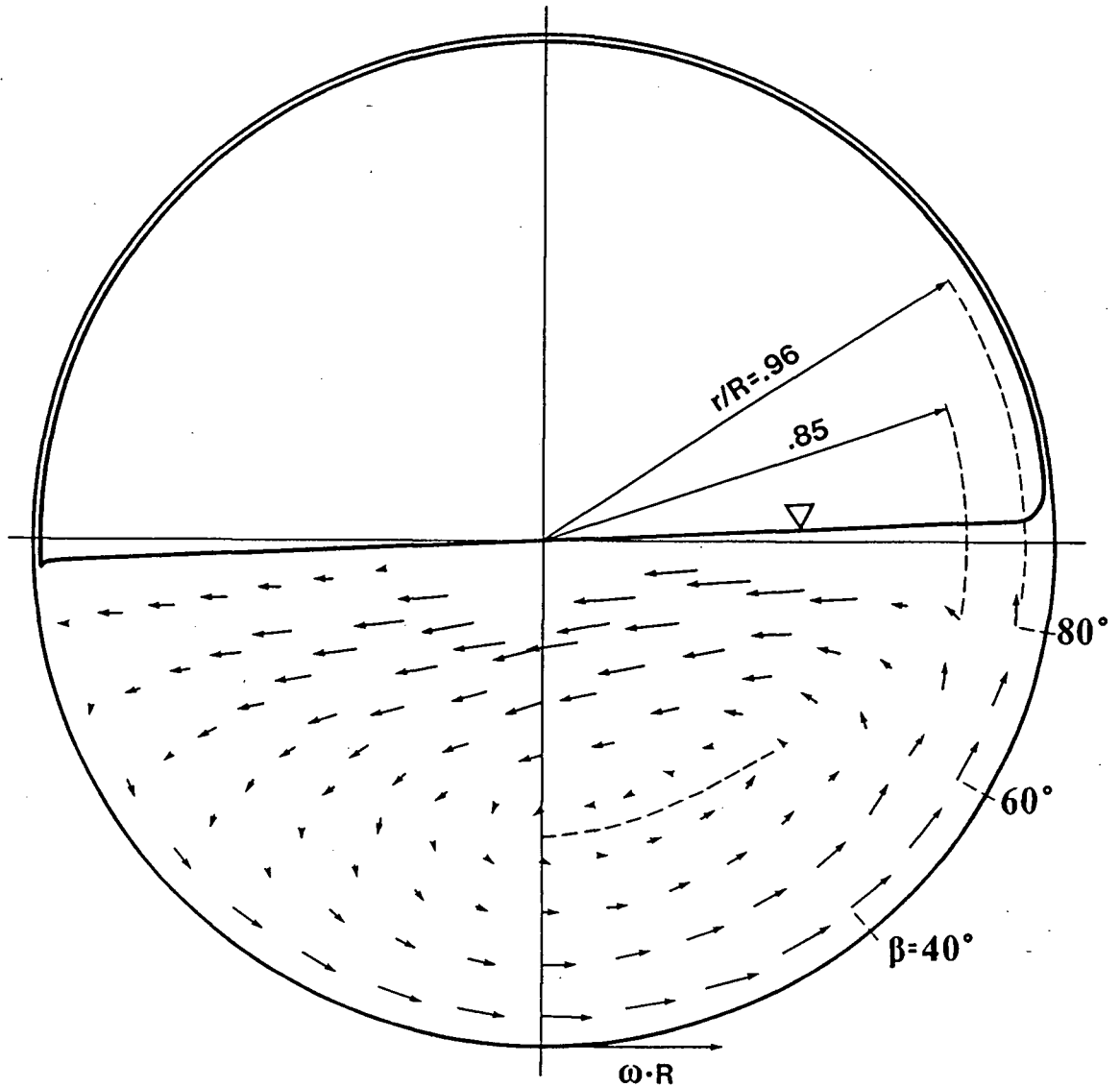


Figure 23. Velocity Vectors for the Case 1 Flow.

Case 3. High viscosity suspending liquid ( $\mu=0.14$  Pa·s). The apparent volumetric concentration of fibres was the same as in Case 2. Type-C flocs did not form.

The velocity vectors for all three cases are shown in Figures 23, 24, and 25. (The data obtained from velocity measurements are in Appendix XXVII.) The velocity vectors

represent the average velocities of the suspending liquid and fibres. The main differences between flows, based on the visual observations and velocity measurements, are listed:

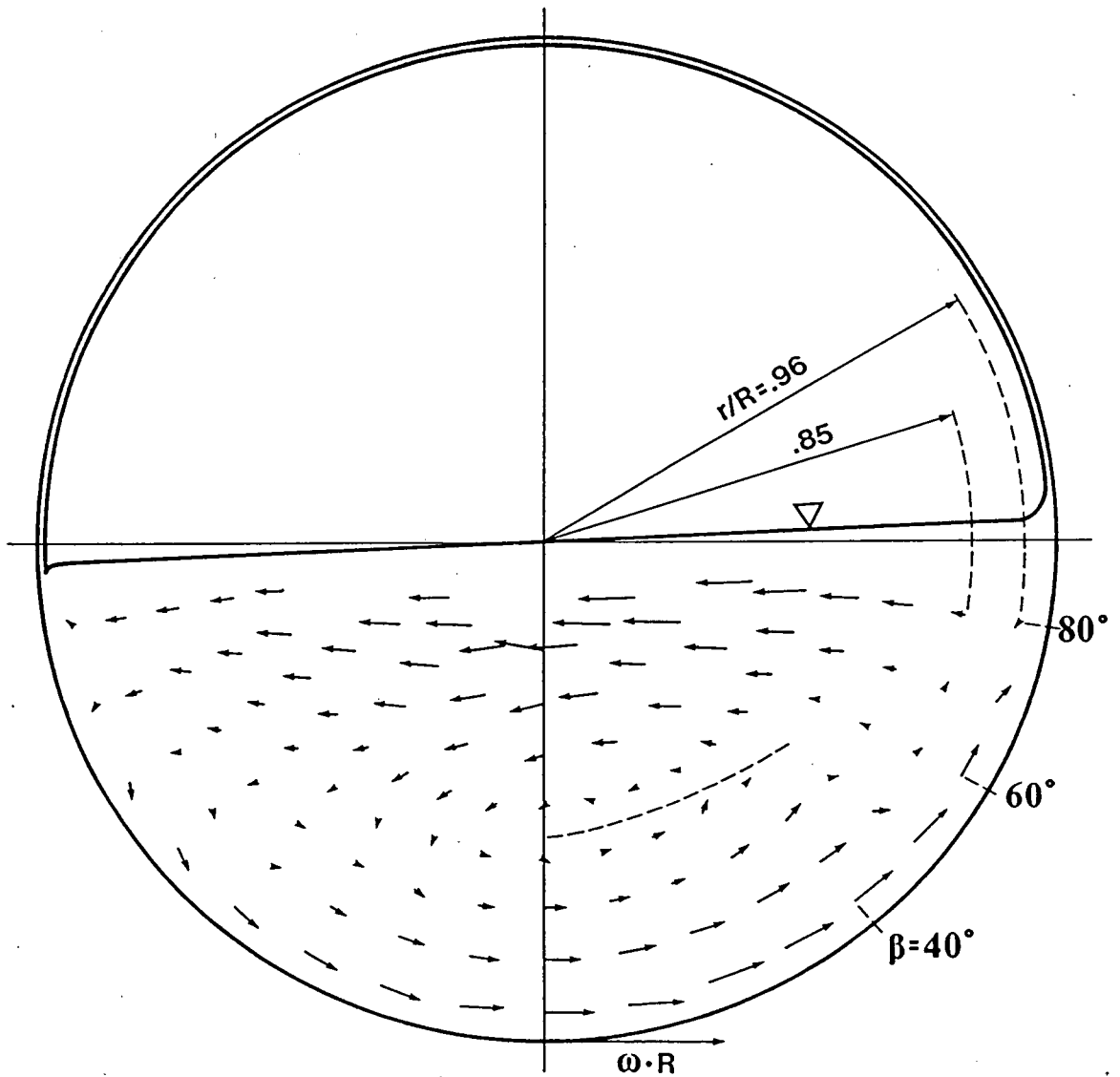


Figure 24. Velocity Vectors for the Case 2 Flow.

## Visual observations

Direct visual observations and visual analysis of films and video tapes aided assessment of the motion of fibres and flocs. The observations are:

1. In Case 2, fibre crowding in the zone between angles  $\beta=50^\circ$  and  $\beta=90^\circ$  at  $r/R>0.6$  was observed. In this zone, groups of fibres moved unsteadily in a tangential direction. At the end of this zone, these groups turned and accelerated across the cylinder. Such fibre crowding had not been observed in the other two flow cases. This important feature of Case 2 flow is discussed in the next subsection.
2. The suspensions of low viscosity (Case 1 and Case 2) produced an almost horizontal free surface, as shown in Figure 23 and 24. In contrast, the suspension of high viscosity (Case 3) produced a free surface inclined to the horizontal as shown in Figure 25.
3. The liquid film thickness on the upper walls of the cylinder ( $\pi/2<\beta<3\cdot\pi/2$ ) increased with increased viscosity of the suspending liquid.
4. The dilute zone marked in Figure 22 did not exist in the Case 3 flow.

## Velocity measurements

LDA measurements gave average velocities of the suspending liquid and fibres at selected points in the central plane of the cylinder. The findings are summarized:

1. In Case 2, the flow velocity decreased sharply between  $\beta=40^\circ$

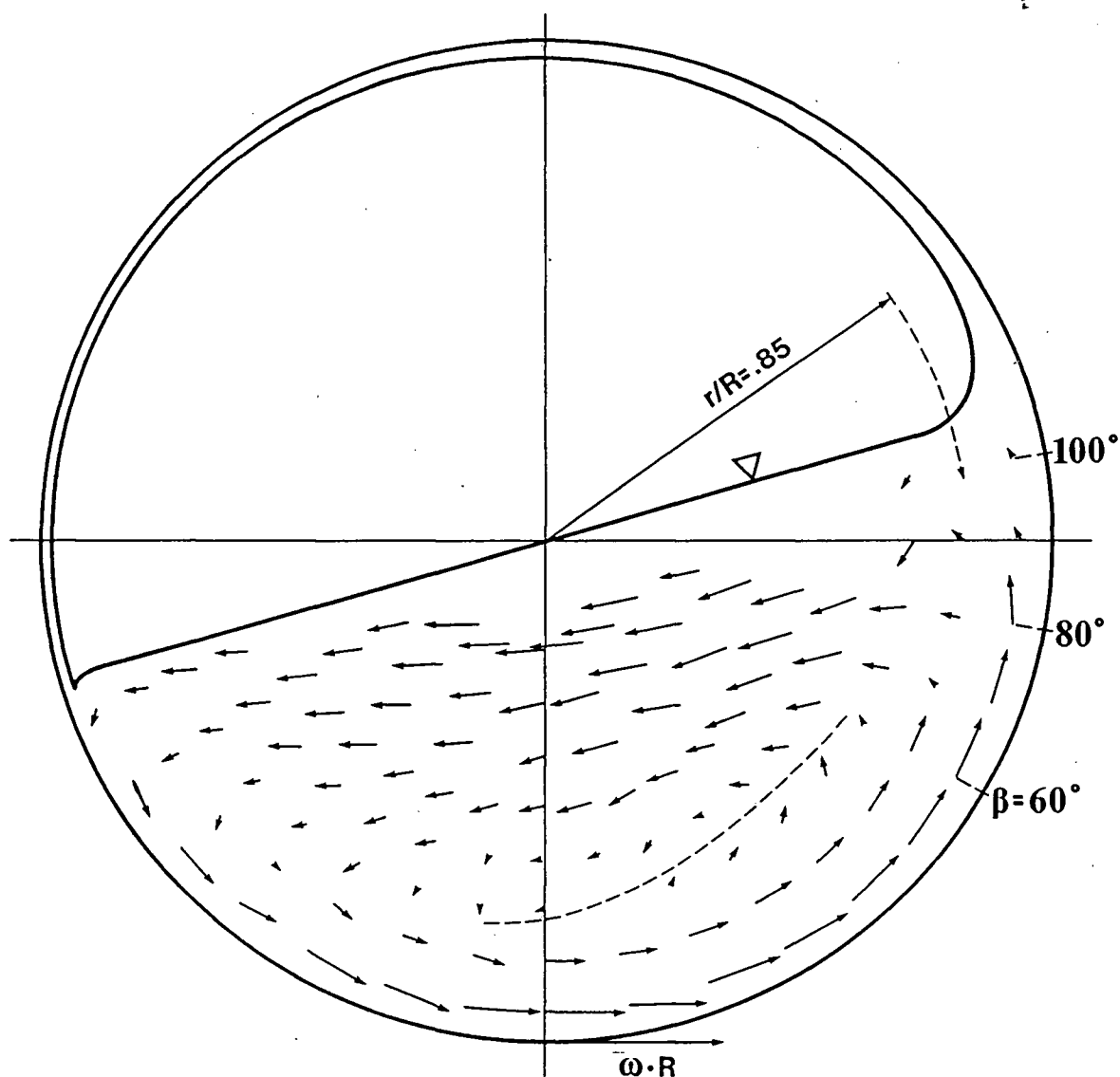


Figure 25. Velocity Vectors for the Case 3 Flow.

and  $\beta=70^\circ$  at  $r/R=0.85$ , and between  $\beta=50^\circ$  and  $\beta=80^\circ$  at  $r/R=0.96$ . In Case 1, the flow velocity decreased gradually between  $\beta=40^\circ$  and  $\beta=80^\circ$  at  $r/R=0.85$ , and between  $\beta=50^\circ$  and  $\beta=80^\circ$  at  $r/R=0.96$  (Figure 26 and Figure 27). Hence, the rates of deceleration differ greatly between Case 2, in which Type-C networks formed, and Case 1, in which they did not.

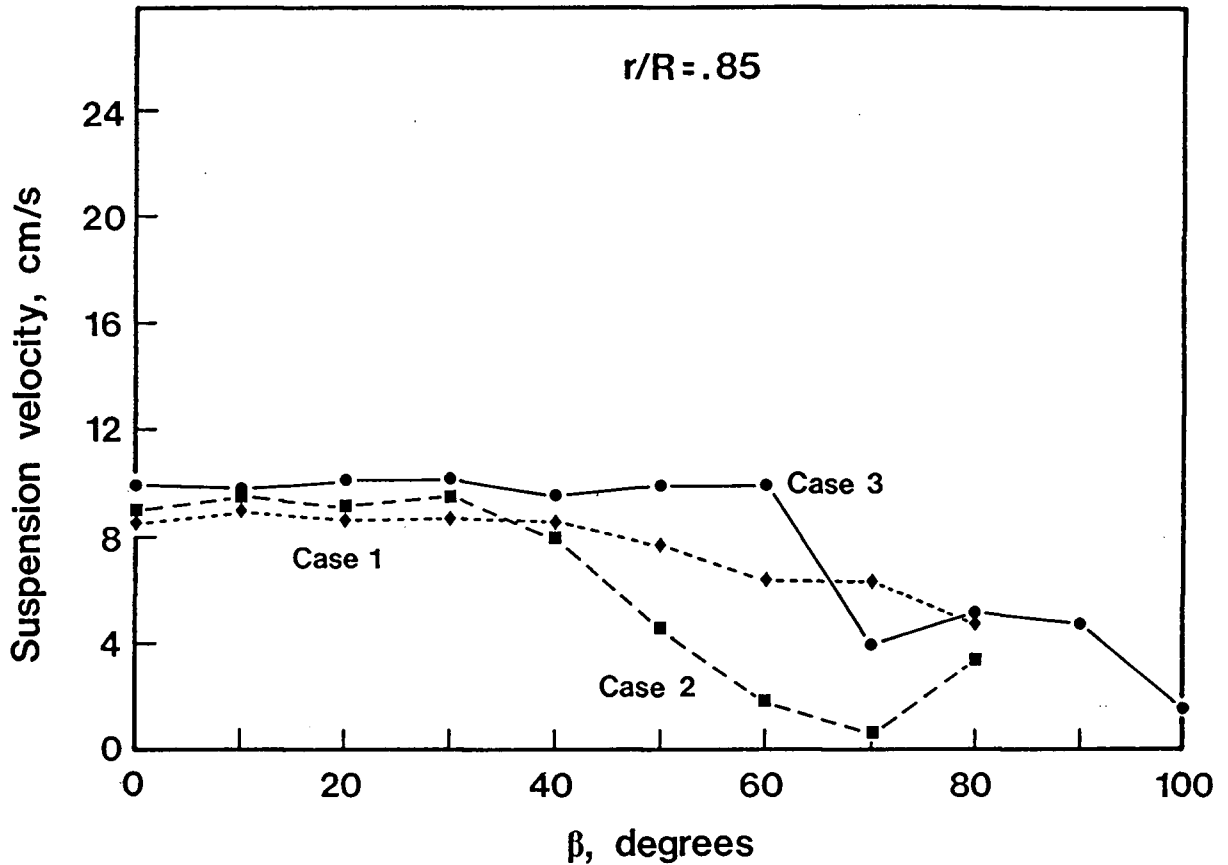


Figure 26. Flow Velocities at  $r/R=0.85$  and  $\beta$  from 0 to 100 degrees. Cylinder peripheral velocity is 0.295 m/s.

In Case 1, the reduction in the flow velocity and the change in flow direction were gradual as indicated by the velocity vectors in Figure 23. The quantitative observations agree with the visual assessment of a smooth flow of fibre suspension. In Case 2, the reduction in the flow velocity and the change in the flow direction were abrupt (Figure 24). This picture corresponds well with the visual observation of the unsteady flow of fibres in which

groups of fibres moved erratically before being accelerated across the cylinder.

In Case 3, the flow velocity decreased and the flow direction changed smoothly between  $\beta=60^\circ$  and  $\beta=80^\circ$ , as in the Case 1 flow. The fibres followed the flow closely, i.e., they did not crowd.

2. In Case 1 and 2, the zero-velocity layer remained at the same radial location,  $r/R=0.64$  (Figure 23 and 24). In Case 3,

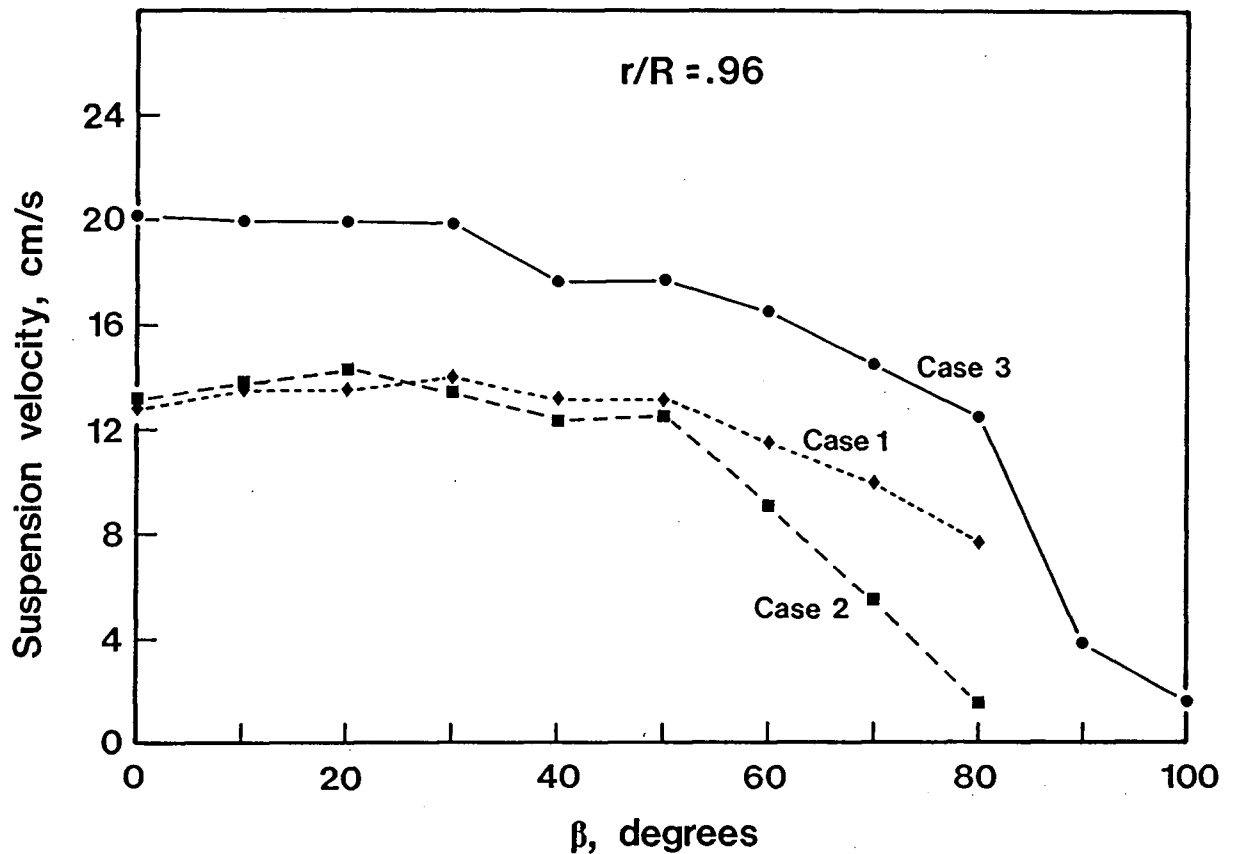


Figure 27. Flow Velocities at  $r/R=0.96$  and  $\beta$  from 0 to 100 degrees. Cylinder peripheral velocity is 0.295 m/s.

the zero-velocity layer was further away from the axis of rotation,  $r/R=0.73$  (Figure 25). The shear zone was approximately twice as long as the corresponding zones in two other flow cases. Calculations of the shear rates between the zero velocity layer and the cylinder wall yielded:  $\Delta V/\Delta r = 26 \text{ s}^{-1}$  for high viscosity liquid, and  $\Delta V/\Delta r = 7.8 \text{ s}^{-1}$  for low viscosity liquid. Hence, in the Case 3 flow, the suspension passing between the wall and the zero velocity layer is subjected to a higher shear rate for longer periods of time. It should be noted that the shear rates of similar magnitude dispersed wood-pulp fibre flocs in water [H8].

3. The viscous interaction between the liquid and the fibres was greater in Case 3 than in the other two cases. This subject has already been discussed in Section 4.3.2.

### Summary

From the visual observations and the velocity measurements, a unifying picture of Type-C flocculation in the partially filled, rotating cylinder emerges. A cyclic flow having acceleration, deceleration, and low shear zones seems required. In addition, the suspension concentration, the properties of fibres, and the properties of the suspending liquid must fulfill conditions which were discussed in Sections 4.3.2 and 4.3.3.

Two consecutive events appear to take place in the recirculating flow: fibre crowding in the deceleration zone, and floc dispersion in the shear zone. Above the threshold

concentration fibre crowding is sufficient to create cohesion in low viscosity fluid and the shear forces are not large enough to disperse such flocs. The high viscosity fluid, on the other hand, appears to prevent network crowding and enhances floc dispersion in the shear zone. A higher average suspension concentration would be expected to be needed to reach the threshold concentration as the suspending liquid viscosity increases. This trend is shown in Figure 16.

At low suspending liquid viscosities, the flocs survive through the shear zone and return to the crowding zone where they undergo further compaction. Cyclic exposure to compaction densifies Type-C flocs. Floc densification coexists with the dilution of the inter-floc-space. In diluted inter-floc-space below the threshold concentration fibres cannot crowd. Floc densification is stopped and formation of new flocs is prevented. Only a portion of suspended fibres ends up in flocs, i.e., the number of Type-C flocs is fixed.

Wahren et al. [M10,S12,T9] postulated that vigorous agitation of a suspension and subsequent decay of agitation are needed to form Type-C flocs. The present work shows that Type-C flocs form in a continuously agitated suspension. Work of others [A9,C1,F1,G5,R2,V1] points to intense agitation as a means of coherent network formation. It is possible that neither high nor low intensity of agitation is exclusively responsible for Type-C network formation, but that a spectrum of agitation intensities exist within which such flocs form. If this is the case, the present work has been conducted at the lower end of this

spectrum.

For completeness of flow characterization the average velocities and Root-Mean-Squares (RMS) of velocity fluctuation are reported in Appendix XXXI for low viscosity suspending liquid only. The calculations of the RMS of velocity fluctuation of fibre suspensions were unreliable because the LDA signal was validated only for a small fraction of time, e.g., less than 10% of the test time, in the fibre crowding zone.

A suspending liquid of high viscosity causes fibres to follow the flow more closely, and thereby prevents localized crowding of fibres which is a first requirement in the formation of Type-C flocs. It follows that the explanation of Attanasio et al. [A17] ascribing a lubricating property to the suspending liquid may be incorrect. Neither the explanation of Steenberg et al. [S12], based on longer decay times for more viscous liquids, seem to be a correct explanation for Type-C floc formation.

#### 4.5.2 Other types of flow

As described in Section 3.2.1, other flows were examined for production of Type-C flocs. Shearing a suspension in a gap between two concentric cylinders did not produce Type-C flocs under either laminar, transition, or turbulent flow conditions with gradually increased fibre concentration from below to above threshold concentration. Type-C flocs did not form in a channel through which a grid was passed up and down in a cyclic manner. On the other hand, Type-C flocs did form in a suspension agitated

by a stirrer in a tank. These flocs existed outside the zone of high shear which surrounds the impellers. High shear dispersed flocs. This explains why Forgacs et al. [F1] did not produce coherent networks from rayon fibres ( $L/d=150$ ) although the limiting concentration was greatly exceeded.

These supplementary experiments confirm the observation that Type-C flocs form in cyclic flows having acceleration and deceleration zone where crowding occurs. Another flow requirement appears to be that flocs not be forced to pass through a zone of very high shear. Although high shear may exist locally in the flow, the flocs should be free to pass outside of this zone. Such is the case of cyclic flow in the rotating cylinder and mixing tank, but not in the case of repeated passage of suspension through the grid. In summary, the flow conditions should be suitable to impart strength to a floc during the crowding process and produce cohesive forces larger than the subsequent forces exerted on the floc to break it apart during passage through the shear zone.

#### 4.6 Observations of Floc Structure

The mathematical models of past theoretical studies describe randomly distributed straight fibres segments in 3-D [C5,M10,O1]. Two of these models [C5,M10] are of interest because they relate fibre geometry and the number of contacts per fibre to the volumetric concentration of fibre network. These models have been discussed earlier, in Section 2.3.2 as equations (2) and (3).

No experimental studies of truly 3-D fibre networks can be found in the literature. Elias [E4], however, came the closest by studying compacted mats of glass fibres and counting fibre contacts. The mats merely had a 2-D structure and therefore did not provide good experimental results to test these models. Consequently, an experiment was designed to visually count number of contacts between fibres in Type-C flocs. The method relies on sugar deposition at the contact points as water evaporates from the aqueous-sugar solution. The deposited sugar bonded the

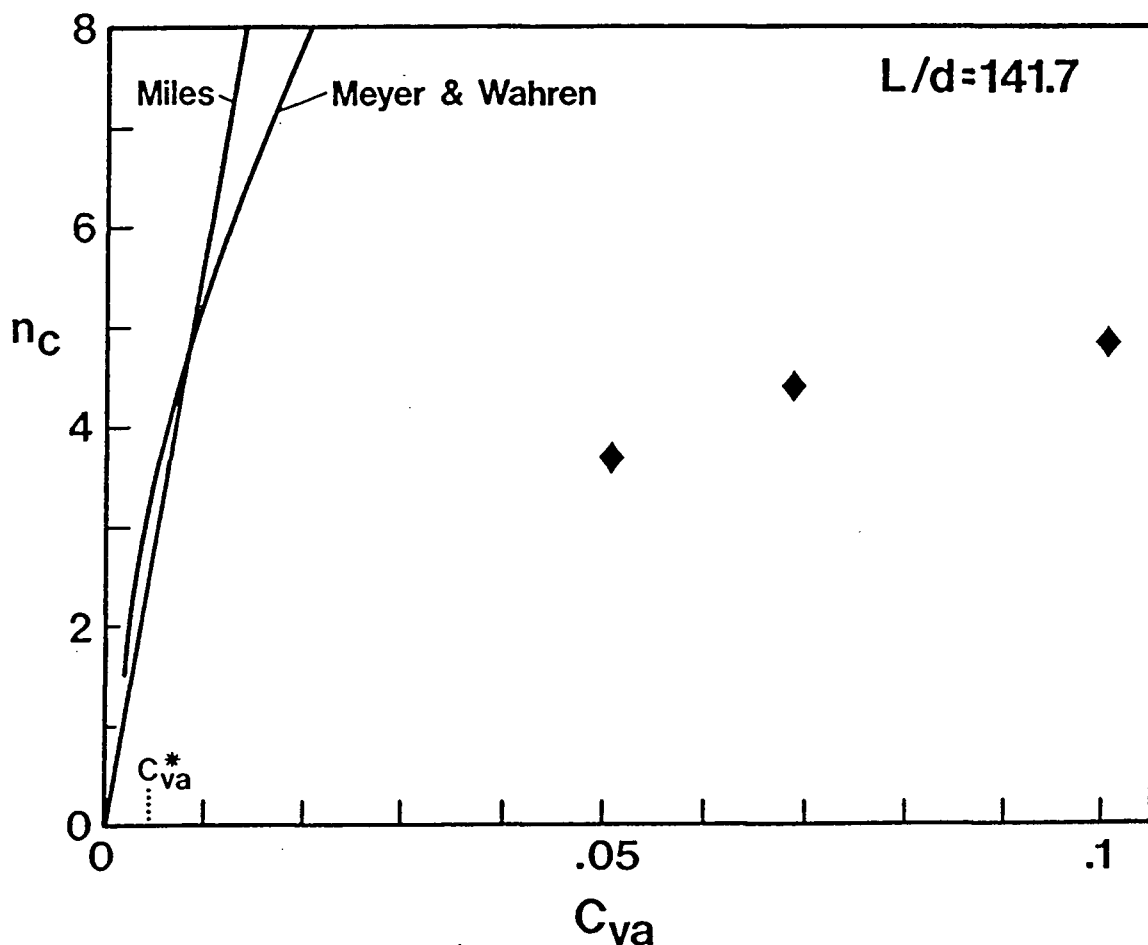


Figure 28. Number of Contacts per Fibre versus Fibre Concentration in Flocs ( $L=6.26$  mm,  $d=44.2$   $\mu\text{m}$ ).

fibres. The fibre contact points were counted by progressive bond breaking and fibre removal.

The numbers of contact points per fibre are shown in Figure 28 for fibres of  $L=6.26$  mm and  $d=44.2$   $\mu\text{m}$  and in Figure 29 for fibres of  $L=45.9$  mm and  $d=559$   $\mu\text{m}$ . The threshold concentration is marked in Figure 28. The predicted number of contacts from equations (2) and (3) for these conditions are also shown. Evidently both models greatly overestimate the number of

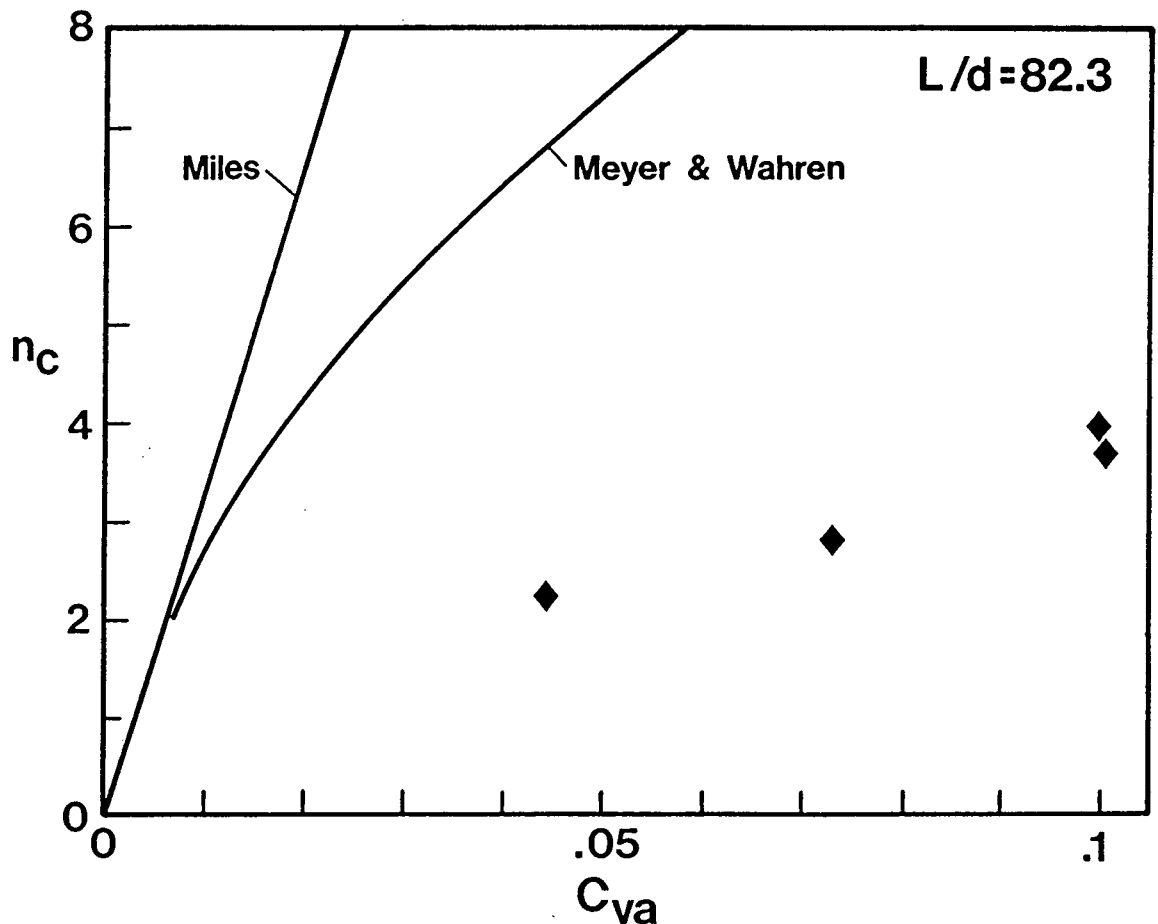


Figure 29. Number of Contacts per Fibre versus Fibre Concentration in Flocs ( $L=45.9$  mm,  $d=559$   $\mu\text{m}$ ).

contacts per fibre in Type-C flocs. The discrepancy between the statistical models and the experiment is large. Models' agreement with the threshold concentration data has already been questioned in Section 4.4. Here, the discrepancy between the statistical theories and experimental values is larger.

Observations of contact point location on fibre surfaces revealed that contacts rarely occur on alternate sides of fibre in a given plane, as shown in the simplistic illustrations of Parker [P3] and Kerekes et al. [K7]. In reality, most of the contacts are distributed around a fibre perimeter. Moreover, it was observed that, on average, less than three contact points per fibre exist in Type-C floc, cf. Figure 29. These observations indicate that fibres interlock in a more complex way than was previously understood [P3,K7]. Many fibres (a few hundred) constitute one coherent floc so that interlocking is a three-dimensional event requiring spatial interaction of fibres.

#### 4.7 Tensile Strength of Type-C Flocs

After examination of the structure of coherent flocs, their tensile strength was measured. Measurements using the procedure described in Section 3.6 were carried out in a THWING/ALBERT tensile tester. The data from these measurements is in Appendix XXVIII. A typical load-separation curve is shown in Figure 30. The load increased steadily from zero (A) to a maximum (B). The ordinate corresponding to the maximum on the curve represents a measure of floc strength. Beyond this point (B), the load decreased jaggedly while the floc separated into

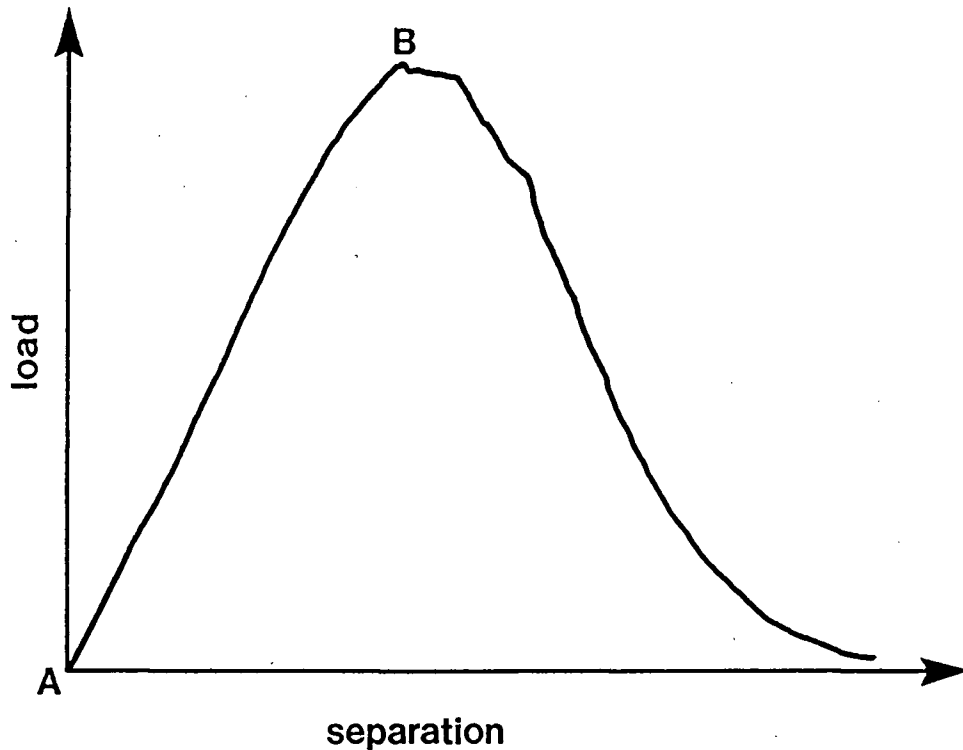


Figure 30. Typical Shape of Load-separation Curve.

two segments. The tensile stress was calculated by the floc strength being divided by the cross-section area of a break zone. The tensile stress varied with floc concentration, as shown in Figures 31 to 37 and it also varied with the length of fibres having the same diameter. The flocs formed from long fibres are stronger than flocs from short fibres at the same concentration, cf. Figures 31 to 33 for  $d=44.2 \mu\text{m}$ , and Figures 34 to 36 for  $d=27.9 \mu\text{m}$ . This effect was anticipated because longer fibres at a given volumetric concentration yield a larger number of contacts with other fibres.

Fits made by a power relationship to the data points allowed comparison of the tensile strength of nylon flocs with the other strengths reported in the literature.

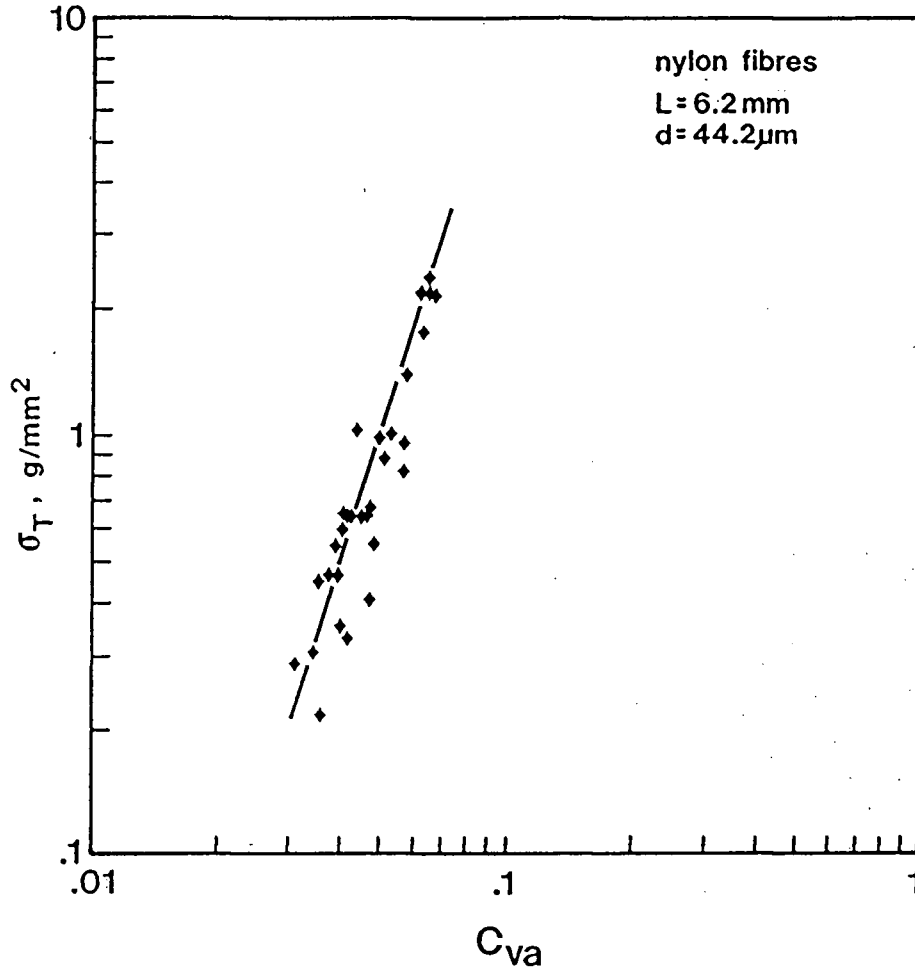


Figure 31. Tensile Stress versus Floc Apparent Volume Concentration.

$$\sigma_T = a^{***} \cdot C_{va}^{b^{**}} \quad (18)$$

The fitted lines are shown in Figures 31 to 37 and the fit coefficients are listed in Table XV along with the ranges of floc concentration.

Whether fibre networks rupture in a tensile or shear mode, the microscopic mechanism of network disruption is the same - fibres are pulled apart. This justifies comparison of results

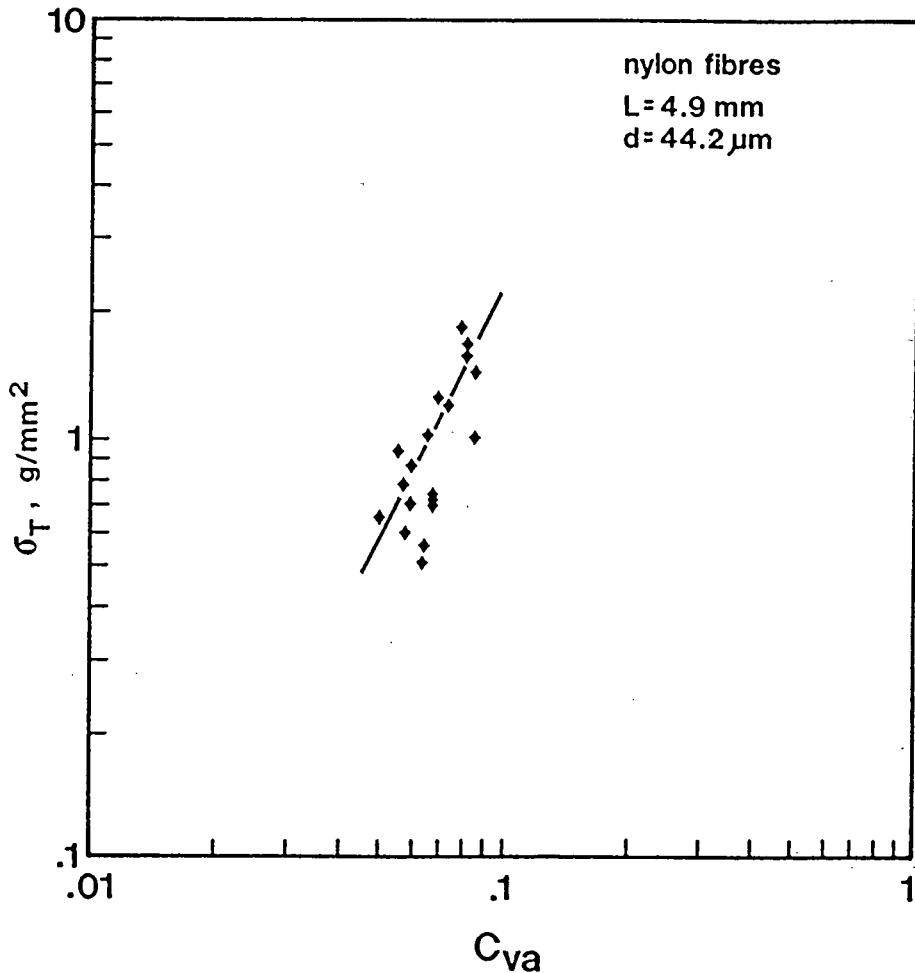


Figure 33. Tensile stress versus floc apparent volume concentration.

from tensile strength experiments and shear strength measurements reported in the literature [H6]. Indeed, the strengths are of the same magnitude as illustrated in Figure 38 by the group of lines marked (1) and (2). The average value of exponent of fitted lines to the nylon floc strength data is 2.65. It is below exponent values from the yield stress measurements of nylon fibre slurries, cf. Tables XV and III. The ranges of concentrations investigated are also comparable. The tensile strength of nylon flocs is somewhat larger than the yield stress

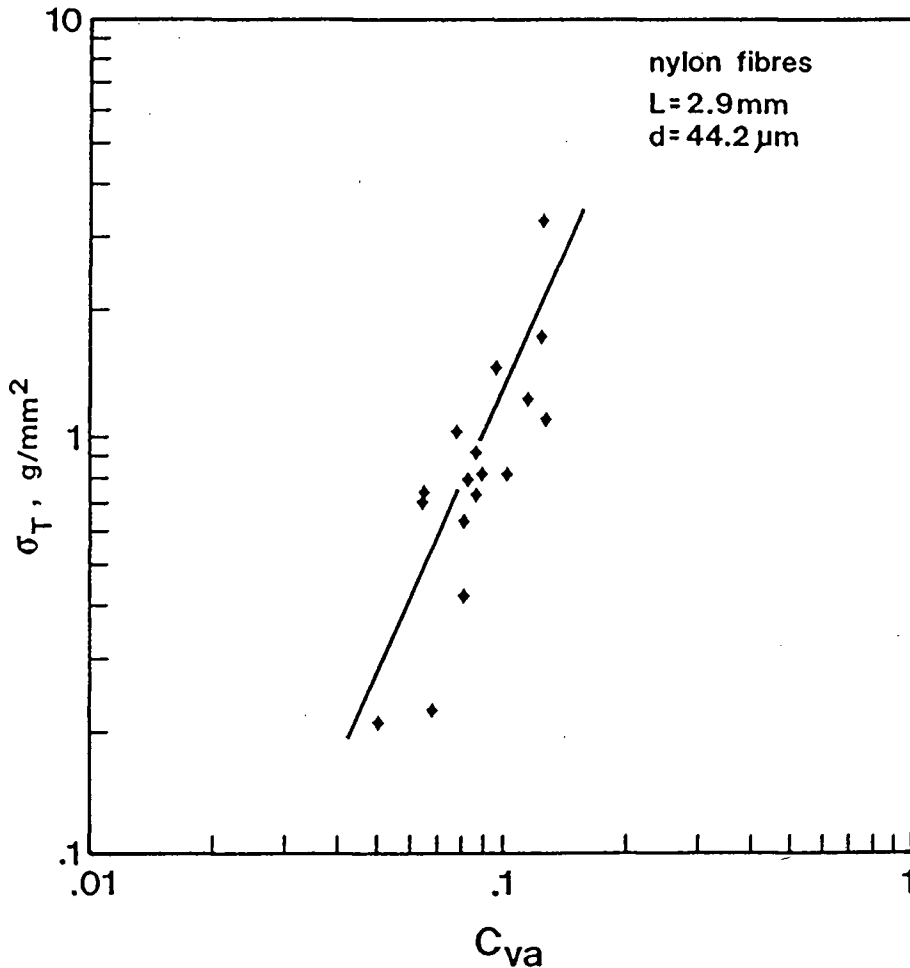


Figure 33. Tensile Stress versus Floc Apparent Volume Concentration.

in shear. As already pointed out in Section 2.3.3, the experimental conditions may alter the way in which forces are applied to the fibre network.

The application of force through bristles and vanes resulted in higher shear strengths at a given concentration than application of force through solid, smooth surfaces, cf. line (3) and line (4) in Figure 38. However, the mode of application of the tensile force in this study resulted in even higher strengths

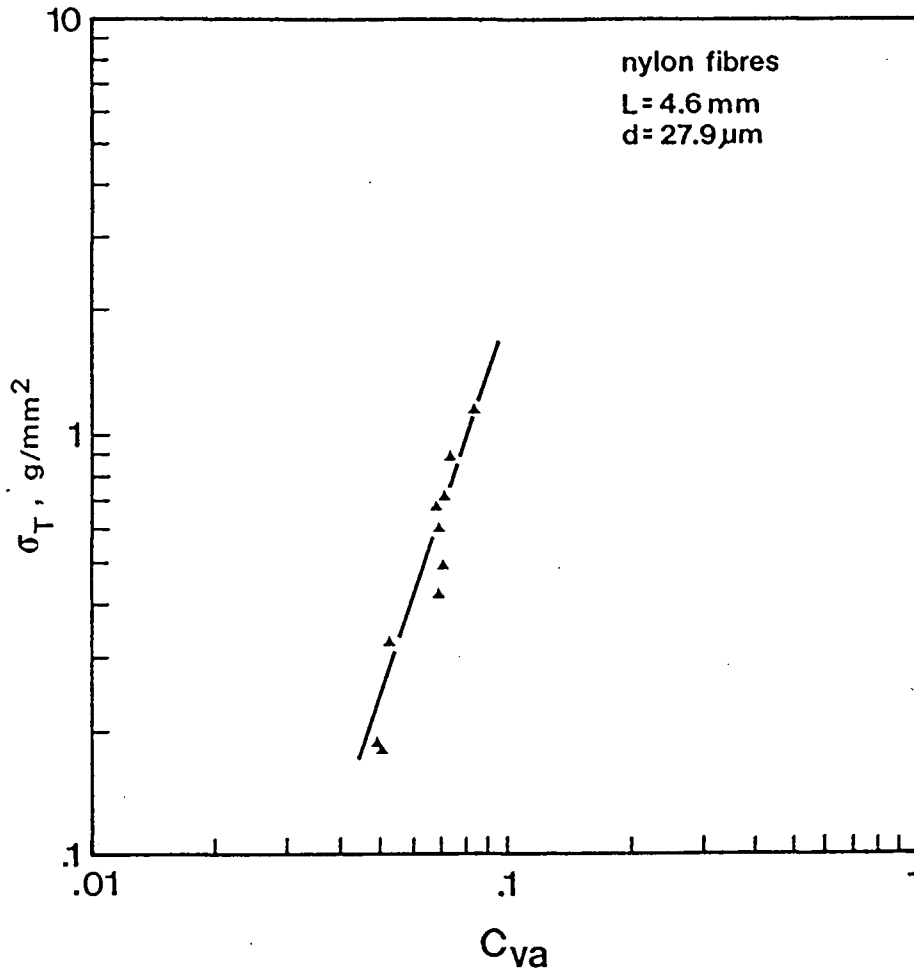


Figure 34. Tensile Stress versus Floc Apparent Volume Concentration.

(group of lines marked (1)). It is possible that all shear methods, regardless of their accuracy, recorded an average strength of the weak and strong zones in the fibre network [M16]. Such an average would be less than the strength of a relatively uniform individual floc. Comparison of the tensile strength for nylon flocs with the shear strength of wood-pulp fibre suspensions by the direct methods (line (3)) reveals a significant difference in the magnitude of recorded stresses but nearly similar slopes of stress dependence on concentration: 2.65

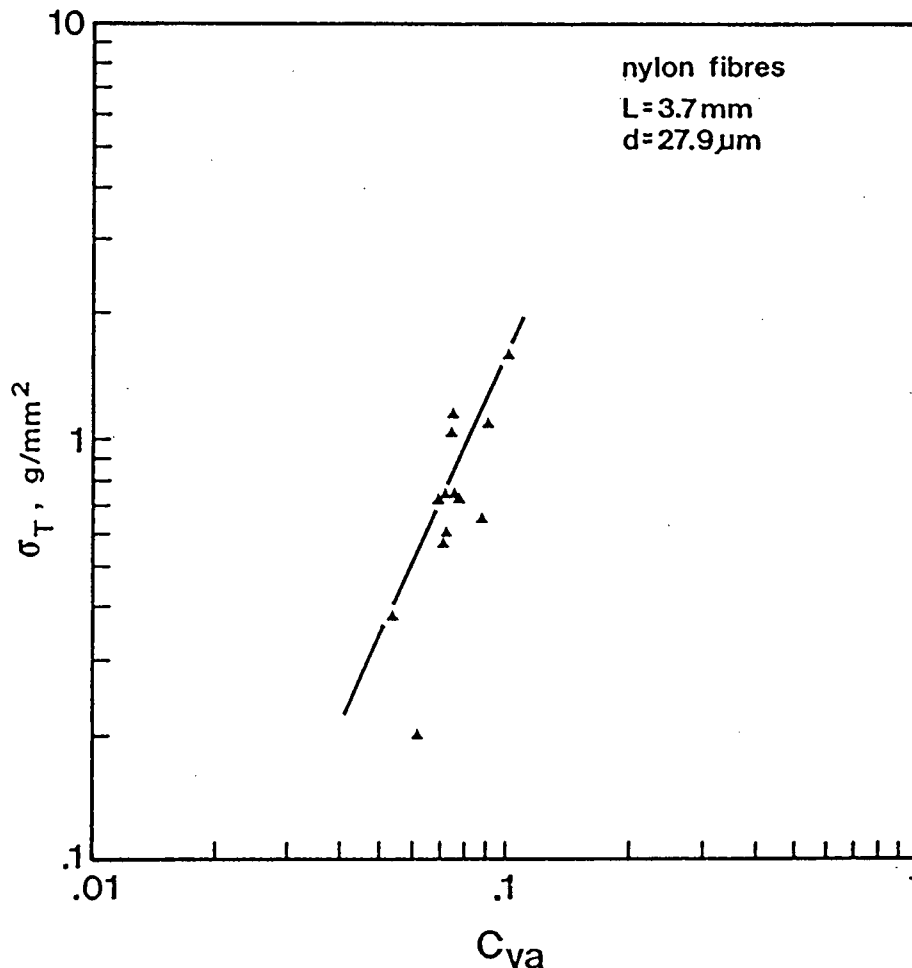


Figure 35. Tensile Stress versus Floc Apparent Volume Concentration.

versus 2.46.

Two published works deal with the strength of individual flocs of wood-pulp fibres. Lee [L2,L3] studied floc dispersion in the turbulent shear, and Garner [G2] measured the tensile strength of air-formed flocs of various moisture content. Lee's work which aimed solely at the phenomena of floc dispersion did not lead to any relationship between the floc strength and consistency. Garner's work, which was reviewed in Section 2.3.3,

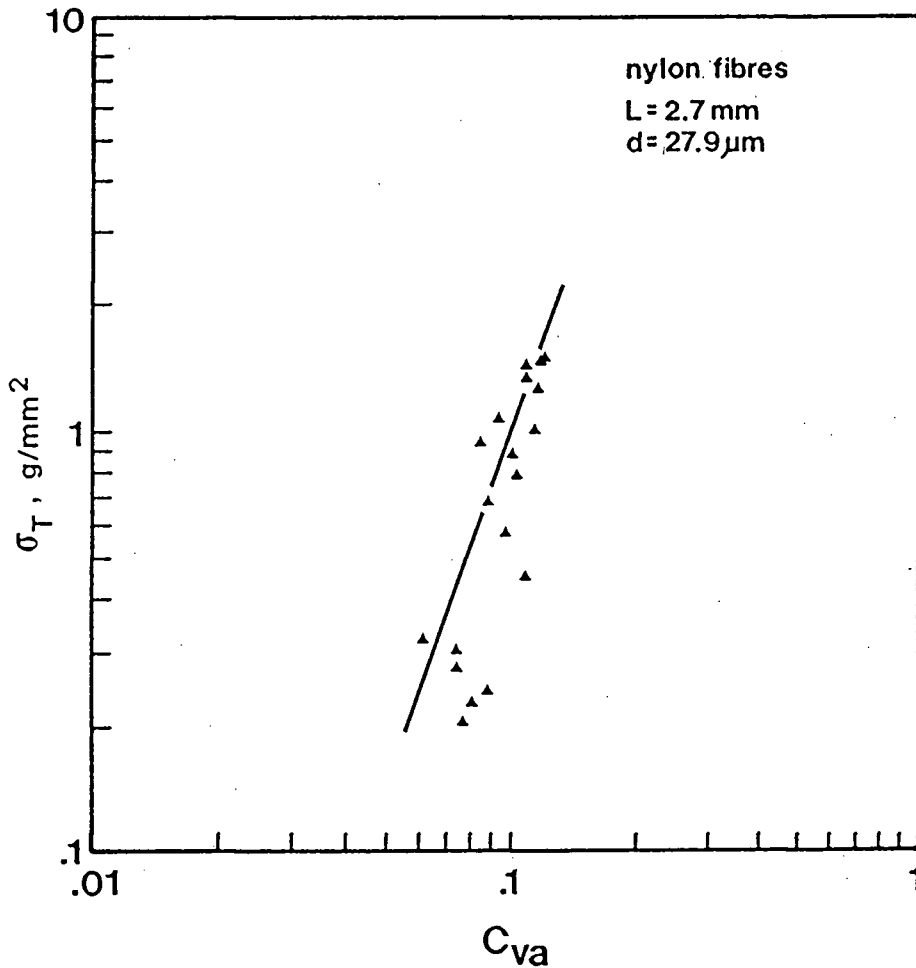


Figure 37. Tensile Stress versus Floc Apparent Volume Concentration.

produced a correlation between the bulk density of flocs and their tensile strength. The data for softwood-pulp fibres are included in Figure 38 as line (5). The magnitude of the tensile strength of dry pulp flocs is below the tensile strength of Type-C flocs (lines (1)). Garner's flocs were formed from highly curled and contorted wood-pulp fibres, whereas the nylon fibres of this study were relatively straight. The contorted nature of Garner's fibres probably introduced significant Type-B cohesion. This is suggested by the jagged shape of the falling slope of

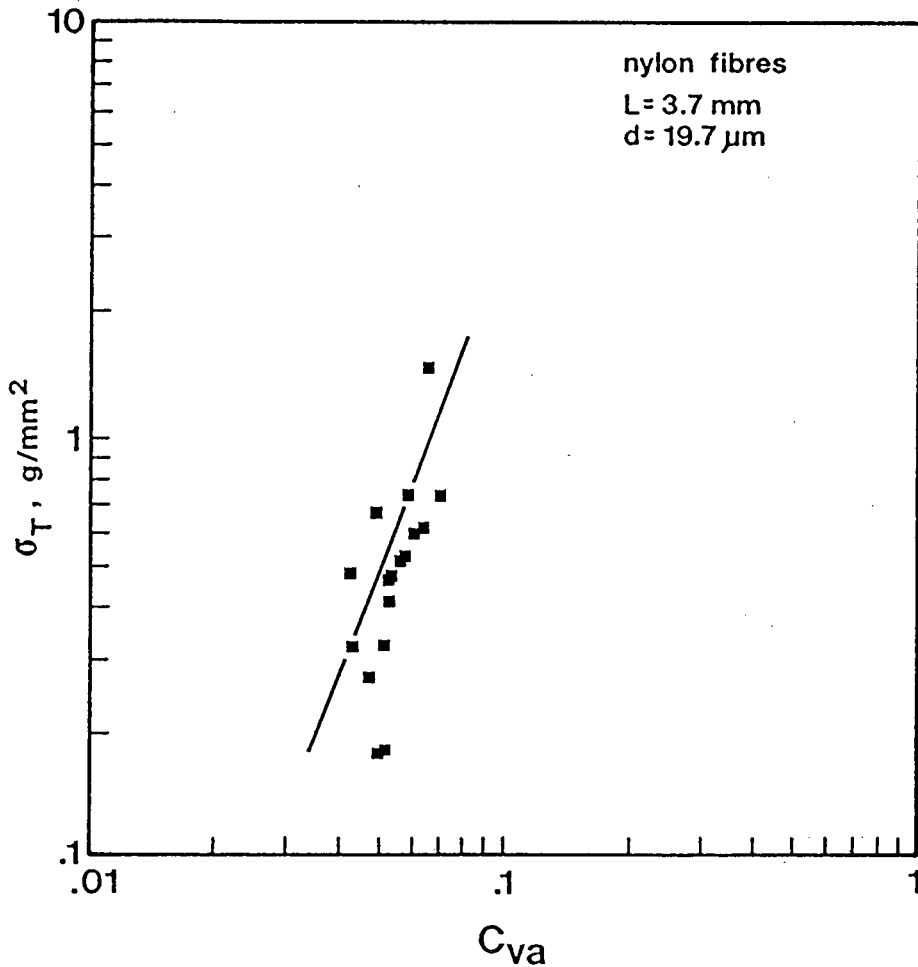


Figure 37. Tensile Stress versus Floc Apparent Volume Concentration.

Garner's tensile load-elongation curves as postulated by Kerekes et al. [K7]. The range of concentrations at which Garner's flocs formed is substantially lower than that for Type-C nylon flocs. These ranges reflect the basic difference in the process of floc formation. Type-B and Type-C cohesions are mutually exclusive; fibres suitable for Type-B cohesion (short, kinked, contorted) are not likely to produce Type-C cohesion. Similar observations were made by Jacquelin [J5,J6] concerning *fragile* and *coherent* flocs. It is possible that wood-pulp plugs were of

Table XV. Power Fit Parameters of Tensile Strength Data.

$$\sigma_T (\text{N/m}^2) = a''' \cdot C_{va} (\%) b'''$$

FIBRE DIAMETER d  μm	AVERAGE FIBRE LENGTH L  mm	POWER FIT PARAMETERS		APPARENT VOLUME CONCENTRATION C <sub>va</sub>  %
		a'''  N/m <sup>2</sup>	b'''  -	
19.76	3.737	67.35	2.68	4.06-6.86
27.95	2.757	14.49	2.86	6.08-11.8
	3.718	100.1	2.23	5.22-9.85
	4.666	12.71	3.31	4.79-8.30
44.19	2.947	83.53	2.22	4.91-12.3
	4.973	23.73	2.02	4.96-8.33
	6.261	62.21	3.23	3.03-6.62

fragile nature (line(6)).

Comparison of tensile strengths between softwood-pulp networks (line (6)) and Type-C flocs (line (1)) reveals the largest difference in the magnitude of recorded strengths and the slopes of fitted lines: 1.59 (Table VI) versus 2.65 an average of b''' from Table XV. Although the plugs (line(6)) were *coherent fibre networks* [F1] or *innerlocked networks* [C1], the nature of cohesion seems to be *fragile* [J5].

As described earlier, the strength of fibre networks in suspension has been experimentally determined by various methods and the results differ widely, cf. Figure 38, over the ranges of concentration and strength measured. The direct test methods

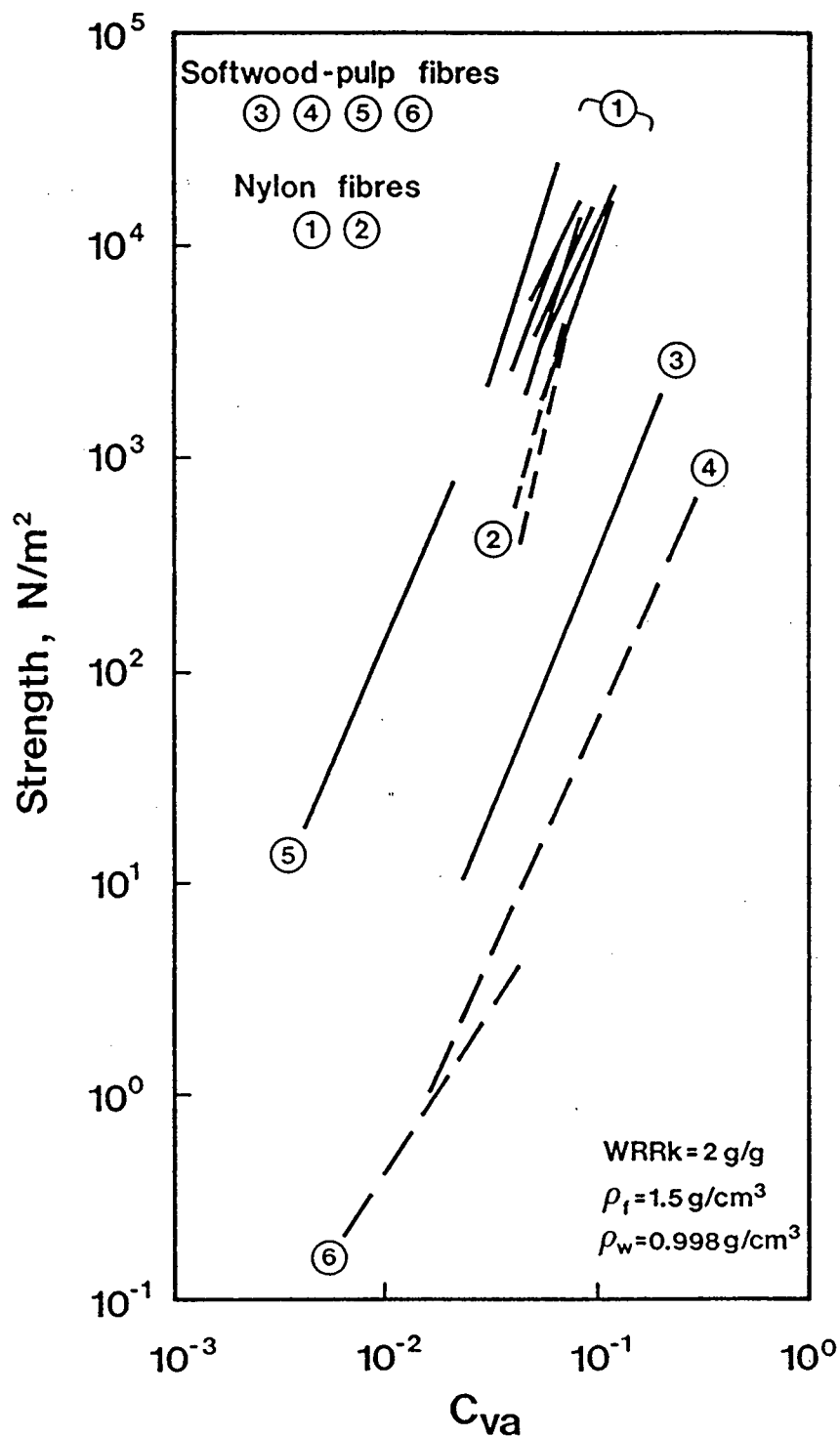


Figure 38. Breaking Stresses versus Suspension Concentration. Tensile of nylon flocs (1). Shear of nylon fibre slurries (2); shear (3,4) and tensile (5,6) of softwood fibre networks from Tables III to VII.

(line (3)) gave higher strengths than the indirect test methods (line (4)) over the same range of fibre concentration and for the same type of fibres. The spread between line group (1) and line (5) can only be attributed to the type of fibres that form networks because the test methods were direct. The similarity of the slopes of these lines (2.65 versus 2.29) is a sign of a common mechanism of strength buildup in the stressed nylon and wood-pulp fibre networks. If this mechanism was purely frictional, the magnitudes of those strengths would depend on the number of contacts between fibres per unit area of the break zone, the normal forces at the contact points, and the coefficient of friction. A mathematical model developed for the tensile strength of Type-C flocs is tested against experimental results in the next section.

#### 4.8 Mathematical Model of Tensile Strength of Type-C Flocs

The mathematical model is based on the assumption that the strength of Type-C network comes from friction forces developed at the contact points when elastically bent fibres press against each other. Development of this model is given in Appendix XVII. This model predicts that floc strength,  $\sigma_T$ , will behave according to:

$$\sigma_T = \frac{F}{B} = \frac{3}{16} \cdot \sin \gamma \cdot k_c \cdot k_d \cdot k_f \cdot \phi_d \cdot E \cdot \frac{d^2}{L^3} \cdot \delta_{\max} \cdot C_{va} \cdot n_c^4 \quad (19)$$

The variables in this equation fall into three groups. One encompassing factors describing fibre properties contains  $(d/L)^2$

which is proportional to  $C_{va}$  as indicated by equation (7).

$$P_f = \phi_d \cdot E \cdot \frac{d^2}{L^3} \quad (20)$$

Another group contains network parameters, and is related to fibre and network geometry, e.g., as  $L/d$  increases, the number of contact per fibre increases at a constant  $C_{va}$ , cf. Figure 27 and 28. This group is:

$$\delta_{max} \cdot C_{va} \cdot n_c^4 \quad (21)$$

The third group containing parameters constant for a given type of fibre network is symbolized by  $P_c$ .

$$P_c = \frac{3}{16} \cdot \sin \gamma \cdot k_c \cdot k_d \cdot k_f \quad (22)$$

Now, equation (19) may be concisely written:

$$\sigma_T = P_c \cdot P_f \cdot \delta_{max} \cdot C_{va} \cdot n_c^4 \quad (23)$$

It appears that the relationship between  $\sigma_T$  and  $C_{va}$  is linear. However, since the parameters,  $P_f$ ,  $\delta_{max}$ , and  $n_c$  are related to  $C_{va}$  in some unknown way, the following relationship should be expected to hold:

$$\sigma_T = D \cdot C_{va}^x \quad (24)$$

where  $D$  is a constant.

The results of tensile tests of this investigation (Section 4.7) indicate that  $x$  is 3.23 for fibres of  $L/d=141.7$ . The proposed mathematical model was tested against experiment while the exponent of  $C_{va}$  equal 3.4 was kept constant. This is explained further in assumption 5. Constants  $D$  and  $a''$  were compared for all types of fibre tested. The results of this test are presented in Table XVI where the constants  $D$  and  $a''$  are shown in the last two rows. In this test the following assumptions have been made:

1. The wet-friction coefficient for 15 denier nylon was assumed to be the same as that for 6 denier nylon.
2. The coefficients  $k_c$  and  $k_f$  were assumed to be at their maxima.
3. Fibres crossing the rupture plane did not change their orientation during floc separation into two parts, i.e., they were randomly oriented.
4. The maximum fibre deflection was assumed to be no more than one fibre diameter.
5. The relationship between the number of contact points per fibre and the apparent volumetric concentration was assumed to be the same for all fibre geometries. It was determined on the basis of the experimental data for 15 denier fibres having  $L/d=141.7$ . The fit

$$n_c = X \cdot C_{va}^Y \quad (25)$$

to the data shown in Figure 28 gave:

Table XVI. Evaluation of the Mathematical Model of Tensile Strength.

VARIABLE OR CONSTANT	3 DENIER FIBRES	6 DENIER FIBRES			15 DENIER FIBRES		
L/d	189.1	98.65	133.0	166.9	66.69	112.5	141.7
E, N/m <sup>2</sup>	1.69×10 <sup>9</sup>	1.78×10 <sup>9</sup>			1.76×10 <sup>9</sup>		
φ <sub>d</sub>	0.273	0.196			0.196		
d, m	19.76×10 <sup>-6</sup>	27.95×10 <sup>-6</sup>			44.19×10 <sup>-6</sup>		
L, m	3.737×10 <sup>-3</sup>	2.757×10 <sup>-3</sup>	3.718×10 <sup>-3</sup>	4.666×10 <sup>-3</sup>	2.947×10 <sup>-3</sup>	4.973×10 <sup>-3</sup>	6.261×10 <sup>-3</sup>
P <sub>f</sub> , N/m <sup>2</sup>	3.452×10 <sup>6</sup>	13.01×10 <sup>6</sup>	5.303×10 <sup>6</sup>	2.583×10 <sup>6</sup>	26.32×10 <sup>6</sup>	5.477×10 <sup>6</sup>	2.744×10 <sup>6</sup>
3 sin(0.57)/16	0.10307	0.10307			0.10307		
k <sub>f</sub>	0.5	0.5			0.5		
k <sub>c</sub>	0.25	0.25			0.25		
k <sub>d</sub> =sin(0.57)	0.540	0.540			0.540		
P <sub>c</sub> , --	6.957×10 <sup>-3</sup>	6.957×10 <sup>-3</sup>			6.957×10 <sup>-3</sup>		
δ <sub>max</sub> , m	19.76×10 <sup>-6</sup>	27.95×10 <sup>-6</sup>			44.19×10 <sup>-6</sup>		
n <sub>c</sub> <sup>4</sup> C <sub>va</sub> (%)	0.205 C <sub>va</sub> <sup>2.4</sup>	0.205 C <sub>va</sub> <sup>2.4</sup>			0.205 C <sub>va</sub> <sup>2.4</sup>		
D, N/m <sup>2</sup>	0.0967	0.520	0.211	0.103	1.662	0.346	0.173
a <sup>'''</sup> , N/m <sup>2</sup>	27.29	8.06	9.78	27.25	7.69	13.57	82.06

$$n_c = 2.129 \cdot C_{va} (\%)^{0.352} \quad (26)$$

The assumption that equation (26) holds for all fibre geometries is the best in the present circumstances. The exponent  $x$  in equation (24) is now  $4 \cdot 0.352 + 2 = 3.4$  and is close to the experimental value of 3.23.

The predictions of the model turned out to be poor especially for fibres of large aspect ratio in which the calculated  $D$ 's are much lower than the constants  $a''$  obtained from experiments. This was expected because only part of the floc break phenomenon was modelled and many additional assumptions were necessary. Forces resisting fibre pullout from the floc can be of frictional and interweaving nature. Only forces of frictional nature and only those which result from fibre-to-fibre interaction from elastic fibre bending were accounted for in this model. The maximum deflection ( $\delta_{max}$ ) of each fibre was assumed to be only one fibre diameter (assumption 4). In reality, fibre deflection can be many times larger than fibre diameter and extend beyond elastic deformation of fibre. Other effects, such as fibre reorientation or fibre wedging at the crossings with other fibres, were not accounted for either. A closer study of the process of floc breakup can only determine the presence and importance of these unaccounted-for effects. The last assumption is the most risky and has probably caused the constant  $D$  to decrease with increasing  $L/d$ , whereas the trend of experimental parameter  $a''$  is the reverse. More experimental

work is needed to determine the relationships between  $n_c$  and  $C_{va}$  for a wide range of  $L/d$ 's. The dependence of  $\delta_{max}$  on floc concentration, also unknown, was not included in the model.

This analysis, which has taken the knowledge of floc strength forward, shows experimental problems and indicates areas in which further research should be done. The most important finding is that the frictional mechanism of load buildup during floc straining can be tackled from fundamental principles.

## 5 SUMMARY

The findings of this study are:

1. The existence of Type-C cohesion between fibres has been experimentally verified for the first time. The cohesion between fibres in a 3-dimensional fibre structures has been shown to arise from elastically bent fibres that are prevented from straightening by the presence of other fibres.
2. Type-C coherent flocs have been found to form at a well defined concentration for fibres of relatively uniform length and diameter in a unique recirculating flow in a partially filled rotating cylinder. This concentration was termed the

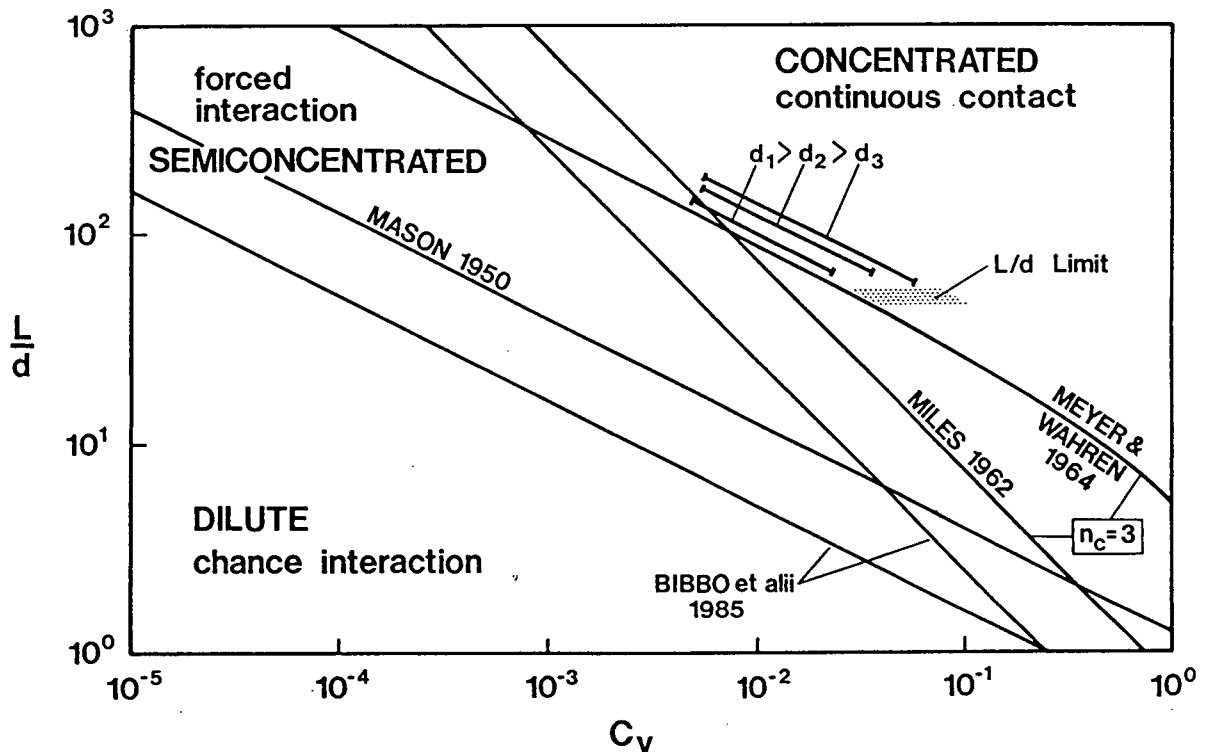


Figure 39. Concepts of Fibre Crowding in Suspensions and Fitted Lines to the Threshold Concentration Data.

"threshold concentration." For the specific conditions of these tests, the threshold concentration appeared to be uniquely related to fibre geometry. The lines shown in Figure 39 correspond to the threshold concentrations for the three diameters of fibres,  $d_1$ ,  $d_2$ ,  $d_3$ .

3. There is a lower limit of either fibre length or fibre aspect ratio (about  $L/d=50$ ) below which Type-C cohesion does not occur at any concentration. The shaded area in Figure 39 marks this limit.
4. It was verified that the sediment concentration is an approximate measure of the threshold concentration.
5. There is an upper limit of viscosity of the suspending liquid above which Type-C cohesion will not form. This limit was found to be close to 0.013 Pa·s for the experimental conditions of this study.
6. The Meyer-Wahren model for predicting the limiting concentration from fibre length, diameter, and number of contacts per fibre predicts the threshold concentration reasonably well when the number of contacts is assumed to be 4. The model of Miles does not predict the threshold concentration well because it depends on  $d/L$  to the first power (equation (2)). Both statistical models do not account for the effect of fibre diameter.
7. Calculations of the number of fibres within a unit volume having the dimension of one fibre length indicate that a large number of fibres exist in the vicinity of one fibre at the threshold concentration. Under these conditions, fibres do not rotate freely when the suspension is sheared.

8. A cyclic flow that imposes deceleration, acceleration and rotation without subjecting flocs to disruptive shear appears to be required for Type-C floc formation.
9. Type-C coherent networks can be produced in flows other than ones having a cessation of vigorous agitation (Wahren *et alli*, quote on p.23). These networks can form in a moderately agitated suspension with decelerating/accelerating flow. The fibres crowd locally in the deceleration zone and interlock elastically as a result of compaction of crowded fibres. An irreversible frictional interlocking occurs and makes fibre networks strong enough to successfully resist the dispersing forces existing in the flow.
10. The existing mathematical models do not describe the isotropic, 3-D networks well; they overestimate the number of contact points per fibre at a given fibre concentration.
11. The tensile strength of individual Type-C flocs was greater than any other strength reported in the literature for either man-made or wood-pulp fibre networks. The power relationship between stress and concentration yielded similar exponents as indicated by the published shear and tensile studies. A mathematical model of tensile strength buildup based on frictional fibre-to-fibre interaction indicates that the phenomenon of strength development can be in part attributed to frictional forces that develop at fibre contact points during floc straining.

## 6 RECOMMENDATIONS FOR FURTHER WORK

This work has opened a new field of study for experimental scientists and theoreticians. There is room for considerable additional work on fibre flocculation and Type-C coherence in particular.

Specifically, it would be useful to establish whether wood-pulp fibres interlock elastically and under what conditions. Investigation should start with fibres as close as possible in geometry to nylon fibres, i.e., sodium chlorite ( $\text{NaClO}_2$ )-cooked fibres from softwood species. This pulping process produces straight, mechanically undamaged fibres. When the first step has been accomplished, i.e., flocs are formed, the effect of other variables (Table I) may be studied.

Extension of the experimental data on the structure of coherent networks to include a broad range of aspect ratios would be useful. The derivation of the expression for the limiting concentration from purely geometrical considerations should be attempted.

No less important than the structure of flocs is their strength. A worthwhile effort would be to study the mechanism of floc breakup to determine the interplay of various factors. An attempt should be made to perfect the tensile and shear tests for the evaluation of the magnitudes of network strength from various types of cohesion, e.g., Type-B and Type-C.

## NOMENCLATURE

### Greek letters

$a$  - dimensionless factor determined by the shape, dimensions, and orientation of suspended particles,

$a_1$  - coefficient,

$\beta$  - angular coordinate,

$\gamma$  - average angle between fibre axis and the plane dissecting a random 3-D fibre network,

$\delta_{\max}$  - maximum fibre deflection in bending,

$\theta$  - spherical polar coordinate, angle,

$\mu$  - viscosity,

$\mu_0$  - viscosity of a suspending liquid,

$\mu_r = \mu / \mu_0$  - relative viscosity of suspensions of cylindrical rods,

$\pi$  - ratio between circumference and diameter of a circle,

$\rho$  - density,

$\sigma$  - tensile stress,

$\tau$  - shear stress,

$\tau_y$  - yield stress in shear,

$\phi_d$  - dynamic coefficient of friction.

$\Phi$  - spherical polar coordinate, angle,

### Roman letters

$a$  - power fit coefficient,

$b$  - power fit exponent,

$d$  - fibre diameter,

$g$  - gravitational acceleration =  $9.80665 \text{ m/s}^2$ ,

$k_c$  - half of the fraction of sliding contacts,  
 $k_d$  - direction coefficient,  
 $k_f$  - half of the fraction of fibres crossing the break plane,  
 $n_c$  - average number of contact points per fibre,  
 $r$  - radial coordinate,  
 $w$  - fibre width,  
 $x$  - exponent in equation (24),  
 $C$  - concentration,  
 $C_b$  - bulk concentration,  
 $C_m$  - mass concentration,  
 $C_v$  - volumetric concentration,  
 $C_{v,min}$  - limiting volumetric concentration,  
 $C_{va}$  - apparent volumetric concentration,  
 $D$  - constant in equation (24),  
 $E$  - elastic modulus,  
 $G$  - shear rate,  
 $I$  - bending moment of inertia,  
 $K_1$  to  $K_6$  - parameters in equations (15), (16), and (17),  
 $L$  - fibre length,  
 $L_w$  - average weighed fibre length,  
 $N_f$  - number of fibres,  
 $N_{fc}$  - number of fibres in a cube of side= $L$ ,  
 $N_{fs}$  - number of fibres in a sphere of diameter= $L$ ,  
 $P_c$  - parameter in equation (22),  
 $P_f$  - parameter in equation (20),  
 $PL$  - plug length,  
 $R$  - internal radius of a cylinder, radius of curvature of

fibres

Re - Reynolds number,

S - fibre stiffness in bending,

V - volume,

### Subscripts

a - apparent,

b - bulk,

c - cube, contact point,

d - dynamic,

cr - critical,

fm - oven-dry fibre mass,

m - mass,

min - minimum,

s - sphere,

v - volumetric,

w - water, weighed,

y - yield,

T - tensile,

### Superscripts

\* - threshold,

- - average,

' - associated with shear strength of wood-pulp networks,

'' - associated with tensile strength of wood-pulp networks,

''' - associated with tensile strength of flocs made of "dry" wood-pulp fibres,

"" - associated with tensile strength of Type-C flocs.

## LIST OF REFERENCES

- A1. ANDERSSON, O., Svensk Papperstid., 60 (5):153 (1957).
- A2. ANDERSSON, O., Svensk Papperstid., 60 (9):341 (1957).
- A3. ANDERSSON, O., Svensk Papperstid., 63 (4):86 (1960).
- A4. ANDERSSON, O., Svensk Papperstid., 63 (5):119 (1960).
- A5. ANDERSSON, O., Svensk Papperstid., 64 (11):417 (1961).
- A6. ANDERSSON, O., BRUNSVIK, J.-J., Svensk Papperstid., 64 (13):493 (1961).
- A7. ANDERSSON, O., Svensk Papperstid., 64 (14):517 (1961).
- A8. ANDERSSON, O., Svensk Pappersitd., 64 (15):248 (1961).
- A9. ANDERSSON, O., Svensk Papperstid., 69 (2):23 (1966).
- A10. APPEL, D.W., "Web formation and Consolidation." EUCEPA 79, London, May 1979, Prep., p.345.
- A11. ARLOV, A.P., FORGACS, O.L., MASON, S.G., Svensk Papperstid., 61 (3):61 (1958).
- A12. ASTM, Annual Book of ASTM Standards, Section 3, Vol.03.01, Designation: E 111-82 (1985).
- A13. ASTM, Annual Book of ASTM Standards, Section 11, Vol.11.01, Designation: D 1125-82 (1985).
- A14. ASTM, Annual Book of ASTM Standards, Section 7, Vol.07.01, Designation: D 885M-85 (1985).
- A15. ASTM, Annual Book of ASTM Standards, Section 7, Vol.07.01, Designation: D 3334-80 (1985).
- A16. ASTM, Annual Book of ASTM Standards, Section 11, Vol.11.01, Designation: D 1293-84 (1985).
- A17. ATTANASIO, A., BERNINI, U., SEGRE, G., J. of Colloid and Interface Sci. 29 (1):81 (1969).
- A18. ATTANASIO, A., BERNINI, V., GALLOPPO, P., SEGRE, G., Trans. Soc. Rheology, 16 (1):147 (1972).
- B1. BAINES, W.D., Svensk Papperstid., 62 (22):823 (1959).
- B3. BALODIS, V., Appita, 18 (5):184 (1965).
- B3. BALDWIN, P.C., VAN DEN AKKER, J.A., Tech. Assoc. Papers, 22 :317 (1939).

- B4. BALODIS, V., MCKENZIE, A.W., HARRINGTON, K.J., HIGGINS, H.G., "Consolidation of Paper Web", B.P.&B.M.A., F. Bolam ed., London, 1966, p.639.
- B5. BALODIS, V., *Appita*, 21 (3):96 (1967).
- B6. BEASLEY, D.E., *Tappi*, 36 (9):159A (1953).
- B7. BENNET, C.A., FRANKLIN, N.L., "Statistical Analysis in Chemistry and in Chemical Industry", John Wiley & Sons Inc., New York, Chapman & Hall Ltd., London (1954).
- B8. BERGMAN, J., TAKAMURA, N., *Svensk Papperstid.*, 68 (20):703 (1965).
- B9. BIBBO, M.A., DINH, S.M., ARMSTRONG, R.C., J. *Rheology*, 29 (6):905 (1985).
- B10. BJELLFORS, C., ERIKSSON, K.-E., JOHANSON, F., *Svensk Papperstid.*, 68 (24):865 (1965).
- B11. BLAKENEY, W.R., J. *Colloid Interface Sci.*, 22 :324 (1966).
- B12. BROADBENT, F.D., HARRISON, H.A., T.S. *Proc. of the Paper Makers' Assoc. of G.B. and Ireland, Part II*, 21:213 (1940).
- C1. CHANG, M.Y., ROBERTSON, A.A., *Pulp & Paper Mag. Canada*, 68 (9):T438 (1967).
- C2. CLARK, J., "Pulp Technology and Treatment for Paper", Miller Freeman Publications Inc., San Francisco (1985).
- C3. COHEN, W.E., FARFANT, G., WATSON, A.J., *Appita Proceedings* p.176 (1950).
- C4. CONDOLIOS, E., CONSTANS, J., *A.T.I.P. Bull.* 17 (1):18 (1963).
- C5. CORTE, H., KALLMES, O.J., "Formation and Structure of Paper", *Trans. Symp. Oxford 1961*, F. Bolam ed., T.S.B.P. & B.M.A., London, Vol. 1, p.13 (1985).
- C6. CLIFT, R., GRACE, J.R., WEBER, M.E., "Bubbles, Drops and Particles", Academic Press (1978).
- C7. COX, R.G., J. *Fluid Mechanics*, 44 (4):791 (1970).
- C8. CPPA, Standard Test Method, D16-1986.
- C9. CPPA, Standard Test Method, C1-1981.
- C10. CRC Handbook of Chemistry and Physics, 66-th ed. (1986)

- D1. DAILY, J.W., BUGLIARELLO, G., Tech. Note No.2, MIT Hydrodynamics Laboratory, (1957).
- D2. DAILY, J.W., BUGLIARELLO, G., Tech. Rep. No.30, MIT Hydrodynamics Laboratory, (1958).
- D3. DOI, M., KUZUU, N.Y., J. Polymer Science: Polymer Physics Ed. 18 :409 (1980).
- D4. DUFFY, G.G., TITCHENER, A.L., Svensk Papperstid., 78 (13):474 (1975).
- D5. DUFFY, G.G., Appita, 28 (5):309 (1975).
- D6. DUFFY, G.G., TITCHENER, A.L., LEE, P.F.W., MOLLER, K., Appita, 29 (5):363 (1976).
- D7. DuPONT CANADA, Technical Service Bulletin, X-43, "Properties of DuPont Filament Yarns for Industrial Uses" (1976).
- D8. DURST, F., MELLING, A., WHITELAW, J.H., "Principles and Practice of Laser-Doppler Anemometers.", Academic Press Inc. (1976).
- E1. EHRNROOTH, E.M.L., Svensk Papperstid., 87 (12):R64 (1984).
- E2. EISSA, Y.Z., USUDA, M., KADOYA, T., KUGA, S., J. Japan Wood Res. Soc. 25 (3):233 (1979).
- E3. ELGIE, D.V., B.A.Sc. Thesis, University of British Columbia, Department of Chemical Engineering (1981).
- E4. ELIAS, T.C., Tappi, 50 (3):125 (1967).
- E5. ELLIS, E.R., JEWETT, K.B., SMITH, K.A., CECKLER, W.H., THOMPSON, E.V., JPPS Trans. CPPA, 9 (1):T12 (1983).
- E6. ERSPAMER, A., Paper Trade J. Vol.110, p.33, June13, (1940).
- E7. ERIKSSON, L., HILL, J., Svensk Papperstid., 75 (13):540 (1972).
- F1. FORGACS, O.L., ROBERTSON, A.A., MASON, S.G., Pulp & Paper Mag. Canada, 59 (5):117 (1958), also, "Fundamentals of Papermaking Fibres", Trans. Symp. Cambridge 1957, F. Bolam ed., T.S.B.P. & B.M.A., London, p.447 (1958).
- F2. FORGACS, O.L., MASON, S.G., Tappi, 41 (11):695 (1958).
- F3. FREEMAN, H., BOADWAY, J.D., Tappi, 36 (5):236 (1953).

- G1. GANANI, E., POWELL, R.L., J. Composite Materials, 19 :194 (1985).
- G2. GARNER, R.G., Tappi J., 69 (2):96 (1986).
- G3. GATES, S.C., Byte, 9 (5):366 (1984).
- G4. GAVELIN, G., Pulp Paper Mag. Canada, Convention Issue, p.191 (1954).
- G5. GIESE, E., GIESE, J., Zelstoff und Papier, 16 (6):163 (1976).
- G6. GRAY, J.L., VAN DEN AKKER, J.A., Paper Trade J., 118 (17):29 (1944).
- G7. GUENTER, T.E., CEAGLSKE, N.H., Tappi, 34 (3):140 (1951).
- G8. GULLICHSEN, J., HARKONEN, E., Tappi J., 64 (6):69 (1981).
- H1. HAJI-SHEIKH, A., LAKSHIMANARAYANAN, R., LOU, D.Y.S., RYAN, P.J., Transactions of ASME, 106 :270 (1984).
- H2. HARRIS, M., "Handbook of Textile Fibres", Harris Research Lab. Inc., Washington D.C. (1954).
- H3. HEAD. V.P., Tappi, 35 (6):260 (1952).
- H4. HEARLE, J.W.S., PETERS, R.H., "Fibre Structure", The Textile Institute Butterworths, Manchester & London (1963).
- H5. HILL, J., ERIKSSON, L., Pulp and Paper Canada, 77 (4):T80 (1976).
- H6. HORIE, M., Ph.D. Thesis, "Time Dependent Shear Flow of Artificial Slurries", Chem. Eng. Dept., University of British Columbia (1978).
- H7. HORIE, M., PINDER, K.L., Canadian J. Chem. Eng., 57 (4):125 (1979).
- H8. HUBLEY, C.E., ROBERTSON, A.A., MASON, S.G., Canadian J. of Research, 28 sec.B, p.770 (1950).
- H9. HUGHSON, G.D., Tappi, 37 (5):162A (1954).
- I1. I.P.C., "The Status of the Sheet-Forming Process. A Critical Review" (1965).
- I2. IPPEN, A.T., DAILY, J.W., BUGLIARELLO, G., Tappi, 40 (6):478 (1957).

- I3. ISENBERG, I.H., "Pulpwoods of the United States and Canada", Vol.1 & 2, The I.P.C., Appleton, Wisconsin (1980).
- I4. ISRAELASCHVILI, J.N., ADAMS, G.E., J. Chem. Soc. Faraday Trans., 174 :975 (1978).
- J1. JACQUELIN, G., A.T.I.P. Bull., 4 :287 (1961).
- J2. JACQUELIN, G., Svensk Papperstid., 66 (20):801 (1963).
- J3. JACQUELIN, G., Techniques et Recherches Papetieres, No.7 p.22 (1966).
- J4. JACQUELIN, G., "Consolidation of Paper Web", B.P. & B.M.A., F. Bolam ed., London, 1966, p.299.
- J5. JACQUELIN, G., C.T.I.P.C.&C., C.T.P. Document No.322 39 :9 (1968).
- J6. JACQUELIN, G., A.T.I.P. Revue, 22 (2):129 (1968).
- J7. JACQUELIN, G., "Method for Treating Suspensions of Fiber to Form Fibrous Aggregates", U.S. Patent 3,679,542 (1972).
- J8. JAYME, G., Tappi, 41 (11):180A (1958).
- K1. KAO, S.V., MASON, S.G., Nature, 253 (5493):619 (1975).
- K2. KARTER, E.M., DURST, R.E., Tappi 49 (6):82A (1966).
- K3. KASWELL, E.R., "Textile Fibres, Yarns, and Fabrics", Reinhold Publishing Corp., New York, N.Y. (1953).
- K4. KENNEDY, G.A., Appita, 16 (4):95 (1963).
- K5. KEREKES, R.J., Tappi, 66 (1):88 (1983), also, Tappi Eng. Conf., p.197 (1982).
- K6. KEREKES, R.J., JPPS, 9 (3):TR86 (1983).
- K7. KEREKES, R.J., SOSZYNSKI, R.M., TAM DOO, P.A., "Papermaking Raw Materials", Trans. Fund. Res. Symp., Oxford 1985, Mechanical Eng. Pub. Ltd., London, Vol.1, p.265 (1985).
- K8. KLIMOV, V.I., Tr. Leningrad Tekhnol. Inst. Tsellyul.-Bumazh. Prom. No.29, pp.99-107, (1973).
- K9. KORNREICH, E. "Introduction to Fibres and Fabrics.", The National Trade Press Ltd., London, 1952 (p.17, Fig.9).

- K10. KRYSKI, K., B.A.Sc. Thesis, Chem. Eng. Dept., University of British Columbia (1982).
- L1. LAFAYE, J.-F., Revue A.T.I.P., 23 (3):195 (1969).
- L2. LEE, C.W., Ph.D. Thesis, "A Visual Study of Fibre and Fluid Interactions", The Ohio State University, (1982).
- L3. LEE, C.W., BRODKEY, R.S., AIChE J., 33 (2):297 (1987).
- L4. LEUTHEUSSER, H.J., CHU, V.H., J. Hydraulics Division, Proc. ASCE, 97 HY-9:1269 (1971).
- M1. MARDON, J., VAN DER MEER, W., Pulp and Paper Mag. of Canada, 55 (11):107 (1954).
- M2. MARK'S Standard Handbook for Mechanical Engineers, Eight Ed., McGraw Hill Book Company (1978).
- M3. MARTON, R., ROBIE, J.D., Tappi, 52 (12):2400 (1969).
- M4. MASON, S.G., Pulp & Paper Mag. Canada, 49 (13):99 (1948).
- M5. MASON, S.G., Pulp & Paper Mag. Canada, 51 (5):93 (1950).
- M6. MASON, S.G., Pulp & Paper Mag. Canada, 51 (10):94 (1950), also, Tappi, 33 (9):440 (1950).
- M7. MASON, S.G., Pulp & Paper Mag. Canada, 55 (13):96 (1954), also, Tappi, 37 (11):494 (1954).
- M8. MASON, S.G., MANLEY, R.St J., Proc. Roy. Soc. of London, A238 :117 (1956).
- M9. MATTHEW'S Textile Fibres, John Wiley & Sons Inc., New York, Chapman & Hall Ltd., London, 1954.
- M10. MEYER, R., WAHREN, D., Svensk Papperstid., 67 (10):432 (1964).
- M11. MCGUIRE, T.A., HOFREITER, B.T., MEHLTRETTER, C.L., RIST, C.E., Tappi, 51 (2):94 (1968).
- M12. MIH, W., PARKER, J., Tappi, 50 (5):237 (1967).
- M13. MOLLER, K., DUFFY, G.G., TITCHENER, A.L., Svensk Papperstid., 76 (13):493 (1973).
- M14. MOLLER, K., NORMAN, B., Svensk Papperstid., 78 (16):582 (1975).
- M15. MOLLER, K., Svensk Papperstid., 81 (16):506 (1978).
- M16. MORRISON, S.R., HARPER, J.C., I. & E.C. 4 (2):176 (1965).

- M17. MUHONEN, J.M., WILLIAMS, D.G., Tappi, 56 (10):117 (1973).
- N1. NAPPER, D.H., "Polimeric Stabilization of Colloidal Dispersions.", Academic Press (1983).
- N2. NAWAB, M.A., MASON, S.G., J. Physical Chemistry, 62 :1248 (1958).
- N3. NERELIUS, L., NORMAN, B., WAHREN, D., Tappi, 55 (4):574 (1972).
- N4. NORMAN, B., NERELIUS, L., HANSTROM, G., WAHREN, D., Svensk Papperstid., 75 (13):536 (1972).
- O1. OGSTON, A.G., Trans. Faraday Soc. 54 :1754, (1959).
- O2. ONOGI, S., SASAGURI, K., Tappi, 44 (12):874 (1961).
- P1. PANSHIN, A.J., de ZEEUW, C., "Textbook of Wood Technology", 4-th ed., McGraw-Hill Book Company (1980).
- P2. PARKER, J.D., Tappi, 44 (4):162A (1961).
- P3. PARKER, J.D., "The Sheet Forming Process", Tappi STAP No.9, (1972).
- P4. PRESTON, "Fibre Science", The Textile Institute, Manchester (1953).
- R1. RAIJ, U., WAHREN, D., Svensk Papperstid., 67 (5):186 (1964).
- R2. REEVES, D.C., GERISCHER, G.F.R., Appita 35 (4):316 (1982).
- R3. REEVES, D.C., GERISCHER, G.F.R., South African Forestry J., 113 :50 (1980).
- R4. ROBERTSON, A.A., MASON, S.G., Pulp & Paper Mag. Canada, 55 (3):263 (1954).
- R5. ROBERTSON, A.A., MASON, S.G., Pulp & Paper Mag. Canada, 57 (6):121 (1956).
- R6. ROBERTSON, A.A., MASON, S.G., Tappi, 40 (5):326 (1957).
- R7. ROBERTSON, A.A., MEINDERSMA, E., MASON, S.G., Pulp & Paper Mag. Canada, 62 (1):T-3 (1961).
- R8. ROBERTSON, A.A., Tappi, 48 (10):568 (1965).
- R9. de ROOS, A.J., Tappi, 41 (7):354 (1958).
- R10. RYDHOLM, S.A., "Pulping Processes", Interscience Publishers of Wiley & Sons, Inc. (1965).

- S1. SAMUELSSON, L.-G., Svensk Papperstid., 67 (22):905 (1964).
- S2. SCALLAN, A.M., CARLES, J.E., Svensk Papperstid., 75 (17):699 (1972).
- S3. SCALLAN, A.M., GREEN, H.V., Wood and Fibre, 5 (4):323 (1974).
- S4. SCALLAN, A.M., GREEN, H.V., Wood and Fibre, 7 (3):323 (1976).
- S5. SEDIVY, O., NOLL, J., Svensk Papperstid., 72 (5):138 (1969).
- S6. SCHNIEWIND, A.P., IFJU, G., BRINK, D.L., "Consolidation of the Paper Web", T.S.B.P. & B.M.A., F. Bolam ed., London, Vol.1, p.538 (1966).
- S7. SEIBOLD Manual, Wien. M 2.038
- S8. SERGEN DIAGNOSTICS, Indianapolis, IN, U.S.A., Uniform Latex Particles Catalogue (1984).
- S9. SERWINSKI, M., KEMBLAWSKI, Z., KIELBASA, J., ICIEK, J., Int. Chem. Eng., 8 (3):453 (1968).
- S10. SPEKMAN, J.B., SAVILLE, A.K., Textile Institute Journal, Proceedings, Vol.37, p.271 (1946).
- S11. STEADMAN, R., LUNER, P., "Papermaking Raw Materials", Trans. Fund. Res. Symp. Oxford 1985, Mechanical Eng. Pub., London Vol.1, p.311 (1985).
- S12. STEENBERG, B., THALEN, N., WAHREN, D., T.S.B.P. & B.M.A., F.Bolam ed., London, p.177 (1966).
- S13. STAMM, A.J., Tappi, 33 (9):435 (1950).
- S14. STONE, J.E., SCALLAN, A.M., Pulp & Paper Mag. of Canada, 66 (7):T407 (1965).
- S15. STONE, J.E., SCALLAN, A.M., ABERSON, G.M.A., Pulp & Paper Mag. of Canada, 67 (5):T263 (1966).
- S16. STONE, J.E., SCALLAN, A.M., "Consolidation of the Paper Web", Trans. Symp. Cambridge 1965, F. Bolam ed., T.S.B.P. & B.M.A., London, Vol.1, p.145 (1966).
- S17. STONE, J.E., SCALLAN, A.M., Tappi, 50 (10):496 (1967).
- S18. STRELIS, I., KENEDY, R.W., "Identification of North American Commercial Pulpwoods and Pulp Fibres", University of Toronto Press, (1967).

- T1. TAM DOO, P.A., KEREKES, R.J., Tappi Annual Meeting, p.169 (1981).
- T2. TAM DOO, P.A., KEREKES, R.J., Tappi 64 (3):113 (1981).
- T3. TAKEUCHI, N., SENDA, S., NAMBA, K., KUWABARA, G., Appita, 37 (3):223 (1983). also, Australia and New Zealand Pulp & Paper Ann. Meet. (1981).
- T4. TAPPI, Official Test Method - T503 om-84 (1984).
- T5. TAPPI, Official Test Method - T227 om-85 (1985).
- T6. TAPPI, Official Test Method - T240 om-81 (1981).
- T7. TASMAN, J.E., Tappi, 55 (1):136 (1972).
- T8. THALEN, N., WAHREN, D., Svensk Papperstid., 67 (7):259 (1964).
- T9. THALEN, N., WAHREN, D., Svensk Papperstid., 67 (11):474 (1964).
- T10. THODE, E.F., BERGOMI, J.G. Jr., UNSON, R.E., Tappi, 43 (5):505 (1960).
- T11. TREVELYAN, B.J., MASON, S.G., J. Colloid Science, 6 :354 (1951).
- T12. TURNER, J.C., TITCHENER, A.L., DUFFY, G.G., Appita, 30 (1):41 (1976).
- U1. UNBEHEND, J.E., Tappi, 59 (10):74 (1976).
- V1. VEINOV, K.A., IZYKSON, B.M., KOSTROMINA, O.E., SURNIN, B.M., BABURIN, S.V., Sb. Tr. Tsentr. Nauch.-Issled. Inst. Bumagi, (8):239 (1973)
- V2. VONDRAKOVA, M., NOLL, J., A.T.I.P. Revue, 22 (3):167 (1968).
- W1. WAHREN, D., Svensk Papperstid., 67 (13):536 (1964).
- W2. WAHREN, D., Svensk Papperstid., 70 (21):725 (1967).
- W3. WAHREN, D., Proc. of the I.P.C. Conf. on Paper Science and Technology, p.112 (1979).
- W4. WAHREN, D., I.P.C. Appleton WI 54912, "Paper Technology, Part 1: Fundamentals.", Lecture Notes. Ed. E.J. Bonano, (1980).
- W5. WASSER, R.B., Tappi, 61 (11):115 (1978).

- W6. WENZL, H.F.J., "The Chemical Technology of Wood", Academic Press, New York, London (1970).
- W7. WOLLWAGE, J.C., Ph.D. Thesis, "The Flocculation of Papermaking Fibres", Lawrence College, Appleton, Wisconsin (1938).
- W8. WOLLWAGE, J.C., Paper Trade J., 108 (12):41 (1939), 108 (13):25 (1939), also, Tappi, 22:578 (1939).
- W9. WRIST, P.E., "Fundamentals of Papermaking Fibres", Trans. Symp. Cambridge 1957, F. Bolam ed., T.S.B.P. & B.M.A., London, p.485 (1961).
- W10. WRIST, P.E., in "Surfaces and Coatings Related to Paper and Wood", ed. R.H. Marchessault and C. Skaar, Syracuse University Press (1967).

## GLOSSARY

APPARENT DENSITY is the ratio of apparent mass to apparent volume of a hydrophilic particle.

APPARENT MASS is a sum of masses of all materials constituting a particle.

APPARENT VOLUME is a space occupied by all materials constituting a particle.

APPARENT VOLUMETRIC CONCENTRATION is a ratio of the apparent volume of particles to the suspension volume. It is also a ratio of the apparent volume of fibres to the Type-C floc volume.

COHERENT FLOC is a denser part of fibre network having strength.

COHERENT FIBRE NETWORK is a physically interlocked system of fibres that exhibits strength. A coherent floc is a coherent network, but not every part of a coherent network is a floc, only the denser parts are.

CONSISTENCY is a term commonly used by paper makers with reference to PULP CONSISTENCY or PULP MASS CONCENTRATION. See term PULP CONSISTENCY.

FIBRE NETWORK is a physically interconnected system of fibres where forces can be transferred at contact points.

FLOC is a part of suspension having larger mass concentration than the surroundings.

FLOCCULATION INDEX is a ratio  $\sigma/N_0$ .  $\sigma$  is the spread of the experimental curve relative to the normalized distribution function  $N=N_0 \cdot p(s) \cdot [1-p(s)]$  in which  $p(s)$  is the probability of a deviation exceeding  $s$  when the standard deviation is unity.  $N$  is the number of pulses per centimeter at a given level of light transmission and  $N_0$  is a constant.

LIMITING CONCENTRATION is defined by equation (3).

LIMITING VISCOSITY NUMBER is a term in the equation for reduced viscosity of suspensions.

$$\frac{\mu_{sp}}{C_v} = [\mu] + a_1 \cdot C_v$$

Where,  $\mu_{sp}/C_v$  is the reduced viscosity,  $[\mu]$  is the limiting viscosity number,  $a_1$  is a coefficient, and  $C_v$  represents volumetric concentration.

NETWORK - see FIBRE NETWORK.

ORIENTATION FACTOR is  $\sin^4\theta \cdot \sin^2(2\Phi)$ . It is a component of dimensionless factor  $a$  which is shown below.

$$a = [(L/d)^2 / 6(\ln(2L/d) - 1.80)] \cdot \sin^4\theta \cdot \sin^2(2L\Phi)$$

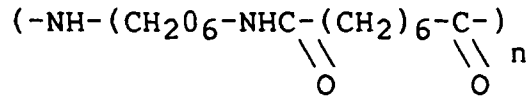
The factor  $a$  is in turn a term in the expression for the relative viscosity of suspensions of cylindrical particles,  $\mu_r$ .

$$\mu_r = 1 + a \cdot C_v$$

Where,  $L$ ,  $d$ ,  $C_v$  are cylinder length, cylinder diameter, volumetric concentration, and  $\theta$ ,  $\Phi$  are spherical polar

coordinates (angles).

NYLON 6-6 - condensation polymer of hexamethylene diamine with adipic acid.



PULP CONSISTENCY or, more properly "pulp mass concentration" is defined as the weight in grams of oven dry fibre in 100 grams of pulp-water mixture [C8,T6], and reported in %. In this dissertation, pulp consistencies are reported as fractions.

SUGAR  $\text{C}_{12}\text{H}_{22}\text{O}_{11}$ , molecular weight=342.3, density  $\rho=1580.5$   $\text{kg/m}^3$ .

THRESHOLD CONCENTRATION is an average suspension concentration at the onset of coherent floc formation under given flow conditions. In this dissertation it is always expressed in terms of apparent volumetric concentration.

TYPE-C COHESION - fibre interlocking by elastic bending.

WRR - Water Retention Ratio is the ratio of mass of the imbibed water to the dry mass of a particle.

WRR<sub>k</sub> - Water Retention Ratio at the "knee" (see Appendix I and II). For nylon it is simply a WRR at saturation. For wood-pulp fibres, it is a WRR when lumen is full of water and fibre walls are at the saturation point.

### Appendix I. Water Retention Ratio of Wood Pulp Fibres.

In the literature, the concentration of fibres in water is frequently given as the ratio of the dry fibre mass to the mass or volume of the whole suspension. Though such representation is precise, it gives only a fraction of the full picture. Knowledge of the volumetric concentration is also needed to assess the degree of fibre crowding or to relate fibre dimensions to the number of fibre-to-fibre contacts. The results of studies on man-made fibres should only be compared with those for wood-pulp fibres on the basis of volumetric concentration. Determination

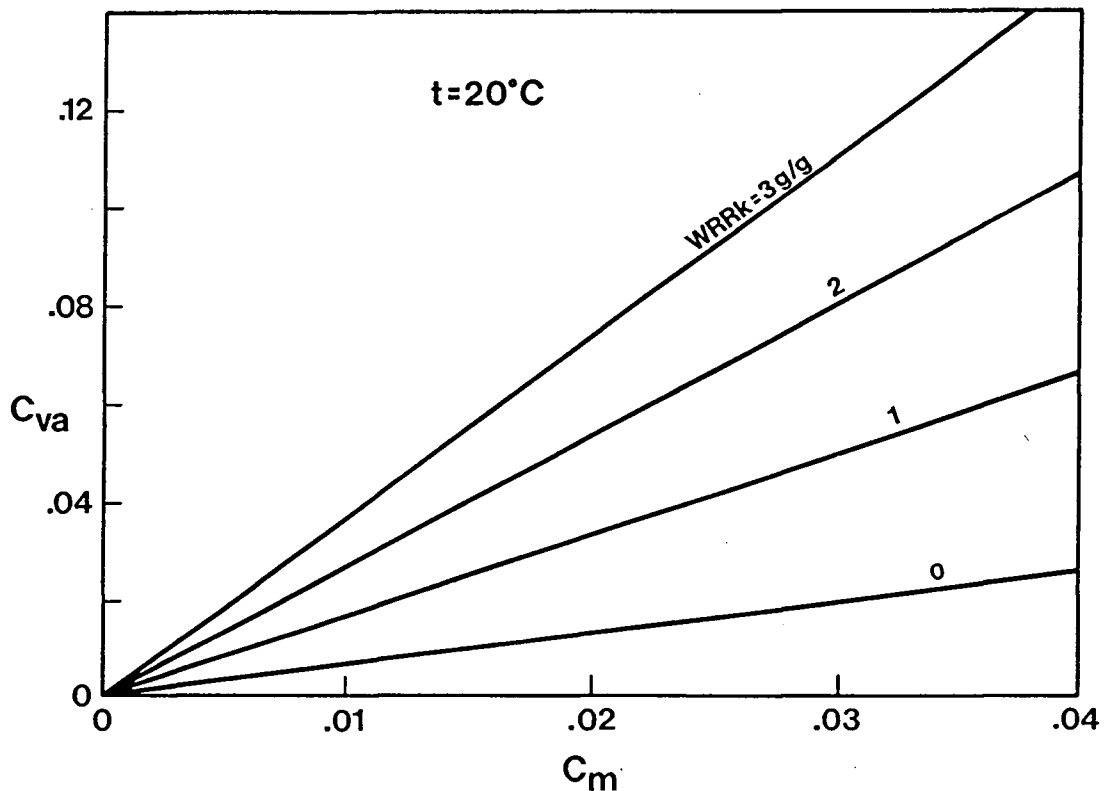


Figure I-40. Apparent Volume Concentration versus Mass Concentration for Wood-pulp Fibres.

of the volumetric concentration is complicated by the fact that wood pulp fibres are very hydrophilic. Often unknown are the volume of water held in the fibre lumen or by the fibre walls and the extent to which the fibre walls swell.

The importance of the amount of water held by fibres cannot be overemphasized. This is illustrated in Figure I-40 in which the relationships between mass concentration,  $C_m$ , and apparent volumetric concentration,  $C_{va}$ , are compared for wood-pulp fibres. In the calculation of the apparent volumetric concentration typical Water Retention Ratios (WRRk) were used (see Appendix II for discussion of WRRk and Appendix VII for derivation of the relationship). It is apparent that  $C_{va}$  may vary considerably for any given  $C_m$ . The most common value of WRRk is 2 g/g (grams of water per one gram of dry fibre) for softwood-pulps [E5]. At this WRRk, the value of  $C_{va}$  is about 2.7 times larger than  $C_m$ . For hardwood-pulps, WRRk=1.7 g/g and  $C_{va}$  is about 2.4 times larger than  $C_m$ .

WRRk can be calculated from the known dimensions of fibres, the density of fibre walls and the amount of water absorbed by fibre walls. The average dimensions of wood fibres are reported in several publications [I3,P1,R10,S3]. The average dimensions for North American species are reproduced in Table I-XVII for softwoods tracheids and hardwood fibres. The reduced dimensions after soda pulping to 60% yield, a typical yield, are also given. The calculation of WRRk values assumed that all fibres are regular tubes of rectangular cross-section having walls of 1500 kg/m<sup>3</sup> density [S4] and that their walls absorb 0.40 g of water

Table I-XVII. Average Dimensions of Wood Fibres and Pulp Fibres.

SOURCE	SOFTWOOD TRACHEIDS			HARDWOOD FIBRES		
	$\bar{L}$ mm	$\bar{w}$ $\mu\text{m}$	$\bar{t}$ $\mu\text{m}$	$\bar{L}$ mm	$\bar{w}$ $\mu\text{m}$	$\bar{t}$ $\mu\text{m}$
[P1]	3.53	36.2		1.61		
[R10]	3.89			1.20		
[I3]	3.28	34.1	3.75	1.05	19.3	3.62
[I3]	2.95	36.6		1.27	26.6	
[S4]		29.2	2.75		13.9	2.23
average	3.41	34.0	3.25	1.28	19.9	2.92
[S4] pulped	3.37	30.3	2.24	1.23	17.7	2.00

per 1g of dry wall material [S17]. WRRk values were: 2.0 g/g for softwood-pulp and 1.3 g/g for hardwood-pulp. Although these two values were calculated from average fibre dimensions, they are in surprisingly good agreement with the values reported in the Ellis et al. study [E5].

## Appendix II. Apparent Density of Wood Pulp Fibres in Aqueous Suspensions.

The selection of a substitute for wood-pulp fibres requires knowledge of all fibre properties. One of these properties is the apparent density of wood-pulp fibres in water. This topic has not been adequately addressed in the literature.

Wood pulp fibres are hydrophilic and must be dealt with as entities having an apparent mass and volume. Their mass is a sum of the mass of solid material constituting fibre walls and the mass of imbibed water which is defined as the water that can be quantitatively removed without changing the composition of fibre material [S13]. The quantity of imbibed water is a function of fibre morphology and chemical or physical treatment to which fibre was exposed.

The apparent density of wood pulp fibre is defined as:

$$\rho_a = \frac{\rho_{\text{water}} \cdot V_{\text{water}} + \rho_{\text{wall}} \cdot V_{\text{wall}}}{V_{\text{water}} + V_{\text{wall}}} \quad (\text{II-1})$$

where

$\rho_{\text{water}}$  - density of water,

$\rho_{\text{wall}}$  - density of fibre wall solids,

$V_{\text{water}}$  - volume of water,

$V_{\text{wall}}$  - volume of fibre wall solids.

Wood fibres are tube-like with closed and pointed ends. The space enclosed by the tube walls is called a "lumen." The tube walls are composed of cellulose, hemicellulose and lignin. Cellulose forms a skeleton of the fibre wall while hemicellulose

and lignin fill up a space within the cellulose fibril matrix. Chemical pulping alters the chemical composition and physical structure of the fibre walls. Lignin and hemicellulose which are gradually removed leave open spaces between fibrillae [S14,S16]. The spaces can be enlarged or new spaces created through mechanical or chemical treatment. In the wet state, water fills up these spaces and the lumen.

From a hydrodynamic point of view, wood pulp fibres are elongated, solid particles. Imbibed water that constitutes part of the particle is retained within the solid in three distinct ways:

- a) Fibre walls are swollen with water. The mass of water held by the walls,  $M_w$ , corresponds to the Fibre Saturation Point (FSP) [S17]. The degree of cooking affects the amount of water imbibed by fibre walls. The FSP of kraft cooked black spruce was reported to be 0.67 g/g at 92.4% yield and 1.14 g/g at 48.7% yield as determined by porous plate method at the relative vapour pressure of water  $p/p_0=0.9975$  [S17]. The larger water content of a cell wall was attributed to the increase in the wall thickness. Any changes to fibre length or fibre diameter were undetectable [S16,S15]. As the fibre wall swelled inward, the space occupied by the lumen diminished [S17].
- b) The lumen is filled with water. A certain mass of water  $M_l$ , depending upon the morphology of the fibres and the state of fibre collapse, is held in it.
- c) Water mass  $M_f$  is trapped by microfibrils which develop on the

Table II-XVIII. WRR at the "knee" for Various Never-dried Pulp.

PULP	WRR at the "knee" g/g
Unbeaten unbleached softwood kraft pulp	2.1
Unbeaten unbleached hardwood kraft pulp	1.8
Bleached softwood kraft pulp	
670 mL CSF	2.0
605 mL CSF	2.2
302 mL CSF	2.4
200 mL CSF	2.4
100 mL CSF	2.5
Bleached hardwood kraft pulp	
600 mL CSF	1.7
300 mL CSF	2.1

external surfaces of fibres particularly after mechanical treatment.

Determining the amount of imbibed water, i.e., the sum of  $M_w$ ,  $M_l$ , and  $M_f$  is extremely difficult. One relatively fast method is removal of water from the pulp pad by centrifugation. However, the interstices between the pad fibres form a capillary system that holds an additional mass of water  $M_i$ . This mass augments the difficulties in interpretation of method's results.

The amount of water retained by a pulp pad decreases with increasing applied centrifugal force. Water would first be forced out of inter-fibre spaces and laminae at lower centrifugal force because of their large capillary sizes in comparison with

the intra-wall pores. The transition from one mechanism of water removal to another is gradual within a range of centrifugal acceleration from  $3923 \text{ m/s}^2$  to  $29420 \text{ m/s}^2$  [S2], and not precisely defined. The water is likely partly confined within partially dried fibre walls and in intra-fibre spaces or lumina. There was no well-defined centrifugal force where a point of inflection might be identified.

The point of inflection was clearly noticeable when a greater range of centrifugal acceleration, from  $490 \text{ m/s}^2$  to  $490000 \text{ m/s}^2$  [E5] was used. This point was defined as an intercept between two straight lines drawn through the data points, and was called "a knee in water retention curve" [E5]. "The knee" is the best possible estimate of the ratio of the mass of imbibed water to the mass of dry, solid, fibre material. Table II-XVIII shows Water Retention Ratios (WRR) at the "knee" for various never-dried pulps [E5]. WRR's were determined with the following mathematical expression:

$$\text{WRR} = \frac{\text{moist pad weight after centrifuging}}{\text{oven-dry pad weight}} - 1 \quad (\text{II-2})$$

Knowing that

$$\text{WRR}_k = \frac{\rho_{\text{water}} \cdot V_{\text{water},k}}{\rho_{\text{wall}} \cdot V_{\text{wall}}} \quad (\text{II-3})$$

equation (II-1) can be transformed to:

Table II-XIX. Apparent Density of Wood Pulp Fibres at Selected WRRk Values.

WRRk	$\rho_a$
g/g	g/cm <sup>3</sup>
1.7	1.152
1.8	1.145
1.9	1.140
2.0	1.134
2.1	1.129
2.2	1.125
2.3	1.121
2.4	1.116
2.5	1.113

$$\rho_a = \frac{\rho_{\text{water}} \cdot (1 + \text{WRRk})}{\frac{\rho_{\text{water}}}{\rho_{\text{wall}}} + \text{WRRk}} \quad (\text{II-4})$$

With cellulose density = 1500 kg/m<sup>3</sup> [S4,S15] and water density = 998 kg/m<sup>3</sup> (at 20°C) [C10], values of the apparent density for different WRRk's were calculated and are shown in Table II-XIX. These values change slightly over a range of typical WRRk.

It should be noted that nylon 6-6 has 1140 kg/m<sup>3</sup> density when dry. Its density at saturation is slightly lower, i.e., about 1130 kg/m<sup>3</sup> as it absorbs about 7.4% of water.<sup>1</sup> Thus, nylon

<sup>1</sup> Experimental determination of moisture absorption by nylon 6-6 is described in Appendix VI.

fibres and wood pulp fibres of similar shapes and dimensions should, from the hydrodynamic point of view, behave alike.

### Appendix III. Estimates of Magnitudes of Various Cohesion Forces.

The magnitude of electro-chemical attractive forces between nylon 6-6 fibres in the concentrated aqueous-sugar solutions is unknown. It is not even known whether the mechanism of fibre interaction involves repulsive double-layer forces, attractive van der Waals forces, short distance repulsive forces [I4] and steric forces [N1] at the same time. Only a direct measurement could clarify this; however, experimental work hitherto not done and using equipment capable of measuring very small forces [I4] would be required. Because such equipment is unavailable, this study used a simpler approach. The net buoyant force on an individual fibre was used as the driving force to separate the forcibly brought-to-contact fibres with the permanently mounted monofilament. This force gave the estimate of the electro-chemical attraction between fibres and was compared to the forces needed to deflect (bend) simply supported fibres.

The deflection forces applied at the centre of simply supported fibres, as shown in Figure XVII-64, were calculated and are presented in Table III-XX. The shortest and the longest fibres of each diameter were considered to be supported at their ends.<sup>1</sup> The maximum fibre deflection was assumed to be equal to fibre diameter which in all cases did not exceed the elastic deformation regime [M2]. This approach provides a range of deflection forces for all types and lengths of fibres. The values of fibre stiffness in a wet state were used.<sup>2</sup>

---

<sup>1</sup> Fibre dimensions are discussed in Appendix V.

<sup>2</sup> See Appendix VIII.

Table III-XX. Forces Deflecting Simply Supported Fibres.

NYLON	FIBRE DIAMETER $\mu\text{m}$	FORCE, nN	
		LONG SPAN	SHORT SPAN
3	19.76	229	1813
6	27.95	704	11630
15	44.19	2847	27299

Nylon fibres, 4.666 mm long and 27.95  $\mu\text{m}$  in diameter, were suspended in aqueous-sugar solutions of increasing sugar content. The solutions prepared had 1100, 1110, and 1120  $\text{kg/m}^3$  density.<sup>1</sup> The apparent density of nylon fibres in pure water at 23°C was 1130  $\text{kg/m}^3$ .<sup>2</sup> The difference of 10  $\text{kg/m}^3$  between fibre and liquid densities produced the net buoyancy force of 0.28 nN.

Fibres brought into physical contact with the monofilament displayed no permanent stickiness in all three solutions. The conclusion is that the forces of attraction must be smaller than 0.28 nN. Clearly the forces presented in Table III-XX are at least three orders of magnitude larger than the upper limit placed on the electro-chemical attraction. If elastic fibre deflections in Type-C networks are about one fibre diameter, the normal forces at contact points are thousand times larger than the attractive colloidal forces.

<sup>1</sup> Solution preparation is described in Appendix XI.

<sup>2</sup> See Appendix II.

#### Appendix IV. Filament Cutting Procedure.

The fifteen-denier nylon 6-6 was obtained as fibres. The six- and three-denier nylon 6-6 was provided by DuPont Canada in the form of multifilaments. These multifilaments had to be cut for fibres to be produced. A cutting procedure which produced fibres of relatively uniform length was invented.

A sheet of A7 size millimeter graph-paper was folded in half with the line pattern on the outside. Two adhesive tabs were attached to the bottom part of the folded sheet at its opposite free edges so that half of the adhesive surfaces were exposed. The exposed surfaces coincided with the blank side of the folded

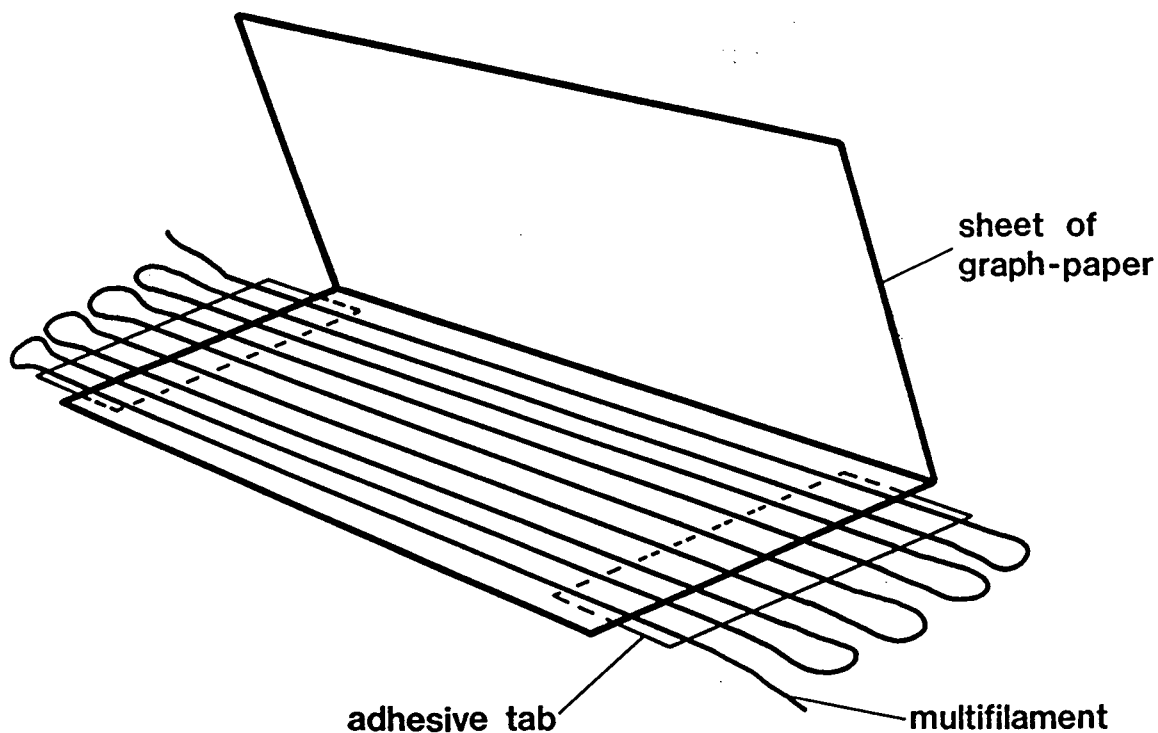


Figure IV-41. Multifilament Preparation for Cutting.

sheet. A nylon multifilament laid across the piece of paper was secured to the adhesive tabs, as shown in Figure IV-41. The top side of the folded sheet covered the filaments and was pressed down by a flat piece of metal. The paper and sandwiched nylon multifilaments were cut on a hand-operated guillotine. The printed millimeter grid helped align the sandwich and facilitated even spacing between cuts. The shearing action of the guillotine and the top pressure on the sandwich kept the multifilaments stretched.

## Appendix V. Measurement of Fibre Length and Curvature.

Fibre samples were enclosed in slide-mounts for fibre length and curvature determination. First, fibres were deposited on the wetted surface of the bottom glass window. For assurance that fibre deposited flat on the surface and could be easily recognized, the number of fibres per slide-mount was limited. Second, the top window was placed over the bottom window. The glass-windows spaced about 0.4 mm apart enclosed a volume totally filled with water. Two parallel black lines on the bottom glass window served as calibration marks. The distance between these marks had been determined by a traversing microscope and was

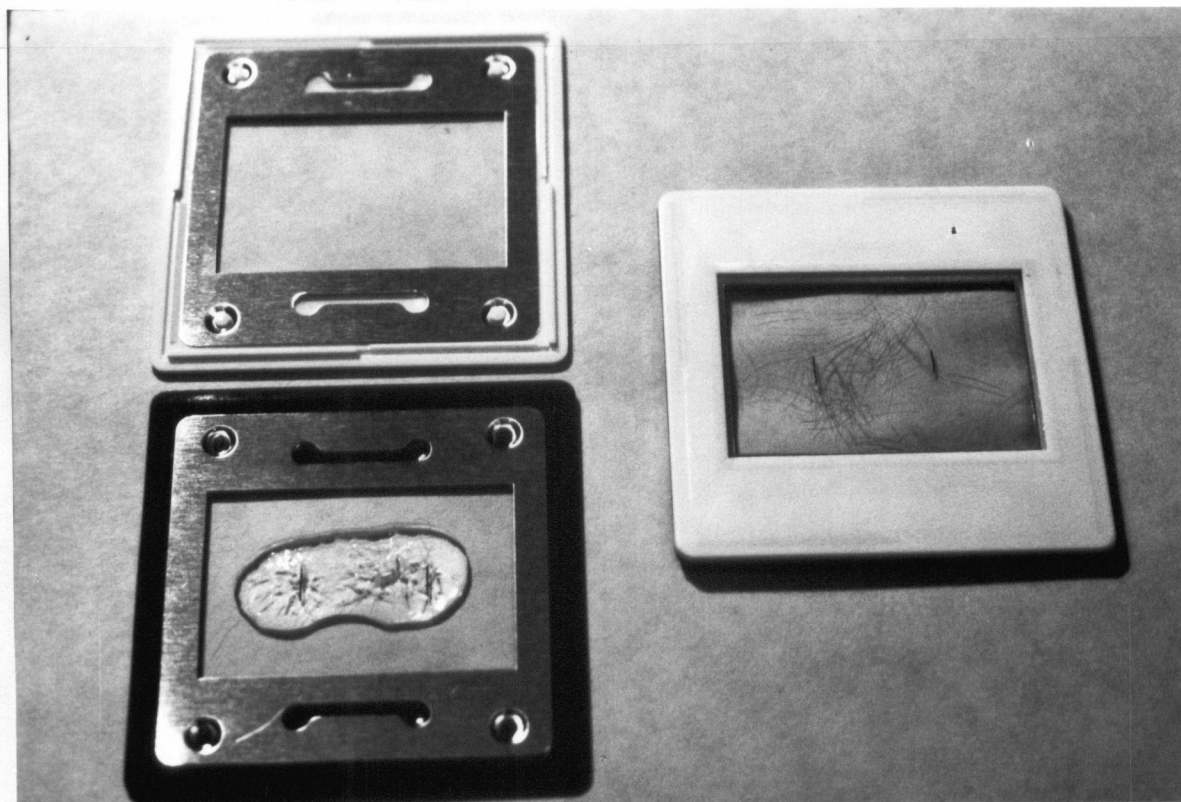


Figure V-42. Sample of Fibres deposited on the Slide Mount and Closed in It.

employed as a calibration constant. A photograph of an open and closed slide-mount is shown in Figure V-42.

Each slide-mount was installed in the slide-projector, and the images of fibres themselves were projected onto the digitizing pad. Magnification of about twelve times was achieved by the 24x36 mm frame being projected on the 300x450 mm active area of the pad. The shortest fibres had about 10 mm of projected length and the longest about 75 mm. The resolution of the digitizer which was set to 0.1 mm led to a maximum  $\pm 2\%$  error for straight fibres. Other sources of error arose from the fuzzy lines of fibre ends and fibre curvature. The maximum overall

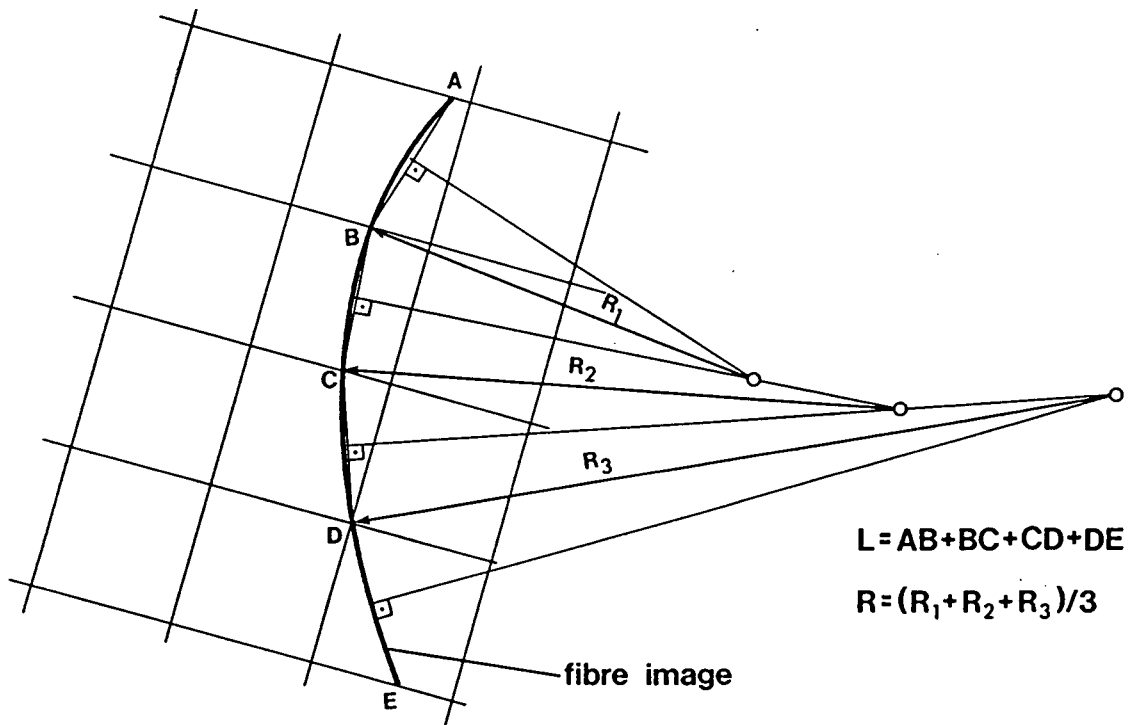


Figure V-43. Principle of Fibre Length and Radius of Curvature Measurements.

error was estimated to be less than  $\pm 3\%$ .

Fibre length was approximated by the sum of straight-line segments. The number of such segments per fibre, arbitrarily chosen, depended on fibre length and fibre curvature. More curved fibres needed more segments. Figure V-43 illustrates the measuring principle. The projected fibre image was delimited by two parallel lines on a millimeter graph paper. These lines touched the fibre ends and established the first and the last node. The millimeter paper facilitated division of the fibre image into sections of almost equal length. Thicker lines on the millimeter paper, such as the one-centimeter or half-centimeter line, crossed the fibre contour establishing additional nodes. The sum of straight line distances between the nodes constituted an approximation of a projected fibre length.

Each pair of straight line segments was also employed in calculations of a local radius of curvature. These segments were analytically halved. Straight lines normal to these segments were analytically constructed at the mid-points of each dissection. These lines intercepted if the fibre was curved, as shown in Figure V-43. The distance between the intercept point and the common point of neighboring segments was taken as the local radius of curvature. Each fibre had several local radii from which an average radius of curvature was calculated.

The length and curvature data were stored on a floppy-disk in a digital form. This digital information was transferred to the main-frame computer for analysis. The photograph of data

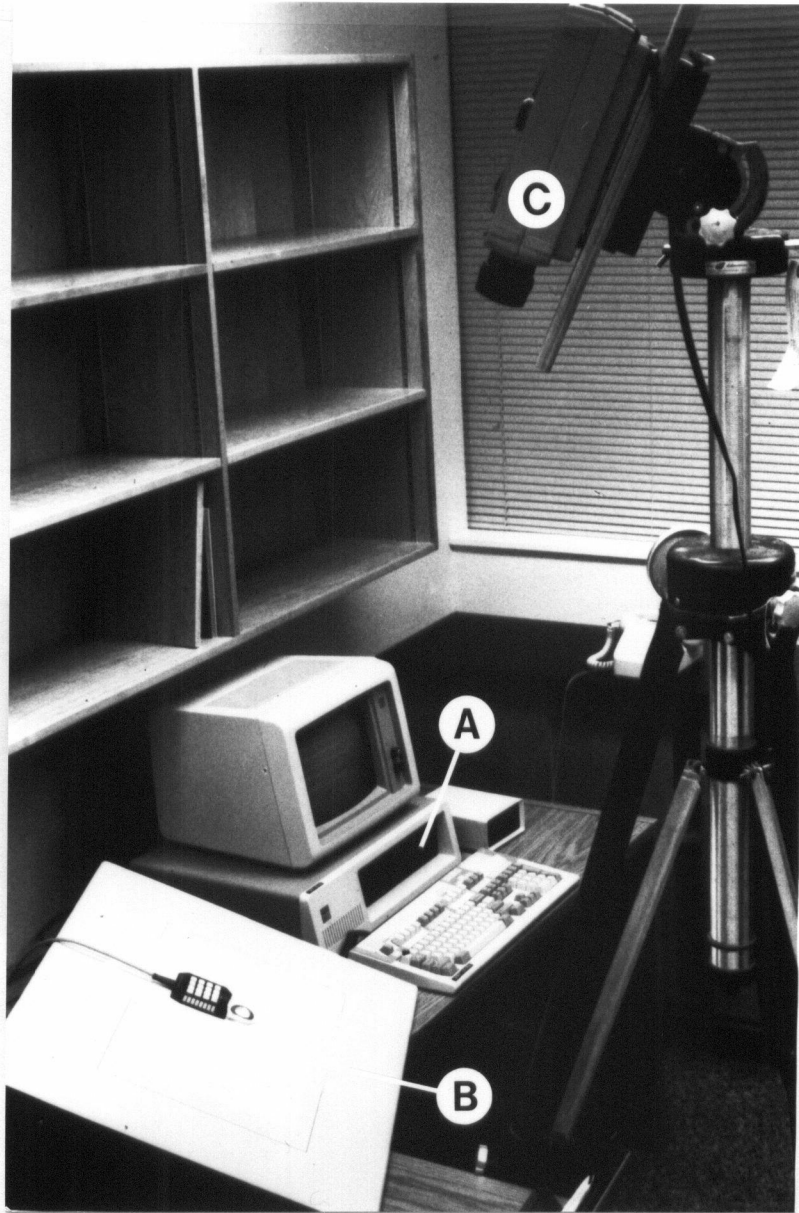


Figure V-44. Data Acquisition System for Fibre Length and Fibre Curvature Measurements.

acquisition hardware is shown in Figure V-44. The major components were: the IBM Personal Computer (8088 microprocessor) (A), the digitizer (Summagraphics Microgrid, model MG1218) (B), and the slide-projector (C).

The data acquisition program written in BASIC is listed in Appendix XIX. The additional software packages that enabled data processing and transfer were: PC-DOS version 2.1, Basic Interpreter version 1.0, Michigan Communication Protocol (to transfer files between the UBC-MTS and IBM-PC), and \*FREQ (statistical program available from UBC-MTS library). The results of statistical analysis in terms of first four moments are presented in Table V-XXI and Table V-XXII.

The coefficient of skewness is a measure of asymmetry of distribution. If the coefficient of skewness is positive, an excess of positive deviations from the mean is indicated. In such a case, the distribution is said to be "positively skewed." If the coefficient of skewness is negative, the distribution is said to be "negatively skewed." The coefficient of skewness is zero when the distribution is symmetrical.

The coefficients of skewness of fibre length distributions which are positive and negative indicate the excess of either longer or shorter than average fibres in each sample. The coefficients of skewness of fibre curvature distributions, all positive, indicate excess of straight fibres.

Kurtosis refers to peakedness of a distribution. If the distribution is very peaked and has relatively wide tails, it is referred to as "leptokurtic." The coefficient of kurtosis is positive. If the distribution is rather flat in the middle and has relatively thin tails, it is called "platykurtic." The coefficient of kurtosis is negative. For a Gaussian

Table V-XXI. Nylon Fibres in Wet State. Fibre Length Statistics.

TYPE OF FIBRE	DIAMETER d	SAMPLE SIZE	FIBRE LENGTH		ASPECT RATIO L/d	SKEWNESS COEFFICIENT	KURTOSIS COEFFICIENT
			AVERAGE LENGTH L	STANDARD DEVIATION			
denier*	$\mu\text{m}$		mm	mm			
3	19.76	1062	0.9158	0.08484	46.35	-0.06787	1.298
		1054	1.875	0.09244	94.88	-1.564	67.15
		1231	2.815	0.1019	142.5	5.268	-297.2
		1117	3.737	0.1122	189.1	5.572	-552.9
6	27.95	1237	0.9139	0.08322	32.70	0.02546	1.926
		1138	1.832	0.09898	65.55	-1.279	49.87
		1042	2.757	0.1267	98.65	1.642	-66.22
		1049	3.718	0.1576	133.0	2.354	-138.9
		1024	4.666	0.1338	166.9	-4.929	403.1
15	44.19	1038	1.560	0.1009	35.30	-0.3115	1.920
		1162	2.947	0.1081	66.69	4.566	-249.1
		1001	4.973	0.1762	112.5	-3.211	235.7
		1006	6.261	0.1769	141.7	-13.38	729.9

\* Denier is a weight in grams of 9000 meters long monofilament.

Table V-XXII. Nylon Fibres in Wet State. Curvature Statistics.

TYPE OF FIBRE	DIAMETER d	SAMPLE SIZE	FIBRE CURVATURE		SKEWNESS COEFFICIENT	KURTOSIS COEFFICIENT
			AVERAGE 1/R **	STANDARD DEVIATION		
denier*	$\mu\text{m}$		$\text{mm}^{-1}$	$\text{mm}^{-1}$		
3	19.76	1062	0.3094	0.21323	0.7796	0.3561
		1054	0.25533	0.17189	0.7765	0.4457
		1231	0.28114	0.19328	0.8155	0.4324
		1117	0.28547	0.18807	0.7543	0.3127
6	27.95	1237	0.16965	0.14534	1.850	7.250
		1138	0.15223	0.11126	1.124	1.742
		1042	0.16181	0.11952	1.250	2.397
		1049	0.12968	0.10034	1.476	3.660
		1024	0.13701	0.10336	1.259	2.088
15	44.19	1038	0.08366	0.08033	3.384	25.30
		1162	0.07240	0.06239	3.289	27.45
		1001	0.07107	0.05731	1.730	4.297
		1006	0.06060	0.05105	1.983	7.636

\* Denier is a weight in grams of 9000 meters long monofilament.

\*\* R denotes a radius of curvature.

distribution, the coefficient of kurtosis is zero.

The distributions of fibre length are both lepto- and platykurtic whereas the distributions of fibre curvature are always leptokurtic. The coefficients of skewness and kurtosis indicate that length and curvature distributions cannot be considered as Gaussian [B7].

The standard deviations of the means of fibre length and curvature indicate very narrow distributions of both. Low fibre curvatures and narrow length distributions justify the use of these fibres in testing the statistical theories developed by Miles [C5] and Meyer and Wahren [M10].

Fibre diameters were calculated from the information on weight per unit length of multifilament, the number of monofilaments, and the material density. The diameters were corrected for water swelling effect under the assumption that fibres swell uniformly in every direction. Some evidence suggests this is not so. The nylon fibres swelled more laterally (4.8%) than longitudinally (1.2%), increasing fibre volume by 11.1% [S10]. If uniform swelling upon absorption of 7.4%<sup>1</sup> of water is assumed, the diameter increase of 2.4% is calculated. Such a small discrepancy in the diameter estimate (2.4% vs. 3.2%) did not justify further extensive experimental investigation. Hence, the 2.4% increase was used in calculations of wet fibre diameters.

---

<sup>1</sup> Water absorption by nylon 6-6 is described in Appendix VI.

## Appendix VI. Water Absorption by Nylon Fibres.

All three types of nylon were tested for water absorption. Figure VI-45 shows a photograph of the experimental setup. The oven-dry sample, weighing few grams, was placed in 98% relative humidity (RH) environment and its weight increase recorded.

A relative humidity of 98% was created in the desiccator (A) containing a large amount of saturated aqueous solution of cupric sulphate ( $\text{CuSO}_4 \cdot 5\text{H}_2\text{O}$ ) (B) [C10]. The nylon sample (C) was placed in the glass dish (D) located immediately above the cupric sulphate. The dish was suspended in the wire-basket (E) hooked on to the AE183 Mettler balance (F) from underneath. The



Figure VI-45. Experimental Setup for Water Absorption by Nylon Fibres.

suspending wire through a small hole in the desiccator lid reached the balance's hook. The balance was electrically connected to the IBM-PC (G) through an Option-012 data interface. Control over data acquisition was made possible through a BASIC program which is listed in Appendix XX. Every increase in weight equal to or slightly larger than 0.001 g was stored in a data file along with the TIMER readings in seconds. The data were transferred to the UBC-MTS system through a modem for analysis and plotting. The water absorption data for 15 denier

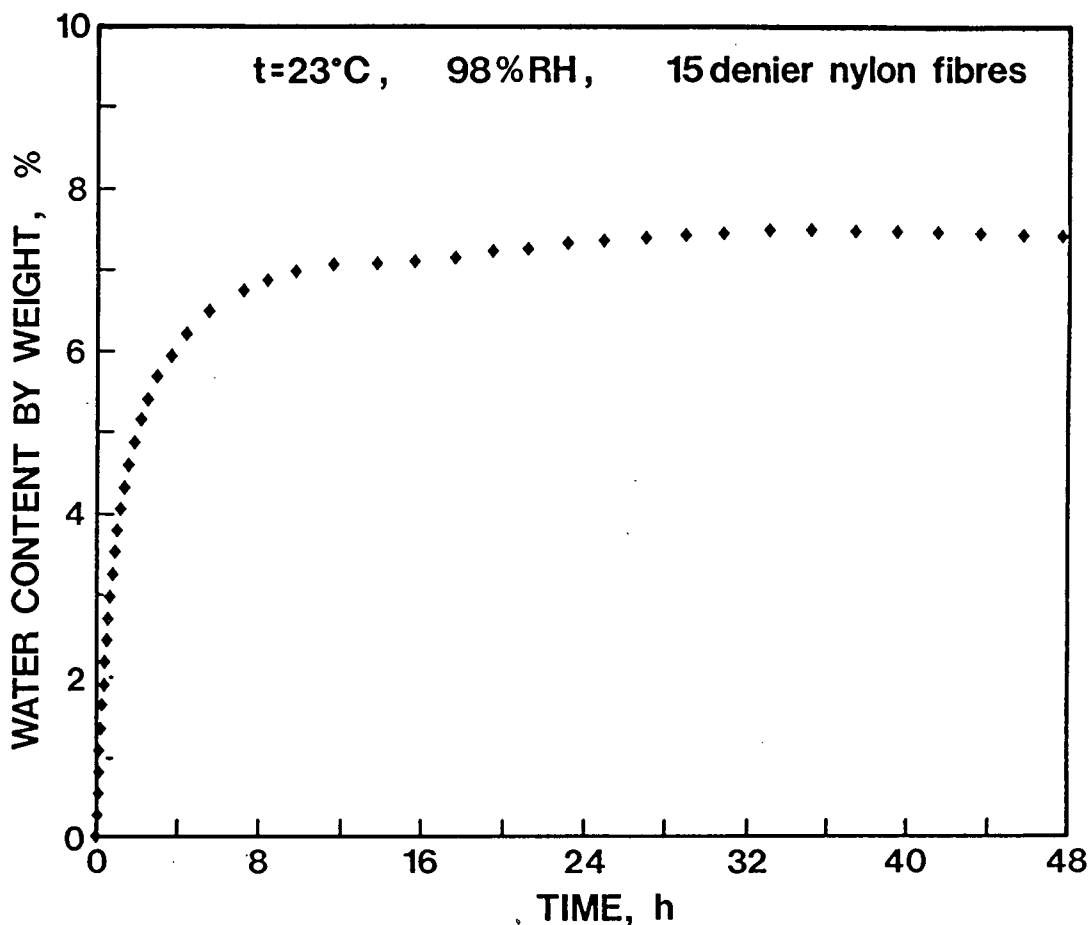


Figure VI-46. Water Absorption by Nylon Fibres in 98% RH Environment.

nylon are shown in Figure VI-46 in which only every tenth experimental point is plotted. Similar curves were obtained for 6 and 3 denier nylon fibres. It can be seen that, after 48 hours of exposure, the water content levelled off.

Longer periods of exposure were also checked. Table VI-XXIII shows the weights of samples after 48, 72, and 96 hours of exposure. Variations in ambient temperature were small. These data indicate that no further water absorption took place beyond a 48 hour period. The average water content for 15 samples and three time periods was accepted as the representative water to nylon mass ratio at saturation. This ratio can be substituted as  $WRR_k$  in the calculations of mass and volume concentrations. The water content of nylon material at 100% RH is slightly greater [S10], but the water content at 98% RH satisfactorily approximates it. An advantage of experiments conducted at 98% RH is that water condensation due to ambient temperature fluctuations is avoided.

Table VI-XXIII. Water Absorption by Nylon Fibres in 98% Relative Humidity Environment.

TYPE OF NYLON	SAMPLE NUMBER	SAMPLE WEIGHT				MOISTURE RETENTION	
		OVEN - DRY	EXPOSED TO 98% R.H. ENVIRONMENT			IN NYLON FILAMENTS	
			AFTER 48 HOURS T=22.7°C	AFTER 72 HOURS T=21.7°C	AFTER 96 HOURS T=21.8°C	AVERAGE	STANDARD DEVIATION
denier*	#	g	g	g	g	g/g	g/g
3	1	1.1189	1.3172	1.3187	1.3158	0.07250	0.002423
	2	1.5896	1.7052	1.7073	1.7046		
	3	1.6870	1.8098	1.8103	1.8077		
	4	1.7736	1.9027	1.9042	1.9002		
	5	1.9166	2.0546	2.0572	2.0548		
6	6	2.9235	3.1415	3.1352	3.1393	0.07329	0.002315
	7	3.0768	3.3015	3.2956	3.3007		
	8	3.3618	3.6120	3.6086	3.6076		
	9	3.4039	3.6526	3.6515	3.6540		
	10	3.5055	3.7649	3.7649	3.7630		
15	11	1.0274	1.1053	1.1053	1.1047	0.07689	0.004941
	12	1.7767	1.9138	1.9197	1.9122		
	13	1.7897	1.9320	1.9251	1.9256		
	14	1.9118	2.0621	2.0535	2.0564		
	15	1.9887	2.1470	2.1423	2.1403		
FOR ALL OBSERVATIONS						0.07423**	0.003478

\* Denier is a weight in grams of 9000 meters long monofilament.

\*\* This average value was accepted as WRRk in calculations of mass or volume concentrations.

**Appendix VII. Relationship Between Mass and Volume Concentration of Hydrophilic Particles Suspended in Aqueous-Solute Solutions.**

The majority of the experimental works in the literature contains findings reported in terms of suspension mass concentration or as a ratio of oven-dry fibre mass to the suspension volume. This is so because the oven-dry fibre mass is easily determined with commonly available equipment - an oven and a balance. Using the available information from the literature requires recalculation of mass concentration or mass content into volume concentration. The coherence and structure of fibre networks are closely related to the spatial arrangement of fibres and the volume they occupy. Thus, comparison of experimental results or interpretation of theoretical calculations requires recalculation of mass concentrations into volume concentrations or vice versa. Such a task is frequently repeated and, if the necessary relationships are not readily available, becomes an unnecessary burden. If all possible relationships for hydrophilic particles are derived from the following basic parameters compiled in this Appendix, the task is avoided:

$V_p$  - moisture-free particle volume (solid substance),

$V_w$  - volume of water absorbed by particles,

$V_l$  - volume of suspending liquid (aqueous-solvent solution),

$V_p + V_w$  - apparent particle volume,

$\rho_p$  - moisture-free particle density (solid substance),

$\rho_w$  - water density,

$\rho_l$  - suspending liquid density,

$C_m$  - mass concentration,

$C_{ma}$  - apparent mass concentration,  
 $C_v$  - volume concentration,  
 $C_{va}$  - apparent volume concentration,

Wood-pulp fibres and nylon fibres are hydrophilic. A wood-pulp fibre absorbs water into its cellulosic wall and imbibes water into its lumen. A nylon fibre retains water solely by absorption. Regardless of the mechanism of absorption, both fibres have a certain mass of water in them at saturation. A concept of Water Retention Ratio at saturation (WRRk) introduced in Appendix II can be used for any hydrophilic material.

$$WRRk = \frac{\rho_w \cdot V_{wk}}{\rho_p \cdot V_p} \quad (VII-1)$$

$$C_m = \frac{V_p \cdot \rho_p}{V_p \cdot \rho_p + V_{wk} \cdot \rho_w + V_l \cdot \rho_l} \quad (VII-2)$$

$$C_{ma} = \frac{V_p \cdot \rho_p + V_{wk} \cdot \rho_w}{V_p \cdot \rho_p + V_{wk} \cdot \rho_w + V_l \cdot \rho_l} \quad (VII-3)$$

$$C_v = \frac{V_p}{V_p + V_{wk} + V_l} \quad (VII-4)$$

$$C_{va} = \frac{V_p + V_{wk}}{V_p + V_{wk} + V_l} \quad (VII-5)$$

The expression (VII-1) introduced to equations (VII-2, VII-3, VII-4, VII-5) yields the following relationships:

$$C_m = \frac{1}{1 + WRRk + \frac{V_1 \cdot \rho_1}{V_p \cdot \rho_p}} \quad (\text{VII-6})$$

$$C_{ma} = \frac{1}{1 + \frac{(V_1 \cdot \rho_1) / (V_p \cdot \rho_p)}{1 + WRRk}} \quad (\text{VII-7})$$

$$C_v = \frac{1}{1 + \frac{\rho_p \cdot WRRk}{\rho_w} + \frac{V_1}{V_p}} \quad (\text{VII-8})$$

$$C_{va} = \frac{1}{1 + \frac{V_1/V_p}{1 + (\rho_p/\rho_w) \cdot WRRk}} \quad (\text{VII-9})$$

Table VII-XXIV provides relationships between mass and volume concentrations derived from equations (VII-6), (VII-7), (VII-8) and (VII-9). In the case of nylon fibres, the WRRk should be replaced by water to nylon mass ratio at the saturation point. Appendix VI contains a description of the empirical evaluation of water absorption by nylon fibres.

Table VII-XXIV. Relationships Between Mass and Volume Concentration of Hygrophilic Particles in Suspensions.

$C_m =$	$C_{ma} =$	$C_v =$	$C_{va} =$
$C_m$	$(1+WRRk)C_m$	$\frac{1}{1 + \left(\frac{\rho_p}{\rho_w} \frac{\rho_p}{\rho_1}\right) WRRk + \frac{\rho_p}{\rho_1} \left(\frac{1}{C_m} - 1\right)}$	$\frac{\frac{\rho_p}{1 + \frac{1}{WRRk}}}{\rho_w} \frac{1}{1 + WRRk \left(\frac{\rho_p}{\rho_w} \frac{\rho_p}{\rho_1}\right) + \frac{\rho_p}{\rho_1} \left(\frac{1}{C_m} - 1\right)}$
$\frac{C_{ma}}{1+WRRk}$	$C_{ma}$	$\frac{1}{\left(\frac{1}{C_{ma}} - 1\right) \left(1+WRRk\right) + \frac{\rho_1}{\rho_p} \left(1 + \frac{\rho_p}{WRRk}\right)}$	$\frac{\frac{\rho_p}{1 + \frac{1}{WRRk}}}{\rho_w} \frac{1}{1 + WRRk \left(\frac{\rho_p}{\rho_w} \frac{\rho_p}{\rho_1}\right) + \frac{1}{C_{ma}} \left(1+WRRk\right) \frac{\rho_p}{\rho_1}}$
$\frac{1}{1 + WRRk \left(1 + \frac{\rho_1}{\rho_w} \left(\frac{1}{C_v} - 1\right)\right) + \frac{\rho_1}{\rho_p} \left(\frac{1}{C_v} - 1\right)}$	$\frac{1}{1 + \frac{\frac{1}{C_v} \rho_1 \rho_p}{\rho_p \rho_w} \left(1 + \frac{1}{WRRk}\right)}$	$C_v$	$\frac{\rho_p}{\rho_w} \left(1 + \frac{1}{WRRk}\right) C_v$
$\frac{1}{1 + WRRk + \left(\frac{1}{C_{va}} - 1\right) \left(\frac{\rho_1}{\rho_p} + \frac{\rho_1}{\rho_w} WRRk\right)}$	$\frac{1}{1 + \frac{\frac{\rho_1}{\rho_p} \left(1 + \frac{1}{WRRk}\right) \rho_p}{\rho_p C_{va} \rho_w}}$	$\frac{C_{va}}{\left(1 + \frac{\rho_p}{WRRk}\right) \rho_w}$	$C_{va}$

## Appendix VIII. Measurement of the Elastic Moduli of Fibres.

Two methods of measurement were considered: fibre bending in a cross flow of water and tensile testing of wet filaments. The bending method has been used in studies of wood-pulp fibre flexibility in the PAPRICAN laboratory at the UBC. The apparatus was readily available. The experimental technique and theoretical background are described elsewhere [T1,T2]. This test method and computational method were applied without change. It was found that the calculated elastic modulus of a given nylon fibre varied nonlinearly with the degree of fibre deflection. Accordingly, the computational part of this method was judged to be unreliable and was discarded. The experimentally determined deflections were kept and used to evaluate the ratio between elastic moduli.

The tensile method, probably the most popular, relies on the load-elongation character of a material in its elastic regime. This method has been standardized in material testing [A12,A14]. Nylon 6-6 filaments were heat treated at 105°C for four hours and soaked in water for 48 hours before being tested. Groups of filaments or a single filament were elongated at a constant rate of 10.5 mm/min in the THWING/ALBERT tensile tester. However, the tester clamps were too coarse for adequate clamping of filaments, and therefore the tests were conducted with two distinctly different span lengths, one twice as long as the other. The rationale for such change which starts with the equation defining the elastic modulus is:

$$E = \frac{\sigma}{\epsilon} = \frac{F/A}{\Delta L/L} = \frac{F \cdot L}{A \cdot \Delta L} \quad (\text{VIII-1})$$

where

E - elastic modulus,

$\sigma$  - stress corresponding to strain  $\epsilon$ ,

$\epsilon$  - strain within elastic regime,

A - cross-section area of a test sample,

F =  $\sigma \cdot A$  - force,

L - test span, distance between clamps,

$\Delta L$  - elongation under applied force F,

Equation (VIII-1) can be transformed to:

$$\Delta L = \frac{F \cdot L}{A \cdot E} \quad (\text{VIII-2})$$

Under imperfect clamping conditions, the observed elongation is different from that expressed by equation (VIII-2) by the amount of slip,  $\delta$ .

$$\Delta L' = \Delta L + \delta \quad (\text{VIII-3})$$

If experimentally obtained  $\Delta L'$  was used in the calculation of the elastic modulus, it would result in an underestimate. Such an error can easily be eliminated by the testing of two sets of samples, one having substantially different test span from the other. In practice it is convenient for one test span to be twice the length of the other. The apparent elongations would then be:

$$\Delta L_s = \Delta L + \delta = \frac{F \cdot L}{A \cdot E} \quad (\text{VIII-4})$$

for the short-span samples, and

$$\Delta L_1 = 2 \cdot \Delta L + \delta = \frac{F \cdot 2L}{A \cdot E} \quad (\text{VIII-5})$$

for the long-span samples.

The amount of slip should be identical in both experiments, and the difference between apparent elongations yields the true elongation for short-span samples.

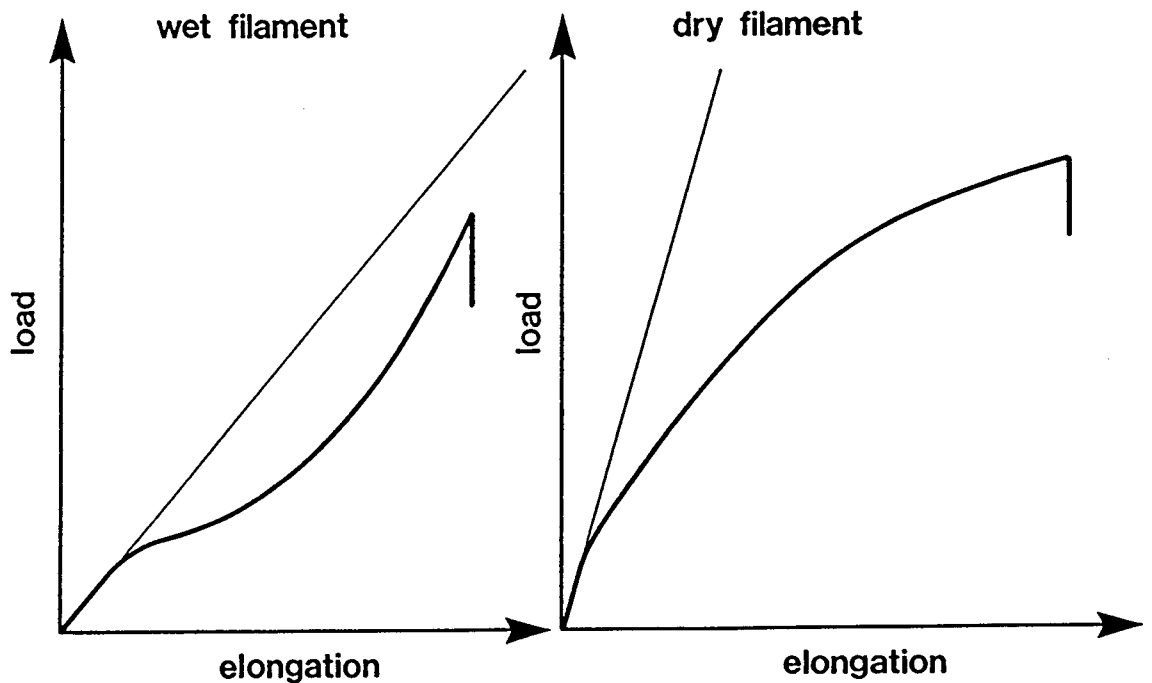


Figure VIII-47. Typical Load-elongation Curves for 3 Denier Nylon Filaments in Wet and Dry State.

$$\Delta L = \Delta L_1 - \Delta L_s \quad (\text{VIII-6})$$

The apparent elongations were recorded on charts along with the applied loads. Typical load-elongation curves for 3 denier nylon filaments are shown in Figure VIII-47. The different slopes of the initial parts of load-elongation curves for wet and dry filaments are clearly distinguishable.

The elastic modulus of 15 denier nylon was not measured because it was pre-cut into fibres too short to be clamped. The 3 and 6 denier filaments were tested. Table VIII-XXV shows the test conditions and the elastic moduli.

Clearly, air-dry filaments exhibit about three times higher elastic moduli than heat-treated, saturated-with-water filaments. These empirical findings agree with those cited in the literature [S10,M9]. For example, at 50%RH the elastic modulus was reported to be  $3.12 \cdot 10^9 \text{ N/m}^2$ , and at 100%RH it was only  $1.17 \cdot 10^9 \text{ N/m}^2$  [M9].

Since 15 denier nylon could not be tensile tested, the results of fibre flexing were used to evaluate its elastic modulus. The deflection,  $y_{\max}$ , of the fibre beam and the flow rate of water through the glass capillary tube,  $Q$ , had been measured. Plotting the deflection and the bulk Reynolds number established a deflection ratio between 6 and 15 denier fibres from which the ratio of elastic moduli could be obtained. When this ratio was known, the elastic modulus for 15 denier, heat-treated, wet nylon could be calculated from the elastic

Table VIII-XXV. Elastic Moduli of 3 and 6 Denier Nylon Filaments.

ELASTIC MODULUS N/m <sup>2</sup>		TEST CONDITIONS
3 denier	6 denier	
4.95·10 <sup>9</sup>	5.45·10 <sup>9</sup>	23°C 22% RH
1.69·10 <sup>9</sup>	1.78·10 <sup>9</sup>	4 hours at 105°C rewetted for 48h

modulus of 6 denier nylon.

The geometry of a bent fibre is shown in Figure VIII-48 with the shape of the velocity profile of the flow causing the deflection [T1]. The water flow rate is related to the velocity distribution as follows:

$$dQ = 2 \cdot \pi \cdot r \cdot V(r) \cdot dr \quad (\text{VIII-7})$$

Integration and division of (VIII-7) by the cross-sectional area of the glass tube yields the bulk velocity,  $V_b$ .

$$V_b = \frac{2}{(c/2)^2} \cdot \int_0^{c/2} V(r) \cdot r \cdot dr \quad (\text{VIII-8})$$

The bulk Reynolds number based on fibre diameter is defined as

$$Re_b = \frac{\rho \cdot V_b \cdot d}{\mu} = \frac{2}{(c/2)^2} \cdot \int_0^{c/2} Re(r) \cdot r \cdot dr \quad (\text{VIII-9})$$

The maximum fibre deflection is governed by the equation

Tam Doo & Kerekes  
(1981)

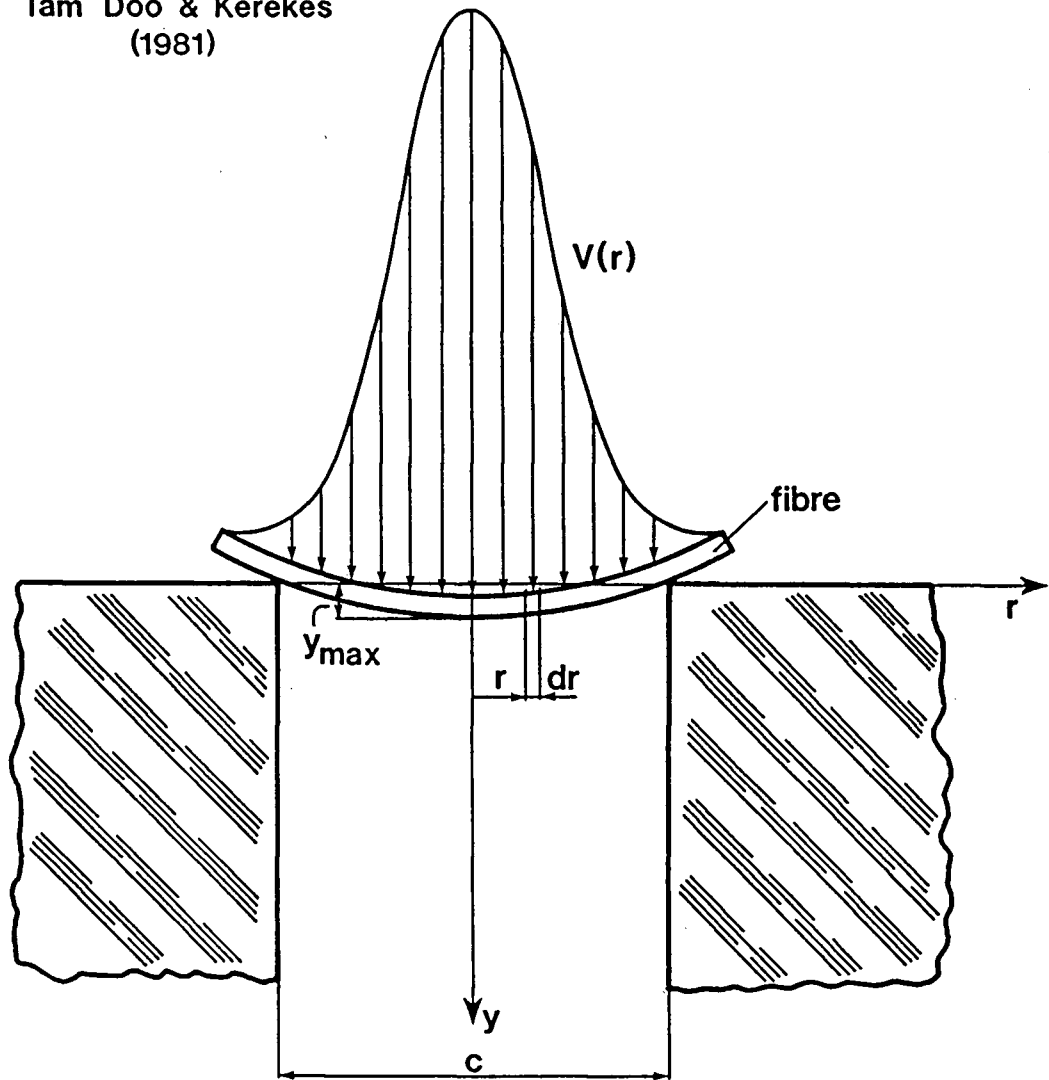


Figure VIII-48. Simply supported Fibre deflects in a Cross-flow.  
Figure taken from [T1].

$$y_{\max} = \frac{F \cdot c^3}{k \cdot E \cdot I} \quad (\text{VIII-10})$$

of the small-deflection beam theory. Where,

$c$  - beam span, i.e., capillary tube diameter,

$k$  - constant depending on the type of beam support and the shape

of the velocity distribution across the capillary tube,  
 F - the resultant force from the hydrodynamic drag which  
 depends on the velocity distribution along fibre beam:

$$F = C_D \cdot \rho \cdot d \cdot \int_0^{c/2} v^2(r) \cdot dr \quad (\text{VIII-11})$$

It can also be expressed in terms of Reynolds number:

$$F = C_D \cdot \frac{\mu^2}{\rho \cdot d} \cdot \int_0^{c/2} Re^2(r) \cdot dr \quad (\text{VIII-12})$$

Since the velocity distribution profiles behind the fibre beam do not change over the range of Reynolds numbers used [T1], drag forces expressed in terms of Reynolds number can be compared. Substitution of (VIII-12) into (VIII-10) yields a relationship between the fibre deflection and the Reynolds number:

$$y \cdot E = \frac{64 \cdot C_D \cdot \mu^2 \cdot l^3}{\pi \cdot k \cdot \rho \cdot d^5} \cdot \int_0^{c/2} Re^2(r) \cdot dr \quad (\text{VIII-13})$$

When  $Re(r)$  distributions for two different fibres are identical, the drag coefficients are equal and the ratio of  $y \cdot E$  between 6 and 15 denier fibres depends solely on fibre geometry:

$$\frac{y_6 \cdot E_6}{y_{15} \cdot E_{15}} = \left[ \frac{d_{15}}{d_6} \right]^5 \quad (\text{VIII-14})$$

The same holds if the bulk Reynolds numbers are identical, cf. equation (VIII-9). The plot of fibre deflection versus bulk Reynolds number is shown in Figure VIII-49. Solid lines

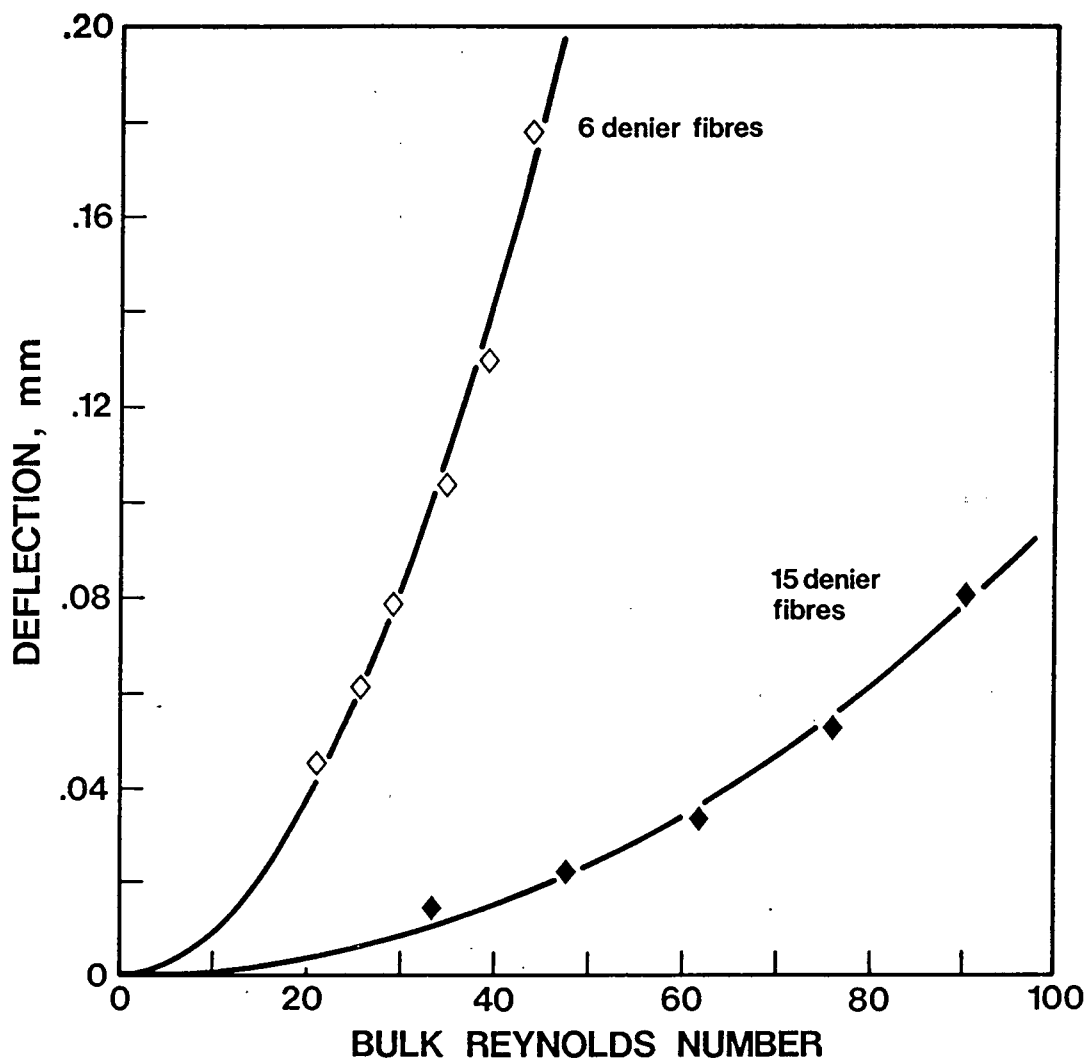


Figure VIII-49. Fibre Deflection versus Bulk Reynolds Number.

represent the power curve fits of the form,

$$y = a \cdot (Re_b)^b \quad (\text{VIII-15})$$

Satisfactory agreement between the theory (equation (VIII-14)) and experiment exists (Appendix XXI, point f). The desired ratio of fibre deflections can be calculated from

$$\frac{y_6}{y_{15}} = \frac{1}{Re_{b2} + Re_{b1}} \cdot \frac{a_6}{a_{15}} \cdot \int_{Re_{b1}}^{Re_{b2}} Re_b^{(b6-b15)} dRe_b \quad (\text{VIII-16})$$

for a chosen range of the bulk Reynolds numbers.

With  $Re_{b1}=20.$  and  $Re_{b2}=50.$  for the integral limits, the deflection ratio is 9.78. The elastic modulus for 15 denier, wet nylon fibre can be now calculated from the following expression.

$$E_{15} = E_6 \cdot \frac{y_6}{y_{15}} \cdot \left[ \frac{d_6}{d_{15}} \right]^5 \quad (\text{VIII-17})$$

Its value is  $1.76 \cdot 10^9 \text{ N/m}^2.$

All elastic moduli and stiffness for wet nylon fibres are shown in Table VIII-XXVI.

**Table VIII-XXVI. Elastic Moduli and Stiffness of Wet Nylon Fibres.**

NYLON denier	DIAMETER $\mu\text{m}$	ELASTIC MODULUS $\text{N/m}^2$	STIFFNESS $\text{N}\cdot\text{m}^2$
3	19.76	$1.69 \cdot 10^9$	$12.6 \cdot 10^{-12}$
6	27.95	$1.78 \cdot 10^9$	$53.3 \cdot 10^{-12}$
15	44.19	$1.76 \cdot 10^9$	$329.4 \cdot 10^{-12}$

The FORTRAN program that processes raw data, calls NL2SOL curve fitting subroutine, and plots the results, is listed in Appendix XXI. The listing of deflection data, and calibration fits for GILMONT flowmeter and micrometer eye-piece are also given there.

## Appendix IX. Friction Between Wet Fibre Surfaces.

An inclined plane method [A15,T4] was used to determine the friction coefficients between wet nylon fibre surfaces. Both coefficients, static and dynamic, have been measured. Figure IX-50 illustrates the experimental principle.

The acrylic tank (A) filled with an aqueous sugar solution housed the inclined plane (B) and the sled (C). The sled and the plane were covered with tightly wound multifilaments of nylon (D). One end of the plane was pulled up by the string (E) at the constant speed of 10 mm/min. At the moment when the sled started to slide down the slope, the pull was halted and the angle  $\alpha$

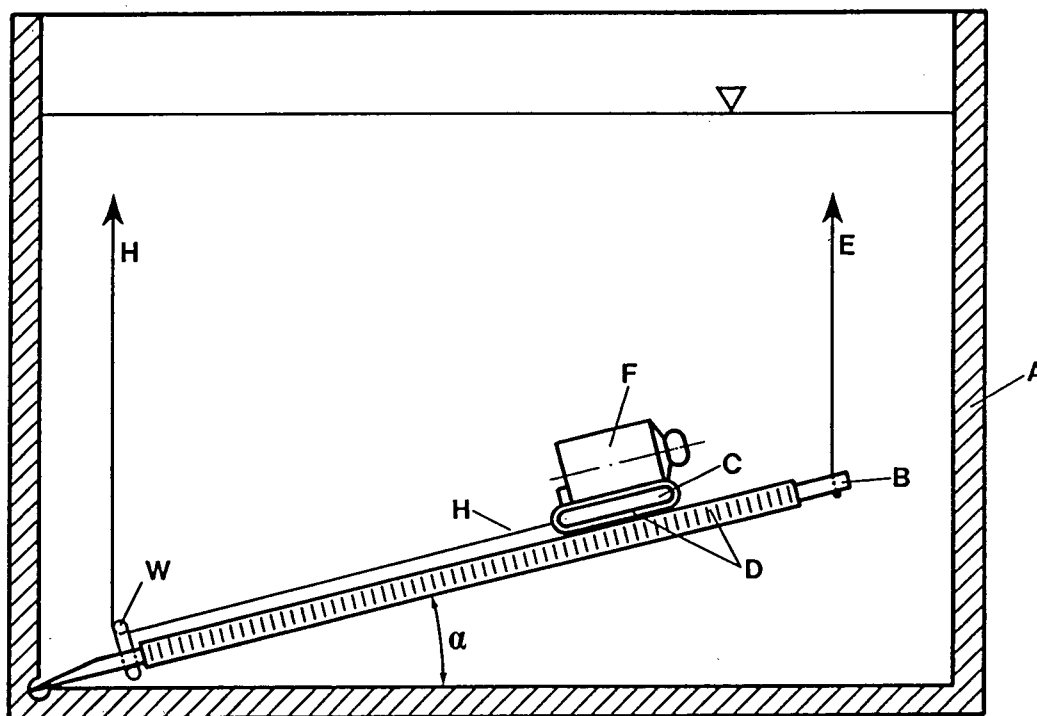


Figure IX-50. Method of Friction Measurement.

measured. The tangent of the slip angle,  $\alpha$ , which is the static coefficient of friction,  $\phi_s$ , was calculated.

$$\phi_s = T/N = \tan(\alpha) \quad (\text{XXI-1})$$

This procedure has been repeated with various weights (F) placed on the sled. Figures IX-51 and IX-52 show plots of

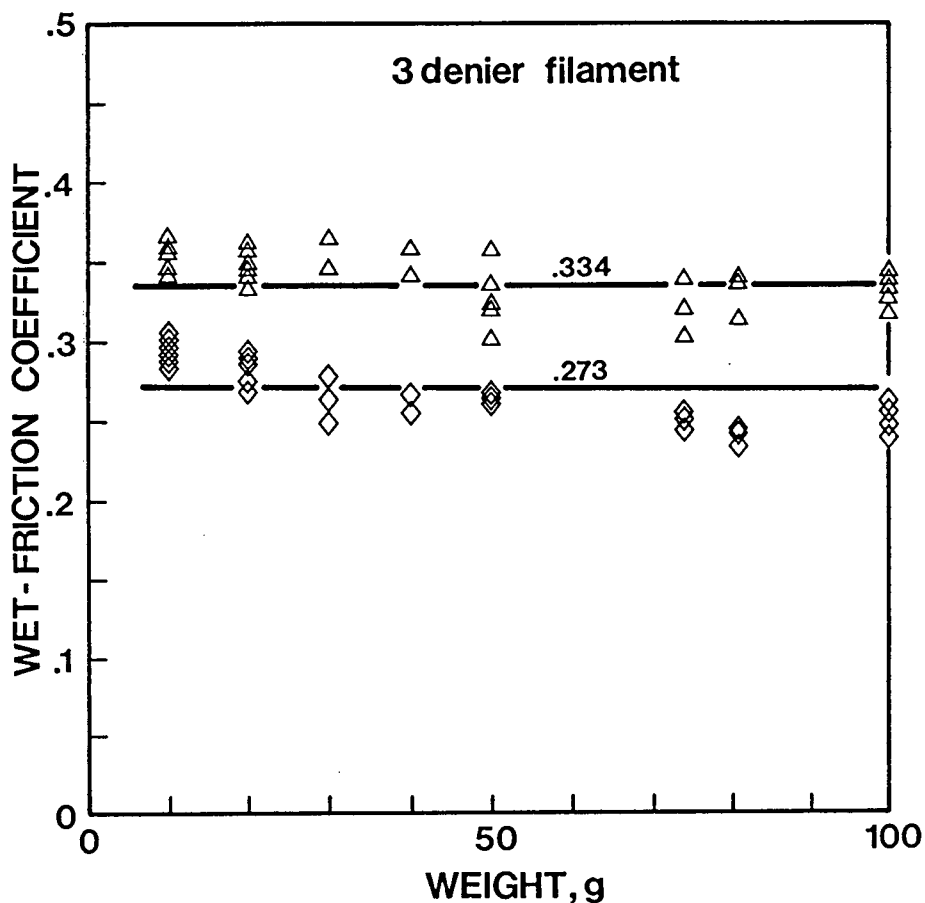


Figure IX-51. Wet-friction Coefficient versus Sled Loading for 3 Denier Nylon Filaments.

friction coefficients versus sled loading. In both figures the lower groups of points represent the data for the dynamic coefficient of friction  $\phi_d$ . The experimental setup for its measurement was slightly different from that for the static coefficient of friction. A string (H) attached to the front of the sled went around wire (W) to be connected to the constant speed drawing mechanism. During an experiment, both strings (E) and (H), were pulled simultaneously with a speed of 10 mm/min.

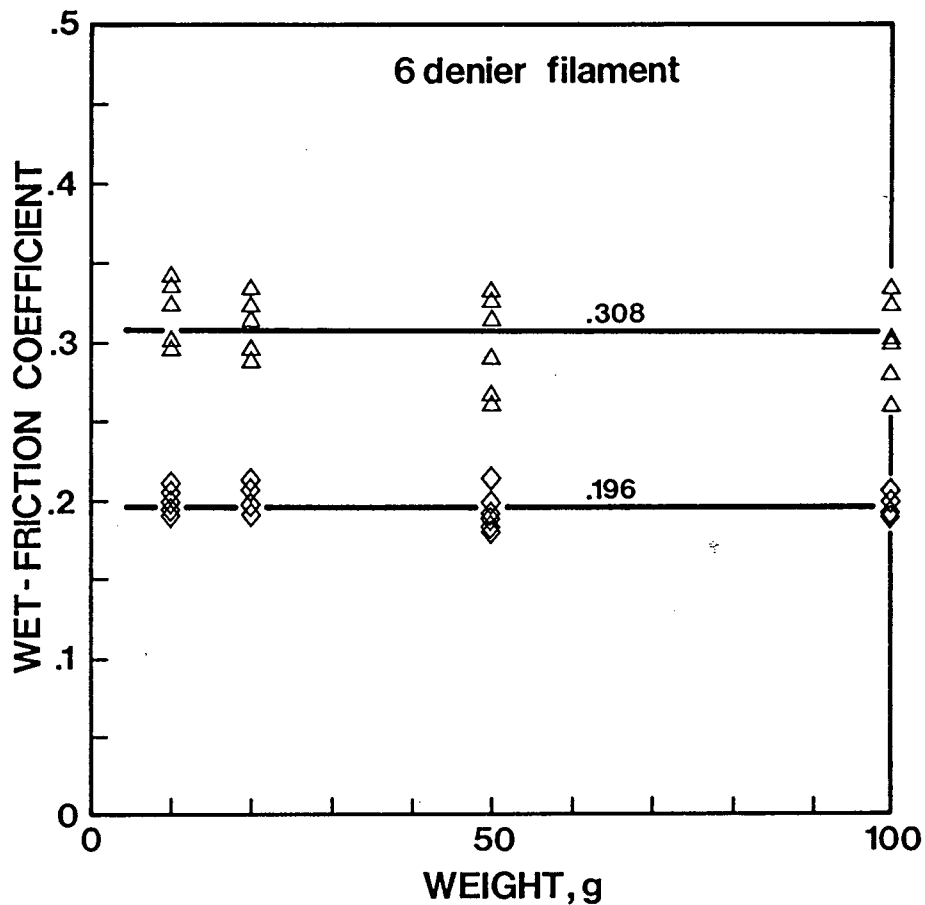


Figure IX-52. Wet-friction Coefficients versus Sled Loading for 6 Denier Nylon Filaments.

Table IX-XXVII. Static and Dynamic Coefficients of Friction for Wet Nylon Fibres.

NYLON FILAMENT	FRICTION COEFFICIENT			
	STATIC		DYNAMIC	
	AVERAGE	S.D.	AVERAGE	S.D.
3 denier	0.334	0.0318	0.273	0.0267
6 denier	0.308	0.0256	0.196	0.0090

Thus, the sled was pulled down the slope with a speed of about 10 mm/min. At the moment when the sled started to slide down the plane by itself, the draw mechanism was stopped and the tangent of  $\alpha$  calculated. The average values and the standard deviations of friction coefficients are shown in Table IX-XXVII. These values are comparable with the dry coefficients of friction reported elsewhere [H2,K3].

In principle the incline plane method is independent of the magnitude of the load placed on the sled, but in practice the compressibility of wound filaments affected the friction angle especially at the sled loadings of less than ten grams. These low loadings were excluded from data analysis.

In all measurements, the effect of viscous drag on the sled can be neglected because it was calculated to be six orders of magnitude smaller than the smallest sled loading, i.e., 10 g.

### Appendix X. Rotating Cylinder Apparatus.

A relatively simple mechanism, shown in Figure X-53, was devised to roll cylinders filled with suspensions. It consisted of an inclining table (A) with rollers (B,C) on stand (S). The table could be inclined at  $0^\circ$ ,  $15^\circ$ ,  $30^\circ$ ,  $45^\circ$ , and  $60^\circ$  to the horizontal, and secured in position by the threaded pin (N). The rollers were grooved to accommodate "O"-rings (H) through which propelling torque was transmitted to the cylinder (D). The torque was applied from an electric motor (F) connected to one roller through the flexible shaft (J). The electric motor was driven by the solid-state power controller (K) (COLE-PARMER INST. Co.) giving a 6 to 600 rpm speed range. The rotational speed was

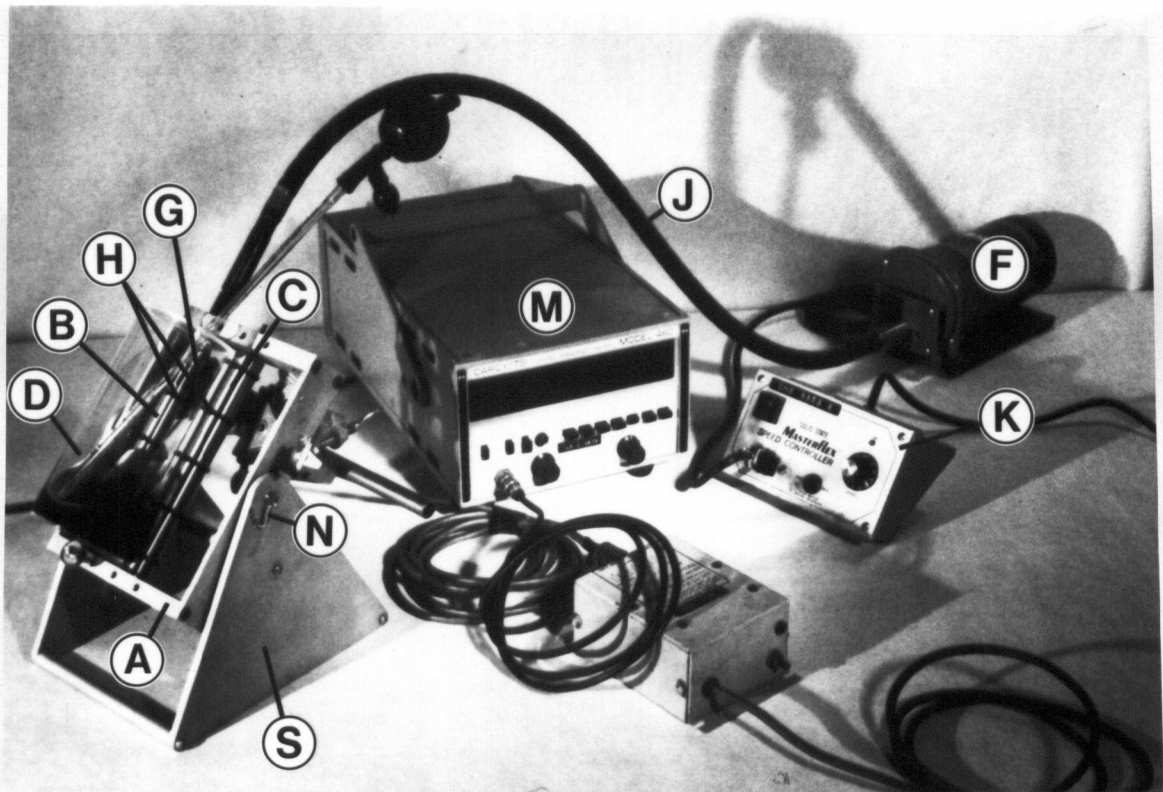


Figure X-53. Rotating Cylinder Apparatus.

monitored by the digital frequency meter (DARCY/TSI, model 460) (M) and a photo-reflective sensing pickup (model 863) consisting of a light source and a photodetector probe (G). The light pulses were picked up directly from the roller, transformed into electric pulses which were counted and their frequency displayed on the digital frequency meter. The rotational speed of the cylinder was calculated from:

$$\omega = 2 \cdot \pi \cdot (f/8) \cdot \frac{d_1}{d_2} \quad (\text{X-1})$$

where

$f$  - measured frequency,  $s^{-1}$ ,

$d_1$  - "O"-ring outside diameter, mm,

$d_2$  - cylinder outside diameter, mm.

In equation (X-1), measured frequency is divided by 8 because of 8 light pulses detected per one revolution of the roller.

**Appendix XI. Suspension Preparation and Type-C Floc Formation.**

Fibres were first washed in hot water with a detergent to remove impurities acquired during the manufacturing process. Subsequently they were thoroughly rinsed in deionized water, dewatered in a Buchner funnel, and oven-dried at 105°C for four hours. Oven-dry nylon was weighed on a Mettler 163F balance with 0.0001 g precision to prepare fibre samples. The samples were then soaked in deionized and ultrafiltered water (conductivity  $\leq 0.2 \mu\text{S}$ ).<sup>1</sup> After 24 hours soaking, full saturation of nylon with water had occurred.<sup>2</sup> The suspending water was removed in the Buchner funnel. The fibre mat collected on the filter paper was kept wet and this mat was slowly immersed in the suspending liquid (deionized, ultrafiltered water or aqueous-sugar solution). The immersion technique of wetted fibres insured complete exclusion of air bubbles from the suspension. The presence of air bubbles could introduce cohesion due to surface tension forces [H9,K7,M6].

A sample of rewetted fibres was first placed in a one-liter graduated cylinder fully filled with the suspending liquid. The concentration was very low, about one tenth of the sediment concentration. At this concentration any fibre aggregates were easily dispersed by several strokes of a plunger having a perforated rubber disk at one end. The plunger fitted loosely inside the graduated cylinder.

---

<sup>1</sup> Measurements of water conductivity are described in Appendix XVIII.

<sup>2</sup> Appendix VI contains details of water absorption by nylon.

Next, the suspension was thickened by slow removal of the liquid by suction into a 100 mL pipet. The pipet's tip covered with a 200-mesh screen prevented fibre removal. When the suspension volume in the cylinder reached 500 mL, the suspension was transferred to the plexiglas cylinder. The cylinder was mounted on the rolling mechanism and rotated at constant speed. Further liquid removal was achieved in 5 mL increments, i.e., each time 25 mL was removed, 20 mL was reintroduced. When it was observed that flocs did not disperse upon redilution, the procedure was halted and the suspension volume was measured. The precision of volume measurement in a 500 mL graduated cylinder was  $\pm 5$  mL.

The aqueous-sugar solution was prepared from deionized, ultrafiltered water and a grocery store sucrose. The electric conductivity for all sucrose solutions was less than  $15 \mu\text{S}$ . In most instances the aqueous-sugar solutions matched the apparent nylon density of  $1130 \text{ kg/m}^3$ . The solution density was measured with the Universal Beaumé Hydrometer graduated every  $10 \text{ kg/m}^3$ .

## Appendix XII. Sediment Concentration Measurements.

The sediment concentrations were measured by a simple procedure. The samples of oven-dried fibres having weights from 0.3 g (long fibres) to 6 g (short fibres) were first soaked for 48 hours in water, dewatered in a Buchner funnel, and dispersed well in one liter of aqueous-sugar solution. Dewatering in the Buchner funnel removed all air bubbles that attach to fibre surfaces and produce differential sedimentation. Subsequent immersion in the suspending liquid prevented small bubbles from attaching themselves to fibres. Uniform fibre dispersion was achieved in turbulent shear produced behind a plunger consisting of a perforated rubber disk fastened to the end of a glass rod. The disk fitted loosely inside the graduated glass cylinder of 60.3 mm ID. Aqueous-sugar solutions of  $1100 \text{ kg/m}^3$  density used as the suspending medium allowed slow sedimentation with little settling of the formed pad. Two hours after the fibres began settling, the pad volume was read off with  $\pm 5 \text{ mL}$  precision. The known volume of fibre sample divided by the pad volume gave the sediment concentration. The pad volume determination was done with an error which was related to the wall effect. At the cylinder vertical wall, in the annulus of about one half fibre length, the fibres form a less dense pad. The maximum estimated error is 8.3% for the longest fibres (6.26 mm) and 1.3% for the shortest fibres (0.913 mm).

### Appendix XIII. Flow Velocity Measurement in Fibre Suspensions in Horizontal Rotating Cylinder.

A non-intrusive technique of fluid velocity measurement, Laser Doppler Anemometry, was used in the study of flow patterns in a horizontal rotating cylinder. The experimental setup is shown in Figure XIII-54. The plexiglas cylinder (D) was rotated by the mechanism described in Appendix X. The mechanism consisted of: a rolling table (A), a flexible shaft (J), and a velocity-controlled motor (F). The fluid velocity measurement system was the TSI dual beam laser Doppler system working in the transmission mode. The experimental setup consisted of: an Argon-ion laser (L) (LEXEL, model 85) a polarizer, a beam

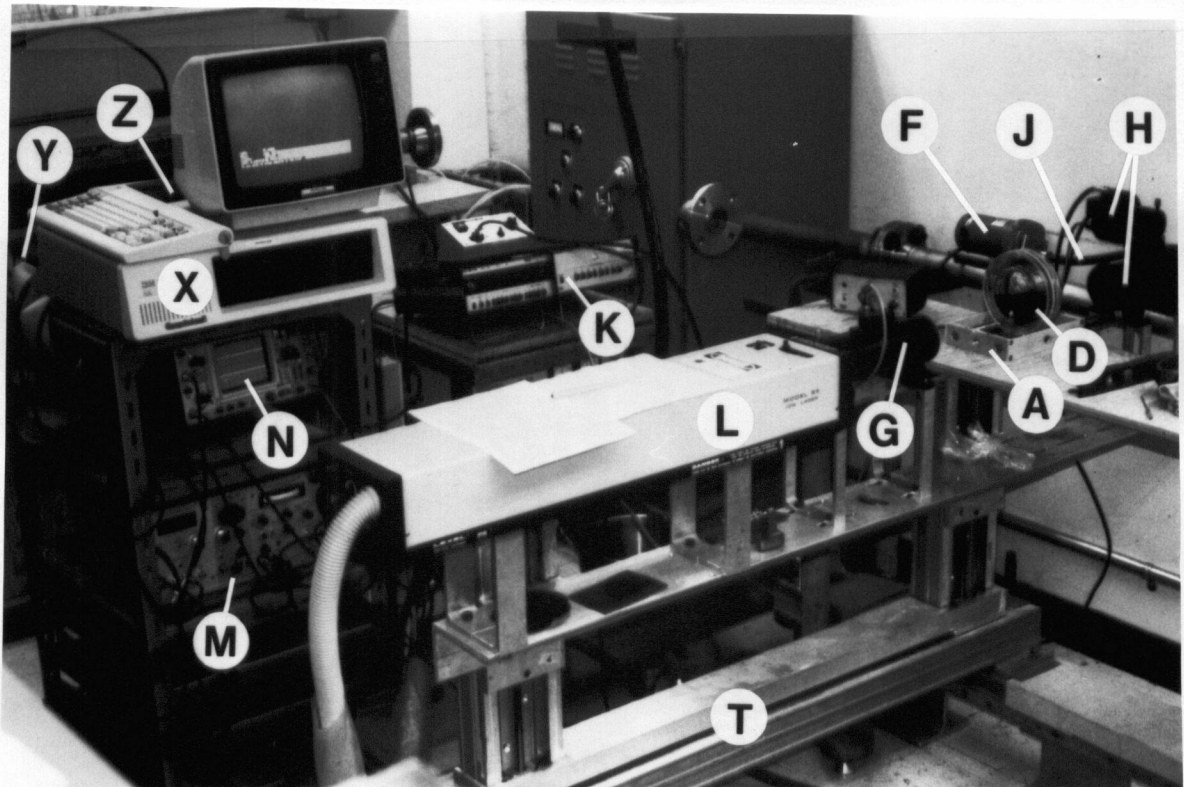


Figure XIII-54. Experimental Setup for Velocity Measurements in a Horizontal Rotating Cylinder.

splitter, a Bragg cell, and focusing optics (G); a photo-detector and receiving optics (H); a Bragg cell driver with the frequency downmix circuit (K); a signal tracker and the signal processor (M); a two-channel oscilloscope (N). The laser was mounted on the "UniSlide" assembly (T) which provided XYZ coordinate motion. The data acquisition equipment consisted of the analog-to-digital conversion board (Scientific Solutions Inc.) (Y), the IBM-PC (X), and the Epson-80 printer (Z).

The principles of Laser Doppler Anemometry are described in numerous publications [D8]. Some principles briefly discussed here emphasize the important aspects of the existing experimental setup.

A basic principle of dual beam anemometry is the crossing of two laser beams of equal intensity at a measuring volume in the fluid. Where these beams cross, they interfere with each other to form "fringes." The fringes caused by the coherent light in the two beams cancel each other in some regions and complement each other in others. The beam-crossing geometry is shown in Figure XIII-55. The distance between the brightest lines of the two neighboring fringes,  $d_f$ , measured within a cross-plane of the beams depends on the light wavelength,  $\lambda$ , and the beam crossing angle,  $\Psi$ .

$$d_f = \frac{\lambda}{2 \cdot \sin(\Psi/2)} = \frac{514.5\text{nm}}{2 \cdot \sin(11.03^\circ/2)} = 2.6767\mu\text{m} \quad (\text{XIII-1})$$

A particle in the fluid moving through the measuring volume and in the cross-plane of two beams generates light pulsing of



volume does not change during optics rotation.

The LDA employed measured two orthogonal velocity components, one horizontal and the other vertical. Velocity directional ambiguity did not exist in the system. The system could distinguish the "forward" flow from the "reverse" because of a Bragg cell which introduced a travelling wave across the beam. A 40 MHz frequency generated by the Bragg cell in the "reference" beam produced "moving" fringes within measuring volume. Hence, when a particle is stationary in the measuring volume, it generates 40 MHz light pulses. Particle movement in the same direction as the "moving" fringes lowers the frequency of the light pulses, while movement in the opposite direction raises it. The directions of "moving" fringes were set to be opposite to the positive direction of x and y axis shown in Figure XIII-56.

The shape of the measuring volume and its main dimensions are shown in Figure XIII-55. If the laser beam diameter,  $D_{e^{-2}}$ , includes all of the beam intensity greater than  $e^{-2}$  of the centerline, the corresponding diameter at the focal point is:

$$d_e = \frac{4}{\pi} \cdot \lambda \cdot \frac{F_D}{D_{e^{-2}}} = \frac{4}{\pi} \cdot 514.5 \text{ nm} \cdot \frac{250.4 \text{ mm}}{1.1 \text{ mm}} = 0.1491 \text{ mm} \quad (\text{XIII-3})$$

where  $F_D$  is the focal length of the lens.

Two other dimensions of the measuring volume,  $d_m$  and  $l_m$  are related to  $d_e$  as follows:

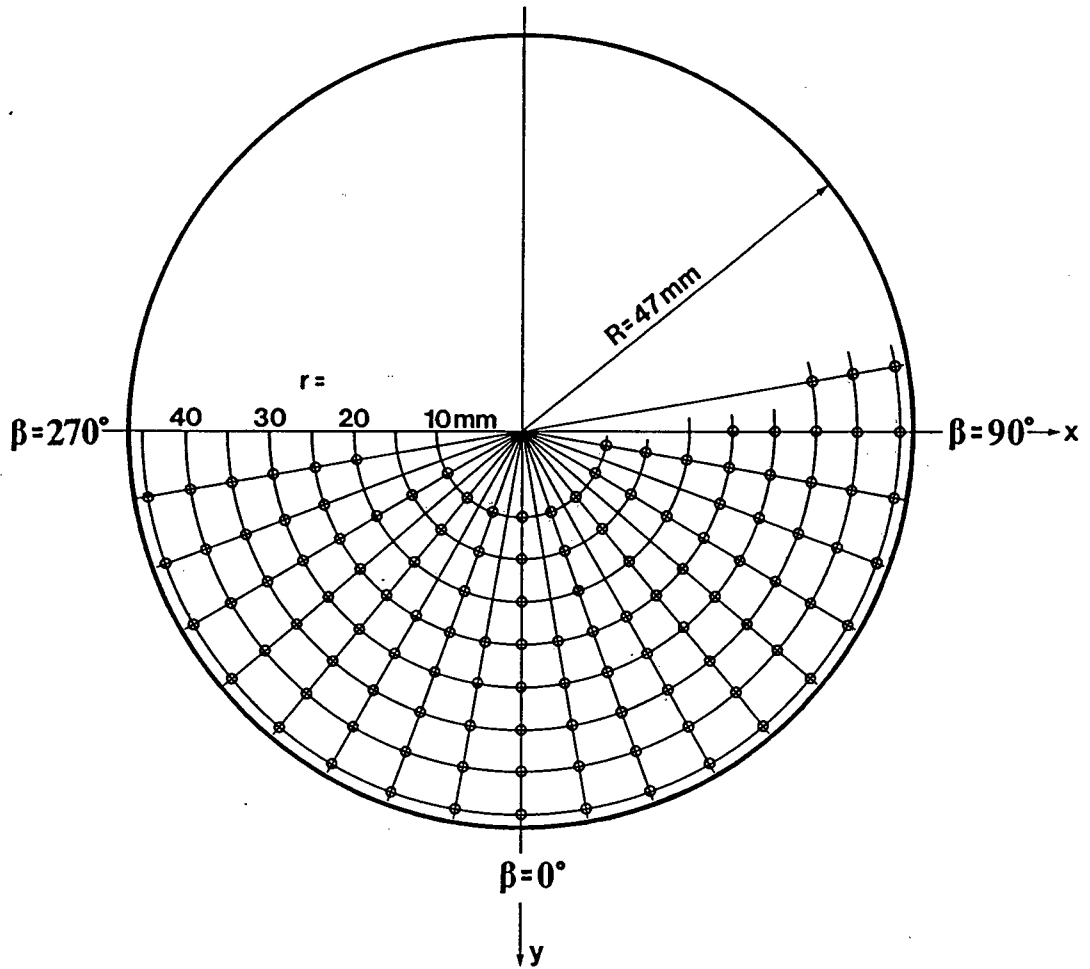


Figure XIII-56. Locations of Measuring Points within the Central Plane of the Cylinder.

$$d_m = \frac{d_e}{\cos(\Psi/2)} = \frac{0.1491\text{mm}}{\cos(11.03^\circ/2)} = 0.1498\text{mm} \quad (\text{XIII-4})$$

$$l_m = \frac{d_e}{\sin(\Psi/2)} = \frac{0.1491\text{mm}}{\sin(11.03^\circ/2)} = 1.551\text{mm} \quad (\text{XIII-5})$$

In the forward scatter mode, the dimensions  $l_m$  and  $d_m$  determine the size of the measuring volume and the spatial resolution of

the system.

The number of fringes at the central section of the measuring volume is:

$$N_{FR} = \frac{d_m}{d_f} = \frac{.1498\text{mm}}{2.676722\mu\text{m}} = 55.96 \quad (\text{XIII-6})$$

In other sections of the measuring volume, the number of fringes decreases as they approach each end of the length  $l_m$ .

If a single particle having a size smaller than  $d_f$  crossed the center of the measuring volume, it would generate  $N_{FR}$  of Doppler cycles. In reality, the number of Doppler cycles seen by the photodetector is smaller due to the small size of the aperture. This aperture blocks light arriving from locations other than the beam crossing volume and thereby improves the signal to noise ratio. In the Thermo System Inc. photodetector, the effective beam diameter is:

$$d_a = 0.7 \cdot d_m \cdot \frac{F_A}{F_D} = 0.7 \cdot 0.1873 \cdot \frac{250.0}{250.4} = 0.1309\text{mm} \quad (\text{XIII-7})$$

Where,  $F_A$  is a focal length of the scattered light focusing lens and  $F_D$  is a focal length of the collecting lens, and 0.7 is a design constant. The number of fringes from the central section which is seen by the photodetector is:

$$N_{EFR} = \frac{d_a}{d_f} = \frac{130.9\mu\text{m}}{2.676722\mu\text{m}} = 48.9 \quad (\text{XIII-8})$$

The LDA system measures the velocity of the particles entrained by the fluid. For fluid velocity to be measured with a

laser anemometer, the particles must follow the fluid flow. An additional requirement is that there be a sufficient number of particles to produce an uninterrupted stream of Doppler cycles. Since the suspending liquid was prepared from ultrafiltered water and pure sugar, the seed particles had to be introduced. White polystyrene particles having the average diameter of  $1.091 \mu\text{m}$  (S.D.= $0.0082 \mu\text{m}$ ) were used [S8]. They had  $1050 \text{ kg/m}^3$  density, and were shown to follow closely the flow of water [D8]. Addition of one drop of suspended particles (10% solids) to 125 mL of aqueous sugar solution was satisfactory as indicated by the number of samples per second and the time fraction of the validated signal displayed by the signal tracker.

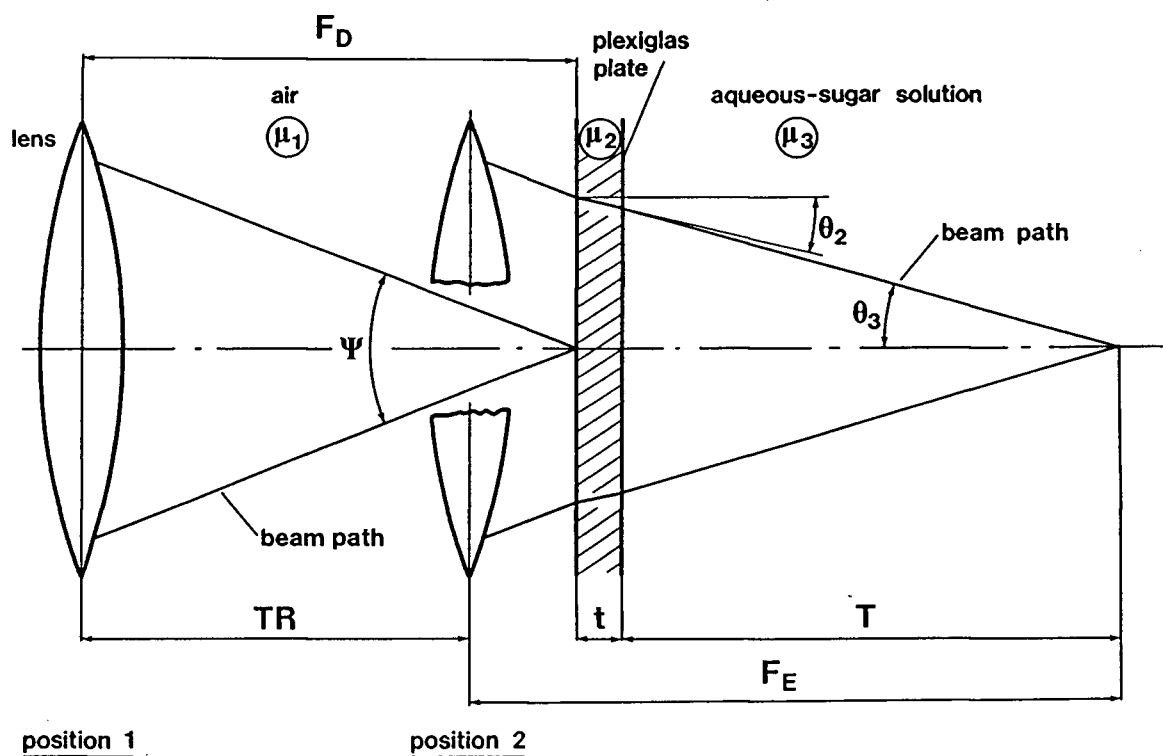


Figure XIII-57. Change in Focal Length caused by Various Indices of Refraction.

The suspension in which velocities were to be measured was confined between the cylinder walls. Two laser beams must pass through one plexiglas plate and the suspension before arriving at the measuring location. The plexiglas and the aqueous-sugar solution have different indices of refraction than has the air. This displaces the measuring volume location and changes the intersection angle of two beams, as illustrated in Figure XIII-57 (position 2). This change in refraction indices does not affect the calibration factor, i.e., the spacing between fringes. The equation (XIII-1) holds because the wavelength and the sine of the angle depend equally on the refraction indices. Since the measuring volume had to be located in the central plane of the cylinder, a reliable method of finding this plane was required.

The laser and the optics were located on a three-directional traversing rig which could be moved with respect to the stationary axis of the cylinder. The location of the measuring volume within the central plane of the cylinder was obtained by the coordinate setting which followed the predetermined pattern of measurement points shown in Figure XIII-56. For the measuring volume to be placed in the central plane of the cylinder, both beams had to go through 3 mm thick plexiglas and penetrate 18 mm into the suspension. The traversing rig, however, had to be displaced by the distance  $TR$  from position 1 to position 2, as marked in Figure XIII-57.  $F_E$  is an effective focal length [D8].

$$F_E = (TR - t \cdot \frac{\tan\theta_2}{\tan\theta_1}) \cdot \frac{\tan\theta_1}{\tan\theta_3} + t + F_D - TR \quad (\text{XIII-9})$$

but  $F_E = F_D - TR + t + T$  and TR obtained from equation (XIII-9) is,

$$TR = T \cdot \frac{\tan\theta_3}{\tan\theta_1} + t \cdot \frac{\tan\theta_2}{\tan\theta_1} \quad (\text{XIII-10})$$

where

$\theta_1 = \Psi/2$  - half of the beam crossing angle,

$$\theta_2 = \sin^{-1} \left( \frac{\sin\Psi/2}{\mu_2} \right)$$

$$\theta_3 = \sin^{-1} \left( \frac{\sin\Psi/2}{\mu_3} \right)$$

$\mu_1$  - index of refraction of air, =1,

$\mu_2$  - index of refraction of plexiglas,

$\mu_3$  - index of refraction of 1.13 g/cm<sup>3</sup> aqueous-sugar solution,

$F_D$  - lens focal distance in the air,

$F_E$  - lens effective focal distance,

t - plexiglas thickness,

T - penetration distance into suspension.

TR can be calculated from (XIII-10) for  $F_D = 250.4$  mm,  $\mu_2 = 1.65$ ,  $\mu_3 = 1.382$  [C10],  $\Psi = 11.03^\circ$ ,  $t = 3$  mm,  $T = 18$  mm. Thus,  $TR = 14.8$  mm.

Light pulses having a frequency close to 40 MHz were transformed into electric signal by the photodetector. This signal entered the frequency shift circuit. The 40 MHz frequency shift was undesirably large and needed to be decreased through downmixing. The purpose of the downmix is to bring the frequency

into the range of the signal processor or, even better, to the optimum part of this range.

The horizontal cylinder was rotated with constant angular speed  $\omega=2\pi$  rad/s. Its peripheral speed was  $R\cdot\omega=0.295$  m/s where  $R$  denotes internal cylinder radius. The measuring volume could not be located closer to the cylinder wall than 3 mm due to the geometry of the crossing beams and the beam diameter. In consequence, the expected maximum speed to be measured was estimated to be about 0.240 m/s. The corresponding Doppler frequency from a stationary fringe pattern would be 90 kHz. The downmix frequencies were 100 kHz or 200 kHz so that only the lowest detection range (2-500 kHz) of the signal tracker was used.

From the frequency downmix circuit, the LDA signal went to the signal tracker. Here, the signal was amplified to the optimum amplitude level and passed to the signal validation processor which eliminates spurious signals. The validation processor works on the principle of a phase lock loop which locks onto the incoming frequency and can "track" the frequency variations within  $\pm 15\%$  frequency window. The lock detector starts one of two counters of Doppler cycles. At a count of 8, the hold mode is initiated and the second counter starts sampling. Though sampling was stopped by the first counter after 8 Doppler cycles, the signal was not validated and released to the output until 10 cycles. This important feature of the signal tracker means that only frequencies one tenth or less than the Doppler frequency can be measured as the validated signal, in

this case 20 kHz or less.

The count of samples per second is derived from the switching off of the sample-and-hold circuits. The percent signal is a measure of the fraction of time the phase lock loop is "in lock." These two readouts give sufficient information to assess whether the validation circuit is working properly. When this has been established, the readouts can be used to determine the optimum dose of the seed particles.

The phase lock circuit gives an output voltage which is linearly proportional to the frequency deviation from the center frequency of the detection range. The proportionality constant is 0.01 V/kHz for the detection range 2-500 kHz. If no new signal is validated, the last voltage is kept by the circuit. The validated signal is passed on to the signal processor in which it can be offset and/or filtered. For convenience, the voltage was offset to read 0.0 volts while the velocity was 0.0 m/s. The signal was collected by the IBM-PC through the analog to digital converter (TM-40, Scientific Solutions Inc.). The program that acquired the data is listed in Appendix XXII. At each measurement point, 25000 voltage readings were taken at the rate of 5000 readings per second. The average voltage, Volt, was used for the calculation of each orthogonal velocity component.

$$u_x = \text{Volt} \cdot d_e (\mu\text{m}) / 0.01 (\text{V/kHz}) = 0.26767 \cdot \text{Volt} (\text{m/s}) \quad (\text{XIII-11})$$

The data were subsequently transferred to the UBC main-frame computer system with the help of MCP-WINDOW software. The

experimental data are in Appendix XXVII.

**Appendix XIV. Floc Preparation and Contact Counting Procedures.**

For the study of the relationship between floc concentration and the number of contact points per fibre, strong nylon flocs were formed at increasing levels of fibre concentration in the rotating cylinder. Fibres of 44.19  $\mu\text{m}$  diameter and 4.9 mm long were used ( $L/d=141.7$ ). First, nuclei were formed of red fibres. Next, the nuclei were introduced to suspension of translucent fibres. A layer of translucent fibres interlocked with and around nuclei. The suspension circulated for two minutes at a given concentration and the floc was removed and dried in the ambient air. Slow motion movies of the drying process were made for observation of any changes in floc structure occurring during drying. No changes in floc shape or structure were observed. Since each floc had a spheroidal shape, the three major, orthogonal dimensions were measured.

During drying, the sugar from the solution deposited on the fibre surfaces and preferentially at the fibre contact points. This deposition led to bonding between fibres. Each contact-counting procedure consisted of the floc being dried and then individual fibres being freed from it under microscope. The fibres were freed by the individual bonds being progressively broken. The contacts made by the red fibres with the red and translucent fibres were only counted. After the floc was completely dismantled, all red fibres were counted and an average number of contact points was calculated.

Studies under microscope proved very demanding on the eyes. Consequently, a similar procedure was adopted for scaled-up flocs made of about ten times larger nylon fibres, i.e., 45.9 mm long and 0.559 mm in diameter ( $L/d=82.3$ ). The flocs were formed by hand in an aqueous-sugar solution. Increasing floc density was achieved by flocs being squeezed similarly to a snow-ball being rolled. Three hundred dyed fibres, each hundred with a different colour, formed floc nucleus. The nucleus was surrounded by the translucent fibres. Floc dismemberment proceeded the same as before. The coloured fibres facilitated contact point recognition. Table XIV-XXVIII contains data on floc

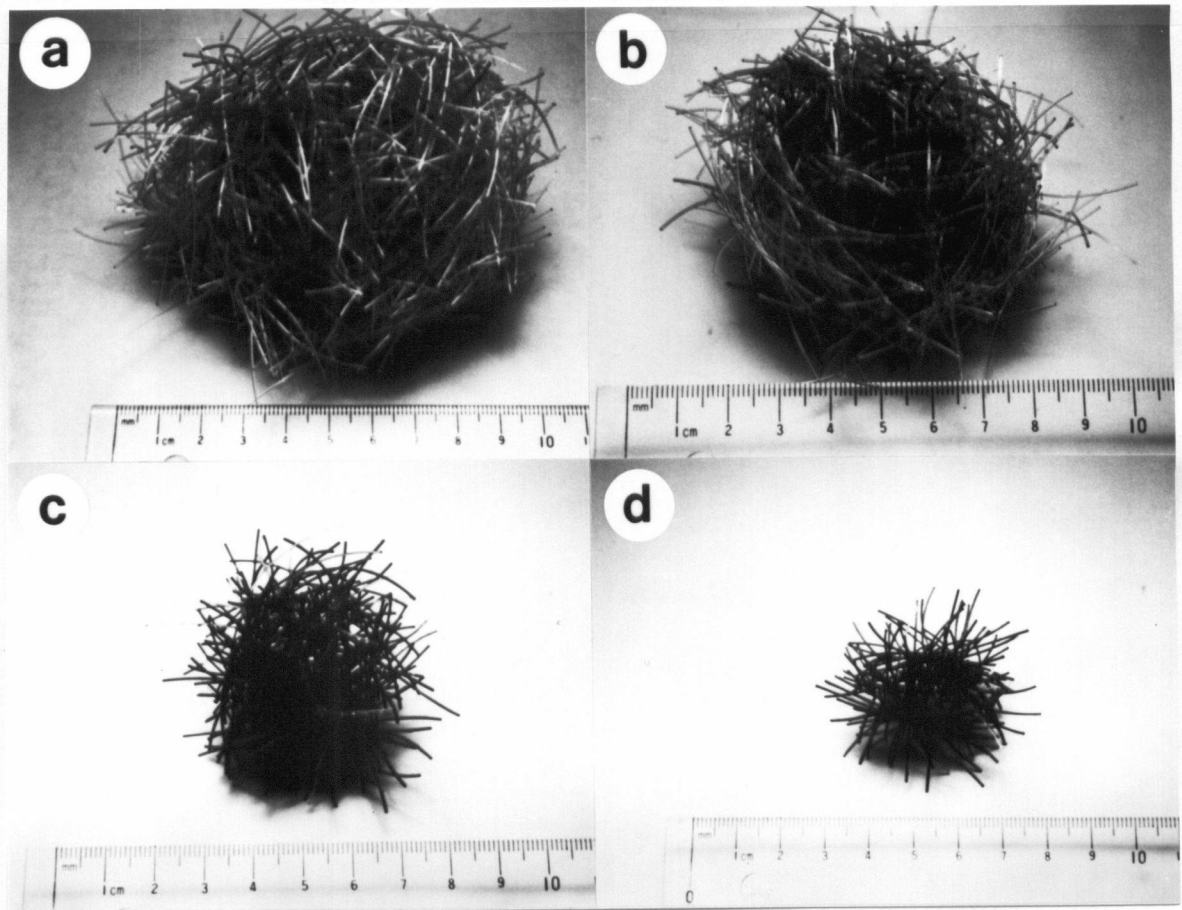


Figure XIV-58. Progressive Dismemberment of Type-C Floc.

disassembly. A sequence illustrating floc dismemberment is shown in Figure XIV-58.

Table XIV-XXVIII. Contact Points in Type-C Flocs.

L/d	FLOC NUMBER	TOTAL NUMBER OF FIBRES	NUMBER OF COLORED FIBRES	VOLUMETRIC CONCENTRATION OF FIBRES	NUMBER OF CONTACTS PER FIBRE
82.3	1	863	300	0.0445	2.26
	2	1154	300	0.0731	2.81
	3	1205	300	0.1005	3.97
	4	1370	300	0.1027	3.68
141.7	1	--	332	0.0512	3.68
	2	--	623	0.0687	4.40
	3	--	491	0.1083	4.84

## Appendix XV. Tensile Strength of Wet Nylon Floccs.

Coherent floccs of various fibre concentration were produced in the inclined rotating cylinder for tensile testing. For increased floc density, the suspension concentration in the cylinder was gradually increased starting from the threshold concentration. At each concentration, rolling continued for two minutes. Only floccs having a shape close to spherical were selected for testing.

Before tensile testing, the floc volume was determined. It was assumed that the floc boundaries were defined by the surface of the liquid associated with the floc when the floc had been

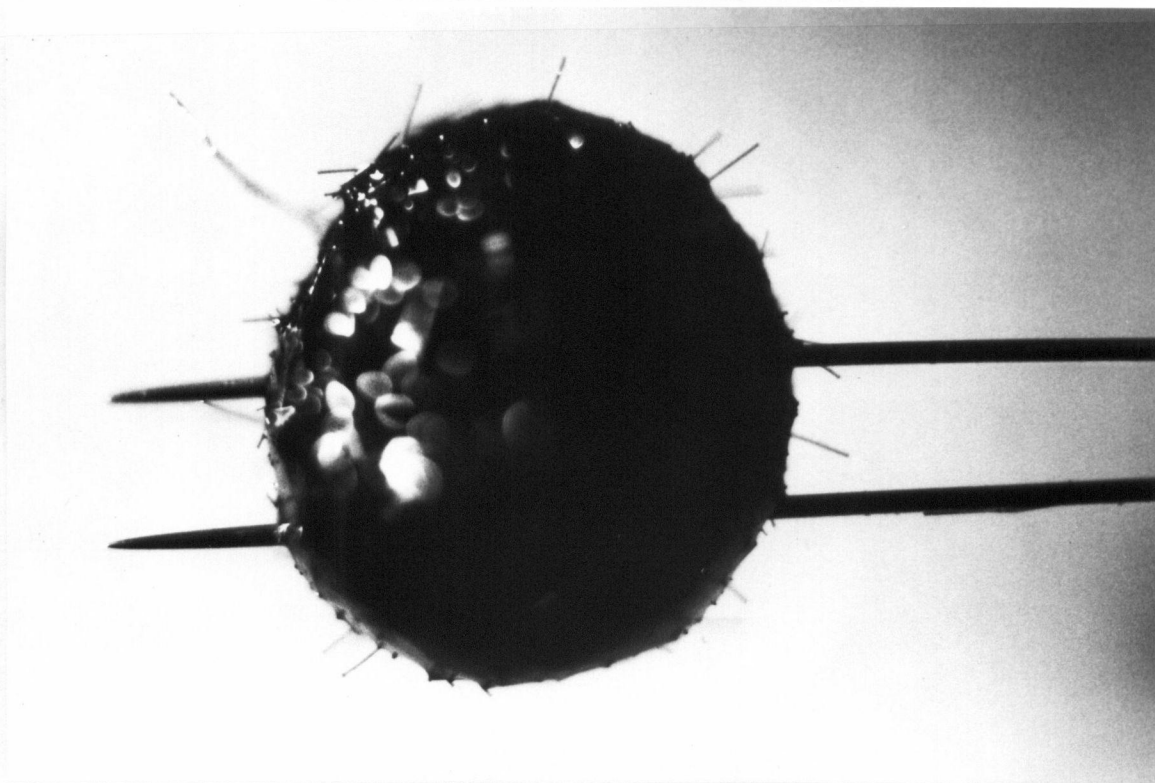


Figure XV-59. Coherent Floc removed from the Suspension by the Fork.

removed from the suspension. Each floc was removed by a fork made of two beading needles. Figure XV-59 depicts the fork and a floc transfixed on it. This step did not damage the floc. The floc was weighed and its volume calculated by the floc's weight being divided by its density. The density of floc matter was uniform throughout since the fibres were rendered neutrally buoyant during floc formation. The floc was then ready to be mounted in the tensile tester.

Figure XV-60 shows the assembly of the tensile test equipment. The equipment consisted of: a Thwing-Albert tensile tester (A), a load cell (B), a signal amplifier (C), an analog-to-digital converter (D), an IBM-PC (E), a plexiglas tank

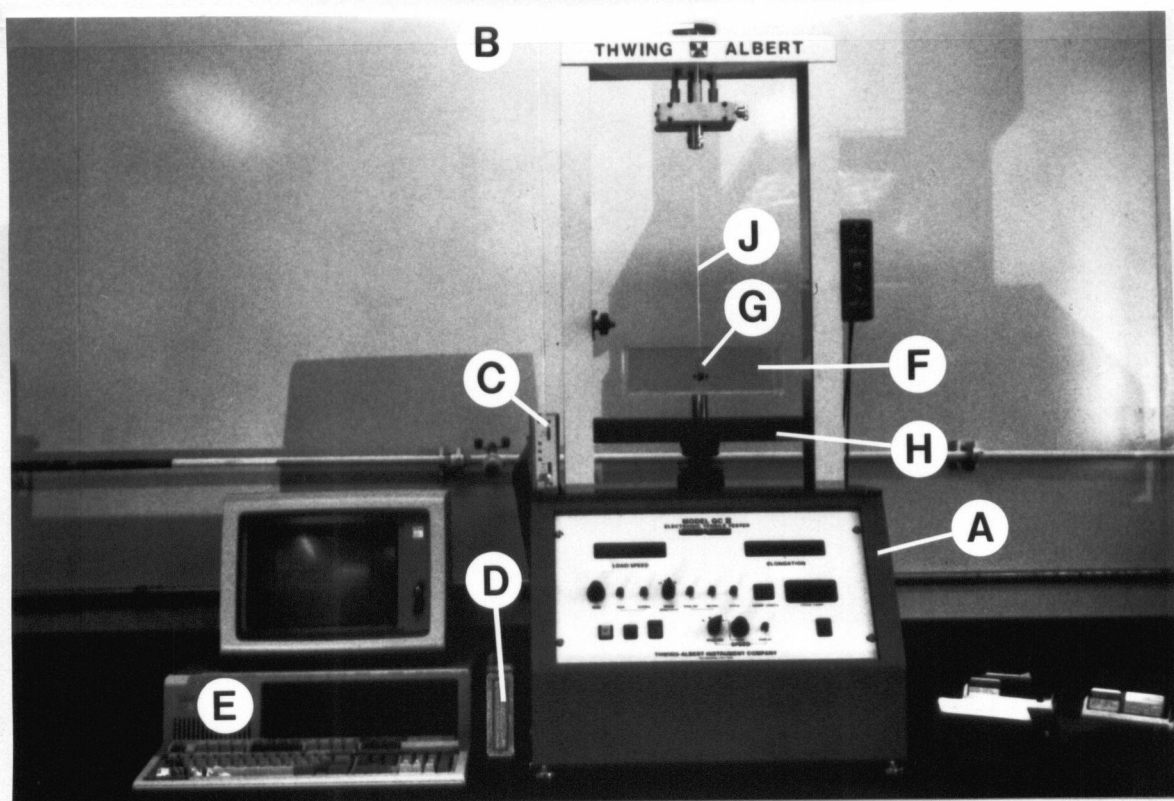


Figure XV-60. Tensile Test Equipment.

(F) and two combs with a floc (G). The plexiglas tank was filled with an aqueous sugar solution. The tank and the lower comb were attached to the cross-head (H) of the Thwing-Albert tester. The upper comb was suspended from the load cell on a flexible string (J). Each comb was comprised of No.10 beading needles ( $D=0.4$  mm) inserted horizontally through the holes drilled in the "L" shaped plexiglas fixtures. The needles were spaced evenly in a 16 mm long row. A closer photograph of the tank is shown in Figure XV-61. One comb (K) was firmly secured to the bottom of the tank, while the other comb (L) was secured to the load-cell by a long, flexible string (J). The floc (M) and the combs were submerged in an aqueous-sugar solution during the test.

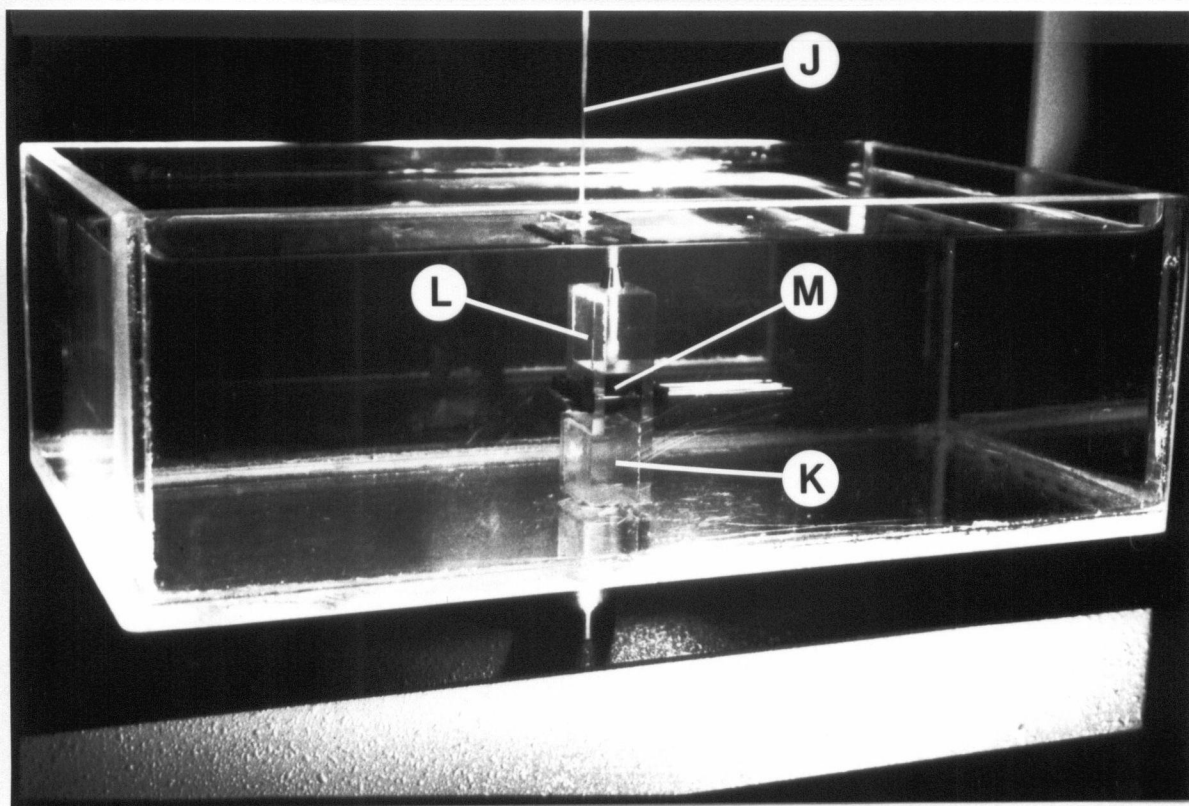


Figure XV-61. Device for Tensile Testing of Nylon Flocs.

Floc mounting on the needles was straight-forward: (1) the floc was pierced in the middle by the bottom set of needles; (2) the top comb was put into place; (3) the top set of needles was inserted into the floc. The floc was ready to be strained. A constant speed of 10 mm/min was applied to the bottom comb by the driving mechanism of the Thwing-Albert tester. The tank and the bottom comb moved downward. The upper comb remained immobile. The floc started to deform and its resistance to deformation grew steadily. The force opposing the pull was sensed by the load cell which converted the force to an electric signal. The signal from the load cell was amplified and sampled by the digital to analog converter (TM-40, Scientific Solutions Inc.) at the rate of 30 readings per second. The force, in its digital form, was stored in data files by the IBM-PC. Data acquisition program is listed in Appendix XXIII.

The area of the break zone was photographed while the separated piece was still attached to the upper comb but the comb was removed from the suspending liquid as shown in Figure XV-62. This was necessary for the size of the cross-sectional area to be determined so that the number of fibres crossing the break plane could be calculated. Slides of each area were projected on the digitizer and the area was measured by polygonal approximation. A data acquisition setup similar to that for fibre length measurements was used. The BASIC program which accomplished this is listed in Appendix XXIV.

Both separated pieces of floc were removed from combs, washed, dried at 105°C for four hours, and weighed. Washing was

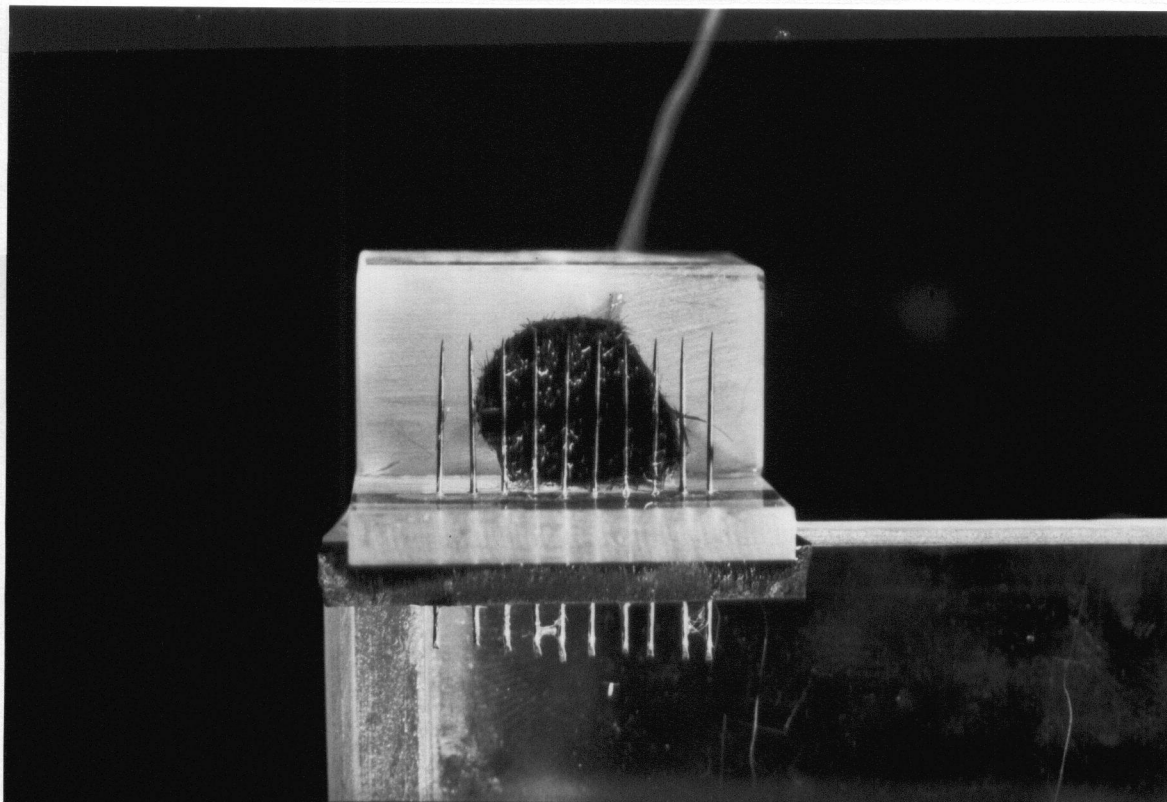


Figure XV-62. Plane View of the Break Zone.

crucial because the residual sugar could contribute to the dry fibre weight. Consequently, the fibres were washed four times with total dilution ratio being 1:256 to reduce the amount of residual sugar to less than 0.001 g. The weight of air in the weighing bottles could contribute to inaccurate results if weighing was done before bottles were cooled. The difference in weight of 20 mL of air when cooled from 100°C to 23°C is 0.005 g. This amount is not large with respect to the dry floc weights ranging from 0.1 to 0.8 g, but can cause an error of 5% in measurements of the weight of light flocs. Since the bottles were always cooled in the desiccator, the total weighing error was less than 2% even in the most unfavorable case. The

concentration of fibres in the floc was calculated from its initial volume and the dry-weight of fibres.

## Appendix XVI. Computer Model of Fibre Deposition into 3-D Networks.

An understanding of 3-D fibre networks can be achieved through experimental studies of laboratory constructed networks. A faster procedure models such networks on a computer where the parameters (fibre length and diameter) can be easily changed. The creation of a computer program requires the choice of suitable programming language which uses an inexpensive compiler. The FORTRAN language was chosen. The program should also accommodate the size limitation of the computer memory. Such a program has been written for deposition of fibres because the process of sediment formation was known.

The space in which fibre deposition was modelled was discrete and shaped as a square-base parallelepiped. The base side was three fibre lengths long as shown in Figure XVI-63. A two-dimensional array containing INTEGER\*2 elements constituted the base of the parallelepiped. Each array element stored the height of the deposited mat of fibres. This choice of space accommodating fibres of a large aspect ratio (up to 1000) did not exceed the memory capacity of the UBC main-frame computer.

Fibres were deposited at random within the parallelepiped, i.e., their initial orientation and the location of their centres were determined by pseudo-random process. The fibres were oriented horizontally during approach to the mat; however, upon deposition on the mat, they could rotate and/or slide to rest on the top of the mat or could penetrate the mat. The direction of rotation was determined by the relative position of the first

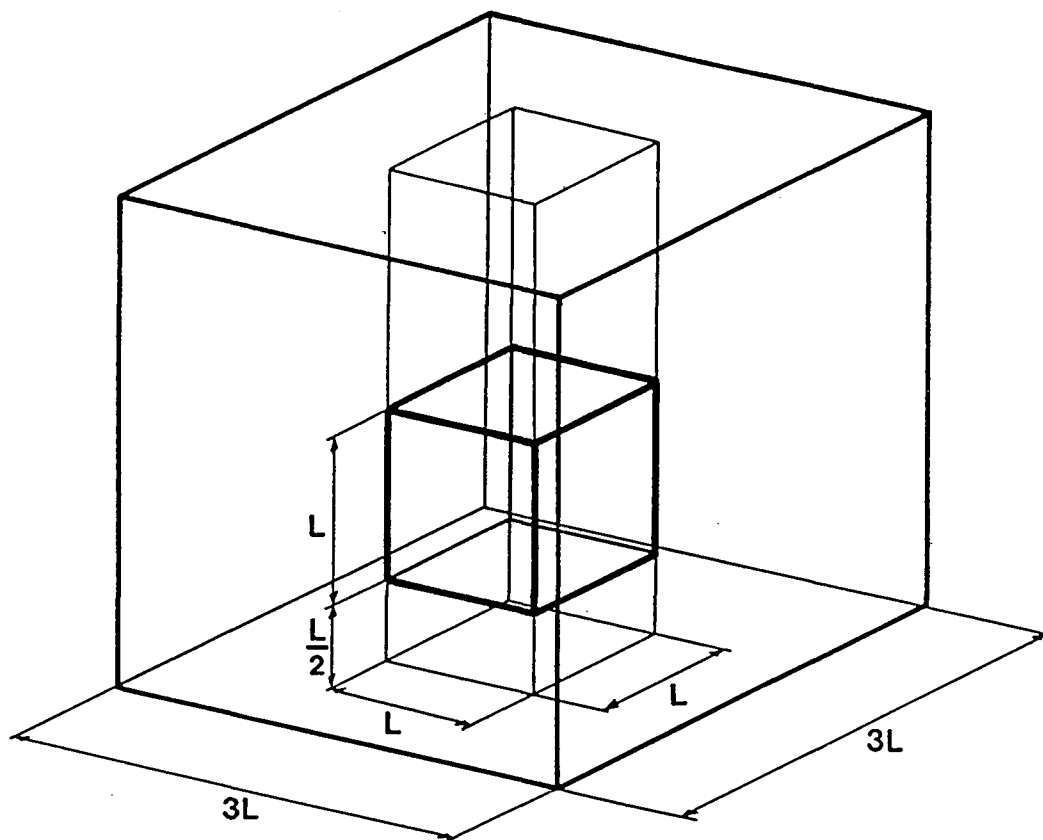


Figure XVI-63. Parallelepiped in which Fibre deposition was Modeled.

contact point with respect to the fibre centre. The slide angle was set equal to the arcus tangens of the static coefficient of friction determined experimentally (see Appendix IX).

A desired number of fibres is deposited before the program calculates the concentration of deposited fibres, number of contacts between fibres, inter-contact distances, angles of deposition and fraction of surface coverage. These calculations are limited to a space defined by a cube shown in Figure XVI-63. This cube has the sides of one fibre length and is raised one-half of a fibre length above the base of the large parallelepiped.

Before the straight line segments were deposited, the bottom of the large parallelepiped was covered with fibres forming a mat having 3-D structure. On top of this mat the straight line segments were deposited and their number was calculated.

## Appendix XVII. Mathematical Analysis of the Tensile Strength of Type-C Floccs.

If it is assumed that the build up of load is a process of gradual engagement of fibres in frictional interaction. The fibres embedded in a floc above the rupture plane slide along fibres embedded in the part of the floc below the rupture plane in monotonously increasing numbers. If it is further assumed that only the dynamic frictional interaction exists at the contact points, the total load developing in a strained floc can be expressed mathematically by:

$$F = k_f \cdot \sum_{i=1}^{N_f} (k_{ci} \cdot \sum_{j=1}^{n_{ci}} T_{ij}) \quad (\text{XVII-1})$$

where

$F$  - total load carried by the strained floc,

$N_f$  - number of fibres crossing the "rupture plane",

$k_f$  - fraction of fibres that carry the load,

$n_{ci}$  - number of contacts of  $j$ -th fibre with other fibres,

$k_{ci}$  - fraction of  $n_{ci}$ , i.e., fraction of sliding contacts,

$T_{ij}$  - frictional force component parallel to the direction of

floc separation produced at  $j$ -th contact on  $i$ -th fibre,

The frictional forces opposing floc separation develop within the plane of each fibre-to-fibre contact. Such planes are randomly oriented at the beginning of the deformation process.

Not all contact points along one fibre are sliding. Most are firmly associated with either the top or the bottom part of

the floc. The coefficient  $k_{ci}$  represents the fraction of contacts which slide. The sum of "embedding" forces is greater than the sum of "sliding" forces on each fibre. It is possible for one half of the contact points to slide and the other half to be embedded since the dynamic coefficient of friction is smaller than the static. The sum of "sliding" forces is summed up in equation (XVII-1).

The assumption that each sliding fibre from the top part of the floc has its counterpart embedded in the bottom part of the floc is reasonable. In other words, the fibre separation is 50/50. This assumption would certainly hold for large and uniformly dense flocs. Moreover, not all the fibres that cross the break plane contribute to the load-bearing capacity of the floc. Those fibres which lie near the peripheries of the floc do not. Some fibres in the core of the floc may not be active either, especially in less dense flocs. The coefficient  $k_f$  is introduced to account for this.

The frictional component  $T_{ij}$  can be expressed in terms of normal force,  $R_{ij}$ , and the dynamic coefficient of friction,  $\phi_d$ .

$$T_{ij} = k_{dj} \cdot R_{ij} \cdot \phi_d \quad (\text{XVII-2})$$

where  $k_{dj}$  is a direction coefficient, or sine of the angle between the frictional force and the direction of floc separation.

If average quantities for  $k_{ci}$ ,  $n_{ci}$ ,  $k_{dj}$ , and  $R_{ij}$  are introduced, the following equality holds:

$$k_{ci} \cdot \sum_{j=1}^{n_{ci}} k_{dj} \cdot R_{ij} \cdot \phi_d = k_c \cdot n_c \cdot k_d \cdot R \cdot \phi_d \quad (\text{XVII-3})$$

where

$n_c$  - average number of contact points per fibre,

$k_c$  - half of the fraction of sliding contacts,

$R$  - average normal force at a contact point,

$k_d$  - average direction coefficient; average sine of an angle between the friction force acting along fibre principal axis and the break plane.

The average number of contact points per fibre can be estimated from the experimental findings presented in Section 4.6.

Introducing (XVII-3) into (XVII-1) yields

$$F = k_f \cdot N_f \cdot k_c \cdot n_c \cdot k_d \cdot R \cdot \phi_d \quad (\text{XVII-4})$$

The average normal force,  $R$ , can be expressed in terms of an average fibre deflection,  $\delta$ , the elastic modulus of wet fibre,  $E$ , the bending moment of inertia,  $I$ , and the average distance between the adjacent, alternate contact points,  $l$  [M2]. Here, only the elastic deformation of fibres is accounted for because such deformation was postulated to develop in Type-C networks. It is possible that the fibres, while the floc is separated, bend more than is necessary to interlock; this is not included in the present mathematical model. First, the case of  $n_c=3$  which is depicted in Figure XVII-64 is considered. The expression for

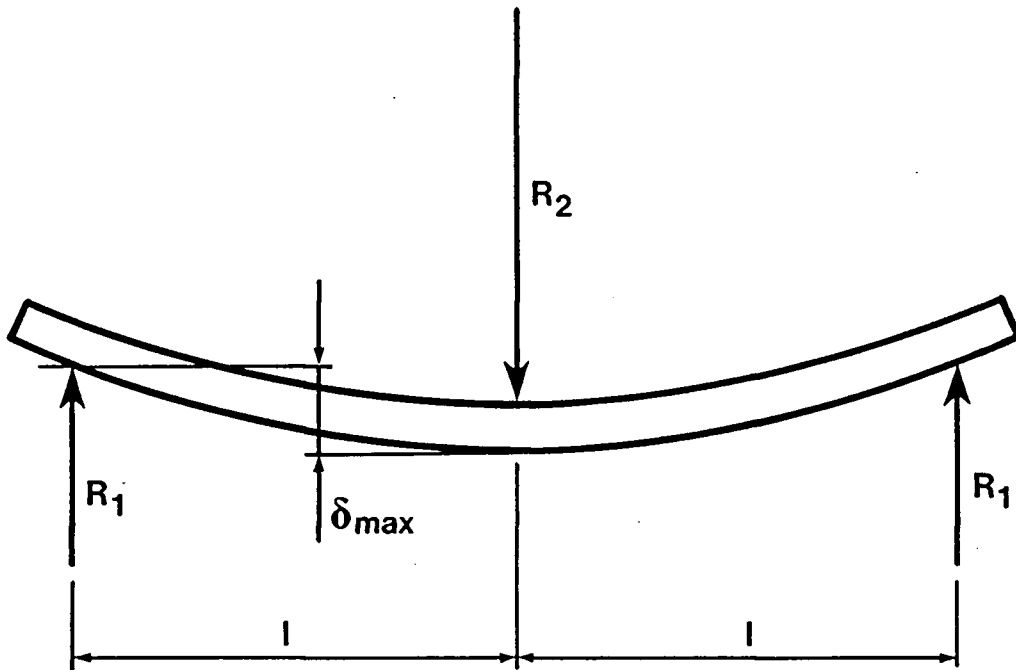


Figure XVII-64. Bending Forces acting on Fibre.

the maximum fibre deflection is:

$$\delta_{max} = \frac{R_1 \cdot l^3}{3 \cdot E \cdot I} = \frac{R_2 \cdot l^3}{6 \cdot E \cdot I} \quad (\text{XVII-5})$$

and for force  $R_1$  is:

$$R_1 = \frac{3 \cdot E \cdot I \cdot \delta_{max}}{l^3} \quad (\text{XVII-6})$$

If this fibre had been pulled out as in a tensile test, most likely only one contact point would slide. The other two contacts would be associated with one of two separating parts of the floc. Therefore, only  $R_1$  would contribute to the total force,  $F$ . The situation becomes more complex when  $n_c$  is greater

than three. In this case, more contact points would slide, each contributing to the total force. If it is assumed that every additional sliding contact develops the average force  $R_1 \cdot \phi_d \cdot k_d$ .

The inter-contact distance, measured along fibre axis is approximated by

$$l = \frac{L}{n_c} \quad (\text{XVII-7})$$

The bending moment of inertia for a circular profile is

$$I = \frac{\pi \cdot d^4}{64} \quad (\text{XVII-8})$$

In non-oriented fibre networks, the average angle between fibre longitudinal axis and the dissecting plane is [W3]

$$\bar{\gamma} = \int_0^{\pi/2} \gamma \cdot \cos \gamma \cdot d\gamma = 0.57 \quad (\text{XVII-9})$$

$$\bar{\gamma} = 32.7^\circ \quad (\text{XVII-10})$$

An average fibre cross-section laying within the break plane is

$$\bar{A}_f = \frac{\pi \cdot d^2}{4 \cdot \sin \gamma} \quad (\text{XVII-11})$$

This equation is valid for  $\gamma$  from arcus tangens( $d/L$ ) to  $\pi/2$ , i.e., this analysis excludes all fibres inclined at angles smaller than arcus tangens( $d/L$ ) to the plane of break. The number of fibres crossing the break cross-section can be estimated from:

$$N_f = \frac{B \cdot C_{va}}{\bar{A}_f} = \frac{4 \cdot B \cdot \sin \gamma}{\pi \cdot d^2} \cdot C_{va} \quad (\text{XVII-12})$$

Where, B is a cross-section area of the break zone. Equation (XVII-4) can now be rewritten in terms of breaking stress.

$$\sigma_T = \frac{F}{B} = \frac{3}{16} \cdot \sin \gamma \cdot k_c \cdot k_d \cdot k_f \cdot \phi_d \cdot E \cdot \frac{d^2}{L^3} \cdot \delta_{\max} \cdot C_{va} \cdot n_c^4 \quad (\text{XVII-13})$$

The components of this equation are further discussed in Section 4.8.

## Appendix XVIII. Conductivity and pH Measurements.

### Conductivity Measurements.

The water used in all experiments was deionized in the deionizer installed in the Chemical Engineering building, and was further ultrafiltered by being passed through the Ultrapore Cartridge (Syborn/Barnstead). The conductivity of the deionized and ultrafiltered water was frequently measured with the Seibold (type LTB) conductivity meter.

Before the conductivity measurements proceeded, the functioning of the instrument and the measuring cell constant was examined. This was necessary because the instrument was in considerable disrepair. Determination of the cell constant required potassium chloride solutions of various concentrations [A13,S7].

For the measuring cell constant to be determined, the standard and the empirical conductivities were compared. Measuring conductivities of KCl solutions followed the standard procedure [A13]; the results are shown in Figure XVIII-65. Since the average temperature of KCl solutions was 22.98°C (S.D.=0.798°C), the standard conductivities at 23°C were taken from the tables in references [A13,S7]. The straight-line fits obtained by a least-squares method were made to the base-ten logarithms of concentrations and conductivities.

$$\text{LOG}_{10}(\text{conductivity}) = a + b \cdot \text{LOG}_{10}(\text{concentration}) \quad (\text{XVIII-1})$$

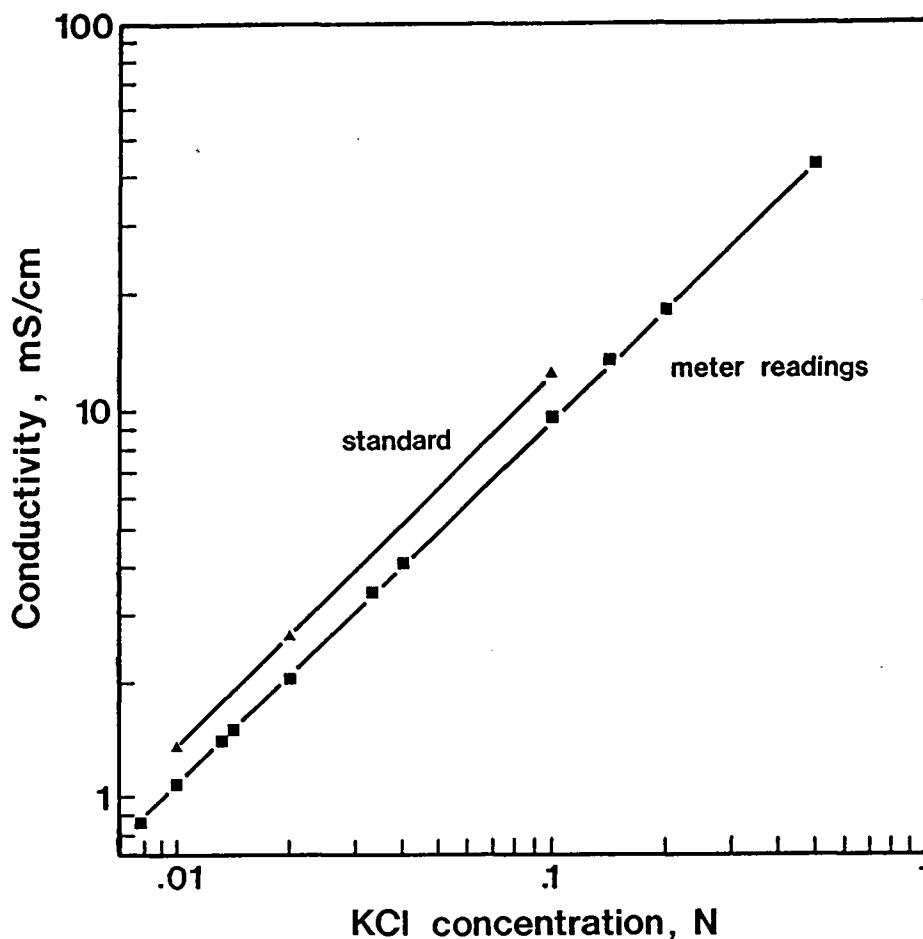


Figure XVIII-65. Standard and Seibold Conductivities versus KCl Concentration in Solutions.

where  $a$  and  $b$  are the fit parameters.

Listing of the FORTRAN program used for the linear regression and plotting is given in Appendix XXV along with the listings of the data files. The fit parameters are shown in Table XVIII-XXIX.

The cell constant,  $K_c$ , is the ratio of standard to empirical conductivities over the range of concentrations measured.

Table XVIII-XXIX. Fit Parameters for Two Straight Lines Shown in Figure XVIII-65.

	a	b	SUM OF SQUARES
SEIBOLD @ 22.98°C	1.919863	0.9473736	$1.415678 \cdot 10^{-2}$
STANDARD @ 23.0°C	2.052766	0.9592081	$4.132784 \cdot 10^{-6}$

$$\frac{\text{CONDUCTIVITY}_{\text{STANDARD}}}{\text{CONDUCTIVITY}_{\text{SEIBOLD}}} = K_c \quad (\text{XVIII-2})$$

Two concentrations, 0.01N and 0.1N, were taken as the lower and the upper limit of integration.

$$K_c = \frac{\int_{.01}^{.1} (10^{a_1} + \text{CONCENTRATION}^{b_1}) d\text{CONCENTRATION}}{\int_{.01}^{.1} (10^{a_2} + \text{CONCENTRATION}^{b_2}) d\text{CONCENTRATION}} \quad (\text{XVIII-3})$$

Taking  $a_1=2.052766$ ,  $b_1=0.9592081$ ,  $a_2=1.919863$ , and  $b_2=0.9473736$  and integrating equation (XVIII-3) yields  $K_c=1.3577$ .

### pH measurements

Water and solutions pH were monitored with the Beckman combination electrode (531013) connected to the Beckman (Model 4500) digital pH meter according to the standard procedure [A16].

Prior to each new batch of experiments, the meter was checked and the slope was adjusted with standard buffer solutions of 4 and 7pH.

Appendix XIX. Data Collection Program for Fibre Length and Fibre Curvature Measurements.

```
10 REM THIS PROGRAM COLLECTS FIBRE LENGTH AND CURVATURE DATA USING
20 REM SUMMAGRAPHICS MICROGRID DIGITIZER.
30 REM FIBRE LENGTH IN mm, NUMBER OF POINTS ALONG THE FIBRE, AND
40 REM LOCAL RADII OF CURVATURE IN mm ARE STORED SEQUENTIALLY IN
50 REM A DISKETTE FILE.
60 CLS:KEY OFF:CLOSE 'Clear screen, soft keys off, close all files or devices
70 DEFINT I-K 'Integer I-K
80 OPTION BASE 1 'The lowest value an array subscript has is one
90 DIM XX(50),YY(50),FF(50),RC(50) 'Coordinates of points along fibre contour, cursor status, local radius of curvature
100 LOCATE 5,1,1,0,7 'Screen location, block cursor on
110 INPUT "INPUT THE NAME OF A NEW DATA FILE :",$F$
120 LOCATE 25,1 'Screen location
130 INPUT "DO YOU WANT TO CHANGE THIS NAME, [Y] OR [N] ";A$
140 A=ASC(A$):IF A=89 OR A=121 GOTO 100:A$=""
150 OPEN "COM1:9600" AS #1 'Open communication port with SUMMAGRAPHICS MICROGRID tablet, OPEN statement is short
because of the intentional DIP switches setting on the tablet to fit BASICA's defaults
160 OPEN $F$ FOR APPEND AS #2 'Open data file named $F$ for sequential output
170 PRINT #1,CHR$(27)"Z" 'Tablet reset
180 PRINT #1,CHR$(27)"M1",CHR$(27)"R3" 'Point mode, 10 coordinates/second
190 PRINT #1,CHR$(27)"C1" 'Resolution - metric-low; 10 points/mm
200 LOCATE 6,1
210 INPUT "INPUT THE REAL SIZE OF THE CALIBRATION SCALE IN MILIMETERS :",$C
220 LOCATE 25,1
230 NUM%=0 'Consecutive fibre number
240 INPUT "DO YOU WANT TO CHANGE THIS VALUE, [Y] OR [N] ";A$
250 A=ASC(A$):IF A=89 OR A=121 GOTO 200:A$=""
260 CLS :LOCATE 7,1
270 PRINT "INPUT END COORDINATES OF THE CALIBRATION SCALE."
280 PRINT "PRESS ANY BUTTON ON THE CURSOR FOR EACH COORDINATE."
290 INPUT #1,XX(1),YY(1),FF(1),T
300 PRINT XX(1),YY(1),FF(1)
310 PRINT #1,CHR$(27)"L11" 'Yellow LED on the cursor is on
320 INPUT #1,XX(2),YY(2),FF(2),T
330 PRINT XX(2),YY(2),FF(2)
340 PRINT #1,CHR$(27)"A",CHR$(27)"L10" 'Beeper, yellow LED off
350 LOCATE 25,1,1,4,7
360 INPUT "DO YOU WANT TO REPEAT THE CALIBRATION PROCEDURE, [Y] OR [N] ";A$
370 A=ASC(A$):IF A=89 OR A=121 GOTO 260:A$=""
380 LOCATE 25,1 :PRINT " ";
390 CS=SQR((XX(1)-XX(2))^2+(YY(1)-YY(2))^2) 'Calibration distance, tablet units
400 CS=CS/C 'Calibration distance in units/mm
410 LOCATE 11,1
420 WRITE "CALIBRATION DISTANCES: REAL AND PROJECTED ON THE TABLET."
430 PRINT "C=",$C;CHR$(109)CHR$(109),"CS=";CS;"units/mm"
440 LOCATE 13,1
450 PRINT "INPUT COORDINATES OF UP TO 50 POINTS ALONG THE FIBRE CONTOUR."
460 PRINT "PRESS BUTTON #5 FOR THE FINAL COORDINATES."
```

```

470 FL=0 'Reset cumulative fibre length to zero
480 INPUT #1,XX(1),YY(1),FF(1),T
490 PRINT XX(1),YY(1),FF(1)
500 PRINT #1,CHR$(27)"L11" 'Yellow LED on the cursor is on
510 FOR I=2 TO 50
520 INPUT #1,XX(I),YY(I),FF(I),T
530 PRINT XX(I),YY(I),FF(I)
540 IF FF(I)=6 GOTO 570 'Was Button #5 pressed?
550 IF I=50 GOTO 920 '50 points is maximum
560 NEXT
570 PRINT #1,CHR$(27)"L10",CHR$(27)"A" 'Yellow LED of, beeper
580 PRINT CHR$(10) 'Line feed
590 PRINT "DO YOU ACCEPT THIS INPUT?"
600 PRINT "IF NOT, PRESS F ON THE CURSOR."
610 PRINT "IF YES, PRESS ANY OTHER BUTTON."
620 INPUT #1,X1,Y1,F1,T
630 CLS :LOCATE 1,1,0 'Clear screen, cursor off
640 IF F1=16 GOTO 440 'Repeat last series of readings
650 NUM%=NUM%+1:PRINT "FIBRE NUMBER ";NUM%
660 FL=SQR((XX(1)-XX(2))^2+(YY(1)-YY(2))^2)
670 FOR K=2 TO I-1
680 KM=K-1:KP=K+1
690 X4=(XX(K)+XX(KM))/2:X5=(XX(KP)+XX(K))/2 'Middle point
700 Y4=(YY(K)+YY(KM))/2:Y5=(YY(KP)+YY(K))/2 'coordinates
710 A1=-((XX(KM)-X4)/(YY(KM)-Y4):A2=-((XX(K)-X5)/(YY(K)-Y5) 'Slopes
720 B1=Y4-A1*X4:B2=Y5-A2*X5 'Intercepts with y-axis
730 X6=(B2-B1)/(A1-A2):Y6=A1*X6+B1 'Normal lines intercept coordinates
740 RC(KM)=SQR((X6-XX(K))^2+(Y6-YY(K))^2) 'Radius of curvature, tablet units
750 RC(KM)=RC(KM)/CS 'Radius of curvature in millimeters
760 FL=SQR((XX(KP)-XX(K))^2+(YY(KP)-YY(K))^2)+FL 'Sum of straight line segments
770 NEXT
780 FL=FL/CS 'Total, approximated fibre length
790 PRINT CHR$(10)
800 PRINT "FIBRE LENGTH AND NUMBER OF DATA POINTS ALONG IT:"
810 PRINT "FL=";FL;CHR$(109)CHR$(109),"KP=";KP
820 PRINT "LOCAL RADII OF CURVATURE:"
830 FOR J=1 TO KM
840 PRINT "RC(";J;")=";RC(J);
850 NEXT
860 PRINT #2,FL;KM;
870 FOR J=1 TO KM
880 PRINT #2,RC(J);
890 NEXT
900 PRINT #2,CHR$(13) 'Carriage return
910 GOTO 930
920 PRINT "THIS WAS THE 50-TH POINT ON THE CONTOUR.":GOTO 570
930 PRINT CHR$(10) 'Line feed
940 PRINT "DO YOU WANT TO CONTINUE WITH THE NEXT FIBRE?"
950 PRINT "IF NOT, PRESS F ON THE CURSOR."
960 PRINT "IF YES, PRESS ANY OTHER BUTTON."

```

```
970 INPUT #1,X1,Y1,F1,T
980 IF F1=16 THEN CLOSE #1,#2 ELSE GOTO 440
990 LOCATE 24,1,O :KEY ON          'Cursor off, soft keys on
1000 END
```

Appendix XX. Data Collection Program for Water Absorption by Nylon Fibres.

```
10 REM THIS PROGRAM CONTROLS DATA ACQUISITION FROM
20 REM METTLER BALANCE AE-163 THROUGH DATA INTERFACE
30 REM CARD OPTION O12.
40 REM WEIGHT READING IN GRAMS AND TIMER READING IN SECONDS
50 REM ARE DISPLAYED ON THE SCREEN AND STORED IN A DATA FILE.
60 CLS :KEY OFF           'Clear screen, soft keys off
70 DEL=.001              'Weight increment is 0.001g
80 LOCATE 4,1
90 INPUT "INPUT THE NAME OF A NEW DATA FILE :",$F$
100 LOCATE 25,1
110 INPUT "DO YOU WANT TO CHANGE THE DATA FILE NAME";YY$
120 Y=ASC(YY$):IF Y=89 OR Y=121 GOTO 80
130 OPEN F$ FOR APPEND AS #2      'Open communication with F$ data file
140 OPEN "COM1:2400,e,7,1,LF,PE" AS #1  'Open communication with the balance
150 PRINT #1,"R1"                'Disable the balance single control bar
160 CLS :LOCATE 8,15
170 PRINT "PREPARE BALANCE FOR TARE INPUT."
180 LOCATE 10,15
190 PRINT "PRESS ANY KEY TO INPUT TARE."
200 CLOSE #1:OPEN "COM1:2400,e,7,1,LF,PE" AS #1
210 A$=INKEY$: IF A$="" THEN 210
220 T=TIMER:PRINT #1,CHR$(84)      'Trigger tare procedure
230 INPUT #1,X$:WRITE #2,X$,T      'Store tare and time in file
240 LOCATE 11,15 :PRINT X$,T
250 CLOSE #1:OPEN "COM1:2400,e,7,1,LF,PE" AS #1
260 PRINT #1,"D do it!";" "      'Display text on the balance display
270 LOCATE 13,15
280 PRINT B$ "PREPARE BALANCE FOR MEASUREMENTS."
290 LOCATE 15,15
300 PRINT B$ "PRESS ANY KEY TO START DATA ACQUISITION."
310 A$=INKEY$: IF A$="" THEN 310
320 PRINT #1,"D"                  'Clear the balance display
330 CLOSE #1:OPEN "COM1:2400,e,7,1,LF,PE" AS #1
340 T=TIMER:PRINT #1,"SI"         'Send immediate value - dynamic measurement
350 INPUT #1,X$:LOCATE 16,15:PRINT X$,T  'First recorded load and time
360 Y$=MID$(X$,4,9):Z=VAL(Y$):WRITE #2,Z,T  'Convert string to variable
370 CNT%=0                        'Reading count
380 T=TIMER:PRINT #1,"SI"         'Send immediate value
390 INPUT #1,U$:V$=MID$(U$,4,9):W=VAL(V$)
400 CNT%=CNT%+1                  'Increment the reading count
410 IF CNT%>900 GOTO 480          'Cycle of no change in weight
420 IF ABS(W-Z)<DEL GOTO 380      'Is weight change more than 0.001g?
430 Z=W:WRITE #2,Z,T            'Store weight and time in data file
440 LOCATE 17,15 :PRINT:LOCATE 17,15:PRINT U$,T
450 LOCATE 22,1
460 PRINT "TO STOP PROGRAM PRESS 'Ctrl-Break' THEN TYPE 'Close' AND PRESS Enter"
470 GOTO 370
```

```
480 LOCATE 18,15:PRINT "WEIGHT HAS LEVELED OFF."  
490 WRITE #2,W,T:LOCATE 19,15:PRINT:LOCATE 19,15:PRINT U$,T  
500 GOTO 370  
510 STOP
```

Appendix XXI. Fibre Bending. Data Processing Program, Raw Data, Averages and Standard Deviations of Fibre Deflection, Bulk Reynolds Numbers. Eye-Piece-Micrometer and GILMONT Flowmeter Calibration Data.

(a) FORTRAN program.

C This program calculates average Reynolds numbers and average  
C fibre deflections, uses NL2S0L to fit  $def=A*Reynolds**B$ ,  
C makes a plot.

C Input is taken from (4).

C Output is directed to (7).

```
      IMPLICIT REAL*8(A - H, O - Z), INTEGER(I - N)
      EXTERNAL CALCR, CALCJ
      INTEGER FLAG, LIST(1)
      COMMON XX(50), YY(50)
      DIMENSION A(50), B(50), P(2), V(200), IV(100)
      REAL*4 C(100), D(100), X1, Y1
      DATA LIST /'*/
      PI = 4. * ATAN(1.)
      M = 2
      P(1) = 1.DO
      P(2) = 1.DO
      CALL AXCTRL('SYMS', .2)
      CALL AXCTRL('LABE', 1)
      CALL AXCTRL('DIGI', -1)
      CALL AXCTRL('XORI', 2.0)
      CALL AXCTRL('YORI', 2.0)
      CALL AXPLLOT('BULK REYNOLDS NO.; ', 0.0, 10., 0.0, 10.)
      CALL AXPLLOT('MAX. DEFLECTION UM; ', 90.0, 10., 0.0, 20.)
      CALL PLOT(2.0, 12.0, 3)
      CALL PLOT(12.0, 12.0, 2)
      CALL PLOT(12.0, 2.0, 2)
      FIND (4'7000)
      READ (4,LIST) X, Y, Z, W
      YOLD = Y
10  J = 0
20  I = 0
30  READ (4,LIST,END=150,ERR=170) X, Y, Z, W
      IF (X .EQ. 0.0) GO TO 40
      I = I + 1
      A(I) = .55068D-1*X - .360563D0
      A(I) = A(I) * 4 / PI / .152D0 / .152D0 / 100
      A(I) = A(I) * RHO(W) / VIS(W)
      B(I) = (Z - Y) / .5932D0
      GO TO 30
40  IF (Y .GT. YOLD) GO TO 100
```

C

C Averages, bulk Reynolds number, maximum fibre deflection

SUM1 = 0.DO

SUM2 = 0.DO

```

DO 50 K = 1, I
  SUM1 = SUM1 + A(K) * Y / 100
  SUM2 = SUM2 + B(K)
50 CONTINUE
  AVE1 = SUM1 / I
  AVE2 = SUM2 / I
  J = J + 1
C
C Standard deviations
  XX(J) = AVE1
  YY(J) = AVE2
  SS1 = 0.DO
  SS2 = 0.DO
  DO 60 K = 1, I
    SS1 = SS1 + (A(K) * Y / 100 - AVE1) ** 2
    SS2 = SS2 + (B(K) - AVE2) ** 2
60 CONTINUE
  SIGMA1 = DSQRT(SS1/(I - 1))
  SIGMA2 = DSQRT(SS2/(I - 1))
  WRITE (7,70) Y
70 FORMAT (1X, 'FIBRE DIAMETER = ', F8.6, 'CM'/)
  WRITE (7,80) AVE1, SIGMA1
80 FORMAT (1X, 'AVERAGE RE. # = ', E13.6, ' STD. DEV. =', E13.6/)
  WRITE (7,90) AVE2, SIGMA2
90 FORMAT (1X, 'AVERAGE DEFLEC. = ', E13.6, 'MICROMETERS
1 STD. DEV. =', E13.6/)
  GO TO 20
C
C Set default values in IV() & V()
100 YOLD = Y
  CALL DFALT(IV, V)
  IV(1) = 0
  CALL NL2SOL(J, M, P, CALCR, CALCJ, IV, V, IPARM, RPARM, FPARM)
C
C Write the return code and solution
  WRITE (7,110) IV(1)
110 FORMAT (1X, ' RETURN CODE =', I2)
  WRITE (7,120) (P(K),K=1,M), V(10)
120 FORMAT (1X, ' SOLUTION:', 1P2G16.8/' SUM OF SQUARES/2 =', 1PG16.8)
  L = IFIX(SNGL(XX(J))) + 3
  C(1) = 2.0
  D(1) = 2.0
  DO 130 K = 1, L
    C(K + 1) = FLOAT(K) / 10 + 2.
    D(K + 1) = (P(1)*FLOAT(K)**P(2)) / 20 + 2.
130 CONTINUE
  CALL PLOT(2., 2., 3)
  CALL LINE(C, D, L, 1)
  DO 140 K = 1, J
    X1 = SNGL(XX(K)/10 + 2.)

```

```

        Y1 = SNGL(YY(K)/20 + 2.)
        CALL SYMBOL(X1, Y1, .2, 1, 0.0, -1)
140 CONTINUE
    GO TO 10
150 WRITE (6,160)
160 FORMAT (1X, 'END OF DATA 4 ENCOUNTERED.')
    CALL PLOTND
    STOP
170 M = I + 6
    WRITE (6,180) M
180 FORMAT (1X, 'RECORD', I5, ' IN FILE 4 SKIPPED.')
    GO TO 20
    END

C
    FUNCTION RHO(W)
        RHO = 280.54253D-12 * W
        RHO = (105.56302D-09 - RHO) * W
        RHO = (46.170469D-06 + RHO) * W
        RHO = (7.987041D-03 - RHO) * W
        RHO = (16.945176D0-RHO) * W
        RHO = (999.83952D0+RHO) / (1. + 16.87985D-03*W)
    RETURN
    END

C
    FUNCTION VIS(W)
        VIS = 1.3272D0 * (20.D0-W) - .001053D0 * (W - 20.D0) ** 2
        VIS = VIS / (105.D0+W)
        VIS = 1.002D0 * 10.D0 ** VIS / 1000
    RETURN
    END

C
C FUNCTION g(t)=f(t)-Yi calculations
    SUBROUTINE CALCR(N, M, P, NF, R, IPARM, RPARM, FPARM)
        IMPLICIT REAL*8(A - H, O - Z)
        DIMENSION P(M), R(N)
        COMMON XX(50), YY(50)

C
C Test for exponential overflow
        IF (P(2) .LT. 1.D-1) GO TO 20

C
C Place residuals in R
        DO 10 I = 1, N
            R(I) = P(1) * XX(I) ** P(2) - YY(I)
10 CONTINUE
        RETURN
20 NF = 0
        RETURN
    END

C
C Derivatives df/dA & df/dT calculations

```

```

SUBROUTINE CALCJ(N, M, P, NF, D, IPARM, RPARM, FPARM)
IMPLICIT REAL*8(A - H, O - Z)
DIMENSION P(M), D(N,M)
COMMON XX(50), YY(50)

```

```

C
C Test for exponential overflow
  IF (P(2) .LT. 1.D-1) GO TO 20
C
C Put derivatives into D
  DO 10 I = 1, N
    D(I,1) = XX(I) ** P(2)
    D(I,2) = P(1) * D(I,1) * DLOG(XX(I))
  10 CONTINUE
  RETURN
  20 NF = 0
  RETURN
  END

```

(b) Data on fibre flexing.

Data for two types of nylon: 6 and 15 denier.  
 Data is listed in packets. Each line in a packet contains  
 Guilmont flowmeter reading (mL), initial eye-piece reading, final  
 eye-piece reading, and water temperature (degree Celsius).

6 DENIER FIBRES (diameter=0.0279mm)

0.3000E+02	0.9570E+02	0.1292E+03	0.2205E+02
0.3000E+02	0.9510E+02	0.1254E+03	0.2260E+02
0.3000E+02	0.9540E+02	0.1248E+03	0.2280E+02
0.3000E+02	0.9480E+02	0.1154E+03	0.2310E+02
0.3000E+02	0.9470E+02	0.1208E+03	0.2320E+02
0.3000E+02	0.9540E+02	0.1179E+03	0.2330E+02
0.3000E+02	0.9460E+02	0.1248E+03	0.2330E+02
0.3000E+02	0.9500E+02	0.1177E+03	0.2350E+02
0.3500E+02	0.9570E+02	0.1391E+03	0.2205E+02
0.3500E+02	0.9510E+02	0.1404E+03	0.2260E+02
0.3500E+02	0.9540E+02	0.1348E+03	0.2280E+02
0.3500E+02	0.9480E+02	0.1245E+03	0.2310E+02
0.3500E+02	0.9470E+02	0.1296E+03	0.2320E+02
0.3500E+02	0.9450E+02	0.1223E+03	0.2330E+02
0.3500E+02	0.9460E+02	0.1337E+03	0.2330E+02
0.3500E+02	0.9500E+02	0.1262E+03	0.2350E+02
0.4000E+02	0.9570E+02	0.1514E+03	0.2205E+02
0.4000E+02	0.9510E+02	0.1530E+03	0.8000E+01
0.4000E+02	0.9540E+02	0.1458E+03	0.2280E+02
0.4000E+02	0.9480E+02	0.1317E+03	0.2310E+02
0.4000E+02	0.9470E+02	0.1386E+03	0.2320E+02
0.4000E+02	0.9540E+02	0.1329E+03	0.2330E+02
0.4000E+02	0.9460E+02	0.1469E+03	0.2330E+02

0.4000E+02	0.9500E+02	0.1331E+03	0.2350E+02
0.4500E+02	0.9570E+02	0.1679E+03	0.2205E+02
0.4500E+02	0.9510E+02	0.1772E+03	0.2260E+02
0.4500E+02	0.9540E+02	0.1528E+03	0.2280E+02
0.4500E+02	0.9480E+02	0.1438E+03	0.2310E+02
0.4500E+02	0.9470E+02	0.1530E+03	0.2320E+02
0.4500E+02	0.9540E+02	0.1445E+03	0.2330E+02
0.4500E+02	0.9460E+02	0.1622E+03	0.2330E+02
0.5000E+02	0.9500E+02	0.1499E+03	0.2350E+02
0.5000E+02	0.9570E+02	0.1907E+03	0.2205E+02
0.5000E+02	0.9510E+02	0.1960E+03	0.2260E+02
0.5000E+02	0.9540E+02	0.1643E+03	0.2280E+02
0.5000E+02	0.9480E+02	0.1578E+03	0.2310E+02
0.5000E+02	0.9470E+02	0.1711E+03	0.2320E+02
0.5000E+02	0.9540E+02	0.1445E+03	0.2330E+02
0.5000E+02	0.9460E+02	0.1818E+03	0.2330E+02
0.5000E+02	0.9500E+02	0.1683E+03	0.2350E+02
0.5000E+02	0.9570E+02	0.2175E+03	0.2205E+02
0.5500E+02	0.9510E+02	0.2453E+03	0.2260E+02
0.5500E+02	0.9540E+02	0.1843E+03	0.2280E+02
0.5500E+02	0.9480E+02	0.1770E+03	0.2310E+02
0.5500E+02	0.9470E+02	0.1925E+03	0.2320E+02
0.5500E+02	0.9540E+02	0.1799E+03	0.2330E+02
0.5500E+02	0.9460E+02	0.2193E+03	0.2330E+02
0.5500E+02	0.9500E+02	0.1861E+03	0.2350E+02

15 DENIER FIBRES (diameter=0.0442mm)

0.3000E+02	0.9530E+02	0.1035E+03	0.2290E+02
0.3000E+02	0.9530E+02	0.1075E+03	0.2300E+02
0.3000E+02	0.9520E+02	0.1010E+03	0.2260E+02
0.3000E+02	0.9430E+02	0.1021E+03	0.2260E+02
0.3000E+02	0.9470E+02	0.1043E+03	0.2260E+02
0.3000E+02	0.9450E+02	0.9990E+02	0.2260E+02
0.3000E+02	0.9480E+02	0.1000E+03	0.2260E+02
0.3000E+02	0.9500E+02	0.1107E+03	0.2260E+02
0.3000E+02	0.9510E+02	0.1021E+03	0.2260E+02
0.4000E+02	0.9530E+02	0.1079E+03	0.2290E+02
0.4000E+02	0.9530E+02	0.1119E+03	0.2300E+02
0.4000E+02	0.9520E+02	0.1039E+03	0.2260E+02
0.4000E+02	0.9430E+02	0.1072E+03	0.2260E+02
0.4000E+02	0.9470E+02	0.1111E+03	0.2260E+02
0.4000E+02	0.9450E+02	0.1047E+03	0.2260E+02
0.4000E+02	0.9480E+02	0.1027E+03	0.2260E+02
0.4000E+02	0.9500E+02	0.1161E+03	0.2260E+02
0.4000E+02	0.9510E+02	0.1084E+03	0.2260E+02
0.5000E+02	0.9530E+02	0.1180E+03	0.2290E+02
0.5000E+02	0.9530E+02	0.1184E+03	0.2300E+02
0.5000E+02	0.9520E+02	0.1089E+03	0.2260E+02
0.5000E+02	0.9430E+02	0.1134E+03	0.2260E+02

0.5000E+02	0.9470E+02	0.1197E+03	0.2260E+02
0.5000E+02	0.9450E+02	0.1093E+03	0.2260E+02
0.5000E+02	0.9480E+02	0.1067E+03	0.2260E+02
0.5000E+02	0.9500E+02	0.1222E+03	0.2260E+02
0.5000E+02	0.9510E+02	0.1158E+03	0.2260E+02
0.6000E+02	0.9530E+02	0.1299E+03	0.2290E+02
0.6000E+02	0.9530E+02	0.1258E+03	0.2300E+02
0.6000E+02	0.9520E+02	0.1164E+03	0.2260E+02
0.6000E+02	0.9430E+02	0.1288E+03	0.2260E+02
0.6000E+02	0.9470E+02	0.1345E+03	0.2260E+02
0.6000E+02	0.9450E+02	0.1196E+03	0.2260E+02
0.6000E+02	0.9480E+02	0.1146E+03	0.2260E+02
0.6000E+02	0.9500E+02	0.1361E+03	0.2260E+02
0.6000E+02	0.9510E+02	0.1299E+03	0.2260E+02
0.7000E+02	0.9530E+02	0.1490E+03	0.2290E+02
0.7000E+02	0.9530E+02	0.1432E+03	0.2300E+02
0.7000E+02	0.9520E+02	0.1248E+03	0.2260E+02
0.7000E+02	0.9430E+02	0.1414E+03	0.2260E+02
0.7000E+02	0.9470E+02	0.1522E+03	0.2260E+02
0.7000E+02	0.9450E+02	0.1532E+03	0.2260E+02
0.7000E+02	0.9480E+02	0.1294E+03	0.2260E+02
0.7000E+02	0.9500E+02	0.1488E+03	0.2260E+02
0.7000E+02	0.9510E+02	0.1433E+03	0.2260E+02

(d) Micrometer eye-piece calibration.

First line - Real distance in mm on calibration scale.

Second line - Eyepiece readings in micrometer units.

0.1	0.2	0.3	0.4	0.5	0.6	0.7	0.8	0.9	1.0
59.4	120.0	178.9	237.6	296.1	356.2	413.4	474.4	533.9	594.0

The straight line fit by least squares regression gave:

$R=0.999$ ; intercept  $a=0.0\mu\text{m}$ ; slope  $b=1.6858\mu\text{m/unit}$ .

(e) GILMONT flowmeter calibration.

FLOWMETER READING	TIME INTERVAL MIN:SEC	FLOW RATE mL/s
66	2:32	3.29
60	2:48	2.97
55	3:07	2.67
50	3:29	2.39
45	3:58	2.10
40	4:34	1.82
35	5:26	1.53
30	6:33	1.27
25	8:13	1.01
20	11:01	0.762
15	17:16	0.482
10	40:57	0.203

The straight line fit by least squares regression produced:

R=0.999; intercept a=-.03606mL/s; slope b=0.05507mL/s/flowmeter unit.

(f) Average deflections and bulk Reynolds numbers at each flow rate. Results of power curve fits.

FIBRE DIAMETER $\mu\text{m}$	AVERAGE FIBRE DEFLECTION y $\mu\text{m}$	AVERAGE BULK REYNOLDS NUMBER	POWER CURVE FIT $y = a Re^b$		
			a $\mu\text{m}$	b	sum of squares
27.95	45.37	21.28	.10314	1.9580	185.5
	61.28	25.82			
	78.53	29.17			
	103.4	34.90			
	129.3	39.44			
	177.3	43.98			
44.19	14.40	33.42	.00745	2.0568	38.23
	22.42	47.66			
	33.38	61.91			
	52.71	76.16			
	80.75	90.41			

Appendix XXII. Data Acquisition Program for Flow Velocity Measurements.

a) Main program written in BASIC.

```
10 REM $LINESIZE: 132 $PAGESIZE: 55
20 WIDTH 80:CLS
30 PRINT "DATA COLLECTION PROGRAM FOR LDA ANALYSIS OF FLOW"
40 PRINT "      IN THE HORIZONTAL ROTATING CYLINDER."
50 PRINT
60 PRINT "HARDWARE: Dual-beam LDA, Brag cell, frequency shift,"
70 PRINT "      IBM personal computer,"
80 PRINT "      Tecmar Lab Master A/D & D/A converter,"
90 PRINT "      (0 channel single-ended, gain=10 -1.V to +1.V)"
100 PRINT
110 DEFINT I,J,K
120 DIM A%(25000),L$(3)
130 INPUT "Enter your name.      ",NAM$
140 PRINT "Enter: suspending liquid density, suspension concentration, cylinder"
150 PRINT "rotational speed, LDA orientation, tracker range, frequency shift."
160 INPUT L$(1)
170 INPUT "Enter the number of data points to collect.      (<=25000) ",N%
180 INPUT "Enter the number of data points/second desired.<=30000) ",S
190 INPUT "Enter the name of the file in which data will be stored.",FILN$
200 D$=DATE$: T$=TIME$
210 OPEN FILN$ FOR OUTPUT AS #2
220 PRINT #2,"NAME: ";NAM$,"DATE: ";D$,"TIME: ";T$
230 PRINT #2,L$(1)
240 PRINT #2,"NUMBER OF DATA POINTS: ";N%,"SAMPLING RATE: ";S;"PTS/SEC"
250 PRINT #2,"Data stored in lines contains: radial coordinate-mm,"
260 PRINT #2,"angular coordinate-deg., average voltage, RMS of voltage"
270 PRINT #2,"fluctuations."
280 C%=0 'A/D channel number
290 S%=S: IF S<1 THEN S%=-1!/S 'Convert to proper format for timer routine
300 P%=1:IF S%>2000 THEN P%=0 'Plot if < 2000 pts/sec
310 REM ***** CALIBRATION PROCEDURE
320 CLS
330 PRINT "Prepare tracker for calibration."
340 PRINT "Set zero voltage on the tracker and press any key."
350 I$=INKEY$:IF I$="" THEN 350
360 MUL%=INT(N%/15): NN%=MUL%*15
370 F%=0 'Initialize overrun flag
380 CALL TIMER(A%(1),F%,P%,NN%,C%,S%)
390 IF F%<>0 THEN PRINT "Warning--data taken too fast!":NN%=NN%-F%
400 SUMO=0
410 FOR I=1 TO NN% STEP 15
420 SUM1=0
430 K=I: KK=I+14
440 FOR J=K TO KK
```

```

450 IF A%(J)>32767 THEN A%(J)=A%(J)-65535!
460 SUM1=SUM1+A%(J)
470 NEXT J
480 SUM1=SUM1/15
490 SUMO=SUMO+SUM1
500 NEXT I
510 SUMO=SUMO/MUL%
520 PRINT "SUMO=",SUMO 'digits
530 PRINT "MUL%=",MUL% '# of sets of 15 readings
540 INPUT "Do you wish to repeat calibration? ",Y$
550 IF Y$="y" OR Y$="Y" GOTO 320
560 PRINT "Set traversing rig to new coordinates."
570 INPUT "Radius in millimeters. ",RAD%
580 INPUT "Angle FI in degrees. ",ANG%
590 PRINT "Press any key to start data collection."
600 I$=INKEY$: IF I$="" THEN 600
610 F%=0 'Initialize overrun flag
620 CALL TIMER(A%(1),F%,P%,NN%,C%,S%)
630 IF F%<>0 THEN PRINT "Warning--data taken too fast!":NN%=NN%-F%
640 SUM2=0
650 FOR I=1 TO NN% STEP 15
660 SUM1=0
670 K=I: KK=I+14
680 FOR J=K TO KK
690 IF A%(J) >32767 THEN A%(J)=A%(J)-65535!
700 SUM1=SUM1+A%(J)
710 NEXT J
720 SUM1=SUM1/15
730 SUM2=SUM2+SUM1
740 NEXT I
750 SUM2=SUM2/MUL%
760 PRINT "SUM2=",SUM2 'digits
770 PRINT "MUL%=",MUL% '# of sets of 15 readings
780 DIG=SUM2-SUMO
790 SUM3=0
800 FOR I=1 TO NN% STEP 15
810 SUM1=0
820 K=I: KK=I+14
830 FOR J=K TO KK
840 SUM1=SUM1+(SUM2-A%(J))a2
850 NEXT J
860 SUM1=SUM1/15
870 SUM3=SUM3+SUM1
880 NEXT I
890 SUM3=SUM3/MUL%
900 SUM3=SQR(SUM3)/2048
910 DIG=DIG/2048
920 PRINT "DIGVOL=",DIG
930 PRINT "SQRT=";SUM3;"VOLTS"
940 INPUT "Do you wish to store results in the file? ",Y$

```

```

950 IF Y$="y" OR Y$="Y" GOTO 1000
960 Y$=""
970 INPUT "Next coordinates? ",Y$
980 IF Y$="y" OR Y$="Y" GOTO 560
990 GOTO 1020
1000 PRINT #2,RAD%,ANG%,DIG,SUM3
1010 GOTO 960
1020 END

```

b) Assembler subroutine for INTEL 8088 microprocessor.

```

PAGE ,132
TITLE TIMER
; SUBROUTINE TO DO TIMED DATA COLLECTION FROM TECMAR A/D/A BOARD
; CALL FROM BASIC WITH CALL OF FORM:
; CALL TIMER (A%(1),F%,P%,N%,C%,S%)
; WHERE A% IS ARRAY WHERE DATA ARE TO BE STORED
; F% IS OVERRUN FLAG--SET TO ZERO UPON NORMAL EXIT
; OTHERWISE SET TO VALUE OF CX REGISTER TO GIVE
; NUMBER OF POINTS NOT COLLECTED
; P% IS 0 TO OMIT REAL-TIME PLOT, OTHER TO PLOT
; N% IS NUMBER OF POINTS TO BE COLLECTED
; C% IS CHANNEL NUMBER OF A/D
; S% IS NUMBER OF DATA POINTS PER SECOND
; S% MUST BE <= SPEED OF A/D
; IF S% <0 THAT MEANS WE WANT THAT MANY SEC/POINT
;
CSEG SEGMENT
ASSUME CS:CSEG, DS:NOTHING
HEADER:
DB OFDH ;CODE FOR BLOAD FILE
DW 0
DW 0
DW RTNLEN
TEMP DW ? ;TEMP. STORAGE
PLOT DW ? ;PLOT FLAG
TEMPSI DW ? ;TEMP. STORAGE FOR SI REGISTER
OVRUN DW ? ;OVERRUN OF A/D FLAG
;DEFINITIONS:
ADD0 =1808 ;I/O ADDRESS OF TECMAR BOARD
ADD4 =ADD0+4 ;A/D CONTROL BYTE
ADD5 =ADD0+5 ;A/D CHANNEL NUMBER
ADD6 =ADD0+6 ;SOFTWARE START CONVERSION
ADD8 =ADD0+8 ;TIMER 9513 DATA PORT
ADD9 =ADD0+9 ;TIMER 9513 CONTROL PORT
PAGE
TIMER PROC FAR
PUSH BP ;SAVE BP

```

```

MOV     BP,SP           ;SET BASE PARAMETER LIST
MOV     DI,[BP]+6      ;GET DATA POINTS/SEC.
MOV     AX,[DI]        ; INTO BX REGISTER
MOV     BX,AX
MOV     DI,[BP]+8      ;GET CHANNEL NUMBER
MOV     AX,[DI]        ; AND STORE AS AX
MOV     DX,ADD5        ; AND OUTPUT TO A/D
OUT     DX,AL          ; (USE ONLY LOWER BYTE)
MOV     DI,[BP]+10     ;GET NUMBER OF DATA POINTS
MOV     CX,[DI]        ; STORE IN CX REGISTER
MOV     DI,[BP]+12     ;GET PLOT FLAG
MOV     AX,[DI]        ; STORE IN MEMORY
MOV     PLOT,AX
MOV     AL,128         ;SELECT A/D MODE (DISABLE AUTOINCREMENT,
MOV     DX,ADD4        ; EXTERN. START CONVERSION, ALL INTERRUPTS
OUT     DX,AL          ; GAIN=1)
MOV     AX,0           ;SI IS X-VALUE OF POINT TO BE
MOV     TEMPSI,AX     ; PLOTTED--SAVE FOR LATER
MOV     AX,6           ;SET UP HIGH RESOLUTION GRAPHICS MODE
INT     10H
MOV     DX,ADD6        ;RESET DONE FLIP-FLOP OF A/D
IN      AL,DX
MOV     DX,ADD9        ;SET DATA POINTER TO MASTER MODE REGISTER
MOV     AL,23
OUT     DX,AL
MOV     DX,ADD8        ;SET MASTER MODE REGISTER FOR SCALER CONTROL=
MOV     AL,0           ; BCD DIVISION, ENABLE INCREMENT, 8-BIT BUS,
OUT     DX,AL          ; FOUT ON, DIVIDE BY 16, SOURCE=F1,
MOV     AL,128         ; COMPARATORS DISABLED, TOD DISABLED
OUT     DX,AL
MOV     DX,ADD9        ;SET DATA POINTER TO COUNTER MODE OF
MOV     AL,5           ; REGISTER 5
OUT     DX,AL
MOV     DX,ADD8        ;SET COUNTER 5 FOR COUNT REPETITIVELY,
MOV     AL,33          ;BINARY COUNT, COUNT DOWN, ACTIVE HIGH
OUT     DX,AL          ;TC, DISABLE SPECIAL GATE, RELOAD FROM LOAD,
CMP     BX,31          ;CHECK IF >=31 POINTS/SEC
JGE     FAST           ;IF SO, JUMP TO FAST
CMP     BX,0           ;CHECK IF >0 POINTS/SEC
JG      MED            ;IF SO JUMP
PAGE
; BRANCH TO HERE IF POINTS/SEC < 0, IT MEANS THAT WE WANT
; LESS THAN ONE POINT/SEC.
SLOW:  MOV     AL,15    ;SET TO 100 Hz (NO GATE, RISING EDGE
OUT     DX,AL          ; OF F5)
NEG     BX             ;GET ABSOLUTE VALUE OF BX
MOV     AX,BX         ;AND MULTIPLY BY 100 TO GET COUNT
MOV     DI,100
MUL    DI
JMP     GO

```

```

;BRANCH TO HERE FOR 31 TO 20000 POINTS/SEC--USE 1 MHZ CLOCK
FAST:  MOV     AL,11           ;COUNT AT 1 MHZ (NO GATE, RISING
      OUT     DX,AL          ;  EDGE OF F1)
      MOV     AX,10000        ;DIVIDE 100000 BY PTS/SEC BY
      MOV     DI,100         ;  GETTING 10F6 INTO DX+AX
      MUL     DI
      DIV     BX              ;BX=PTS/SEC; RESULT IN DX+AX. BUT
      ;IGNORE DX, SINCE DX=0
      CMP     AX,200         ;DISABLE INTERRUPTS IF >=5000
      JG      FAST2         ;  POINTS/SEC
      CLI
FAST2:  JMP     GO
;BRANCH TO HERE FOR 1 TO 30 POINTS/SEC--USE 10kHz CLOCK
MED:   MOV     AL,13           ;COUNT AT 10kHz (NO GATE, RISING
      OUT     DX,AL          ;  EDGE OF F3)
      MOV     AX,10000        ;CALCULATE NUMBER OF TICKS OF 10000 HZ CLOCK
      CWD
      DIV     BX              ;PER DATA POINT BY DIVIDING
      ;10000 BY PTS/SEC
;START CLOCK TICKING AT DESIRED RATE
GO:    MOV     DX,ADD8        ; AND LOAD COUNTER 5 WITH TICKS
      DEC     AX              ;(COUNT TO ZERO, DECREMENT AX
      OUT     DX,AL          ;  FOR CORRECT COUNT)
      MOV     AL,AH
      OUT     DX,AL          ; 8 BITS AT A TIME
      MOV     DI,[BP]+14     ;GET OVERRUN FLAG ADDRESS
      MOV     WORD PTR [DI],0 ;ZERO THE FLAG
      MOV     OVRUN,DI       ;AND STORE THE FLAG ADDRESS
      MOV     DI,[BP]+16     ;GET ADDRESS OF DATA ARRAY
      MOV     DX,ADD9        ;LOAD COUNTER 5 FROM LOAD REGISTER
      MOV     AL,112         ; AND ARM (START COUNTING)
      OUT     DX,AL
      MOV     DX,ADD4        ;ENABLE EXTERNAL START (PINES 3,4 OF
      MOV     AL,132         ;  J2 CONNECTOR MUST BE CONNECTED)
      OUT     DX,AL
      PAGE
;BEGIN DATA COLLECTION; COLLECT UPON EXTERNAL START TRIGGER
DONE:  MOV     DX,ADD4        ;CHECK IF DATA READY
      IN      AL,DX
      CMP     AL,128         ;BY CHECKING READY BIT (BIT 7)
      JB      DONE          ;LOOP UNTIL READY
      TEST    AL,64          ;SEE IF DATA OVERRUN FLAG SET
      JNE    ERRMESS        ;IF SO, NOTIFY BASIC PROGRAM AND EXIT
      MOV     DX,ADD5        ;YES, DONE, SO GET LOW BYTE OF DATUM
      IN      AL,DX
      MOV     [DI],AL        ;AND STORE IT
      INC     DI              ;GO TO NEXT LOCATION IN ARRAY (1 BYTE LATER)
      MOV     DX,ADD6        ;GET HIGH BYTE AND STORE IT
      IN      AL,DX
      MOV     [DI],AL
      INC     DI

```

```

        CMP     PLOT,0           ;DON'T PLOT IF PLOT FLAG=0
        JZ      NOPLOT
;PLOT ROUTINE STARTS HERE
        MOV     TEMP,CX         ;SAVE CX FIRST
        MOV     AH,AL           ;GET HIGH BYTE JUST TAKEN
        MOV     AL,[DI-2]       ;AND LOW BYTE FROM STORAGE SO AX=DATUM
        ADD     AX,2047         ;CALCULATE Y-VALUE TO PLOT =
                                ; 199-((DATUM+2047)/21)
        CWD                                ;DIVIDE BY 21--QUOTIENT IN AX
        MOV     BX,21
        DIV     BX
        MOV     DX,AX           ;RESULT INTO DX
        NEG     DX              ;NEGATE AND ADD TO 199
        ADD     DX,199
        MOV     SI,TEMPSI       ;GET X-VALUE OF LAST POINT ON SCREEN
        INC     SI              ;GO TO NEXT LOCATION ON SCREEN
        CMP     SI,640          ;TEST IF AT RIGHT EDGE OF 640x200
        JL      M1              ; SCREEN
        MOV     SI,0            ;IF SO, GO TO LEFT EDGE TO PLOT
M1:     MOV     CX,SI           ;GET X-VALUE INTO CX
        MOV     TEMPSI,SI       ;SAVE X-VALUE
        MOV     AX,3073         ;AH=12,AL=1 TO WRITE DOT TO SCREEN
        INT     10H            ;PLOT POINT
        MOV     CX,TEMP         ;RESTORE CX
NOPL0T: LOOP    DONE           ;DECREMENT CX AND LOOP IF >0
;BRANCH TO HERE UPON FINISH OR OVERRUN
NOGO:   MOV     DX,ADD4         ;TURN OFF A/D
        MOV     AL,0
        OUT     DX,AL
        STI                                ;RESTORE INTERRUPT SERVICE
        POP     BP              ;RESTORE BP
        RET     12              ;6 ARGUMENTS IN CALL X 2=12
ERRMESS: MOV    DI,OVRUN       ;SET OVERRUN FLAG SINCE A/D GOING
        MOV     WORD PTR [DI],CX ;TOO FAST
        JMP     NOGO
TIMER   ENDP
RTNLEN  EQU     $-TEMP         ;LENGTH OF ROUTINE FOR HEADER
CSEG    ENDS
        END     HEADER         ;NEEDED FOR A .BIN FILE CONVERSION

```

This subroutine was taken from [G3].

Appendix XXIII. Data Acquisition Program for Tensile Tests of Wet, Type-C Nylon Flocs.

a) Main program written in BASIC.

```
10 REM $LINESIZE: 132 $PAGESIZE: 55
20 WIDTH 80:CLS
30 PRINT "DATA COLLECTION PROGRAM FOR WET TENSILE STRENGTH"
40 PRINT "      OF NYLON FIBRE AGGREGATES."
50 PRINT
60 PRINT "HARDWARE: Thwing-Albert tensile tester,"
70 PRINT "      IBM personal computer,"
80 PRINT "      20 Newtons load cell,"
90 PRINT "      B-2-F Bofors Electronic amplifier,"
100 PRINT "      (10V excitation, 0-15mV sensitivity range)"
110 PRINT "      Tecmar Lab Master A/D & D/A converter,"
120 PRINT "      (0 channel single-ended, gain=10 -1.V to +1.V)"
130 PRINT
140 DEFINT I,J,K
150 DIM A%(4000),B(4000),SG%(9),L$(3)
160 INPUT "Enter your name.      ",NAM$
170 INPUT "Enter the sample identification (type of nylon).      ",S$
180 INPUT "Enter the number of data points to collect.      (<=4000) ",N%
190 INPUT "Enter the number of data points/second desired.(<=30000) ",S
200 INPUT "Enter cross-head speed in centimeters/minute.      ",CHS
210 C%=0 'A/D channel number
220 S%=S: IF S<1 THEN S%=-1/S 'Convert to proper format for timer routine
230 P%=1:IF S%>2000 THEN P%=0 'Plot if < 2000 pts/sec
240 REM ***** LOAD CALIBRATION PROCEDURE
250 CLS
260 PRINT "Prepare tester for load calibration."
270 PRINT "Set zero load on the load cell and press any key."
280 I$=INKEY$:IF I$="" THEN 280
290 NUM=N%/10: MUL%=INT(NUM/15+1): NN%=MUL%*15
300 F%=0 'Initialize overrun flag
310 CALL TIMER(A%(1),F%,P%,NN%,C%,S%)
320 IF F%<>0 THEN PRINT "Warning--data taken too fast!":NN%=NN%-F%
330 SUMO=0
340 FOR I=1 TO NN% STEP 15
350 SUM1=0
360 K=I: KK=I+14
370 FOR J=K TO KK
380 IF A%(J)>32767 THEN A%(J)=A%(J)-65535!
390 SUM1=SUM1+A%(J)
400 NEXT J
410 SUM1=SUM1/15
420 SUMO=SUMO+SUM1
430 NEXT I
440 SUMO=SUMO/MUL%
```

```

450 PRINT "SUMO=",SUMO
460 PRINT "MUL%=",MUL%
470 PRINT "Hang calibration load on the load cell and"
480 INPUT "enter this load in grams.      ",FSL%
490 F%=0      'Initialize overrun flag
500 CALL TIMER(A%(1),F%,P%,NN%,C%,S%)
510 IF F%<>0 THEN PRINT "Warning--data taken too fast!":NN%=NN%-F%
520 SUM2=0
530 FOR I=1 TO NN% STEP 15
540 SUM1=0
550 K=I: KK=I+14
560 FOR J=K TO KK
570 IF A%(J)>32767 THEN A%(J)=A%(J)-65535!
580 SUM1=SUM1+A%(J)
590 NEXT J
600 SUM1=SUM1/15
610 SUM2=SUM2+SUM1
620 NEXT I
630 SUM2=SUM2/MUL%
640 PRINT "SUM2=",SUM2
650 PRINT "MUL%=",MUL%
660 CAL=(FSL%/(SUM2-SUMO))*100      'centigrams/one digit
670 PRINT "CAL=",CAL
680 INPUT "Do you wish to repeat calibration? ",Y$
690 IF Y$="y" OR Y$="Y" GOTO 240
700 PRINT "Run the cross-head and start data acquisition as the upper comb clears the lower comb."
710 PRINT "Press any key to start the dead run data collection."
720 I$=INKEY$:IF I$="" THEN 720
730 F%=0      'Initialize overrun flag
740 CALL TIMER(A%(1),F%,P%,NN%,C%,S%)
750 IF F%<>0 THEN PRINT "Warning--data taken too fast!":NN%=NN%-F%
760 SUM3=0
770 FOR I=1 TO NN% STEP 15
780 SUM1=0
790 K=I: KK=I+14
800 FOR J=K TO KK
810 IF A%(J)>32767 THEN A%(J)=A%(J)-65535!
820 SUM1=SUM1+A%(J)
830 NEXT J
840 SUM1=SUM1/15
850 SUM3=SUM3+SUM1
860 NEXT I
870 SUM3=SUM3/MUL%
880 SU%=INT((SUM3+2048)*CAL)
890 INPUT "Do you wish to repeat the last run?      ",Y$
900 IF Y$="y" OR Y$="Y" GOTO 700
910 REM ***** DATA COLLECTION
920 CLS
930 PRINT "Prepare sample for testing."
940 INPUT "Enter aggregate description.      ",L$(1)

```

```

950 PRINT "Press any key to start data collection."
960 I$=INKEY$:IF I$="" THEN 960
970 F%=0 'Initialize overrun flag
980 CALL TIMER(A%(1),F%,P%,N%,C%,S%)
990 IF F%<>0 THEN PRINT "Warning--data taken too fast!":N%=N%-F%
1000 FOR I=1 TO N%
1010 IF A%(I)>32767 THEN A%(I)=A%(I)-65535!
1020 A%(I)=INT((A%(I)+2048)*CAL) 'optimum resolution data storage, centigrams at A/D sensitivity range -1.0V to +1.0V
1030 NEXT I
1040 INPUT "Enter comments about finished test. ",L$(2)
1050 CLS: PRINT "Enter a 1 if you wish to recalibrate the load."
1060 PRINT "Enter a 2 to plot data on the screen."
1070 PRINT "Enter a 3 to store data in a file."
1080 PRINT "Enter a 4 to smooth the data."
1090 PRINT "Enter a 5 to do next test."
1100 PRINT "Enter a 6 to exit."
1110 INPUT Y
1120 ON Y GOSUB 240,1160,1330,1500,910,1580
1130 GOTO 1050
1140 '*****SUBROUTINES*****
1150 REM Screen plotting routine.
1160 SCREEN 2: KEY OFF
1170 DEF FNSCALE(Z%)=180!-180!*(Z%-YMIN%)/(YMAX%-YMIN%)
1180 CLS:YMAX%=A%(1): YMIN%=A%(1)
1190 FOR I=1 TO N%
1200 IF A%(I)<YMIN% THEN YMIN%=A%(I) ELSE IF A%(I)>YMAX% THEN YMAX%=A%(I)
1210 NEXT I
1220 PRINT "YMIN=";YMIN%,"YMAX=";YMAX%,"ZERO=";SU%
1230 YPLOT=FNSCALE(A%(1))+10
1240 PSET (60,YPLOT),0
1250 FOR I=2 TO N%: XPLOT=60!+579!*(I-1)/(N%-1): YPLOT=FNSCALE(A%(I))+10: LINE -(XPLOT,YPLOT): NEXT I
1260 LOCATE 25,20:PRINT "Sample-";L$(1),S%;"p/s",CHS;"cm/min";: PSET (60,0): LINE (60,10)-(639,190),,B 'Label and box plot
1270 YPLOT=FNSCALE(SU%)+10
1280 PSET(60,YPLOT),0: LINE -(639,YPLOT)
1290 LOCATE 25,8: PRINT "1";: LOCATE 25,75: PRINT N%;: LOCATE 2,1: PRINT YMAX%;:LOCATE 12,1: PRINT "cg";:LOCATE 24,1: PRINT Y
1300 Y$=INKEY$: IF Y$="" THEN 1300
1310 RETURN
1320 REM Subroutine to store data in file
1330 INPUT "Enter the name of the file in which data will be stored. ",FILN$
1340 D$=DATE$: T$=TIME$
1350 OPEN FILN$ FOR OUTPUT AS #2
1360 PRINT #2,"NAME:";NAM$,"DATE:";D$,"TIME:";T$
1370 PRINT #2, S$ 'Save sample description
1380 PRINT #2,"NUMBER OF DATA POINTS:";N%,"SAMPLING RATE:";S%;"PTS/SEC"
1390 PRINT #2,"CROSS-HEAD SPEED=";CHS;"cm/min","ZERO LOAD=";SU%,"CALIBRATION LOAD=";FSL%;"g"
1400 FOR I=1 TO 2: PRINT #2,L$(I): NEXT I
1410 FOR I=1 TO N%: WRITE #2,A%(I): NEXT I
1420 CLOSE #2: RETURN
1430 REM Subroutine to compute second-order 9-point Savitzki-Golay smooth
1440 REM including smoths at both beginning and and of data

```

```

1450 REM It computes a "smoothed" value for each point by adding together
1460 REM     the 4 points on either side of it, plus itself, each multiplied
1470 REM     by the corresponding coefficient.
1480 REM It then computes the "smoothed value for each successive point
1490 REM     using the original data array.
1500 DATA -21,14,39,54,59,54,39,14,-21: 'Savitzki-Golay coefficients
1510 RESTORE
1520 FOR I=1 TO 9: READ SG%(I): NEXT I
1530 FOR I=1 TO N%: B(I)=0: DF%=0: FOR J=-4 TO +4: IF I+J<1 OR I+J>N% THEN 1550
1540 ZZ=A%(I+J): B(I)=B(I)+ZZ*SG%(J+5): DF%=DF%+SG%(J+5)
1550 NEXT J: B(I)=B(I)/DF%: NEXT I 'Divide by sum of the coefficients used
1560 FOR I=1 TO N%: A%(I)=B(I): NEXT I 'Store back in the original array
1570 RETURN
1580 END

```

b) The assembler subroutine TIMER called from main program has already been listed in Appendix XXII.

Appendix XXIV. Data Collection Program for Determination of Break Area.

```
10 REM BASICA/D, LOAD AREA2, RUN or BASICA AREA2/D - Run commands
20 REM THIS PROGRAM CALCULATES AN AREA OF A REGULAR CLOSED SHAPE
30 REM BY POLYGONAL APPROXIMATION.
40 CLS:KEY OFF:CLOSE 'Clear screen, soft keys off, close all files or devices
50 DEFDBL 0-Z 'Double-precision variables
60 DEFINT I-N 'Integer variables
70 OPTION BASE 1 'The lowest value any array subscript has is one
80 DIM XX(100),YY(100) 'Coordinates of points along contour
90 LOCATE 4,1,1,0,7 'Screen location, block cursor on
100 INPUT "INPUT EXPERIMENT DESCRIPTION. ",F$
110 OPEN "COM1:9600" AS #1 'Open communication port with SUMMAGRAPHICS MICROGRID tablet, OPEN statement is short
because of the intentional DIP switches setting on the tablet to fit BASICA's defaults
120 PRINT #1,CHR$(27)"Z" 'Tablet reset
130 PRINT #1,CHR$(27)"M1",CHR$(27)"R3" 'Point mode, 10 coordinates/second
140 PRINT #1,CHR$(27)"FO" 'Origin in the lower left corner
150 PRINT #1,CHR$(27)"C3" 'Resolution - metric-high, 40 points/m
160 LOCATE 6,1
170 INPUT "INPUT THE SIZE OF THE CALIBRATION SCALE IN MILIMETERS : ",C
180 LOCATE 25,1
190 INPUT "DO YOU WANT TO CHANGE THIS VALUE, [Y] OR [N] ":A$
200 A=ASC(A$):IF A=89 OR A=121 GOTO 160:A$=""
210 CLS :LOCATE 8,1
220 PRINT "INPUT END COORDINATES OF THE CALIBRATION SCALE."
230 PRINT "PRESS ANY BUTTON ON THE CURSOR FOR EACH COORDINATE."
240 INPUT #1,XX(1),YY(1),FF,N
250 PRINT XX(1),YY(1),FF,N
260 PRINT #1,CHR$(27)"L11" 'Yellow LED on the cursor is on
270 INPUT #1,XX(2),YY(2),FF,N
280 PRINT XX(2),YY(2),FF,N
290 PRINT #1,CHR$(27)"L10" 'Yellow LED is off
300 LOCATE 25,1
310 INPUT "DO YOU WANT TO REPEAT THE CALIBRATION PROCEDURE, [Y] OR [N] ":A$
320 A=ASC(A$):IF A=89 OR A=121 GOTO 210:A$=""
330 LOCATE 25,1
340 PRINT " "
350 SS=SQR((XX(1)-XX(2))**2+(YY(1)-YY(2))**2) 'Calibration distance, tablet units
360 SS=SS/C 'Calibration constant, units/mm
370 LPRINT
380 LPRINT F$
390 LPRINT "SCALE LENGTH=";C;"mm","CALIBRATION CONSTANT=";SS;"units/mm"
400 LOCATE 11,1
410 PRINT "SCALE LENGTH=";C;"mm","CALIBRATION CONSTANT=";SS;"units/mm"
420 LPRINT
430 INPUT "FLOC NUMBER: ",FLOC$
440 LPRINT "FLOC NUMBER: ";FLOC$
450 CLS :LOCATE 14,1
460 PRINT "INPUT COORDINATES OF A POINT APPROXIMATELY AT THE CENTRE OF THE AREA"
```

```

470 PRINT #1,CHR$(27)"F1"           'Set the origin with the cursor
480 INPUT #1,XX(3),YY(3),FF,N
490 PRINT #1,CHR$(27)"L11"         'Yellow LED on
500 PRINT XX(3),YY(3),FF,N
510 PRINT CHR$(10)
520 PRINT "INPUT COORDINATES OF POINTS ALONG THE CONTOUR."
530 PRINT "PLACE POINTS AT THE IMAGINARY CORNERS OF A POLYGON"
540 PRINT "WHICH CLOSELY APPROXIMATES THE CONTOUR."
550 SANGLE=0#: SAREA=0#: PI=3.141592654##2: IFLAG=0
560 SBETA=0#
570 I=4
580 INPUT #1,XX(I),YY(I),FF,N      'First point
590 PRINT #1,CHR$(27)"L10"         'Yellow LED off
600 I=I+1
610 INPUT #1,XX(I),YY(I),FF,N
620 J=I-1
630 SA=SQR((XX(J))**2+(YY(J))**2)   'Distance from the origin to point A
640 SB=SQR((XX(I))**2+(YY(I))**2)   'Distance from the origin to point B
650 IF SA>SB GOTO 820
660 S=YY(I)/XX(I): S=SGN(S)*S       'Slope of OB, always positive
670 X1=SQR(SA**2/(1+S**2))          'Point on OB and OA distant from
680 Y1=X1*S                          'the origin 0
690 IF SGN(XX(I))=-1 THEN X1=-X1
700 IF SGN(YY(I))=-1 THEN Y1=-Y1
710 SD=SQR((XX(J)-X1)**2+(YY(J)-Y1)**2)/2 'Distance from A to C
720 X2=(X1+XX(J))/2
730 Y2=(Y1+YY(J))/2
740 SE=SQR(X2**2+Y2**2)              'Distance from origin 0 to C
750 SBETA=ATN(SD/SE)*2               'Angle between OA and OB
760 SH=SIN(SBETA)*SA                 'Distance between A and D
770 SANGLE=SANGLE+SBETA              'Sum of angles
780 IF IFLAG=1 GOTO 980
790 IF SANGLE>PI THEN XX(I)=XX(4): YY(I)=YY(4): IFLAG=1: GOTO 620
800 SAREA=SAREA+SB*SH/2
810 GOTO 600
820 S=YY(J)/XX(J): S=SGN(S)*S       'Slope of OB, always positive
830 X1=SQR(SB**2/(1+S**2))          'Point on OA and OB distant from
840 Y1=X1*S                          'the origin
850 IF SGN(XX(J))=-1 THEN X1=-X1
860 IF SGN(YY(J))=-1 THEN Y1=-Y1
870 SD=SQR((XX(I)-X1)**2+(YY(I)-Y1)**2)/2 'Distance between B and C
880 X2=(X1+XX(I))/2
890 Y2=(Y1+YY(I))/2
900 SE=SQR(X2**2+Y2**2)              'Distance from the origin 0 to C
910 SBETA=ATN(SD/SE)*2               'Angle between OA and OB
920 SH=SIN(SBETA)*SB                 'Sum of angles
930 SANGLE=SANGLE+SBETA
940 IF IFLAG=1 GOTO 1000
950 IF SANGLE>PI THEN XX(I)=XX(4): YY(I)=YY(4): IFLAG=1: GOTO 620
960 SAREA=SAREA+SA*SH/2

```

```

970 GOTO 600
980 K=I-3: SAREA=SAREA+SB*SH/2
990 GOTO 1010
1000 K=I-3: SAREA=SAREA+SA*SH/2
1010 PRINT #1,CHR$(27)"A"          'Beeper
1020 LPRINT "THERE WAS ";K;" POINTS ON THE CONTOUR."
1030 PRINT CHR$(10)
1040 SAREA=SAREA/SS/SS           'Area in mm**2
1050 AREA=CSNG(SAREA)           'Convert to single-precision
1060 PRINT "AREA IS ";AREA;" mm**2"
1070 LPRINT "AREA IS ";AREA;" mm**2"
1080 LPRINT
1090 PRINT "DO YOU WANT TO CONTINUE WITH THE NEXT AREA?"
1100 PRINT "IF NOT, PRESS F ON THE CURSOR."
1110 PRINT "IF YES, PRESS ANY OTHER BUTTON."
1120 INPUT #1,X,Y,F,N
1130 IF F=16 THEN CLOSE #1 ELSE GOTO 430
1140 LOCATE 24,1,O:KEY ON        'Cursor off, soft keys on
1150 END

```

Appendix XXV. FORTRAN Program Processing Conductivity Data. Data Listing.

C This program fits straight line to conductivity data  
C and makes a plot of conductivity versus KCl solution  
C concentration.

C Input is taken from (4).

C Output is directed to (7).

```
IMPLICIT REAL*8(A - H, O - Z), INTEGER(I - N)
INTEGER FLAG, LIST(1)
```

```
DIMENSION A(100), B(100), C(100), YF(100), YD(100), WT(100)
DIMENSION S(3), SIGMA(3), XX(2), YY(2), P(2)
```

```
REAL*4 X1, Y1
```

```
LOGICAL LK
```

```
DATA LIST /'*' /
```

```
LK = .TRUE.
```

```
CALL AXCTRL('SYMS', .2)
```

```
CALL AXCTRL('LABE', 1)
```

```
CALL AXCTRL('LOGS', 1)
```

```
CALL AXCTRL('XORI', 2.0)
```

```
CALL AXCTRL('YORI', 2.0)
```

```
CALL AXPLLOT('CONCENTRATION;', ., 0.0, 10., -2., 0.0)
```

```
CALL AXPLLOT('CONDUCTIVITY;', ., 90.0, 10., 0.0, 2.0)
```

```
CALL PLOT(2.0, 12.0, 3)
```

```
CALL PLOT(12.0, 12.0, 2)
```

```
CALL PLOT(12.0, 2.0, 2)
```

```
FIND (4'7000)
```

```
I = 0
```

```
10 READ (4, LIST, END=80, ERR=100) X, Y, Z
```

```
I = I + 1
```

```
A(I) = DLOG10(1.DO/X)
```

```
B(I) = DLOG10(Y)
```

```
C(I) = Z
```

```
GO TO 10
```

```
80 WRITE (6, 90)
```

```
90 FORMAT (1X, 'END OF DATA 4 ENCOUNTERED.')
```

C

C Averages

```
SUM1 = 0.0
```

```
DO 20 K = 1, I
```

```
SUM1 = SUM1 + C(K)
```

```
20 CONTINUE
```

```
AVE1 = SUM1 / I
```

C

C Standard deviations

```
SS1 = 0.0
```

```
DO 30 K = 1, I
```

```
SS1 = SS1 + (C(K) - AVE1) ** 2
```

```

30 CONTINUE
  SIGMA1 = DSQRT(SS1/(I - 1))
  WRITE (7,40) AVE1, SIGMA1
40 FORMAT (1X, 'AVERAGE TEMP. = ', E13.6, ' STD. DEV. = ', E13.6/)
  CALL DOLSF(1, I, A, B, YF, YD, WT, O, S, SIGMA, XX, YY, SS, LK, P)
  WRITE(7,50) P
50 FORMAT(1X, 'PARAMETER ESTIMATES:', 1P2E13.6)
  WRITE(7,55) SS
55 FORMAT(1X, 'SUM OF SQUARES IS:', 1PE13.6)
  DO 60 K = 1, I
    A(K) = (A(K)+2.DO)*5 + 2.DO
    B(K) = B(K) * 5 + 2.DO
60 CONTINUE
  DO 70 K = 1, I
    X1 = SNGL(A(K))
    Y1 = SNGL(B(K))
    CALL SYMBOL(X1, Y1, .15, 2, 0.0, -1)
70 CONTINUE
  CALL PLOTND
  STOP
100 M = I + 6
  WRITE (6,110) M
110 FORMAT (1X, 'RECORD', I5, ' IN FILE 4 SKIPPED.')
  GO TO 10
1000 WRITE(6,1001)
1001 FORMAT(1X, 'ERROR: SINGULAR MATRIX. SOLUTION FAILED.')
  STOP
  END

```

b) Data Listing.

Readings of conductivity for calibration of Seibold conductivity cell.  
Each line contains: denominator of Normal concentration,  
conductivity (mMhos), temperature of KCl solution (deg. Celsius).

0.2000E+01	0.4300E+02	0.2130E+02
0.5000E+01	0.1800E+02	0.2190E+02
0.7000E+01	0.1340E+02	0.2210E+02
0.1000E+02	0.9600E+01	0.2240E+02
0.3000E+02	0.3400E+01	0.2260E+02
0.4000E+02	0.2600E+01	0.2270E+02
0.5000E+02	0.2030E+01	0.2290E+02
0.7000E+02	0.1500E+01	0.2300E+02
0.1000E+03	0.1080E+01	0.2300E+02
0.5000E+01	0.1820E+02	0.2280E+02
0.1000E+02	0.9580E+01	0.2300E+02
0.2500E+02	0.4040E+01	0.2340E+02
0.5000E+02	0.2040E+01	0.2370E+02

0.7500E+02	0.1400E+01	0.2390E+02
0.1000E+03	0.1080E+01	0.2400E+02
0.1250E+03	0.8570E+00	0.2400E+02
0.1000E+02	0.9800E+01	0.2270E+02
0.7000E+02	0.1600E+01	0.2220E+02
0.1000E+03	0.1150E+01	0.2220E+02
0.1000E+02	0.8200E+01	0.2350E+02
0.5000E+02	0.1920E+01	0.2370E+02
0.1000E+03	0.8800E+00	0.2450E+02
0.1000E+02	0.1239E+02	0.2300E+02
0.5000E+02	0.2659E+01	0.2300E+02
0.1000E+03	0.1359E+01	0.2300E+02

Appendix XXVI. Data from Threshold Concentration Measurements.

Data on threshold concentration from the experiments conducted in aqueous sugar solutions. Each line contains: oven-dry nylon fibre weight (grams), suspension temperature (degrees Celsius), and suspension volume (milliliters).

3 DENIER FIBRES (diameter=0.0197mm)

Fibre length=1.875mm

0.3770E+01	0.2510E+02	0.1750E+03
0.4000E+01	0.2340E+02	0.1950E+03
0.4000E+01	0.2290E+02	0.1950E+03
0.4000E+01	0.2260E+02	0.2000E+03
0.4000E+01	0.2330E+02	0.1900E+03

Mean threshold concentration=0.01979  
Standard deviation=0.0005615  
95% confidence limits=0.01979 ± 0.001787

Fibre length=2.815mm

0.1629E+01	0.2400E+02	0.1650E+03
0.2000E+01	0.2400E+02	0.2100E+03
0.2000E+01	0.2290E+02	0.2100E+03
0.2000E+01	0.2350E+02	0.2100E+03
0.2000E+01	0.2320E+02	0.2050E+03
0.2000E+01	0.2310E+02	0.2050E+03
0.2000E+01	0.2280E+02	0.1950E+03
0.2000E+01	0.2280E+02	0.1950E+03

Mean threshold concentration=0.009333  
Standard deviation=0.0002908  
95% confidence limits=0.009333 ± 0.0006878

Fibre length=3.737mm

0.1000E+01	0.2590E+02	0.1400E+03
0.2000E+01	0.2210E+02	0.3300E+03
0.2000E+01	0.2240E+02	0.3650E+03
0.1000E+01	0.2370E+02	0.1650E+03
0.1000E+01	0.2480E+02	0.1650E+03
0.2000E+01	0.2200E+02	0.3200E+03
0.2000E+01	0.2230E+02	0.3350E+03
0.2000E+01	0.2210E+02	0.3250E+03
0.2000E+01	0.2330E+02	0.3350E+03
0.2000E+01	0.2220E+02	0.3500E+03

Mean threshold concentration=0.005791  
Standard deviation=0.0004116  
95% confidence limits=0.005791 ± 0.0009310

6 DENIER FIBRES (diameter=0.0279mm)

Fibre length=1.832mm

0.8000E+01	0.2570E+02	0.2300E+03
0.8000E+01	0.2470E+02	0.2300E+03
0.8000E+01	0.2420E+02	0.2450E+03
0.8000E+01	0.2350E+02	0.2200E+03
0.8000E+01	0.2450E+02	0.2350E+03
0.8000E+01	0.2380E+02	0.2200E+03

Mean threshold concentration=0.03314  
Standard deviation=0.001350  
95% confidence limits=0.03314 ± 0.003471

Fibre length=2.757mm

0.4000E+01	0.2230E+02	0.2250E+03
0.4000E+01	0.2230E+02	0.2100E+03
0.4000E+01	0.2210E+02	0.2500E+03
0.4000E+01	0.2200E+02	0.2450E+03
0.4000E+01	0.2190E+02	0.2200E+03
0.4000E+01	0.2150E+02	0.2500E+03
0.4000E+01	0.2120E+02	0.2300E+03

Mean threshold concentration=0.01641  
Standard deviation=0.001124  
95% confidence limits=0.01641 ± 0.002751

Fibre length=3.718mm

0.1000E+01	0.2300E+02	0.9000E+02
0.2000E+01	0.2000E+02	0.2350E+03
0.2000E+01	0.2070E+02	0.2200E+03
0.2000E+01	0.2100E+02	0.2250E+03
0.2000E+01	0.2100E+02	0.2200E+03
0.2000E+01	0.2070E+02	0.2100E+03
0.2000E+01	0.2070E+02	0.2250E+03
0.2000E+01	0.2060E+02	0.2300E+03
0.2000E+01	0.2060E+02	0.2300E+03
0.2000E+01	0.2060E+02	0.2500E+03
0.2000E+01	0.2070E+02	0.2400E+03

Mean threshold concentration=0.008549  
Standard deviation=0.0007754  
95% confidence limits=0.008549 ± 0.001728

Fibre length=4.666mm

0.1000E+01	0.2370E+02	0.1750E+03
0.1000E+01	0.2170E+02	0.1950E+03
0.1000E+01	0.2250E+02	0.1800E+03
0.1000E+01	0.2180E+02	0.1850E+03
0.1000E+01	0.2180E+02	0.1900E+03
0.1000E+01	0.2200E+02	0.1850E+03
0.1000E+01	0.2210E+02	0.1950E+03
0.1000E+01	0.2170E+02	0.1950E+03
0.1000E+01	0.2170E+02	0.1850E+03
0.1000E+01	0.2180E+02	0.1800E+03
0.1000E+01	0.2180E+02	0.1900E+03

Mean threshold concentration=0.005099  
Standard deviation=0.0001875  
95% confidence limits=0.005099 ± 0.0004176

15 DENIER FIBRES (diameter=0.0442mm)

Fibre length=2.947mm

0.3200E+01	0.2350E+02	0.1400E+03
0.6400E+01	0.2400E+02	0.2800E+03
0.6400E+01	0.2390E+02	0.2750E+03
0.6400E+01	0.2360E+02	0.2850E+03
0.5000E+01	0.2360E+02	0.2050E+03
0.5000E+01	0.2340E+02	0.2150E+03
0.5000E+01	0.2320E+02	0.2100E+03
0.5000E+01	0.2530E+02	0.2100E+03

Mean threshold concentration=0.02221  
Standard deviation=0.0006022  
95% confidence limits=0.02221 ± 0.004176

Fibre length=4.976mm

0.1600E+01	0.2280E+02	0.1850E+03
0.1600E+01	0.2250E+02	0.1900E+03
0.1600E+01	0.2300E+02	0.1950E+03
0.3200E+01	0.2320E+02	0.3850E+03
0.1600E+01	0.2300E+02	0.1850E+03
0.1600E+01	0.2310E+02	0.1900E+03
0.1600E+01	0.2330E+02	0.1950E+03
0.1600E+01	0.2340E+02	0.2000E+03
0.1600E+01	0.2360E+02	0.2000E+03

Mean threshold concentration=0.007915  
Standard deviation=0.0002300  
95% confidence limits=0.007915 ± 0.005304

Fibre length=6.261mm

0.8000E+00	0.2440E+02	0.1600E+03
0.8000E+00	0.2390E+02	0.1800E+03
0.8000E+00	0.2300E+02	0.1700E+03
0.8000E+00	0.2320E+02	0.1650E+03
0.8000E+00	0.2340E+02	0.1650E+03
0.8000E+00	0.2470E+02	0.1850E+03
0.8000E+00	0.2310E+02	0.1700E+03

Mean threshold concentration=0.004469  
Standard deviation=0.0002267  
95% confidence limits=0.004469 ± 0.0005547

Data on threshold concentration from experiments conducted  
in water as a suspending medium.  
Each line contains: oven-dry nylon fibre weight (grams),  
suspension temperature (degrees Celsius),  
and suspension volume (milliliters).

15 DENIER FIBRES (diameter=0.0442mm)

Fibre length=2.947mm

0.5000E+01	0.2350E+02	0.2400E+03
0.5000E+01	0.2340E+02	0.2500E+03
0.5000E+01	0.2320E+02	0.2550E+03
0.5000E+01	0.2310E+02	0.2500E+03
0.5000E+01	0.2340E+02	0.2600E+03
0.5000E+01	0.2340E+02	0.2550E+03

Mean threshold concentration=0.01892  
Standard deviation=0.0005244  
95% confidence limits=0.01892 ± 0.0001348

Fibre length=4.973mm

0.1600E+01	0.2350E+02	0.2200E+03
0.1600E+01	0.2290E+02	0.2200E+03
0.1600E+01	0.2330E+02	0.2100E+03
0.1600E+01	0.2310E+02	0.2150E+03
0.1600E+01	0.2190E+02	0.2100E+03
0.1600E+01	0.2270E+02	0.2150E+03
0.1600E+01	0.2260E+02	0.2250E+03
0.1600E+01	0.2170E+02	0.2250E+03

Mean threshold concentration=0.007004  
Standard deviation=0.0001925  
95% confidence limits=0.007004 ± 0.0004553

Fibre length=6.261mm

0.8000E+00	0.2110E+02	0.2200E+03
0.8000E+00	0.2200E+02	0.2200E+03
0.8000E+00	0.2240E+02	0.2000E+03
0.8000E+00	0.2280E+02	0.2000E+03
0.8000E+00	0.2350E+02	0.2150E+03
0.8000E+00	0.2320E+02	0.2000E+03
0.8000E+00	0.2470E+02	0.2150E+03
0.8000E+00	0.2220E+02	0.2150E+03

Mean threshold concentration=0.003620  
Standard deviation=0.0001577  
95% confidence limits=0.003620 ± 0.0003727

Data on the effect of cylinder diameter on threshold concentration.  
Each line contains: oven-dry sample weight (grams), suspension  
volume at the onset of Type-C floc formation (mL), suspension  
temperature (degree Celsius), 8 times the rotational speed of driving  
roller (Rev/s), and cylinder incline to the horizontal (degrees).

15 DENIER FIBRES (diameter=0.0442mm), FIBRE LENGTH=4.973mm

Cylinder ID=56mm.

0.7000E+00	0.2420E+02	0.7600E+02	0.2860E+02	0.4500E+02
0.7000E+00	0.2440E+02	0.7200E+02	0.2860E+02	0.4500E+02
0.7000E+00	0.2420E+02	0.7000E+02	0.2860E+02	0.4500E+02
0.7000E+00	0.2400E+02	0.7500E+02	0.2860E+02	0.4500E+02
0.7000E+00	0.2420E+02	0.7500E+02	0.2860E+02	0.4500E+02
0.7000E+00	0.2420E+02	0.8000E+02	0.2860E+02	0.4500E+02

Mean threshold concentration=0.00894  
Standard deviation=0.0004105  
95% confidence limits=0.00894 ± 0.001056

Cylinder ID=69mm.

0.1400E+01	0.2340E+02	0.1400E+03	0.3400E+02	0.4500E+02
0.1400E+01	0.2350E+02	0.1440E+03	0.3400E+02	0.4500E+02
0.1400E+01	0.2400E+02	0.1420E+03	0.3400E+02	0.4500E+02
0.1400E+01	0.2320E+02	0.1400E+03	0.3400E+02	0.4500E+02
0.1400E+01	0.2340E+02	0.1470E+03	0.3400E+02	0.4500E+02
0.1400E+01	0.2360E+02	0.1470E+03	0.3400E+02	0.4500E+02

Mean threshold concentration=0.00930  
Standard deviation=0.0002073  
95% confidence limits=0.00930 ± 0.000533

Cylinder ID=82mm.

0.1600E+01	0.2280E+02	0.1850E+03	0.4000E+02	0.4500E+02
0.1600E+01	0.2250E+02	0.1900E+03	0.4000E+02	0.4500E+02
0.1600E+01	0.2300E+02	0.1950E+03	0.4000E+02	0.4500E+02
0.3200E+01	0.2320E+02	0.3850E+03	0.4000E+02	0.4500E+02
0.1600E+01	0.2300E+02	0.1850E+03	0.4000E+02	0.4500E+02
0.1600E+01	0.2310E+02	0.1900E+03	0.4000E+02	0.4500E+02
0.1600E+01	0.2330E+02	0.1950E+03	0.4000E+02	0.4500E+02
0.1600E+01	0.2340E+02	0.2000E+03	0.4000E+02	0.4500E+02
0.1600E+01	0.2360E+02	0.2000E+03	0.4000E+02	0.4500E+02
0.1600E+01	0.2450E+02	0.2000E+03	0.3970E+02	0.4500E+02

Mean threshold concentration=0.00788

Standard deviation=0.0002370

95% confidence limits=0.00788 ± 0.000536

Cylinder ID=94mm.

0.3000E+01	0.2400E+02	0.3200E+03	0.4550E+02	0.4500E+02
0.3000E+01	0.2440E+02	0.3450E+03	0.4550E+02	0.4500E+02
0.3000E+01	0.2400E+02	0.3100E+03	0.4550E+02	0.4500E+02
0.3000E+01	0.2410E+02	0.3250E+03	0.4550E+02	0.4500E+02
0.3000E+01	0.2420E+02	0.3300E+03	0.4550E+02	0.4500E+02
0.3000E+01	0.2440E+02	0.3200E+03	0.4550E+02	0.4500E+02

Mean threshold concentration=0.00879

Standard deviation=0.0003145

95% confidence limits=0.00879 ± 0.000809

Cylinder ID=121mm.

0.7000E+01	0.2380E+02	0.7500E+03	0.5770E+02	0.4500E+02
0.7000E+01	0.2380E+02	0.7550E+03	0.5770E+02	0.4500E+02
0.7000E+01	0.2390E+02	0.7350E+03	0.5770E+02	0.4500E+02
0.6400E+01	0.2510E+02	0.7000E+03	0.3970E+02	0.4500E+02

Mean threshold concentration=0.00887

Standard deviation=0.0001508

95% confidence limits=0.00887 ± 0.000480

Cylinder ID=146mm.

0.1100E+02	0.2410E+02	0.1220E+04	0.6900E+02	0.4500E+02
0.1100E+02	0.2400E+02	0.1140E+04	0.6900E+02	0.4500E+02
0.1100E+02	0.2400E+02	0.1125E+04	0.6900E+02	0.4500E+02

Mean threshold concentration=0.00902

Standard deviation=0.0003878

95% confidence limits=0.00902 ± 0.001669

Data on the effect of cylinder rotational speed on threshold concentration. Each line contains: oven-dry sample weight (grams), suspension temperature (degree Celsius), and suspension volume (mL). Cylinder ID=82mm.

15 DENIER FIBRES (diameter=0.0442mm) FIBRE LENGTH=4.973mm

Cylinder rotational speed=4.2 rad/s

0.1600E+01	0.2140E+02	0.2150E+03
0.1600E+01	0.2140E+02	0.2250E+03
0.1600E+01	0.2150E+02	0.2300E+03
0.1600E+01	0.2150E+02	0.2150E+03
0.1600E+01	0.2170E+02	0.1950E+03
0.1600E+01	0.2180E+02	0.2150E+03

Mean threshold concentration=0.00707  
Standard deviation=0.0004097  
95% confidence limits=0.00707 ± 0.001053

Cylinder rotational speed=6.8 rad/s

0.1600E+01	0.2160E+02	0.2000E+03
0.1600E+01	0.2160E+02	0.1900E+03
0.1600E+01	0.2170E+02	0.1900E+03
0.1600E+01	0.2180E+02	0.2050E+03
0.1600E+01	0.2170E+02	0.2150E+03
0.1600E+01	0.2170E+02	0.2050E+03

Mean threshold concentration=0.00759  
Standard deviation=0.0003661  
95% confidence limits=0.00759 ± 0.000941

Cylinder rotational speed=11.3 rad/s

0.1600E+01	0.2150E+02	0.1950E+03
0.1600E+01	0.2150E+02	0.2050E+03
0.1600E+01	0.2150E+02	0.2050E+03
0.1600E+01	0.2160E+02	0.1850E+03
0.1600E+01	0.2170E+02	0.1800E+03
0.1600E+01	0.2170E+02	0.2000E+03

Mean threshold concentration=0.00783  
Standard deviation=0.0004307  
95% confidence limits=0.00783 ± 0.001107

Cylinder rotational speed=16.8 rad/s

0.1600E+01	0.2130E+02	0.1850E+03
0.1600E+01	0.2130E+02	0.2050E+03
0.1600E+01	0.2150E+02	0.2100E+03
0.1600E+01	0.2160E+02	0.1850E+03
0.1600E+01	0.2170E+02	0.2050E+03
0.1600E+01	0.2170E+02	0.1850E+03

Mean threshold concentration=0.00780  
Standard deviation=0.0004764  
95% confidence limits=0.00780 ± 0.001225

Cylinder rotational speed=22.1 rad/s

0.1600E+01	0.2140E+02	0.1800E+03
0.1600E+01	0.2150E+02	0.2050E+03
0.1600E+01	0.2150E+02	0.1800E+03
0.1600E+01	0.2140E+02	0.2000E+03
0.1600E+01	0.2160E+02	0.1950E+03
0.1600E+01	0.2170E+02	0.1800E+03

Mean threshold concentration=0.00804  
Standard deviation=0.0004770  
95% confidence limits=0.00804 ± 0.001226

Data on the effect of cylinder incline on threshold concentration.  
Each line contains: oven-dry sample weight (grams),  
suspension temperature (degree Celsius), suspension volume (mL),  
8 times the rotational speed of the driving roller (Rev/s),  
and cylinder incline (degree).  
Cylinder: ID=82mm; OD=88mm.

15 DENIER FIBRES (diameter=0.0442mm), FIBRE LENGTH=4.973mm

0.16E+01	0.211E+02	0.190E+03	0.292E+02	0.0
Threshold concentration=0.00801				
0.16E+01	0.214E+02	0.205E+03	0.304E+02	0.15E+02
Threshold concentration=0.00743				
0.16E+01	0.216E+02	0.200E+03	0.304E+02	0.30E+02
threshold concentration=0.00761				

Data on the effect of viscosity of suspending liquid on threshold  
concentration. Each line contains: oven-dry sample weight (grams),  
suspension temperature (degree Celsius), suspension volume (mL),  
and 8 times the rotational speed of the driving roller (Rev/s).

15 DENIER FIBRES (diameter=0.0442mm) FIBRE LENGTH=4.973mm

Density of the suspending liquid=1.175g/cm\*\*3

0.2000E+01	0.2300E+02	0.1800E+03	0.4000E+02
0.2000E+01	0.2300E+02	0.1750E+03	0.4000E+02
0.2000E+01	0.2310E+02	0.1900E+03	0.4000E+02
0.2000E+01	0.2350E+02	0.1750E+03	0.4000E+02
0.2000E+01	0.2370E+02	0.1850E+03	0.4000E+02
0.2000E+01	0.2380E+02	0.1700E+03	0.4000E+02

Mean threshold concentration=0.0106  
Standard deviation=0.0004323  
95% confidence limits=0.0106 ± 0.001111

Density of the suspending liquid=1.22g/cm\*\*3

0.2000E+01	0.2500E+02	0.1450E+03	0.4010E+02
0.2000E+01	0.2510E+02	0.1550E+03	0.4010E+02
0.2000E+01	0.2540E+02	0.1400E+03	0.4010E+02
0.2000E+01	0.2580E+02	0.1350E+03	0.4010E+02
0.2000E+01	0.2570E+02	0.1500E+03	0.4010E+02
0.2000E+01	0.2570E+02	0.1400E+03	0.4010E+02

Mean threshold concentration=0.0132  
Standard deviation=0.0006662  
95% confidence limits=0.0132 ± 0.001713

Appendix XXVII. Data from Velocity Measurements in Horizontal Rotating Cylinder.

a) Case 1.

NAME:Robert M. Soszynski, DATE:03-01-1986, TIME:23:06:18  
1.13;1.0g in 125mL;1/s;horizontal;2-500kHz or 0.01V/kHz;200kHz  
NUMBER OF DATA POINTS: 25000, SAMPLING RATE: 2500 PTS/SEC  
Data stored in lines contains: radial coordinate - mm,  
angular coordinate - deg., average voltage for horizontal  
and vertical velocity componenets - volts.

10	0	-0.470413E+00	0.109549E+00
15	0	-0.337353E+00	0.122745E+00
20	0	-0.210124E+00	0.777233E-01
25	0	-0.778463E-01	0.671929E-01
30	0	0.724024E-01	0.388355E-01
35	0	0.155700E+00	0.162050E-01
40	0	0.319181E+00	0.390779E-02
45	0	0.481168E+00	0.951210E-02
25	10	0.159210E-01	0.329458E-01
30	10	0.607521E-01	0.613596E-02
35	10	0.203023E+00	-0.153780E-01
40	10	0.330611E+00	-0.636548E-01
45	10	0.504228E+00	-0.797557E-01
10	20	-0.483226E+00	0.750384E-01
15	20	-0.347085E+00	0.723528E-01
20	20	-0.211551E+00	0.602350E-01
25	20	-0.719233E-01	0.519083E-01
30	20	0.102826E+00	-0.382016E-01
35	20	0.200579E+00	-0.804626E-01
40	20	0.341528E+00	-0.106151E+00
45	20	0.487241E+00	-0.143197E+00
25	30	-0.923697E-01	-0.133527E-01
30	30	0.122205E+00	-0.767988E-01
35	30	0.203152E+00	-0.130044E+00
40	30	0.304335E+00	-0.193567E+00
45	30	0.448712E+00	-0.277052E+00
10	40	-0.509067E+00	0.788339E-01
15	40	-0.434588E+00	0.770602E-01
20	40	-0.253258E+00	0.477927E-01
25	40	-0.958958E-01	0.165657E-01
30	40	0.675963E-01	-0.984510E-01
35	40	0.111578E+00	-0.160057E+00
40	40	0.263140E+00	-0.234349E+00
45	40	0.381765E+00	-0.310228E+00
25	50	-0.189692E+00	-0.373345E-01
30	50	-0.645996E-01	-0.826580E-01
35	50	0.859486E-01	-0.107020E+00
40	50	0.178760E+00	-0.279601E+00

45	50	0.307620E+00	-0.385633E+00
10	60	-0.558540E+00	0.590906E-01
15	60	-0.521508E+00	0.679862E-01
20	60	-0.405841E+00	0.545692E-01
25	60	-0.278040E+00	0.183709E-01
30	60	-0.176243E+00	-0.896399E-01
35	60	-0.447635E-01	-0.182338E+00
40	60	0.124532E+00	-0.202449E+00
45	60	0.199724E+00	-0.381822E+00
25	70	-0.377341E+00	0.456746E-02
30	70	-0.250210E+00	-0.391865E-01
35	70	-0.125346E+00	-0.102065E+00
40	70	0.125453E-01	-0.234137E+00
45	70	0.132134E+00	-0.347365E+00
15	80	-0.519270E+00	0.416339E-01
20	80	-0.599522E+00	0.568729E-01
25	80	-0.530196E+00	0.561977E-01
30	80	-0.452165E+00	0.319531E-01
35	80	-0.193317E+00	-0.462316E-01
40	80	-0.138606E+00	-0.115882E+00
45	80	-0.312772E-02	-0.289138E+00
15	280	-0.754685E-01	0.518916E-02
20	280	-0.178243E+00	0.838600E-02
25	280	-0.214551E+00	0.909403E-02
30	280	-0.261155E+00	0.854780E-02
35	280	-0.265733E+00	0.481027E-02
40	280	-0.233377E+00	-0.180281E-01
45	280	-0.908498E-01	0.184510E-02
25	290	-0.365059E+00	0.218813E-01
30	290	-0.292931E+00	0.587402E-01
35	290	-0.209492E+00	0.341299E-01
40	290	-0.128477E+00	0.540412E-01
45	290	-0.159699E-01	0.974093E-01
10	300	-0.483005E+00	0.558972E-01
15	300	-0.465948E+00	0.551656E-01
20	300	-0.419729E+00	0.631033E-01
25	300	-0.350098E+00	0.649176E-01
30	300	-0.240058E+00	0.727243E-01
35	300	-0.146114E+00	0.741315E-01
40	300	-0.843289E-01	0.818717E-01
45	300	0.719724E-01	0.173261E+00
25	310	-0.264593E+00	0.101724E+00
30	310	-0.162274E+00	0.105546E+00
35	310	-0.875978E-01	0.112817E+00
40	310	-0.277126E-01	0.112306E+00
45	310	0.162287E+00	0.205543E+00
10	320	-0.499105E+00	0.763421E-01
15	320	-0.413193E+00	0.958417E-01
20	320	-0.341397E+00	0.102700E+00
25	320	-0.211437E+00	0.109140E+00

30	320	-0.134655E+00	0.920352E-01
35	320	-0.957425E-02	0.115924E+00
40	320	0.367763E-01	0.125297E+00
45	320	0.264417E+00	0.204840E+00
25	330	-0.142671E+00	0.132521E+00
30	330	-0.353827E-01	0.137587E+00
35	330	0.204828E-01	0.138561E+00
40	330	0.136476E+00	0.145843E+00
45	330	0.307774E+00	0.180249E+00
10	340	-0.478917E+00	0.783091E-01
15	340	-0.350344E+00	0.969390E-01
20	340	-0.247264E+00	0.964268E-01
25	340	-0.150155E+00	0.852638E-01
30	340	0.149045E-01	0.987043E-01
35	340	0.936582E-01	0.104633E+00
40	340	0.191197E+00	0.106151E+00
45	340	0.395405E+00	0.141370E+00
25	350	-0.119893E-01	0.665227E-01
30	350	0.505018E-01	0.688755E-01
35	350	0.105004E+00	0.427272E-01
40	350	0.258189E+00	0.646885E-01
45	350	0.436576E+00	0.805734E-01

b) Case 2.

NAME:Robert M. Soszynski, DATE:02-22-1986, TIME:23:56:09  
 1.13;1.5g in 125mL;1/s;horizontal;2-500kHz so 0.01V/kHz;100kHz  
 NUMBER OF DATA POINTS: 25000, SAMPLING RATE: 5000 PTS/SEC  
 Data stored in lines contains: radial coordinate - mm,  
 angular coordinate - deg., average voltage for horizontal  
 and vertical velocity components - volts.

10	0	-0.442774E+00	-0.644879E-01
15	0	-0.301163E+00	0.855581E-01
20	0	-0.170778E+00	0.711411E-01
25	0	-0.385428E-01	0.478650E-01
30	0	0.745004E-01	0.466815E-01
35	0	0.205431E+00	-0.978420E-02
40	0	0.340536E+00	0.979175E-02
45	0	0.494546E+00	0.145979E-01
25	10	-0.399374E-01	-0.272714E-01
30	10	0.123813E+00	-0.289418E-01
35	10	0.190380E+00	-0.460816E-01
40	10	0.358226E+00	-0.694743E-01
45	10	0.512884E+00	-0.595649E-02
10	20	-0.471556E+00	0.590236E-01
15	20	-0.353666E+00	0.515908E-01
20	20	-0.201871E+00	0.184117E-01
25	20	-0.538190E-01	0.403428E-02
30	20	0.963724E-01	-0.421060E-01

35	20	0.121188E+00	-0.567951E-01
40	20	0.319095E+00	-0.112149E+00
45	20	0.506686E+00	-0.178558E+00
25	30	-0.489481E-01	-0.728648E-02
30	30	0.426044E-01	-0.127048E+00
35	30	0.169772E+00	-0.123821E+00
40	30	0.305983E+00	-0.186748E+00
45	30	0.447693E+00	-0.239914E+00
10	40	-0.549264E+00	-0.188259E-01
15	40	-0.338904E+00	-0.150258E-01
20	40	-0.281949E+00	0.783234E-02
25	40	-0.112632E+00	-0.115184E-01
30	40	0.157285E-01	-0.359651E-01
35	40	0.134934E+00	-0.161129E+00
40	40	0.243256E+00	-0.177001E+00
45	40	0.356741E+00	-0.283984E+00
25	50	-0.176273E+00	-0.297930E-02
30	50	-0.310040E-01	-0.996057E-02
35	50	0.505428E-01	-0.679876E-02
40	50	0.168058E+00	-0.132484E-02
45	50	0.325002E+00	-0.334200E+00
10	60	-0.545801E+00	0.130413E-01
15	60	-0.529872E+00	-0.965350E-02
20	60	-0.407095E+00	-0.151016E-01
25	60	-0.257788E+00	-0.142141E-01
30	60	-0.120387E+00	-0.200474E-01
35	60	-0.406489E-01	-0.175827E-01
40	60	0.674721E-01	-0.314138E-01
45	60	0.166266E+00	-0.290666E+00
25	70	-0.348824E+00	-0.184389E-01
30	70	-0.229980E+00	-0.186676E-01
35	70	-0.132801E+00	-0.182364E-01
40	70	0.174301E-01	-0.190713E-01
45	70	0.133407E+00	-0.161213E+00
20	80	-0.514141E+00	0.247231E-01
25	80	-0.491947E+00	0.320376E-01
30	80	-0.369574E+00	-0.168680E-01
35	80	-0.246478E+00	-0.337394E-01
40	80	-0.126153E+00	-0.192849E-01
45	80	-0.339320E-01	0.556065E-01
25	280	-0.225822E+00	0.773563E-02
30	280	-0.221313E+00	0.280551E-01
35	280	-0.212055E+00	0.439743E-01
40	280	-0.173442E+00	0.333430E-01
45	280	-0.650751E-01	-0.678460E-01
25	290	-0.334859E+00	-0.180164E-01
30	290	-0.228486E+00	-0.156173E-01
35	290	-0.209697E+00	-0.155452E-01
40	290	-0.100017E+00	0.332284E-01
45	290	-0.304766E-01	0.414700E-01

10	300	-0.380916E+00	0.352298E-02
15	300	-0.427326E+00	-0.149615E-01
20	300	-0.337120E+00	-0.159127E-01
25	300	-0.271237E+00	-0.129686E-01
30	300	-0.168917E+00	-0.149692E-01
35	300	-0.115265E+00	-0.157204E-01
40	300	-0.387061E-01	-0.131860E-01
45	300	0.318077E-01	0.183620E+00
25	310	-0.201334E+00	0.246496E-02
30	310	-0.126501E+00	0.868433E-02
35	310	-0.660401E-01	0.100183E-01
40	310	-0.740724E-02	0.764792E-02
45	310	0.107230E+00	0.224222E+00
10	320	-0.434412E+00	-0.169510E-01
15	320	-0.367634E+00	-0.225577E-01
20	320	-0.291579E+00	-0.218048E-01
25	320	-0.160952E+00	0.453296E-01
30	320	-0.893036E-01	0.553187E-01
35	320	0.388267E-02	0.181333E-01
40	320	0.107316E+00	0.255200E-01
45	320	0.238240E+00	0.231569E+00
25	330	-0.166888E+00	0.994360E-01
30	330	-0.492859E-01	0.106515E+00
35	330	0.673500E-01	0.597215E-01
40	330	0.142566E+00	0.826791E-01
45	330	0.300848E+00	0.173862E+00
10	340	-0.420787E+00	0.642369E-01
15	340	-0.347557E+00	0.568977E-01
20	340	-0.228392E+00	0.658665E-01
25	340	-0.104167E+00	0.816137E-01
30	340	-0.733647E-02	0.704390E-01
35	340	0.870856E-01	0.879960E-01
40	340	0.276608E+00	0.843433E-01
45	340	0.389298E+00	0.132052E+00
25	350	-0.761341E-01	0.776763E-01
30	350	0.324011E-01	0.272753E-01
35	350	0.145408E+00	0.315864E-01
40	350	0.285605E+00	0.458640E-01
45	350	0.431695E+00	0.206854E-01

c) Case 3.

NAME:Robert M. Soszynski, DATE:02-23-1986, TIME:23:53:58  
 1.456;1.5g in 125mL;1/s;horizontal;2-500kHz or 0.01V/kHz;200kHz  
 NUMBER OF DATA POINTS: 25000, SAMPLING RATE: 5000 PTS/SEC  
 Data stored in lines contains: radial coordinate - mm,  
 angular coordinate - deg., average voltage for horizontal  
 and vertical velocity components - volts.

10	0	-0.451620E+00	0.340755E-01
----	---	---------------	--------------

15	0	-0.427205E+00	0.949689E-01
20	0	-0.231965E+00	0.103178E+00
25	0	-0.228998E+00	0.390461E-01
30	0	-0.134877E+00	0.326238E-01
35	0	-0.829622E-01	0.266744E-01
40	0	0.375195E+00	0.679225E-02
45	0	0.757407E+00	0.775583E-02
25	10	-0.308750E+00	0.101089E+00
30	10	-0.963623E-01	0.518279E-01
35	10	-0.252236E-01	0.110394E-01
40	10	0.359502E+00	-0.391579E-01
45	10	0.747069E+00	-0.103160E-01
10	20	-0.470029E+00	0.313528E-01
15	20	-0.463933E+00	0.120045E+00
20	20	-0.423305E+00	0.122707E+00
25	20	-0.239854E+00	0.141191E+00
30	20	-0.674376E-01	0.111084E+00
35	20	0.321433E-01	-0.655071E-01
40	20	0.381206E+00	-0.127390E+00
45	20	0.686768E+00	-0.257072E+00
25	30	-0.281035E+00	0.945972E-01
30	30	-0.729544E-01	0.370044E-02
35	30	0.857815E-01	-0.118028E+00
40	30	0.338983E+00	-0.220844E+00
45	30	0.628721E+00	-0.341985E+00
10	40	-0.480043E+00	0.743423E-01
15	40	-0.541361E+00	0.899879E-01
20	40	-0.466018E+00	0.672025E-01
25	40	-0.266710E+00	0.594738E-01
30	40	-0.166596E+00	-0.777107E-02
35	40	0.286565E-01	-0.170713E+00
40	40	0.253929E+00	-0.251828E+00
45	40	0.468575E+00	-0.471401E+00
25	50	-0.385922E+00	0.145777E+00
30	50	-0.227183E+00	0.365051E-01
35	50	-0.518643E-01	-0.209074E+00
40	50	0.195145E+00	-0.318236E+00
45	50	0.367002E+00	-0.545870E+00
10	60	-0.527398E+00	0.100375E+00
15	60	-0.532380E+00	0.987549E-01
20	60	-0.518619E+00	0.167420E+00
25	60	-0.424276E+00	0.141389E+00
30	60	-0.295802E+00	0.692990E-01
35	60	-0.488953E-01	-0.111826E+00
40	60	0.145312E+00	-0.348889E+00
45	60	0.248862E+00	-0.565223E+00
25	70	-0.497891E+00	0.146312E+00
30	70	-0.467352E+00	0.921491E-01
35	70	-0.274856E+00	-0.541076E-01
40	70	-0.114857E+00	-0.962816E-01

45	70	0.153395E+00	-0.522856E+00
15	80	-0.371542E+00	0.566213E-01
20	80	-0.495122E+00	0.161321E+00
25	80	-0.488336E+00	0.132021E+00
30	80	-0.441202E+00	0.146161E+00
35	80	-0.358351E+00	0.574343E-02
40	80	-0.190333E+00	-0.233883E-01
45	80	-0.259287E-01	-0.467071E+00
25	90	-0.155485E+00	0.120882E-02
30	90	-0.155598E+00	-0.223294E-01
35	90	-0.144176E+00	0.198558E+00
40	90	-0.143074E+00	-0.108312E+00
45	90	-0.572086E-01	-0.136273E+00
35	100	-0.283926E-01	0.535953E-01
40	100	0.196207E-01	0.593532E-01
45	100	-0.454408E-01	-0.434826E-01
30	290	-0.303205E+00	0.236720E-01
35	290	-0.325674E+00	0.315893E-01
40	290	-0.218251E+00	0.368653E-01
45	290	-0.346835E-01	0.176446E+00
15	300	-0.392113E+00	0.562289E-01
20	300	-0.369683E+00	0.397054E-01
25	300	-0.362807E+00	0.384319E-01
30	300	-0.328171E+00	0.379053E-01
35	300	-0.230924E+00	0.410070E-01
40	300	-0.139634E+00	0.654199E-01
45	300	0.146173E+00	0.356612E+00
25	310	-0.347860E+00	0.953447E-02
30	310	-0.304884E+00	0.963233E-02
35	310	-0.130561E+00	0.272321E-01
40	310	-0.325129E-01	0.153647E+00
45	310	0.311833E+00	0.373477E+00
10	320	-0.499907E+00	0.321594E-02
15	320	-0.477663E+00	0.597591E-02
20	320	-0.356092E+00	-0.426134E-03
25	320	-0.336270E+00	0.455189E-02
30	320	-0.240083E+00	0.753978E-02
35	320	-0.144991E+00	0.204481E-01
40	320	0.226530E-01	0.207729E-01
45	320	0.351344E+00	0.173123E+00
25	330	-0.279009E+00	0.486331E-01
30	330	-0.203130E+00	0.768448E-01
35	330	-0.142827E+00	0.105955E+00
40	330	0.164156E+00	0.141337E+00
45	330	0.531916E+00	0.326905E+00
10	340	-0.454856E+00	0.257170E-01
15	340	-0.387750E+00	0.459753E-01
20	340	-0.365481E+00	0.426211E-01
25	340	-0.278020E+00	0.659819E-01
30	340	-0.195137E+00	0.589397E-01

35	340	-0.595153E-01	0.691274E-01
40	340	0.243954E+00	0.868744E-01
45	340	0.620262E+00	0.251225E+00
25	350	-0.283647E+00	0.998829E-01
30	350	-0.434487E-01	0.890982E-01
35	350	-0.813715E-02	0.914336E-01
40	350	0.309369E+00	0.106373E+00
45	350	0.718170E+00	0.751158E-01

Appendix XXVIII. Raw Data from Tensile Strength Measurements.

This appendix contains the wet-tensile-test results. The data are grouped in packets corresponding to one type of nylon fibres. Each line of data contains from left to right: breaking load (centigrams), "zero"-load (centigrams), oven-dry floc weight (grams), wet floc weight (grams), and break area (millimeters squared).

Fibre length=3.737mm, fibre diameter=0.0197mm.

1306	674	0.510000E-02	0.129700E+00	0.198000E+02
1289	674	0.560000E-02	0.127800E+00	0.226000E+02
1194	674	0.780000E-02	0.168600E+00	0.294000E+02
910	674	0.300000E-02	0.634000E-01	0.133000E+02
1206	674	0.510000E-02	0.106200E+00	0.165000E+02
1602	674	0.610000E-02	0.117300E+00	0.183000E+02
1273	674	0.500000E-02	0.102000E+00	0.126000E+02
1775	674	0.600000E-02	0.111200E+00	0.150000E+02
1451	674	0.440000E-02	0.783000E-01	0.130000E+02
1440	674	0.520000E-02	0.899000E-01	0.124000E+02
1295	674	0.390000E-02	0.819000E-01	0.150000E+02
1384	674	0.430000E-02	0.113600E+00	0.148000E+02
3601	674	0.750000E-02	0.126500E+00	0.198000E+02
1468	674	0.490000E-02	0.104200E+00	0.170000E+02
1870	674	0.550000E-02	0.123600E+00	0.179000E+02
1507	674	0.900000E-02	0.140800E+00	0.113000E+02
1485	674	0.560000E-02	0.108200E+00	0.154000E+02

Fibre length=2.757mm, fibre diameter=0.0279mm.

1236	882	0.600000E-02	0.753000E-01	0.146000E+02
1319	779	0.124000E-01	0.173600E+00	0.265000E+02
1308	744	0.940000E-02	0.166000E+00	0.176000E+02
1135	740	0.980000E-02	0.132200E+00	0.176000E+02
2355	890	0.236000E-01	0.233900E+00	0.322000E+02
1687	841	0.123000E-01	0.178100E+00	0.281000E+02
3446	773	0.156000E-01	0.201100E+00	0.286000E+02
1364	761	0.780000E-02	0.113800E+00	0.221000E+02
4153	723	0.224000E-01	0.210600E+00	0.342000E+02
3407	766	0.209000E-01	0.260600E+00	0.392000E+02
2321	741	0.196000E-01	0.221100E+00	0.277000E+02
3986	712	0.282000E-01	0.301100E+00	0.420000E+02
4883	719	0.225000E-01	0.211200E+00	0.331000E+02
5267	722	0.221000E-01	0.207100E+00	0.310000E+02
5312	703	0.221000E-01	0.200800E+00	0.310000E+02
4098	703	0.139000E-01	0.140100E+00	0.253000E+02

5779	709	0.205000E-01	0.208200E+00	0.359000E+02
3758	691	0.192000E-01	0.210800E+00	0.345000E+02
3931	812	0.129000E-01	0.152700E+00	0.293000E+02

Fibre length=3.718mm, fibre diameter=0.0279mm.

1799	749	0.126000E-01	0.259200E+00	0.277000E+02
2861	700	0.184000E-01	0.275300E+00	0.292000E+02
1335	778	0.144000E-01	0.253300E+00	0.282000E+02
1821	778	0.119000E-01	0.178600E+00	0.174000E+02
3078	745	0.146000E-01	0.226500E+00	0.325000E+02
2486	718	0.134000E-01	0.192100E+00	0.239000E+02
2777	722	0.151000E-01	0.225100E+00	0.199000E+02
2637	708	0.169000E-01	0.256200E+00	0.339000E+02
2475	720	0.158000E-01	0.194900E+00	0.269000E+02
3112	707	0.212000E-01	0.304400E+00	0.333000E+02
5738	713	0.210000E-01	0.229000E+00	0.316000E+02
4654	709	0.154000E-01	0.227500E+00	0.345000E+02
3710	720	0.141000E-01	0.171600E+00	0.275000E+02

Fibre length=4.666mm, fibre diameter=0.0279mm.

1150	866	0.540000E-02	0.120900E+00	0.154000E+02
1166	778	0.690000E-02	0.146800E+00	0.218000E+02
1769	749	0.218000E-01	0.449300E+00	0.315000E+02
2557	775	0.190000E-01	0.298700E+00	0.302000E+02
2026	773	0.203000E-01	0.311400E+00	0.256000E+02
2808	773	0.137000E-01	0.201300E+00	0.231000E+02
1803	775	0.930000E-02	0.146400E+00	0.247000E+02
3617	790	0.146000E-01	0.221100E+00	0.399000E+02
4310	777	0.326000E-01	0.421600E+00	0.312000E+02
3227	758	0.155000E-01	0.251300E+00	0.368000E+02

Fibre length=2.947mm, fibre diameter=0.0442mm.

1179	688	0.129000E-01	0.282100E+00	0.236000E+02
1713	688	0.248000E-01	0.395200E+00	0.457000E+02
2269	688	0.175000E-01	0.234400E+00	0.379000E+02
3109	688	0.122000E-01	0.171000E+00	0.239000E+02
2530	688	0.112000E-01	0.187800E+00	0.263000E+02
4621	688	0.361000E-01	0.382200E+00	0.487000E+02
2958	688	0.179000E-01	0.239100E+00	0.362000E+02
4955	688	0.293000E-01	0.366700E+00	0.464000E+02
2714	688	0.139000E-01	0.229500E+00	0.278000E+02
3231	688	0.181000E-01	0.224700E+00	0.312000E+02
4193	688	0.211000E-01	0.242400E+00	0.242000E+02
2335	688	0.176000E-01	0.226000E+00	0.228000E+02

3314	688	0.176000E-01	0.234900E+00	0.334000E+02
6145	688	0.488000E-01	0.424400E+00	0.504000E+02
7386	688	0.495000E-01	0.477300E+00	0.551000E+02
10711	688	0.294000E-01	0.261200E+00	0.307000E+02
10250	688	0.434000E-01	0.389400E+00	0.558000E+02

Fibre length=4.973mm, fibre diameter=0.0442mm.

3113	809	0.218000E-01	0.356600E+00	0.326000E+02
3715	770	0.253000E-01	0.461900E+00	0.338000E+02
4500	720	0.280000E-01	0.451500E+00	0.542000E+02
3993	709	0.345000E-01	0.746800E+00	0.499000E+02
3286	693	0.262000E-01	0.440600E+00	0.509000E+02
2879	708	0.225000E-01	0.380400E+00	0.390000E+02
3052	697	0.220000E-01	0.415300E+00	0.393000E+02
5107	683	0.330000E-01	0.599600E+00	0.631000E+02
10271	679	0.336000E-01	0.459800E+00	0.524000E+02
4110	689	0.261000E-01	0.504300E+00	0.437000E+02
5419	603	0.237000E-01	0.399800E+00	0.472000E+02
3704	699	0.153000E-01	0.251800E+00	0.415000E+02
7764	694	0.313000E-01	0.498900E+00	0.562000E+02
7118	701	0.228000E-01	0.308500E+00	0.409000E+02
4032	699	0.174000E-01	0.345300E+00	0.356000E+02
7948	709	0.235000E-01	0.317400E+00	0.436000E+02
7090	724	0.334000E-01	0.505400E+00	0.528000E+02
7514	703	0.472000E-01	0.608800E+00	0.674000E+02
6049	694	0.290000E-01	0.373900E+00	0.372000E+02

Fibre length=6.261mm, fibre diameter=0.0442mm.

1670	691	0.109000E-01	0.386000E+00	0.338000E+02
2556	691	0.193000E-01	0.495400E+00	0.563000E+02
1190	691	0.107000E-01	0.320400E+00	0.231000E+02
3357	691	0.276000E-01	0.629000E+00	0.658000E+02
2702	691	0.242000E-01	0.645500E+00	0.578000E+02
2443	691	0.168000E-01	0.465300E+00	0.382000E+02
1658	691	0.100000E-01	0.314700E+00	0.321000E+02
2121	691	0.138000E-01	0.379000E+00	0.263000E+02
2697	691	0.180000E-01	0.544600E+00	0.444000E+02
3304	675	0.184000E-01	0.486700E+00	0.415000E+02
3345	652	0.161000E-01	0.389600E+00	0.421000E+02
3136	652	0.142000E-01	0.380900E+00	0.382000E+02
2441	652	0.137000E-01	0.310800E+00	0.323000E+02
4155	652	0.214000E-01	0.414800E+00	0.375000E+02
1975	652	0.930000E-02	0.271400E+00	0.286000E+02
3125	652	0.155000E-01	0.399600E+00	0.387000E+02
6527	652	0.439000E-01	0.846300E+00	0.727000E+02
2915	652	0.146000E-01	0.347400E+00	0.348000E+02

4574	652	0.227000E-01	0.528900E+00	0.579000E+02
2740	652	0.150000E-01	0.400100E+00	0.353000E+02
6695	679	0.219000E-01	0.408700E+00	0.428000E+02
5421	679	0.165000E-01	0.411000E+00	0.460000E+02
4707	679	0.193000E-01	0.406800E+00	0.454000E+02
5987	679	0.229000E-01	0.470900E+00	0.531000E+02
5449	679	0.173000E-01	0.376500E+00	0.487000E+02
6848	679	0.180000E-01	0.312800E+00	0.283000E+02
9454	679	0.190000E-01	0.308100E+00	0.409000E+02
10854	679	0.207000E-01	0.347000E+00	0.432000E+02
9975	679	0.235000E-01	0.392000E+00	0.422000E+02
8859	679	0.241000E-01	0.411600E+00	0.466000E+02

Appendix XXIX. Data from Sedimentation Experiments.

This file contains sediment volumes (mL) and oven dried weights (grams) of 3, 6, and 15 denier fibres. Suspension temperature was close to 22°C and conductivity was less than  $5.0 \times 10^6$  Mho.

3 DENIER FIBRES (diameter=0.0197mm)

Fibre length=0.915mm

0.167000E+03	0.630900E+01
0.168000E+03	0.630900E+01
0.128000E+03	0.473760E+01
0.129000E+03	0.473760E+01
0.142000E+03	0.516430E+01
0.142000E+03	0.516430E+01

Mean sediment concentration=0.0352  
Standard deviation=0.000568  
95% confidence limits=0.0352  $\pm$  0.00146

Fibre length=1.875mm

0.188000E+03	0.250170E+01
0.189000E+03	0.250170E+01
0.151000E+03	0.231060E+01
0.159000E+03	0.231060E+01
0.140000E+03	0.190480E+01
0.141000E+03	0.190480E+01
0.115000E+03	0.117670E+01
0.110000E+03	0.117670E+01
0.110000E+03	0.102970E+01
0.112000E+03	0.102970E+01
0.115000E+03	0.112720E+01
0.115000E+03	0.112720E+01
0.130000E+03	0.162720E+01
0.129000E+03	0.162720E+01
0.940000E+02	0.116580E+01
0.920000E+02	0.116580E+01
0.135000E+03	0.190420E+01
0.143000E+03	0.190420E+01
0.130000E+03	0.169380E+01
0.130000E+03	0.169380E+01
0.102000E+03	0.120130E+01
0.100000E+03	0.120130E+01
0.105000E+03	0.107380E+01
0.980000E+02	0.107380E+01

Mean sediment concentration=0.0115  
Standard deviation=0.00164  
95% confidence limits=0.0115 ± 0.00339

Fibre length=2.815mm

0.140000E+03	0.928900E+00
0.135000E+03	0.928900E+00
0.150000E+03	0.932000E+00
0.147000E+03	0.932000E+00
0.105000E+03	0.683900E+00
0.110000E+03	0.683900E+00
0.140000E+03	0.765700E+00
0.133000E+03	0.765700E+00
0.103000E+03	0.523400E+00
0.100000E+03	0.513400E+00
0.850000E+02	0.394200E+00
0.820000E+02	0.394200E+00
0.100000E+03	0.522200E+00
0.100000E+03	0.522200E+00
0.112000E+03	0.574000E+00
0.112000E+03	0.574000E+00
0.105000E+03	0.480100E+00
0.104000E+03	0.480100E+00
0.108000E+03	0.648300E+00
0.112000E+03	0.648300E+00
0.740000E+02	0.445100E+00
0.740000E+02	0.445100E+00
0.116000E+03	0.716000E+00
0.120000E+03	0.716000E+00

Mean sediment concentration=0.00537  
Standard deviation=0.000647  
95% confidence limits=0.00537 ± 0.00134

Fibre length=3.737mm

0.135000E+03	0.523700E+00
0.138000E+03	0.523700E+00
0.950000E+02	0.355200E+00
0.950000E+02	0.355200E+00
0.980000E+02	0.336300E+00
0.100000E+03	0.336300E+00
0.140000E+03	0.515300E+00
0.145000E+03	0.515300E+00
0.130000E+03	0.448000E+00
0.135000E+03	0.448000E+00
0.115000E+03	0.363400E+00
0.110000E+03	0.363400E+00
0.125000E+03	0.434300E+00

0.135000E+03	0.434300E+00
0.185000E+03	0.591200E+00
0.195000E+03	0.591200E+00
0.165000E+03	0.504600E+00
0.170000E+03	0.504600E+00
0.145000E+03	0.416900E+00
0.145000E+03	0.416900E+00
0.110000E+03	0.362400E+00
0.108000E+03	0.362400E+00
0.165000E+03	0.433700E+00
0.165000E+03	0.433700E+00

Mean sediment concentration=0.00313  
Standard deviation=0.000332  
95% confidence limits=0.00313 ± 0.000686

6 DENIER FIBRES (diameter=0.0279mm)

Fibre length=0.914mm

0.810000E+02	0.384340E+01
0.810000E+02	0.384340E+01
0.770000E+02	0.349680E+01
0.770000E+02	0.349680E+01
0.113000E+03	0.616910E+01
0.117000E+03	0.616910E+01
0.118000E+03	0.616910E+01
0.900000E+02	0.463690E+01
0.900000E+02	0.463690E+01
0.102000E+03	0.540560E+01
0.104000E+03	0.540560E+01

Mean sediment concentration=0.0479  
Standard deviation=0.00309  
95% confidence limits=0.0479 ± 0.00688

Fibre length=1.832mm

0.136000E+03	0.330900E+01
0.136000E+03	0.330900E+01
0.120000E+03	0.279150E+01
0.121000E+03	0.279150E+01
0.110000E+03	0.255370E+01
0.110000E+03	0.255370E+01
0.150000E+03	0.364140E+01
0.154000E+03	0.364140E+01
0.122000E+03	0.271700E+01
0.121000E+03	0.271700E+01
0.138000E+03	0.291850E+01
0.138000E+03	0.291850E+01

0.105000E+03 0.253630E+01  
 0.105000E+03 0.253630E+01  
 0.660000E+02 0.140440E+01  
 0.650000E+02 0.140440E+01  
 0.730000E+02 0.170530E+01  
 0.780000E+02 0.170530E+01

Mean sediment concentration=0.0218

Standard deviation=0.00109

95% confidence limits=0.0218 ± 0.00232

Fibre length=2.757mm

0.129000E+03 0.119620E+01  
 0.130000E+03 0.119620E+01  
 0.126000E+03 0.118530E+01  
 0.129000E+03 0.118530E+01  
 0.138000E+03 0.157840E+01  
 0.142000E+03 0.157840E+01  
 0.156000E+03 0.140370E+01  
 0.160000E+03 0.140370E+01  
 0.140000E+03 0.130700E+01  
 0.148000E+03 0.130700E+01  
 0.171000E+03 0.148620E+01  
 0.170000E+03 0.148620E+01  
 0.147000E+03 0.115030E+01  
 0.147000E+03 0.115030E+01  
 0.140000E+03 0.989600E+00  
 0.143000E+03 0.989600E+00  
 0.101000E+03 0.782500E+00  
 0.100000E+03 0.782500E+00  
 0.950000E+02 0.652000E+00  
 0.970000E+02 0.652000E+00

Mean sediment concentration=0.00817

Standard deviation=0.00122

95% confidence limits=0.00817 ± 0.00255

Fibre length=3.718mm

0.108000E+03 0.859200E+00  
 0.109000E+03 0.859200E+00  
 0.145000E+03 0.861500E+00  
 0.145000E+03 0.861500E+00  
 0.930000E+02 0.527600E+00  
 0.900000E+02 0.527600E+00  
 0.920000E+02 0.439500E+00  
 0.920000E+02 0.439500E+00  
 0.990000E+02 0.642600E+00  
 0.101000E+03 0.642600E+00

0.126000E+03	0.706000E+00
0.128000E+03	0.706000E+00
0.900000E+02	0.628400E+00
0.890000E+02	0.628400E+00
0.970000E+02	0.643200E+00
0.900000E+02	0.643200E+00
0.161000E+03	0.112690E+01
0.160000E+03	0.112690E+01
0.150000E+03	0.110310E+01
0.158000E+03	0.110310E+01
0.220000E+03	0.138810E+01
0.225000E+03	0.138810E+01
0.170000E+03	0.945500E+00
0.175000E+03	0.945500E+00

Mean sediment concentration=0.00604  
Standard deviation=0.000834  
95% confidence limits=0.00604 ± 0.00172

Fibre length=4.666mm

0.128000E+03	0.588000E+00
0.130000E+03	0.588000E+00
0.900000E+02	0.374800E+00
0.850000E+02	0.374800E+00
0.170000E+03	0.729200E+00
0.165000E+03	0.729200E+00
0.175000E+03	0.736000E+00
0.180000E+03	0.736000E+00
0.115000E+03	0.501400E+00
0.115000E+03	0.501400E+00
0.110000E+03	0.428500E+00
0.110000E+03	0.428500E+00
0.165000E+03	0.648900E+00
0.160000E+03	0.648900E+00
0.980000E+02	0.356600E+00
0.900000E+02	0.356600E+00
0.110000E+03	0.396800E+00
0.105000E+03	0.396800E+00
0.140000E+03	0.538600E+00
0.150000E+03	0.538600E+00
0.105000E+03	0.387400E+00
0.110000E+03	0.387400E+00
0.900000E+02	0.338600E+00
0.950000E+02	0.338600E+00

Mean sediment concentration=0.00381  
Standard deviation=0.000315  
95% confidence limits=0.00381 ± 0.000651

15 DENIER FIBRES (diameter=0.0442mm)

Fibre length=0.931mm

0.112000E+03	0.143900E+02
0.112000E+03	0.143900E+02
0.111000E+03	0.144300E+02
0.111000E+03	0.144300E+02
0.860000E+02	0.116500E+02
0.860000E+02	0.116500E+02
0.100000E+03	0.122000E+02
0.100000E+03	0.122000E+02
0.114000E+03	0.147700E+02
0.116000E+03	0.147700E+02
0.106000E+03	0.143500E+02
0.107000E+03	0.143500E+02

Mean sediment concentration=0.124

Standard deviation=0.00449

95% confidence limits=0.1235 ± 0.00989

Fibre length=1.560mm

0.970000E+02	0.625000E+01
0.960000E+02	0.625000E+01
0.111000E+03	0.681000E+01
0.111000E+03	0.681000E+01
0.700000E+02	0.358000E+01
0.660000E+02	0.358000E+01
0.960000E+02	0.530000E+01
0.920000E+02	0.530000E+01
0.880000E+02	0.530000E+01
0.880000E+02	0.530000E+01
0.950000E+02	0.517000E+01
0.900000E+02	0.517000E+01

Mean sediment concentration=0.0557

Standard deviation=0.00408

95% confidence limits=0.0557 ± 0.00899

Fibre length=2.947mm

0.110000E+03	0.273800E+01
0.110000E+03	0.273800E+01
0.105000E+03	0.274800E+01
0.106000E+03	0.274800E+01
0.111000E+03	0.276500E+01
0.111000E+03	0.276500E+01
0.101000E+03	0.241300E+01
0.990000E+03	0.241300E+01

0.880000E+02 0.226900E+01  
 0.890000E+02 0.226900E+01  
 0.980000E+02 0.240400E+01  
 0.980000E+02 0.240400E+01  
 0.116000E+03 0.275400E+01  
 0.110000E+03 0.275400E+01  
 0.110000E+03 0.271900E+01  
 0.110000E+03 0.271900E+01  
 0.980000E+02 0.271400E+01  
 0.990000E+02 0.271400E+01  
 0.105000E+03 0.270300E+01  
 0.108000E+03 0.270300E+01  
 0.970000E+02 0.249000E+01  
 0.990000E+02 0.249000E+01  
 0.960000E+02 0.278900E+01  
 0.100000E+03 0.278900E+01

Mean sediment concentration=0.0243  
 Standard deviation=0.00125  
 95% confidence limits=0.0243 ± 0.00259

Fibre length=4.973mm

0.980000E+02 0.107200E+01  
 0.950000E+02 0.107200E+01  
 0.120000E+03 0.112700E+01  
 0.110000E+03 0.112700E+01  
 0.980000E+02 0.102500E+01  
 0.950000E+02 0.102500E+01  
 0.105000E+03 0.102400E+01  
 0.100000E+03 0.102400E+01  
 0.110000E+03 0.100100E+01  
 0.100000E+03 0.100100E+01  
 0.900000E+02 0.951000E+00  
 0.800000E+02 0.951000E+00  
 0.850000E+02 0.845500E+00  
 0.850000E+02 0.845500E+00  
 0.850000E+02 0.816500E+00  
 0.800000E+02 0.816500E+00  
 0.850000E+02 0.936900E+00  
 0.800000E+02 0.936900E+00  
 0.900000E+02 0.812700E+00  
 0.900000E+02 0.812700E+00

Mean sediment concentration=0.00976  
 Standard deviation=0.000797  
 95% confidence limits=0.00976 ± 0.00167

Fibre length=6.261mm

0.140000E+03 0.800000E+00  
0.145000E+03 0.800000E+00  
0.135000E+03 0.800000E+00  
0.150000E+03 0.800000E+00  
0.175000E+03 0.800000E+00  
0.135000E+03 0.800000E+00  
0.125000E+03 0.800000E+00  
0.130000E+03 0.800000E+00

Mean sediment concentration=0.00542  
Standard deviation=0.000538  
95% confidence limits=0.00542 ± 0.00127

Appendix XXX. Data from Coefficient of Friction Measurements.

Data from static and dynamic friction measurements between two wet nylon surfaces. Each line contains: load placed on a slide (grams), and tangents of an incline angle for static and dynamic cases.

3 DENIER FILAMENTS (diameter=0.0197mm)

0.100000E+02	0.367400E+00	0.302900E+00
0.100000E+02	0.357500E+00	0.296600E+00
0.100000E+02	0.357500E+00	0.293000E+00
0.200000E+02	0.358400E+00	0.293000E+00
0.200000E+02	0.351200E+00	0.285800E+00
0.200000E+02	0.343200E+00	0.285800E+00
0.500000E+02	0.336900E+00	0.267900E+00
0.500000E+02	0.324400E+00	0.264300E+00
0.500000E+02	0.302000E+00	0.261600E+00
0.100000E+03	0.338700E+00	0.261600E+00
0.100000E+03	0.328800E+00	0.246400E+00
0.100000E+03	0.318100E+00	0.239200E+00
0.100000E+02	0.360000E+00	0.305000E+00
0.100000E+02	0.348000E+00	0.289600E+00
0.100000E+02	0.342000E+00	0.284000E+00
0.200000E+02	0.362000E+00	0.284000E+00
0.200000E+02	0.348000E+00	0.274000E+00
0.200000E+02	0.334000E+00	0.269000E+00
0.300000E+02	0.365000E+00	0.278000E+00
0.300000E+02	0.365000E+00	0.264000E+00
0.300000E+02	0.347000E+00	0.249000E+00
0.400000E+02	0.360000E+00	0.266000E+00
0.400000E+02	0.358000E+00	0.266000E+00
0.400000E+02	0.343000E+00	0.255000E+00
0.740000E+02	0.340000E+00	0.256000E+00
0.740000E+02	0.321000E+00	0.252000E+00
0.740000E+02	0.303000E+00	0.244000E+00
0.810000E+02	0.340000E+00	0.244000E+00
0.810000E+02	0.337000E+00	0.242000E+00
0.810000E+02	0.315000E+00	0.234000E+00
0.500000E+02	0.358000E+00	0.261000E+00
0.500000E+02	0.337000E+00	0.261000E+00
0.500000E+02	0.322600E+00	0.261000E+00
0.100000E+03	0.257000E+00	0.343200E+00
0.100000E+03	0.241000E+00	0.333000E+00
0.100000E+03	0.241000E+00	0.333000E+00

Mean static coefficient of friction=0.334  
Standard deviation=0.0318  
95% confidence limits=0.0334 ± 0.0647

Mean dynamic coefficient of friction=0.273  
Standard deviation=0.0267  
95% confidence limits=0.273 ± 0.0542

6 DENIER FILAMENTS (diameter=0.0279mm)

0.100000E+02	0.302700E+00	0.205300E+00
0.100000E+02	0.342800E+00	0.210700E+00
0.200000E+02	0.296400E+00	0.207100E+00
0.200000E+02	0.315200E+00	0.212500E+00
0.500000E+02	0.261600E+00	0.199100E+00
0.500000E+02	0.291100E+00	0.214200E+00
0.100000E+03	0.259800E+00	0.199100E+00
0.100000E+03	0.279500E+00	0.204800E+00
0.100000E+02	0.343700E+00	0.197300E+00
0.100000E+02	0.325000E+00	0.191100E+00
0.200000E+02	0.335000E+00	0.197300E+00
0.200000E+02	0.324100E+00	0.190200E+00
0.500000E+02	0.334000E+00	0.190200E+00
0.500000E+02	0.327000E+00	0.180400E+00
0.100000E+03	0.334800E+00	0.198600E+00
0.100000E+03	0.325000E+00	0.191100E+00
0.100000E+02	0.296100E+00	0.194400E+00
0.100000E+02	0.336900E+00	0.194400E+00
0.200000E+02	0.288500E+00	0.191700E+00
0.200000E+02	0.288500E+00	0.191700E+00
0.500000E+02	0.267900E+00	0.183700E+00
0.500000E+02	0.315400E+00	0.187500E+00
0.100000E+03	0.302000E+00	0.189100E+00
0.100000E+03	0.303700E+00	0.189100E+00

Mean static coefficient of friction=0.308  
Standard deviation=0.0256  
95% confidence limits=0.308 ± 0.0529

Mean dynamic coefficient of friction=0.196  
Standard deviation=0.00898  
95% confidence limits=0.196 ± 0.0186

Appendix XXXI. Average Velocities and Root-Mean-Squares of Velocity Fluctuation.

Data presented in this appendix are for the low viscosity suspending liquid discussed in Section 4.5.

<u>COORDINATES</u>		<u>AVERAGE VELOCITIES</u>		<u>RMS OF VELOCITIES</u>		<u>RMS/AVERAGE VELOCITY</u>	
<u>r</u>	<u><math>\beta</math></u>	<u>RADIAL</u>	<u>TANGENTIAL</u>	<u>RADIAL</u>	<u>TANGENTIAL</u>	<u>RADIAL</u>	<u>TANGENTIAL</u>
<u>mm</u>	<u>deg.</u>	<u>m/s</u>	<u>m/s</u>	<u>m/s</u>	<u>m/s</u>	<u>--</u>	<u>--</u>
10	0	0.20E-02	-0.61E-02	0.26E-01	0.20E-01	0.13E+02	-0.32E+01
15	0	-0.15E-01	0.83E-02	0.19E-01	0.14E-01	-0.13E+01	0.17E+01
20	0	-0.13E-01	0.18E-01	0.17E-01	0.13E-01	-0.13E+01	0.70E+00
25	0	-0.19E-01	0.29E-01	0.15E-01	0.13E-01	-0.76E+00	0.46E+00
30	0	-0.15E-01	0.19E-01	0.16E-01	0.15E-01	-0.11E+01	0.79E+00
35	0	-0.19E-01	0.88E-02	0.18E-01	0.17E-01	-0.97E+00	0.19E+01
40	0	-0.14E-01	0.18E-01	0.13E-01	0.23E-01	-0.93E+00	0.13E+01
45	0	-0.29E-02	0.11E+00	0.11E-01	0.17E-01	-0.38E+01	0.16E+00
25	10	-0.20E-01	0.10E-01	0.16E-01	0.12E-01	-0.81E+00	0.12E+01
30	10	-0.44E-02	0.15E-01	0.20E-01	0.13E-01	-0.44E+01	0.87E+00
35	10	-0.18E-01	0.28E-01	0.17E-01	0.12E-01	-0.94E+00	0.44E+00
40	10	-0.15E-01	0.28E-01	0.15E-01	0.15E-01	-0.11E+01	0.54E+00
45	10	-0.73E-03	0.11E+00	0.16E-01	0.17E-01	-0.22E+02	0.16E+00
10	20	-0.87E-03	-0.14E-01	0.20E-01	0.10E-01	-0.23E+02	-0.73E+00
15	20	-0.14E-01	0.11E-01	0.21E-01	0.87E-02	-0.15E+01	0.76E+00
20	20	-0.22E-01	0.19E-01	0.27E-01	0.48E-02	-0.12E+01	0.25E+00
25	20	-0.18E-01	0.22E-01	0.17E-01	0.58E-02	-0.96E+00	0.26E+00
30	20	-0.25E-01	0.27E-01	0.17E-01	0.11E-01	-0.67E+00	0.39E+00
35	20	-0.26E-01	0.27E-01	0.19E-01	0.11E-01	-0.74E+00	0.41E+00
40	20	-0.16E-01	0.30E-01	0.18E-01	0.11E-01	-0.11E+01	0.36E+00
45	20	0.22E-02	0.12E+00	0.18E-01	0.84E-02	0.81E+01	0.69E-01
25	30	-0.21E-01	0.25E-01	0.21E-01	0.42E-02	-0.98E+00	0.17E+00
30	30	-0.20E-01	0.27E-01	0.26E-01	0.17E-03	-0.13E+01	0.62E-02
35	30	-0.19E-01	0.22E-01	0.26E-01	0.58E-02	-0.14E+01	0.26E+00
40	30	-0.59E-02	0.42E-01	0.23E-01	0.42E-02	-0.40E+01	0.10E+00
45	30	-0.60E-02	0.12E+00	0.17E-01	0.58E-02	-0.29E+01	0.49E-01
10	40	-0.83E-02	-0.98E-02	0.18E-01	0.66E-03	-0.22E+01	-0.68E-01
15	40	-0.99E-02	0.38E-02	0.19E-01	-0.16E-02	-0.19E+01	-0.42E+00
20	40	-0.11E-01	0.25E-01	0.19E-01	0.87E-03	-0.17E+01	0.35E-01
25	40	-0.13E-01	0.24E-01	0.19E-01	0.31E-02	-0.15E+01	0.13E+00
30	40	-0.15E-01	0.30E-01	0.20E-01	-0.31E-03	-0.14E+01	-0.10E-01
35	40	-0.26E-01	0.30E-01	0.20E-01	0.19E-02	-0.78E+00	0.62E-01
40	40	-0.15E-01	0.51E-01	0.20E-01	0.40E-02	-0.13E+01	0.79E-01
45	40	0.17E-02	0.14E+00	0.18E-01	-0.66E-03	0.10E+02	-0.48E-02
25	50	-0.19E-01	0.93E-02	0.24E-01	0.49E-03	-0.12E+01	0.53E-01
30	50	-0.18E-01	0.35E-01	0.19E-01	-0.15E-02	-0.10E+01	-0.44E-01
35	50	0.29E-02	0.24E-01	0.26E-01	-0.11E-01	0.91E+01	-0.48E+00
40	50	0.39E-02	0.21E-01	0.23E-01	-0.47E-02	0.60E+01	-0.22E+00
45	50	0.27E-02	0.12E+00	0.30E-01	-0.93E-02	0.11E+02	-0.80E-01

10	60	-0.76E-01	-0.43E-01	0.41E-01	0.74E-02	-0.54E+00	-0.17E+00
15	60	-0.73E-03	-0.28E-01	0.27E-01	-0.14E-01	-0.37E+02	0.50E+00
20	60	0.24E-01	-0.32E-01	0.25E-01	-0.22E-01	0.10E+01	0.70E+00
25	60	0.19E-01	-0.15E-01	0.24E-01	-0.25E-01	0.13E+01	0.16E+01
30	60	-0.26E-02	0.14E-01	0.18E-01	-0.89E-02	-0.70E+01	-0.66E+00
35	60	-0.35E-02	0.19E-01	0.22E-01	-0.16E-01	-0.65E+01	-0.85E+00
40	60	-0.38E-02	0.53E-01	0.21E-01	-0.11E-01	-0.56E+01	-0.21E+00
45	60	-0.22E-02	0.14E+00	0.24E-01	-0.94E-02	-0.11E+02	-0.70E-01
25	70	-0.41E-02	0.67E-02	0.13E-01	-0.68E-02	-0.32E+01	-0.10E+01
30	70	-0.20E-02	0.13E-01	0.14E-01	-0.86E-02	-0.68E+01	-0.66E+00
35	70	-0.34E-02	0.20E-01	0.17E-01	-0.12E-01	-0.49E+01	-0.57E+00
40	70	-0.65E-02	0.55E-01	0.19E-01	-0.16E-01	-0.30E+01	-0.29E+00
45	70	0.21E-02	0.15E+00	0.17E-01	-0.99E-02	0.79E+01	-0.64E-01
20	80	-0.15E+00	-0.35E-01	0.23E-01	-0.12E-01	-0.16E+00	0.34E+00
25	80	-0.94E-01	-0.20E-01	0.30E-01	-0.10E-01	-0.32E+00	0.51E+00
30	80	-0.66E-01	-0.81E-02	0.20E-01	-0.13E-01	-0.30E+00	0.16E+01
35	80	-0.48E-01	0.86E-02	0.20E-01	-0.13E-01	-0.42E+00	-0.15E+01
40	80	-0.20E-01	0.41E-01	0.15E-01	-0.20E-01	-0.75E+00	-0.48E+00
45	80	-0.64E-02	0.14E+00	0.15E-01	-0.16E-01	-0.23E+01	-0.12E+00
25	280	0.20E-01	-0.91E-01	0.91E-02	0.36E-01	0.46E+00	-0.39E+00
30	280	0.12E-01	-0.52E-01	0.91E-02	0.48E-01	0.77E+00	-0.93E+00
35	280	0.12E-01	-0.43E-01	0.13E-01	0.34E-01	0.11E+01	-0.81E+00
40	280	0.41E-02	-0.50E-01	0.13E-01	0.39E-01	0.31E+01	-0.78E+00
45	280	-0.22E-01	-0.22E-01	0.19E-01	0.22E-01	-0.83E+00	-0.98E+00
25	290	0.30E-01	-0.47E-01	0.10E-01	0.36E-01	0.34E+00	-0.77E+00
30	290	0.18E-01	-0.20E-01	0.97E-02	0.24E-01	0.55E+00	-0.12E+01
35	290	0.29E-01	-0.39E-01	0.14E-01	0.32E-01	0.49E+00	-0.82E+00
40	290	0.10E-01	-0.16E-01	0.77E-02	0.25E-01	0.74E+00	-0.16E+01
45	290	0.92E-02	0.26E-02	0.13E-01	0.19E-01	0.14E+01	0.74E+01
10	300	0.52E-01	-0.91E-01	-0.60E-02	0.36E-01	-0.12E+00	-0.39E+00
15	300	0.24E-01	-0.40E-01	-0.62E-02	0.43E-01	-0.26E+00	-0.11E+01
20	300	0.16E-01	-0.28E-01	0.54E-02	0.33E-01	0.33E+00	-0.12E+01
25	300	0.16E-01	-0.19E-01	0.60E-02	0.26E-01	0.38E+00	-0.14E+01
30	300	0.68E-02	-0.72E-02	0.49E-02	0.21E-01	0.73E+00	-0.29E+01
35	300	0.12E-01	-0.36E-02	0.36E-02	0.25E-01	0.29E+00	-0.70E+01
40	300	0.92E-02	0.13E-01	0.54E-02	0.18E-01	0.58E+00	0.14E+01
45	300	0.17E-01	0.29E-01	0.68E-02	0.22E-01	0.39E+00	0.74E+00
25	310	0.25E-01	-0.45E-01	-0.74E-02	0.35E-01	-0.29E+00	-0.79E+00
30	310	0.78E-02	-0.21E-01	-0.18E-02	0.21E-01	-0.23E+00	-0.97E+00
35	310	0.13E-01	-0.24E-01	-0.22E-02	0.23E-01	-0.17E+00	-0.98E+00
40	310	0.11E-01	-0.18E-01	-0.41E-03	0.19E-01	-0.37E-01	-0.11E+01
45	310	0.24E-03	0.15E-02	0.65E-03	0.21E-01	0.27E+01	0.14E+02
10	320	0.35E-01	-0.35E-01	-0.18E-01	0.31E-01	-0.51E+00	-0.88E+00
15	320	0.23E-01	-0.32E-01	-0.16E-01	0.31E-01	-0.71E+00	-0.98E+00
20	320	0.25E-01	-0.29E-01	-0.14E-01	0.32E-01	-0.56E+00	-0.11E+01
25	320	0.15E-01	-0.26E-01	-0.84E-02	0.27E-01	-0.56E+00	-0.10E+01
30	320	0.22E-01	-0.28E-01	-0.80E-02	0.24E-01	-0.36E+00	-0.86E+00
35	320	0.61E-02	-0.30E-01	-0.42E-02	0.24E-01	-0.69E+00	-0.81E+00
40	320	0.14E-02	-0.20E-01	-0.10E-02	0.19E-01	-0.75E+00	-0.93E+00
45	320	-0.42E-02	0.19E-01	-0.35E-02	0.22E-01	0.82E+00	0.12E+01

25	330	-0.12E-01	-0.30E-02	-0.73E-02	0.19E-01	0.60E+00	-0.62E+01
30	330	-0.18E-01	0.20E-02	-0.43E-02	0.15E-01	0.24E+00	0.75E+01
35	330	-0.25E-01	0.65E-02	-0.46E-02	0.16E-01	0.19E+00	0.25E+01
40	330	-0.28E-01	0.50E-02	-0.70E-02	0.14E-01	0.25E+00	0.28E+01
45	330	-0.43E-01	0.41E-01	-0.83E-02	0.21E-01	0.19E+00	0.53E+00
10	340	0.21E-01	-0.24E-02	-0.15E-01	0.31E-01	-0.69E+00	-0.13E+02
15	340	-0.87E-02	0.51E-02	-0.61E-02	0.27E-01	0.69E+00	0.54E+01
20	340	-0.24E-01	-0.78E-02	-0.74E-02	0.18E-01	0.31E+00	-0.23E+01
25	340	-0.24E-01	0.27E-02	-0.81E-02	0.18E-01	0.34E+00	0.66E+01
30	340	-0.28E-01	-0.10E-01	-0.67E-02	0.22E-01	0.24E+00	-0.22E+01
35	340	-0.21E-01	-0.10E-01	-0.13E-01	0.18E-01	0.61E+00	-0.17E+01
40	340	-0.40E-01	0.99E-02	-0.85E-02	0.13E-01	0.21E+00	0.13E+01
45	340	-0.76E-01	0.37E-01	-0.14E-01	0.21E-01	0.18E+00	0.57E+00
25	350	-0.18E-01	0.32E-02	-0.13E-01	0.24E-01	0.70E+00	0.75E+01
30	350	-0.23E-01	-0.95E-04	-0.11E-01	0.23E-01	0.49E+00	-0.24E+03
35	350	-0.23E-01	0.66E-02	-0.11E-01	0.16E-01	0.47E+00	0.23E+01
40	350	-0.32E-01	-0.83E-03	-0.11E-01	0.16E-01	0.35E+00	-0.19E+02
45	350	-0.76E-01	0.94E-02	-0.17E-01	0.15E-01	0.22E+00	0.16E+01